TRACKING AND DATA RELAY SATELLITE SYSTEM CONFIGURATION AND TRADEOFF STUDY

Volume 4. TDRS System Operation and Control and Telecommunications Service System

HUGHES
HUGHES AIRCRAFT COMPANY
SPACE AND COMMUNICATIONS GROUP

HUGHES AIRCRAFT COMPANY
SPACE AND COMMUNICATIONS GROUP
El Segundo, California

29 September 1972
Part I Final Report

Prepared for
GODDARD SPACE FLIGHT CENTER
Greenbelt, Maryland 20771

Hughes Reference No. B5033 • SCG 20642R

TECHNICAL REPORT STANDARD TITLE PAGE

1. Report No.	2. Government Accession No.	3. Recipient's Catalog No.
4. Title and Subtitle Tracking and Data Relay Satellite System Configuration and Tradeoff Study		5. Report Date 29 September 1972 6. Performing Organization Code
7 Author(s)		8. Performing Organization Report No. Volume 4, 20642R
9. Performing Organization Name and Address Hughes Aircraft Company Space and Communications Group NASA Systems Division 1950 E. Imperial Highway El Segundo, California 90009		10. Work Unit No. 11. Contract or Grant No. NAS 5-21704
12. Sponsoring Agency Name and Address National Aeronautics and Space Administration Goddard Space Flight Center Greenbelt, Maryland 20771 G. Clark		13. Type of Report and Period Covered Part I Final Report, 25 January 1972 to 21 August 1972 14. Sponsoring Agency Code
15. Supplementary Notes		

16. Abstract

Two major study areas are treated in this volume: 1) Operations and Control and 2) the Telecommunication Service System. The TDRS orbit selection, orbital deployment, Ground Station visibility, sequence of events from launch to final orbit position, and TDRS Control Center functions required for stationkeeping, repositioning, attitude control, and antenna pointing are briefly treated as part of the Operations and Control section. The last topic of this section concerns the operations required for efficiently providing the TDRSS user telecommunication services. The discussion treats functions of the GSFC control and data processing facility, Ground Station, and TDRS Control Center.

The second major portion of this volume deals with the Telecommunication Service System (TSS) which consists of the Ground Station, TDRS Communication equipment and the user transceiver. A summary of the requirements and objectives for the telecommunication services and a brief summary of the TSS capabilities is followed by communication system analysis, signal design, and equipment design. Finally, descriptions of the three TSS elements are presented.

17. Key Words (Selected by Author(s))	18. Distribution Statement
Orbital Deployment, TDRS Control, Telecommunication Operations, Telecommunication Service System, Signal Design, Repeater	

19. Security Classif. (of this report)	20. Security Classif. (of this page)	21. No. of Pages	22. Price*
Unclassified	Unclassified	335	

*For sale by the Clearinghouse for Federal Scientific and Technical Information, Springfield, Virginia 22151.

CONTENTS

APPENDICES

ILLUSTRATIONS

TABLES

1. INTRODUCTION

The results of Phase I of the TDRSS study have been organized into three major categories: 1) operations and control, 2) telecommunication service system, and 3) spacecraft design. This volume contains the material treating topics 1 and 2, and Volume 3 discusses the design of the TDR spacecraft.

Operations and control refer to those aspects of the TDRS system that involve the major system elements such as the spacecraft, ground station, and control facilities. The four major subjects included in this section are 1) orbit selection, 2) launch and orbit insertion, 3) TDRS on-orbit control, and 4) telecommunications service system control.

Orbit selection, discussed in subsection 2.1, relates the TDRS position and orbit inclination to both ground station visibility and user visibility. The impact on spacecraft mass due to orbit inclination is discussed. Subsection 2.2 discusses the major phases required to achieve the selected TDRS orbit, including launch, transfer orbit, apogee injection, and station acquisition.

The discussion of TDRS on-orbit control in subsection 2.3 deals mainly with those functions required for maintaining orbit position and angular orientation (attitude). In addition, TDRS repositioning and antenna pointing are discussed briefly. Subsection 2.4 on telecommunications service system operations discusses the functions of the three major ground based elements of the TDRSS: 1) the GSFC communications control and processing facility, subsequently referred to as GSFC; 2) the TDRS Control Center; and 3) the ground station.

The telecommunications service system(TSS) is the heart of the TDRSS concept. It includes the communication payload on the TDR spacecraft, the user transceiver, and the ground station. This equipment performs all modulation/demodulation and/or RF transmission/reception. Section 3 treats the design of this equipment in a logical progression of subject matter. First requirements and objectives for the TSS design are presented followed by a short summary of the TSS performance and major features. In subsection 3.3 detailed analysis is presented which was the foundation for the selection of baseline signaling and system operation concepts. The analysis is followed by three subsections which discuss respectively the design of the TDRS communication subsystem, the ground station, and the user transceiver.

2. OPERATIONS AND CONTROL

The TDRS system provides telecommunication service with two geosynchronous relay satellites. The TDRSS operations and control comprise three major functions:

- TDRS launch and orbital deployment
- TDRS on-orbit control
- TDRSS telecommuncation service operations

The TDRS orbital inclination of 7 degrees is selected as a compromise between spacecraft mass, inclination biasing requirements, and user coverage. This orbital inclination does not cause any operational difficulties and has a negligible effect on user visibility as compared to a zero inclination orbit. Maximum separation (compatible with ground station elevation constraints) is used between the two TDR satellites to maximize user visibility. The TDRS launch and orbit insertion is quite conventional, e.g., similar to that used for Intelsat IV.

The TDRS on-orbit control operations are as follows:

- E-W stationkeeping
- Attitude correction maneuvers
- S and K band antenna pointing
- TDRS repeater channel settings

All of these operations will be commanded from ground, and they are similar to the control of other synchronous satellites for which considerable orbital experience has been accumulated.

The TDRSS telecommunication service operations have been developed to stress simplicity, economy, flexibility, and ease of operations. Maximum use of existing GSFC network control and scheduling, orbit determination, and data processing capabilities has been planned.

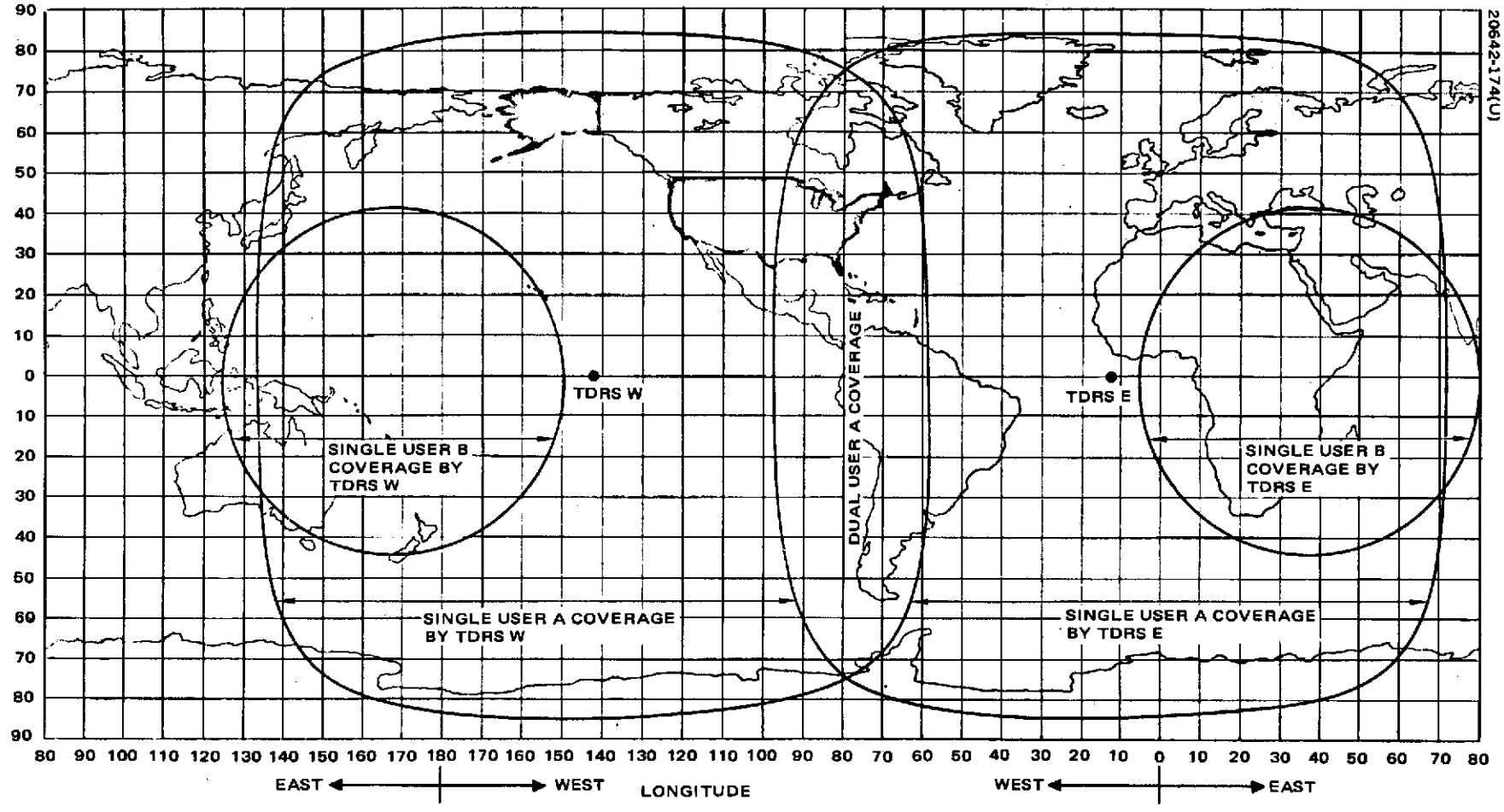

Figure 2-1. Coverage Provided by TDRSs in Equatorial Orbit, User A at 100 km; User B at 5000 km Altitude

2.1 TDRSS ORBIT SELECTION

The proper selection of the optimal orbital geometry for the TDRSS (limited to a class of 24 hour, circular, near equatorial orbits) involves a number of system tradeoffs. As a result, the selected geometry is dependent on which system characteristics are deemed most desirable from a total mission design standpoint. The characteristics of the TDRSS that affect selection of the orbital geometry are maximization of TDRS spacecraft mass, elevation angles from ground station, solar power consideration, station-keeping, orbit determination requirements, and user coverage.

The selection of the optimum orbital geometry for the TRDSS is constrained by the 10 degree minimum elevation to the ground station, assumed to be located near GSFC. It is desired to maximize both the TDRS mass and the percentage time that the user satellite is visible to either TDRS. This selection involves determination of the most favorable longitudinal separation between the two TDRSs, the optimal TDRS orbital inclination, and the acceptable limit on the TDRS drift, consistent with the minimum elevation constraint.

The useful payload from 28.3 degree inclined transfer orbit to a synchronous equatorial final orbit is defined when launch vehicle performance levels and apogee motor characteristics are given. However, two important factors may be utilized to considerably increase the final orbit useful payload. First it can be shown that a small plane change at perigee of the transfer orbit equal to approximately 1 degree for any given apogee motor will maximize the final useful payload. This improvement comes about because the apogee motor fuel savings for the insertion into the final TDRS orbit more than offset the decrease in actual payload into the transfer orbit. The second important factor for increasing useful payload is to bias the final TDRS inclination. For example, assuming a 7 degree TDRS final orbit inclination and a 1 degree perigee plane change allows an increase of approximately 18 kg of useful payload.

2.1.1 Satellite Deployment

It can be shown quite simply that, as the longitudinal separation between the TDRSs increases, the percentage time that a user is visible also increases, until, at 180 degrees separation, continuous global coverage exists for user altitudes above 170 km. Since a separation of 180 degrees precludes continual communication between GSFC and both spacecraft, a separation less than 180 degrees must be used. In the absence of north-south and east-west drifts, the maximum allowable separation between spacecraft will exist when the orbits are equatorial (i.e., inclination at zero degrees) and will equal the value of 130 degrees when a 10 degree visibility angle is maintained at the ground station latitude of 38°N. The TDRSS coverage capability for a 130 degree separation and 0 degree inclination, for users at altitudes of 100 and 5000 km, is shown in Figure 2-1.

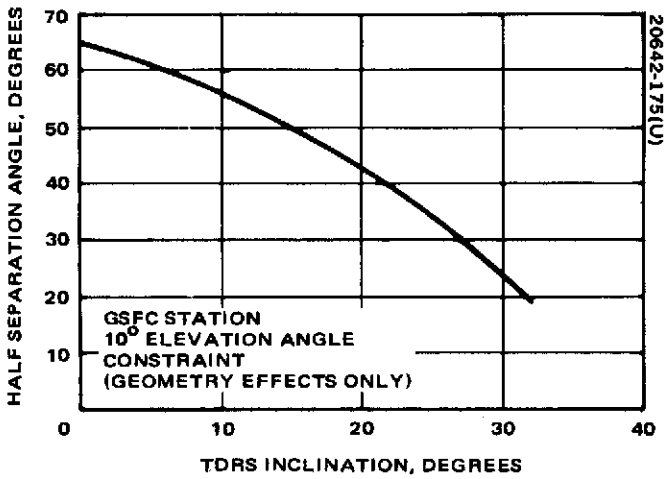

Figure 2-2. Maximum Separation Angle as Function of Increasing TDRS Inclination

In the selection of the optimum TDRS orbital inclination, the diurnal north-south motion at the higher inclinations causes the ground station to appear to move in and out of the satellite coverage area. Therefore, in order to guarantee uninterrupted communication with GSFC, the longitudinal separation between the ground station and each spacecraft must be reduced (see Figure 2-2). In the absence of north-south stationkeeping, the orbital inclination will change at a rate of approximately 0.9 deg/yr as a result of solar/lunar perturbations. To minimize the maximum inclination experienced over the life of the mission, the inclination should be initially biased by at least 3 degrees (for a 7 year lifetime). This procedure avoids the high cost of north-south stationkeeping.

If the TDRS inclination were biased 7 degrees, the north-south stationkeeping could still be eliminated, since proper nodal selection will cause the inclination to decrease over the lifetime. As discussed previously, a substantial increase in useful payload into final orbit may then be accomplished with the only penalty being paid in terms of coverage. As seen in Figure 2-3, the effect on coverage of the 7 degree inclination (compared to Figure 2-1) is to slightly decrease the continuous coverage areas; however, no matter what the TDRS inclination is at any instant in time, it still covers exactly the same total area. As the figure indicates, this total area shifts up and down as the TDRS traverses its orbit. Thus, users can be scheduled to relay their data with no coverage penalties caused by the TDRS orbital inclination.

Considering a typical dead band of ±1 degree for east-west stationkeeping about the nominal satellite location, Figure 2-4 shows the maximum longitudinal separation between ground station and spacecraft as a function of elevation angle and inclination. For an orbital inclination of 7 degrees, it can be seen from the curve that a maximum nominal separation of approximately 59 degrees exists for a minimum elevation angle of

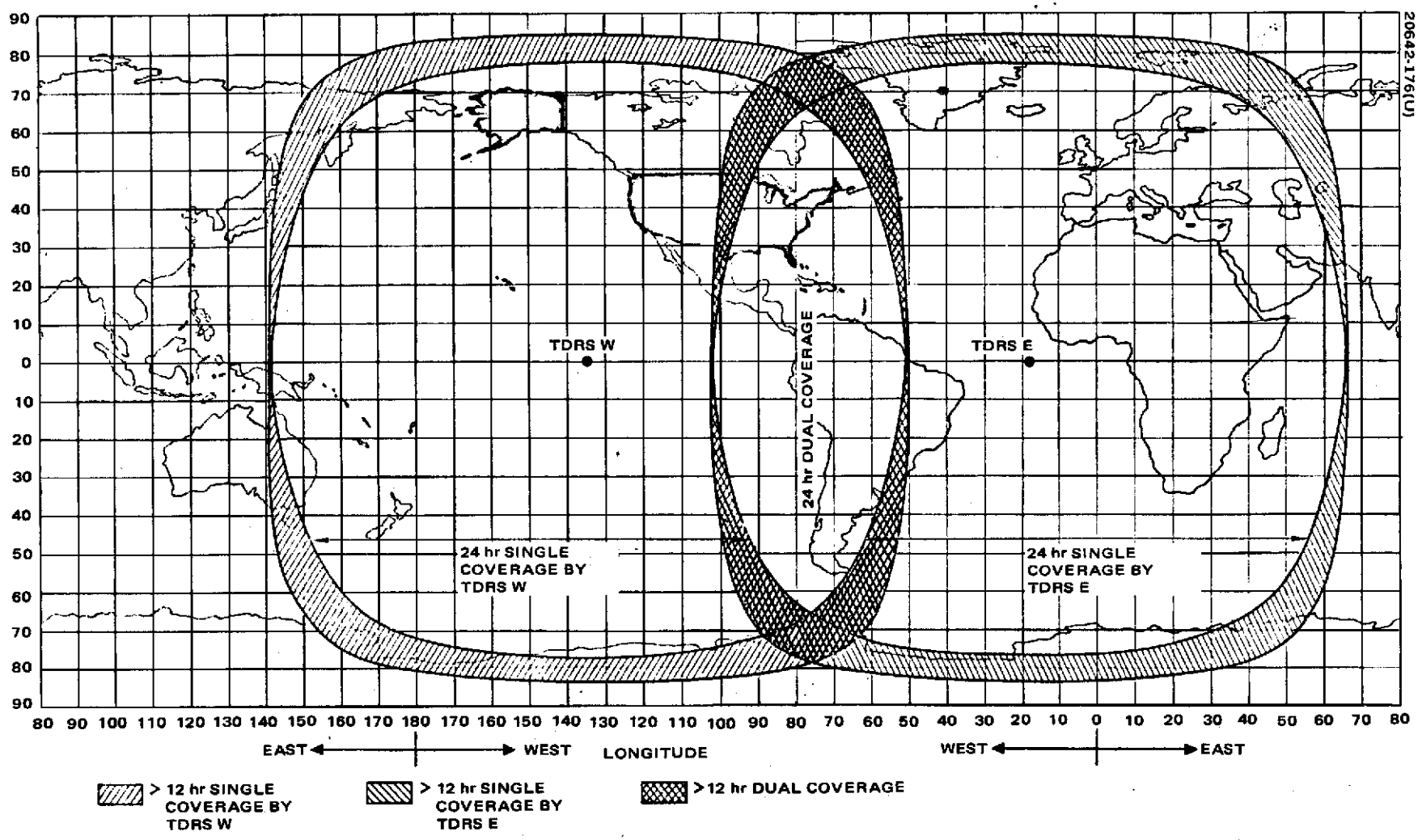

a) User A 100 km Altitude

Figure 2-3. User Coverage Provided by TDRSS in 7 Degree Biased Orbit

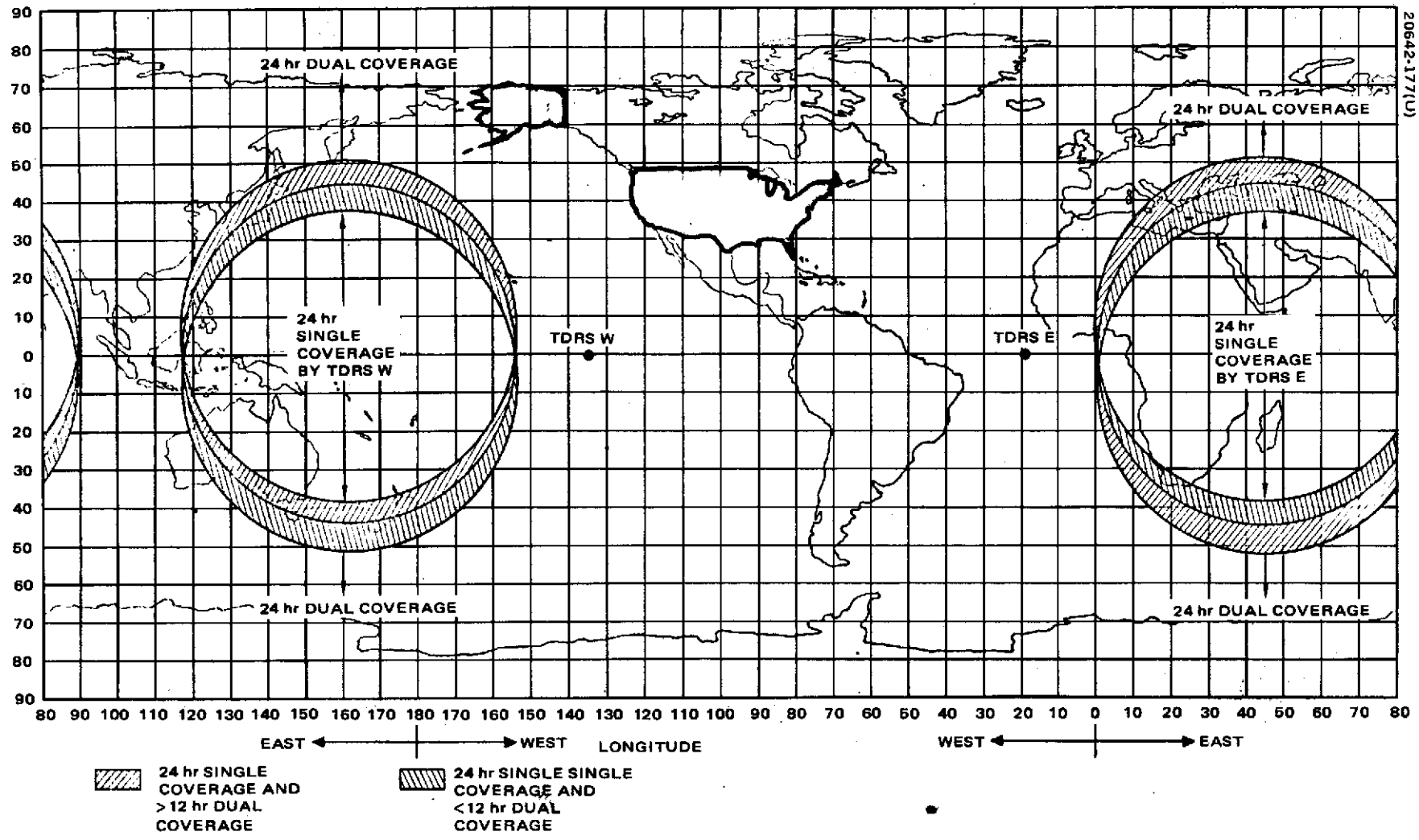

b) User B at 5000 km Altitude

Figure 2-3 (Continued). User Coverage Provided by TDRSS in 7 Degree Biased Orbit

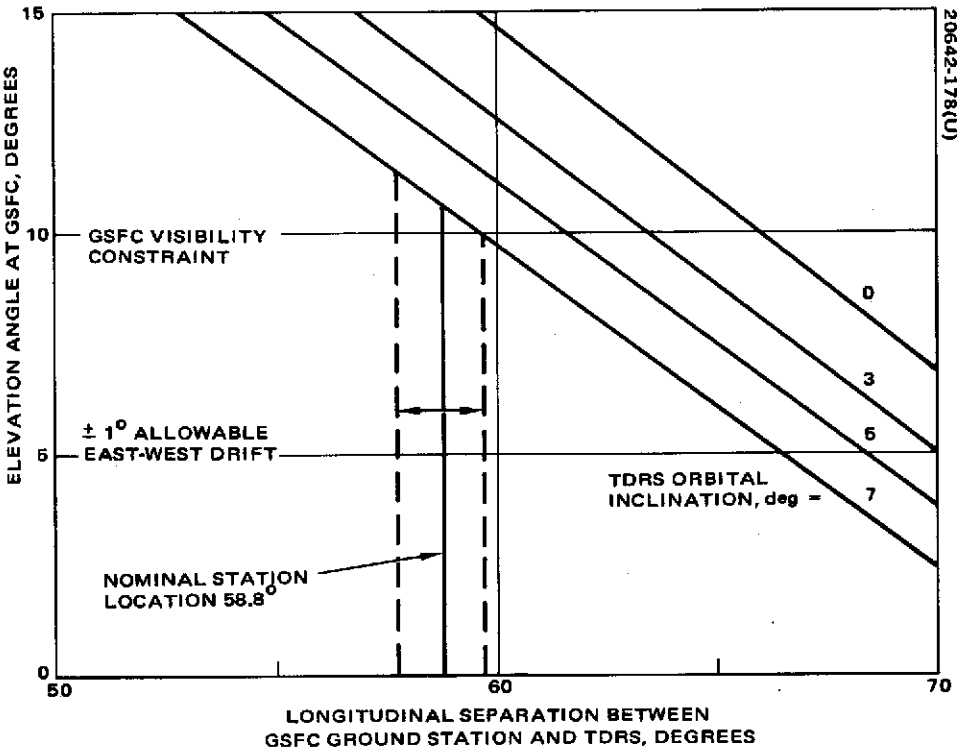

Figure 2-4. Separation Between Ground Station and Spacecraft

10 degrees at GSFC. Thus, it can be concluded that a total separation of 118 degrees between spacecraft is the most that can be allowed in order to maximize the user visibility time and still meet the elevation constraints at the ground station. For a 1 degree limit on east-west motion, any greater separation would result in a periodic communication loss between GSFC and the TDRS at the beginning and end of mission life. It should be noted that the selection of a dead band on satellite drift is somewhat arbitrary, and that a narrower band could be adopted at the cost of more frequent east-west stationkeeping maneuvers.

The solar incidence angles and eclipse durations are not significantly different for the near equatorial synchronous satellites, so power considerations do not enter into the choice of TDRS inclination. From the point of view of tracking accuracy, the effect of varying TDRS inclination can be felt in two ways. Certain TDRS inclinations are considerably more difficult to track from the ground, and so their a priori accuracy and thus, the user tracking accuracy should be poor (this condition occurs at 0 degree TDRS inclination). Also, the user tracking data taken from a TDRS at an inclination when user-TDRS orbit planes are coincident is poor for determining the user orbit.

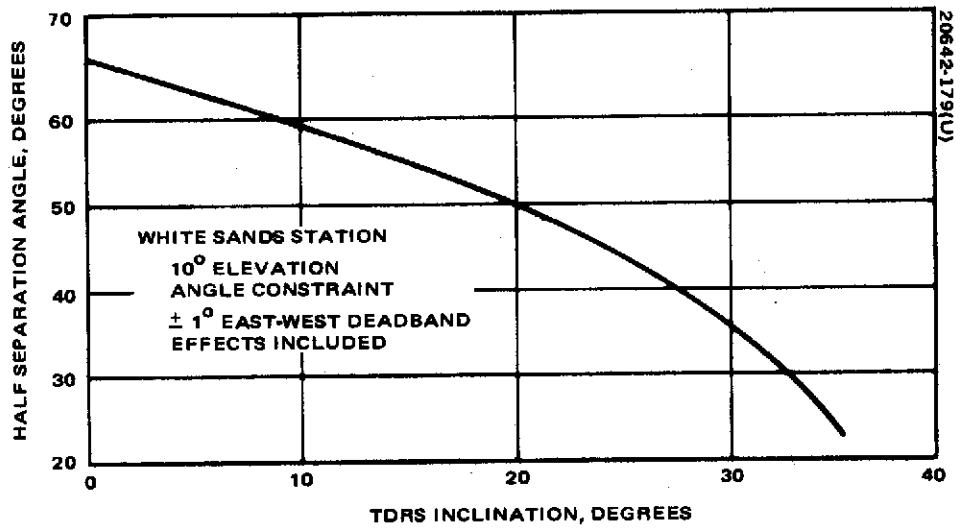

Figure 2-5. Maximum Separation Angle as Function of Increasing TDRS Orbital Inclination

However, neither of these considerations significantly affects the choice of TDRS inclination.

From the above consideration, the choice of a 7 degree TDRS inclination and nominal locations at 18°W and 136°W appears to be the best solution in terms of coverage, visibility, and payload.

2.1.2 Satellite Deployment for Alternate Ground Station Location

To evaluate the possibility of locating the ground station closer to the equator, an alternate location, White Sands, has been assumed. The lower latitude allows increased longitudinal separation between the two TDRSs. As seen in Figures 2-5 and 2-6, the White Sands station permits the allowable longitudinal separation for the 7 degree orbit to be increased to ±61.6 degrees from the station longitude. This increase corresponds to placing the satellites at 45°W and 168°W.

2.1.3 TDRS Orbital Inclination Effects on User Coverage

It is of interest to determine the altitude above which continuous user coverage can be guaranteed for the entire user orbit. Naturally, this critical altitude varies with TDRS longitudinal separation. For example, if the TDRS could be separated by 180 degrees, each would cover half the global area, and continuous coverage would be possible for any user above the 170 km (50 n.mi.) atmosphere. But the TDRS inclination and the ground station elevation constraint limit the allowable separation between TDRS E and TDRS W (Figure 2-6). Critical user altitude is plotted in Figure 2-7 for the White Sands station as a function of TDRS inclination. The critical altitude for the nominal 7 degree inclined TDRS is thus found to be 1750 km.

Of even greater interest to the selection of appropriate orbital geometry is the penalty paid by higher inclinations in terms of percent global coverage as shown in Table 2-1. The table assumes that proper user scheduling is maintained to compensate for the shift in latitude of the coverage area as each TDRS traverses its inclined orbit. Also, a worst case view was adopted in that both TDRSs were assumed to be precisely in phase; i.e., they arrive at their maximum declination at the same time. This case causes their overlapping dual coverage areas to be a maximum and, hence, their percent of global coverage a minimum. As seen in Table 2-1, with proper scheduling the 7 degree orbit yields only a 2.8 percent penalty in user coverage for the 100 km user.

2.2 LAUNCH AND ORBIT INSERTION

2.2.1 Launch Phase and Launch Window

The TDRS will be launched by an advance Thor-Delta launch vehicle, Douglas designation Delta 2914. The Delta 2914 is a three stage launch vehicle with the first two stages being inertially guided; whereas the

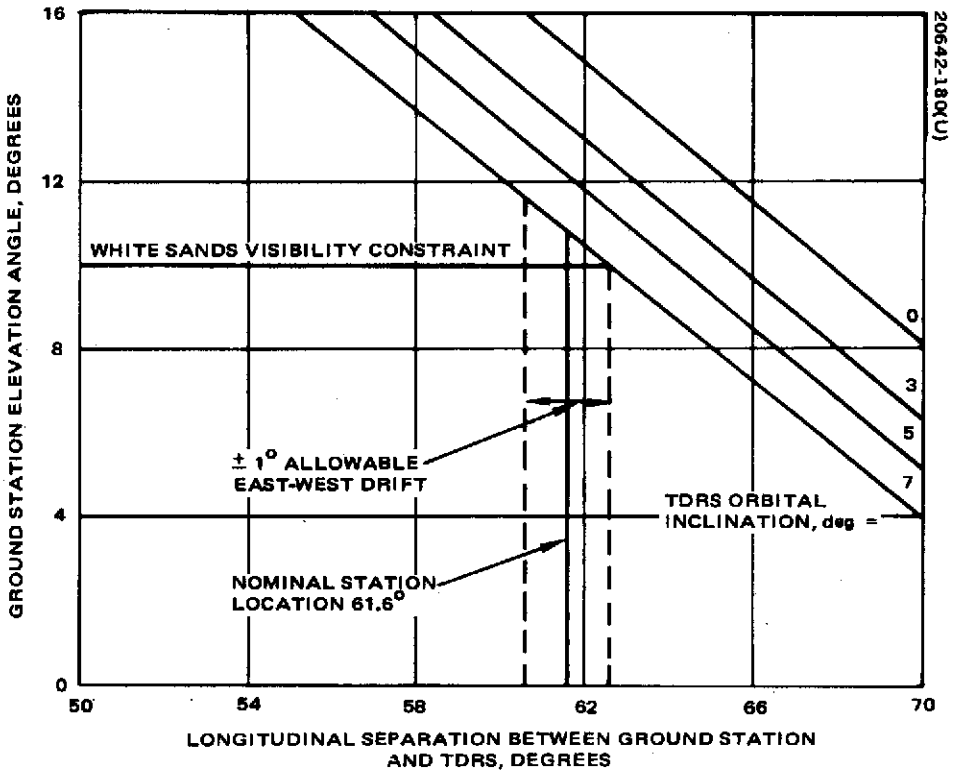

Figure 2-6. Separation Between Ground Station (White Sands) and TDRS

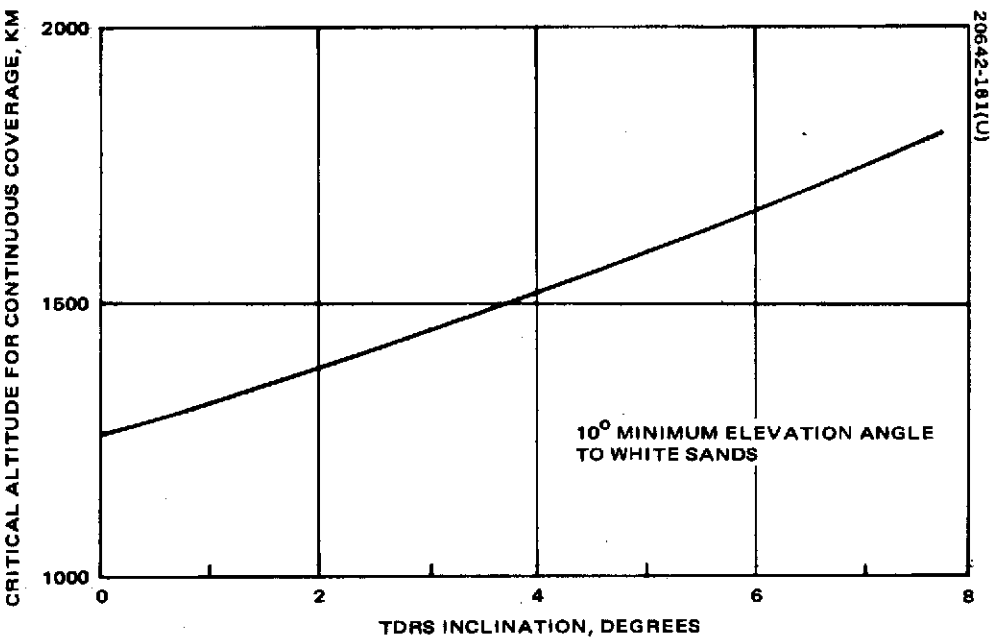

Figure 2-7. Critical User Altitude for Continuous Coverage

TABLE 2-1. PERCENT GLOBAL COVERAGE FOR 100 KM USER

Inclination, degrees	Global Coverage, percent
0	81.4
3	80.2
5	79.4
7	78.6

third stage is unguided and spun up prior to separation from the second stage. The first stage of the vehicle is an extended long tank Thor with a new H-1 main engine. Nine Castor II solids are strapped onto the first stage. The existing second stage is enclosed in a 2.44 meter diameter fairing with no changes in the engine or tankage. A new third stage, the TE364-4, has been added, and the payload fairing has been extended to a 2.44 meter diameter. The vehicle configuration is shown in Figure 2-8 and has a payload capability of 680.4 kg (excluding a payload attach fitting) into a 28.3 degree inclined transfer orbit with a 185.2 km perigee altitude and synchronous apogee altitude.

The TDRS mission starts with a liftoff at a time compatible with the launch window constraints. Following liftoff, the first stage burn and a partial burn of the second stage will place the spacecraft into a 28.3 degree inclined 185.2 km (100 n.mi.) circular parking orbit 555 seconds after liftoff. After a 983 second coast in the parking orbit, the second stage is restarted. The second and third stage burns perform a small plane change and inject the spacecraft into an inclined elliptical transfer orbit 1582 seconds after liftoff. A typical sequence of events is depicted in Figure 2-9 and summarized in Table 2-2.

The magnitude of the perigee plane change depends on the apogee motor characteristics and the desired inclination of the final synchronous orbit (see Figure 2-10). As the final inclination increases, the optimum perigee plane change (where the apogee motor propellant load is matched precisely to the launch vehicle performance capability to maximize spacecraft useful load) decreases. A small plane change of approximately 0.8 degree will maximize the spacecraft useful mass (361 kg) into a 7 degree inclined synchronous orbit.

Launch window constraints are placed on liftoff time due to the design limits of the thermal and power subsystems (Figure 2-11). In particular, the solar incidence angle on the spacecraft and eclipse duration during the

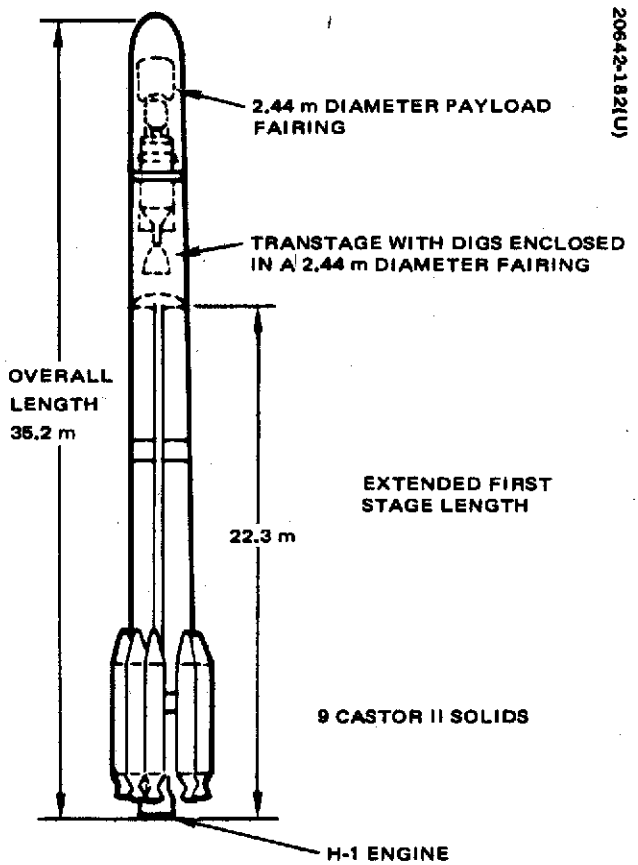

Figure 2-8. Delta 2914 Launch Vehicle

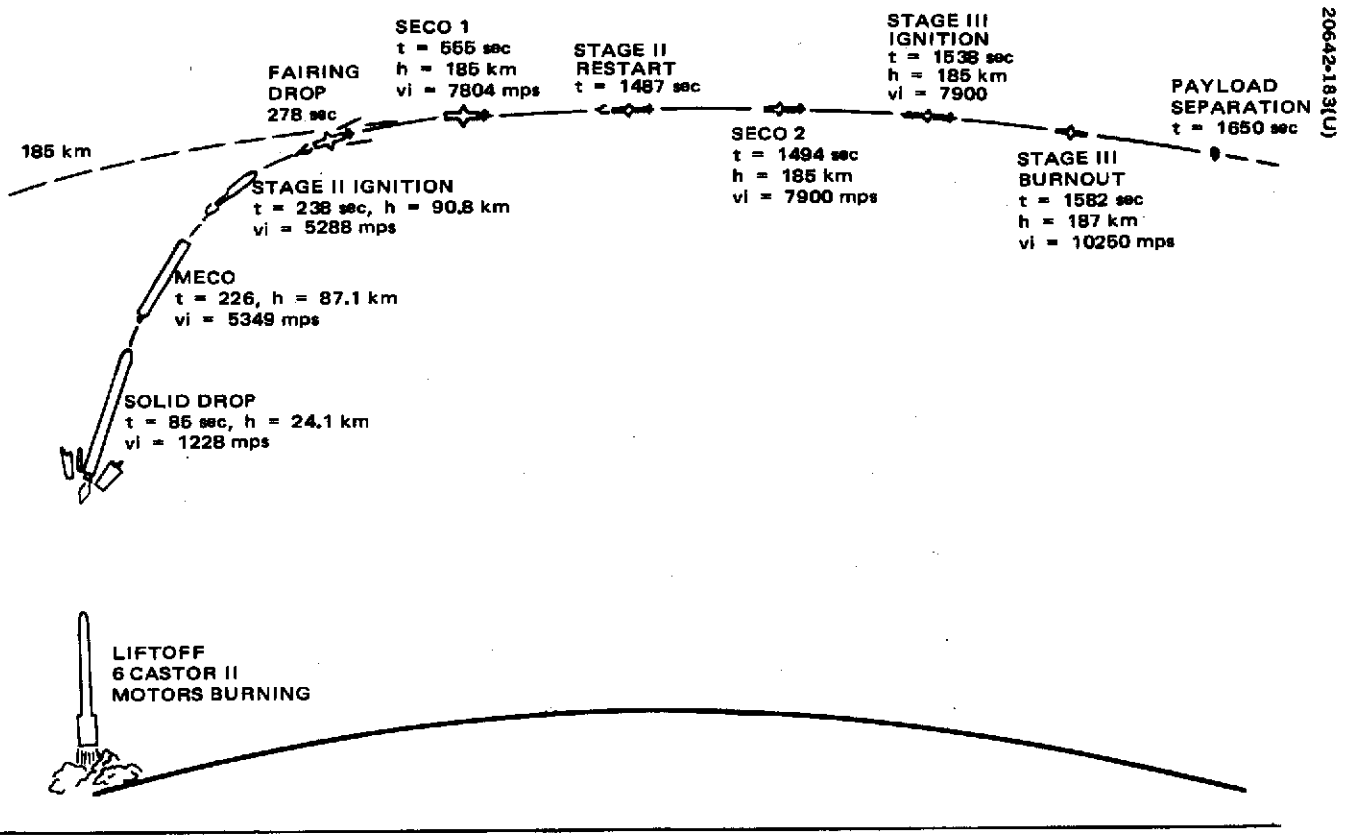

Figure 2-9. Typical Three-Stage Synchronous Mission Profile, Delta 2914-Eastern Test Range Launch (185 km Perigee)

transfer orbit phase impose bounds on the available launch time. The angle between the vehicle spin axis and the sun direction must be between 65 and 115 degrees for the perigee injection and the apogee firing attitudes. Furthermore, eclipse times should be kept under 30 minutes in the transfer orbit. The recommended final orbit inclination of biasing establishes further restrictions on launch time. These restrictions result from the fact that it is necessary to inject into a final synchronous orbit that has an inertial node that allows the solar/lunar perturbations to decrease the inclination during mission life. The allowable range of nodes maps directly into an allowable range of launch times. Figure 2-11 presents the results of a preliminary launch window analysis.

2.2.2 Transfer Orbit

The launch vehicle will inject the spacecraft into an inclined near-synchronous altitude transfer orbit with the following nominal parameters and their 99 percent dispersions:

Perigee latitude	0 ±0.26 degree
Perigee longitude	4°E ±0.48 degree

TABLE 2-2. TYPICAL SEQUENCE OF EVENTS

Time, sec	Event
0.000	Liftoff
7.875	Begin first stage I pitch rate (-2.000000 deg/sec)
13.328	End first stage I pitch rate
13.328	Begin second stage I pitch rate (+1.00000 deg/sec)
15.013	End second stage I pitch rate
15.013	Begin gravity turn
36.990	Maximum dynamic pressure (51,000 Newton/m^2)
38.614	Six Castor II solid motors burnout
39.000	Three Castor II solid motors ignite
77.814	Three Castor II solid motors burnout
85.000	Jettison nine solid motor casings
95.000	End gravity turn
95.000	Begin last stage I pitch rate (-0.10801 deg/sec)
226.337	End last stage I pitch rate
226.337	Booster cutoff (MECO)
226.337 to 227.337	Booster tailoff
227.337 to 232.337	Vernier solo
234.337	Jettison booster
238.337	Stage II ignition
238.637	Begin stage II pitch rate (-0.10763 deg/sec)
276.000	Jettison fairing
555.656	End stage II pitch rate
555.656	Stage II cutoff (SECO I)
555.656	Begin coast
650.656	Begin coast pitch rate (-0.44948 deg/sec)
800.000	End coast pitch rate
1486.275	Stage II restart
1494.230	Stage II final cutoff (SECO II)
1496.230	Third stage spinup
1525.230	Jettison stage II
1538.230	Stage III ignition
1581.630	Stage III cutoff (TECO)
1681.630	Jettison stage III

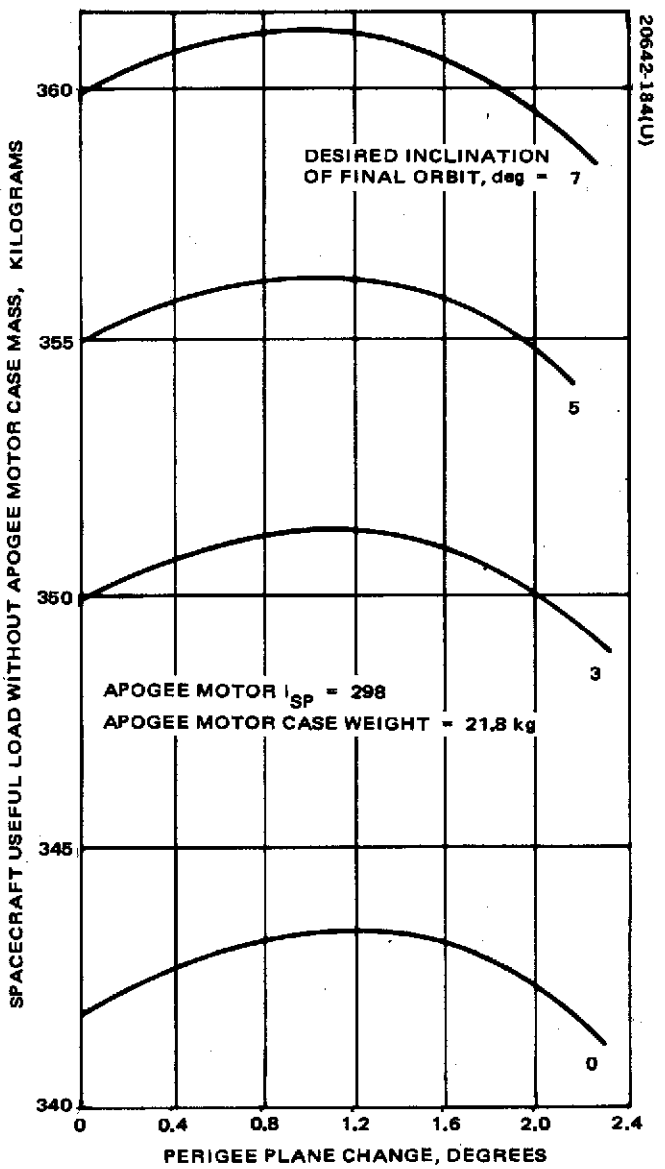

Figure 2-10. Plane Change Performed by Second and Third Stage Burns

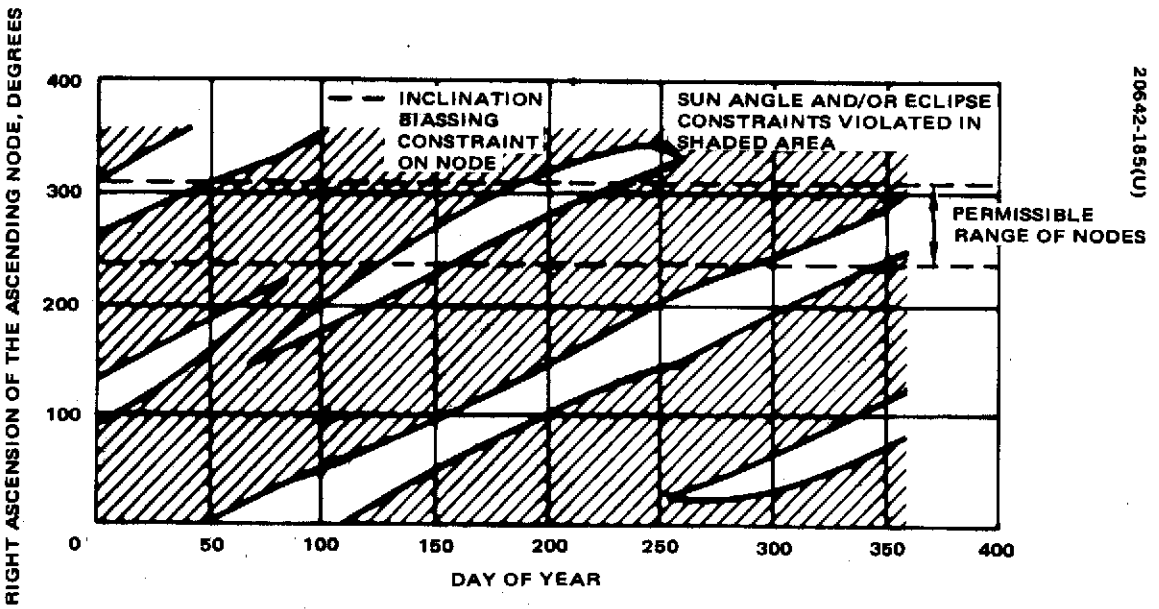

Figure 2-11. Preliminary Launch Window

Perigee altitude	185 ±9 km (100 ±5 n. mi.)
Apogee altitude	35, 800 ±1090 km
Orbital inclination	28. 3 ±0. 55 degrees*
Orbital period	10. 52 ±0. 35 hours

After injection into the transfer orbit, the spacecraft telemetry and command (TT&C) functions, along with ground station tracking will be initiated as soon as ground station visibility permits. Orbit and attitude determination will be initiated within 2 hours of spacecraft acquisition and the spacecraft will be reoriented normal to the orbit plane 5 hours after injection (attitude determination will be accomplished using the sun or earth sensor data as observables). To minimize the reaction control fuel required to compensate for injection errors and for final station acquisition, the spacecraft attitude for apogee motor firing will be adjusted on the basis of orbit determination results. This attitude is selected to produce the desired inclination and right ascension of the ascending node for the final orbit.

The reorientation maneuvers required to achieve the desired attitude will be completed at least 1 hour prior to the second apogee. To limit the time to reach the final station to approximately 3 weeks, an apogee injection

*With no plane change at perigee by the booster.

into the drift orbit sufficiently close to the final station (i.e., second apogee) and compatible with drift rates caused by apogee altitude dispersions will be selected. A schematic transfer orbit profile is shown in Figure 2-12.

During the transfer orbit phase, extensive use of the NASA STDN network will be required for spacecraft T&C and tracking data. To identify the ground station requirements for orbit determination, spacecraft TT&C, and apogee motor firing command, the rise and set times of the spacecraft during the transfer orbit phase have been established for the stations shown in Figure 2-13.

The ground trace of the transfer orbit is shown in Figure 2-14. Note that the ground trace corresponds to the nominal injection conditions. Variations will be introduced by the launch vehicle injection dispersions.

An illustration of the earth visibility as viewed from the spacecraft is shown in Figure 2-15. From the figure, it can be concluded that the limits of earth visibility are given by $A - \Psi/2$ and $A + \Psi/2$; i.e., an antenna or sensor will be able to see the earth when the deployment angle with respect to the spin axis is contained within the above limits. The earth visibility as a function of time is shown in Figure 2-16 for several spacecraft orientations.

2.2.3 Apogee Injection

A nominal apogee injection to achieve a near synchronous altitude, 7 degree inclined orbit has been selected. An apogee motor firing attitude (AMFA) to minimize the dispersions in the final orbit inclination due to launch vehicle injection errors has been planned. Future planning may result in an altitude bias to enhance station acquisition; this bias will be on the order of a few hundred kilometers.

The spacecraft will be oriented into the AMFA 1 hour prior to the selected apogee. Selection of the second apogee in Table 2-3 as the nominal injection apogee for the two TDRSs allows injection into the drift orbit compatible with the expected drift direction obtained from orbit determination. Injection at a later (or earlier) apogee is possible, however, and may be chosen as a nonstandard procedure if the real time mission activities so indicate. For example, for the TDRS at 168° W, if the drift due to dispersions is determined to be westerly, then the second apogee is used. But if the drift is to the east, then injection may then take place on the third apogee to conserve fuel. A review of the transfer orbit apogee locations given in Table 2-3 shows that, in order to establish the final station without an excessive reaction control system fuel expenditure, the choice of the apogees for the motor firings should be compatible with the direction of the desired drifts after the apogee injection.

Following the apogee injection, the attained drift rate will be evaluated from orbit determination results and, if the spacecraft is drifiting in the wrong direction, the reaction control system will be used one orbit later to initiate a drift rate toward the final station.

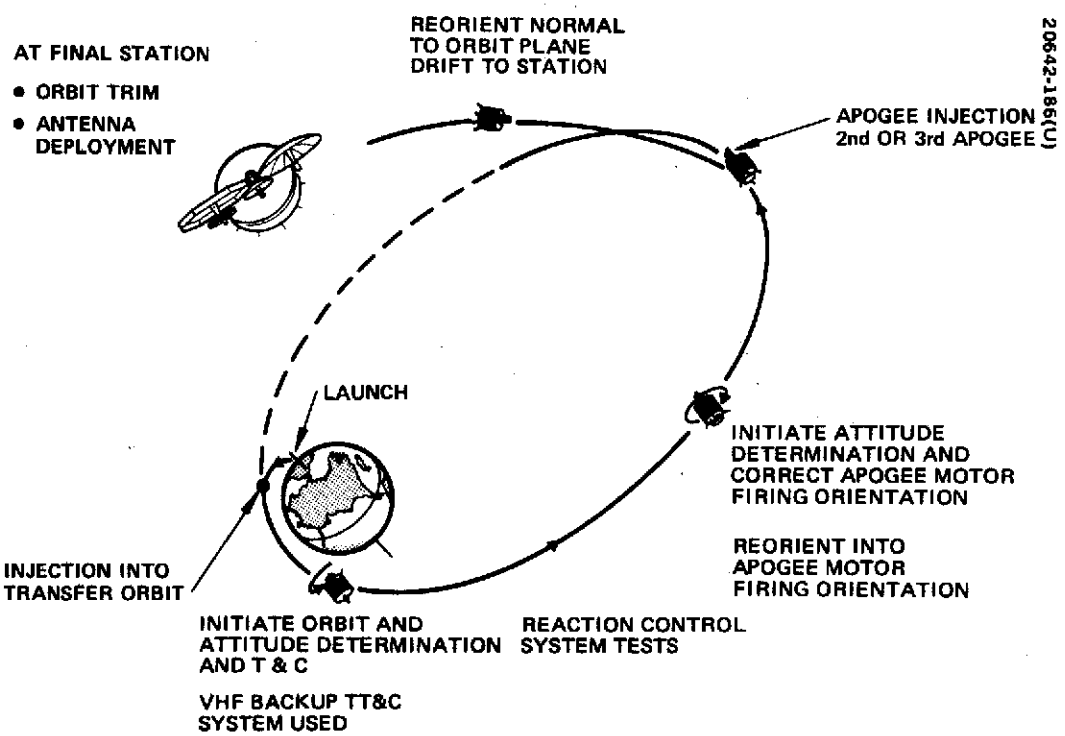

Figure 2-12. TDRS Orbit Insertion Profile

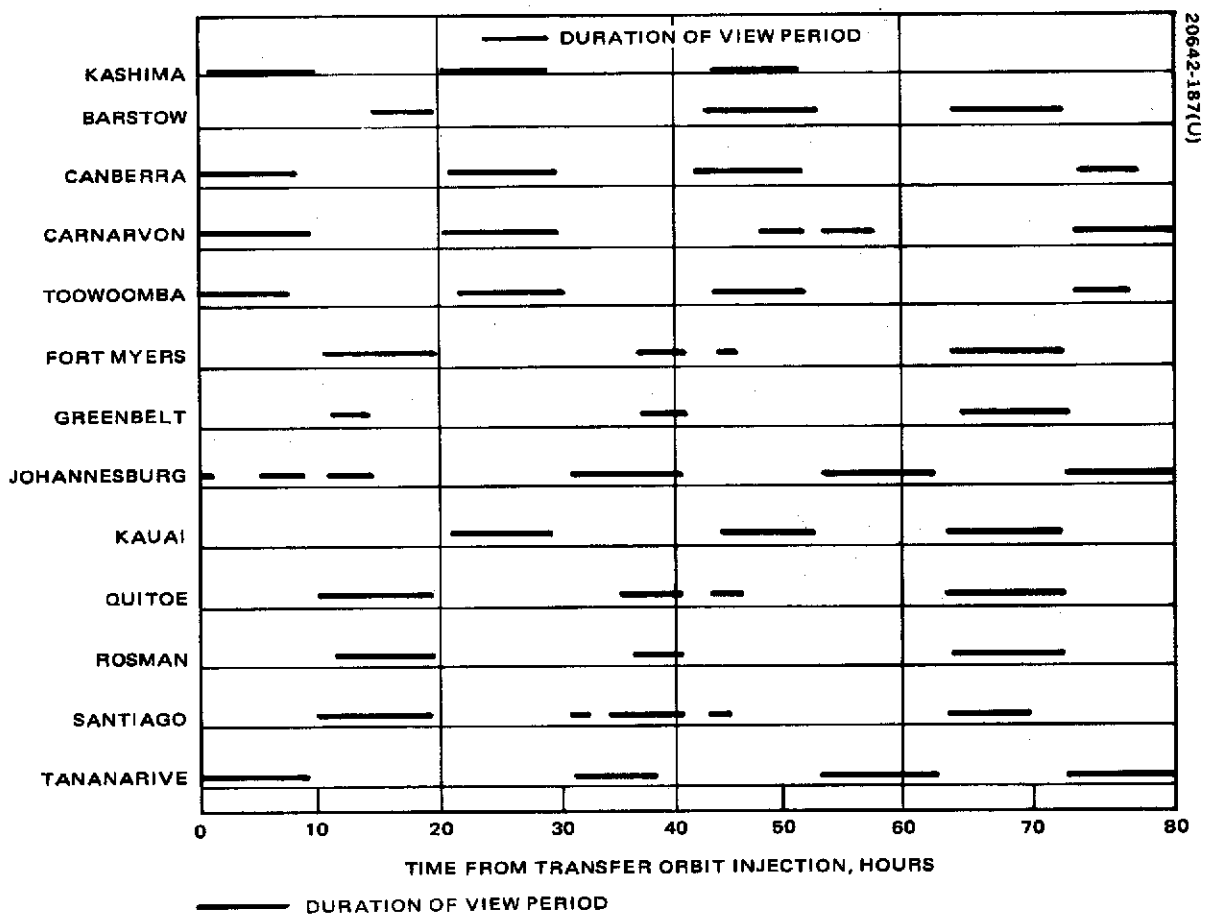

Figure 2-13. Ground Station View Periods

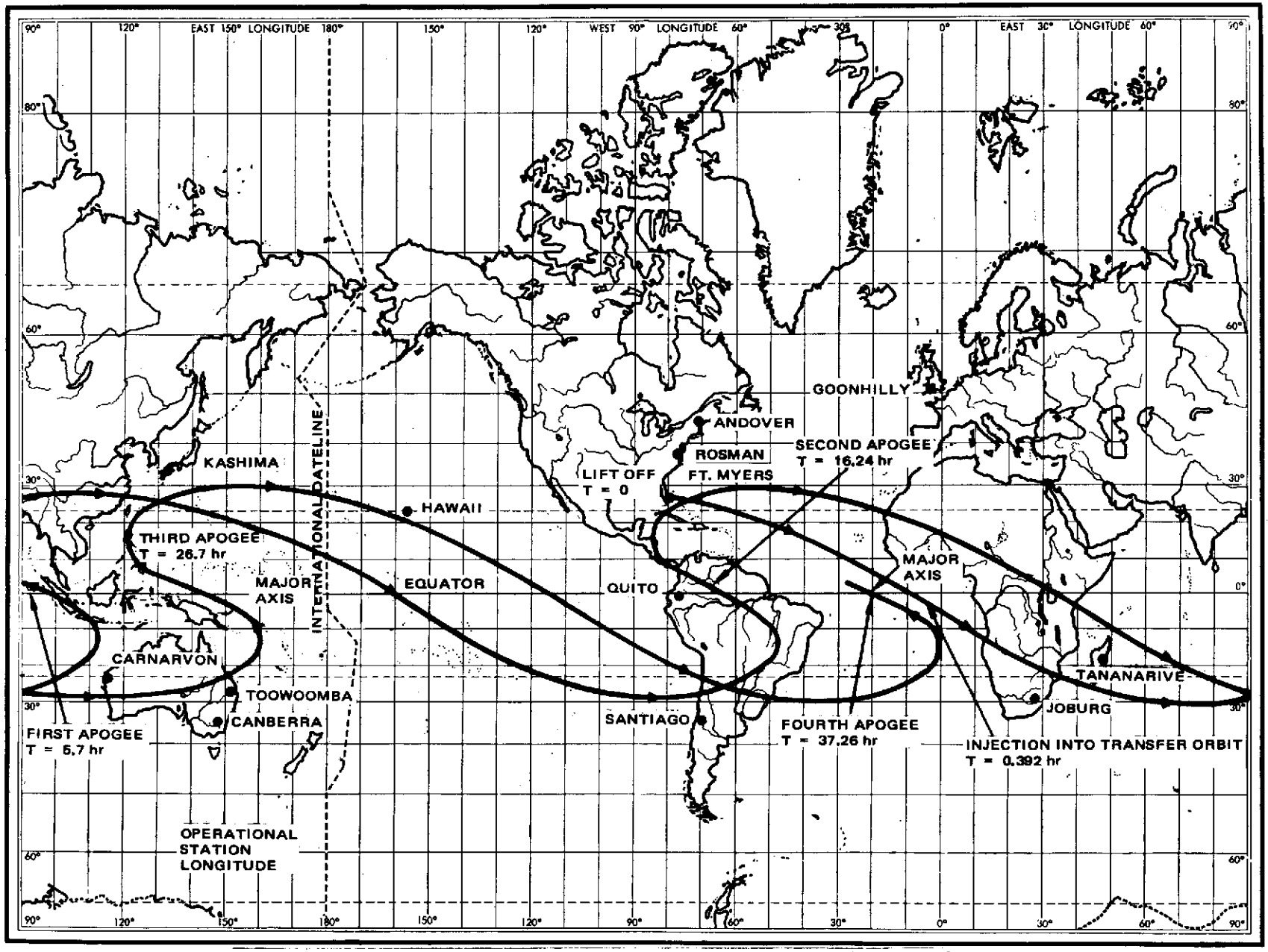

20642-188(U)

Figure 2-14. Approximate Transfer Orbit Ground Track

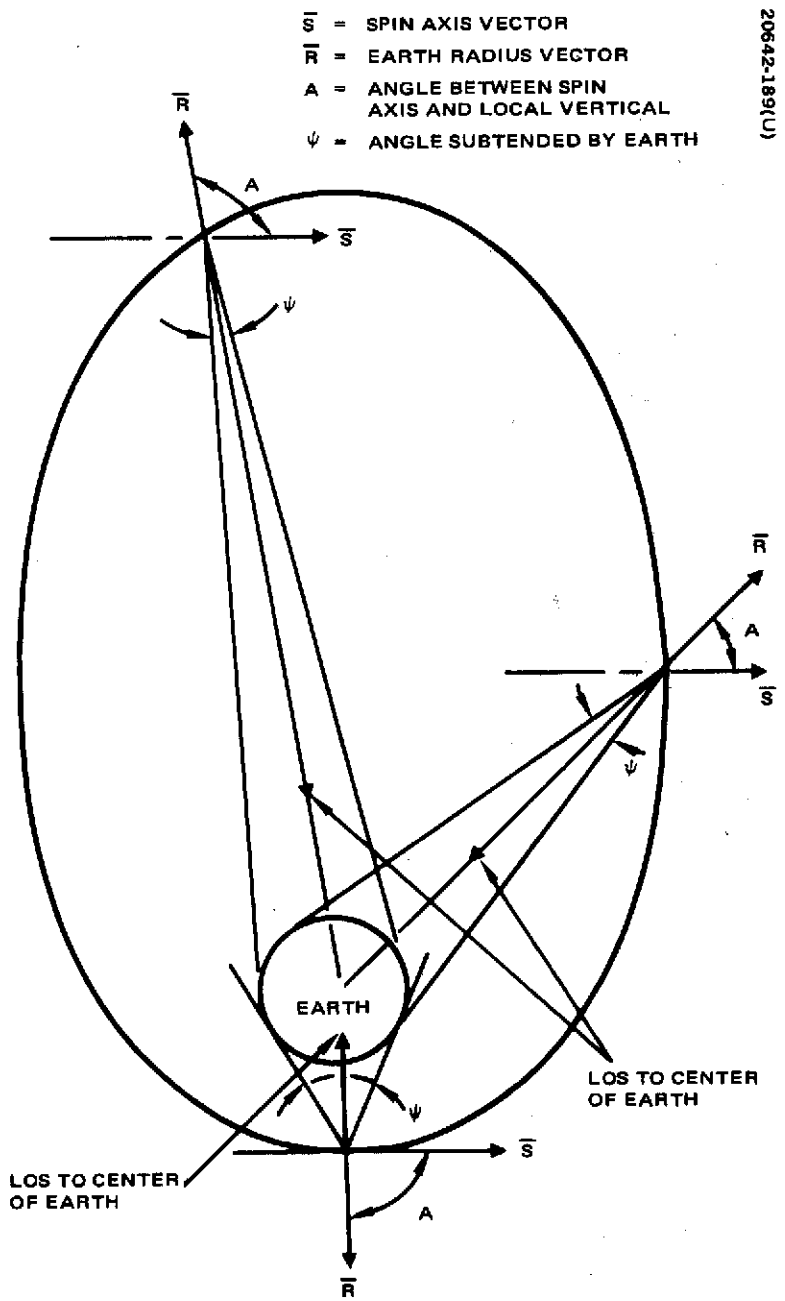

Figure 2-15. Earth Visibility Geometry in Perigee Firing Attitude

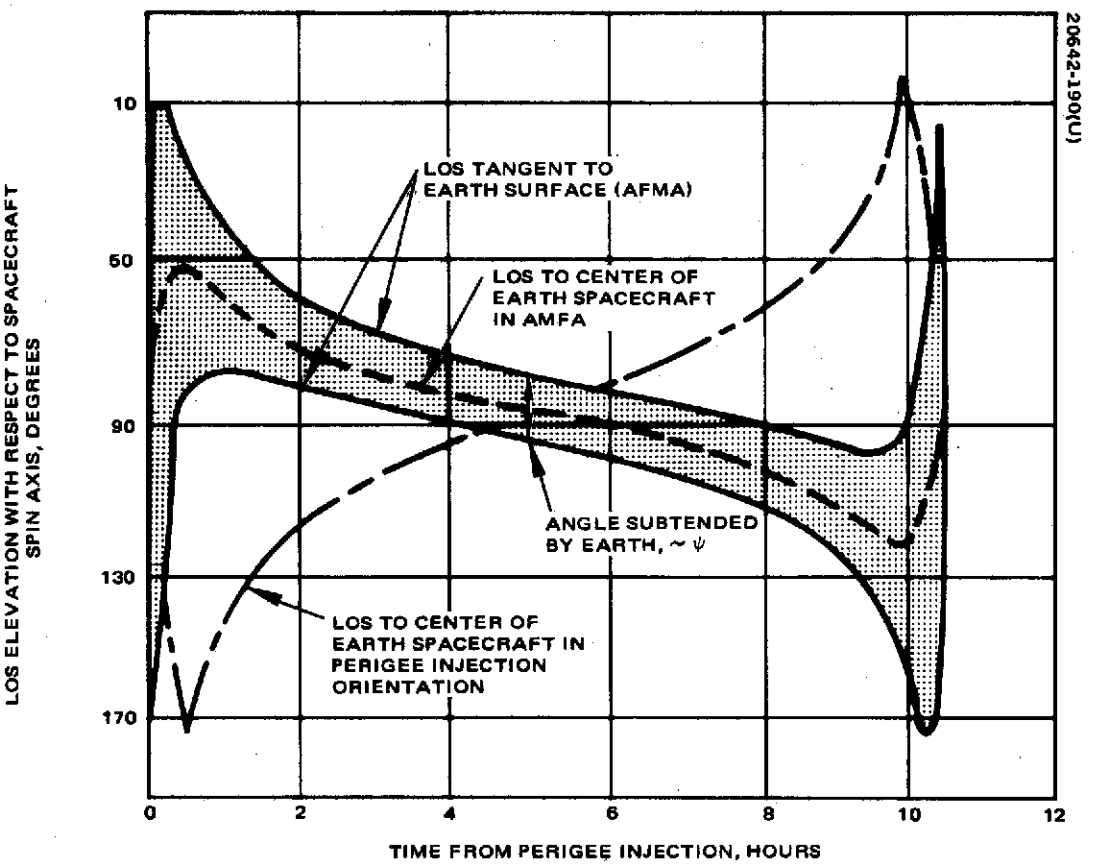

Figure 2-16. Line of Sight From Spacecraft to Earth During Transfer Orbit

TABLE 2-3. TRANSFER ORBIT APOGEE SELECTION

Apogee No.	Nominal Apogee Subpoint Longitude, degrees	±99 percent Dispersions, degrees	Time Required for Station Acquisition, days				
			From Nominal Apogee Location with Drift of 10 deg/day				±99 percent Dispersions
			West		East		
			TDRS W*	TDRS E*	TDRS W*	TDRS E*	
1	101E	2.7	26.9	14.6	9.1	21.4	±0.3
2	57W	8.0	11.1	34.8	24.9	1.2	±0.8
3	145E	13.3	31.3	19.0	4.7	17.0	±1.3
4	13W	18.6	15.5	3.2	20.5	32.8	±1.9
5	171W	23.9	35.7	23.4	0.3	12.6	±2.4**
6	31E	29.3	19.9	7.6	16.1	28.4	±2.9
7	127W	34.6	4.1	27.8	31.9	8.2	±3.5

*TDRS W at 168° W and TDRS E at 45° W.

**When time required from station acquisition for the nominal apogee location is less than the absolute value of the 99 percent dispersion, add 36 days to numbers less than 0 and subtract 36 days from number greater than 36 days. Thus for the fifth apogee, the 99 percent dispersions for west drifts for TDRS W become 33.3 and 1.1 days and the 99 percent dispersions for east drift become 2.7 and 33.9 days.

Under non-nominal conditions, alternate apogees, such as the first, may be chosen for apogee motor firing. It should be pointed out, however, that to prepare for apogee motor firing on first apogee requires many functions to be performed within the first 5 hours of the first transfer orbit. These functions include: evaluation of spacecraft health, evaluation of spacecraft stability, orbit determination, attitude determination, sensor bias determination, spacecraft reorientation to the orbit normal, determination of the AMFA, spacecraft reorientation to the AMFA, reaction control system calibration, and an attitude trim maneuver to the AMFA.

Experience at Hughes, with missions of the TDRS type, has shown that it is not desirable to schedule many activities within a short time span since many human decisions are required during this phase of the mission. Particularly, occasional abnormalities in system performance or data procession occur which may be readily resolved if sufficient data and time are available. Therefore, first apogee for apogee motor firing should be considered to be only a backup — with the second apogee being the nominal firing point.

The actual orbit attained after the apogee motor firing will not be exactly that orbit which was targeted for since it will be affected by the launch vehicle and apogee motor dispersions. The following error sources can be identified:

1) Launch vehicle dispersions at the perigee of the transfer orbit

2) AMFA uncertainties and a deficiency or excess in the velocity delivered by the apogee motor

3) The apogee motor coning during the burn

The magnitudes of the dispersions are summarized in Table 2-4.

The launch vehicle injection dispersions will be evaluated from orbit determination results during the transfer orbit phase. Previous Hughes apogee injection studies indicate that, by a judicious selection of the apogee motor firing attitude, in-plane velocity requirements for injection error removal and station acquisition can be substantially reduced. These analyses have shown that reaiming of the AMFA for apogee boost in the transfer orbit in such a way as to minimize out-of-plane injection errors results in a minimum hydrazine requirement for orbit circularization and inclination control. In particular, if the 3σ apogee dispersions shown in Table 2-4 are assumed, then the total ΔV required for station acquisition, removal of the residual in-plane launch vehicle injection errors, and removal of both in plane and out-of-plane apogee motor firing errors becomes approximately 55.6 m/sec. This reaiming scheme has been adopted as the baseline approach for the TDRS mission. The 3σ dispersions, along with on-orbit fuel requirements, are used for sizing the reaction control system requirements for the TDRS spacecraft.

TABLE 2-4. THREE SIGMA DISPERSIONS

Launch vehicle (99 percent)	
Apogee altitude	1092 km
Perigee altitude	9.26 km
Transfer orbit inclination	0.55 degree
Perigee flight path angle	0.55 degree
Apogee motor	
Orientation	0.1 degree
Total velocity	1.0 percent
Apogee motor burn phase	
Orientation	0.2 degree
Coning	2 degree

2.2.4 Station Acquisition

The apogee injection will result in a synchronous or nearly synchronous orbit. Four distinct types of orbits can be identified (see Figure 2-17):

1) Synchronous altitude circular orbit

2) Elliptical (or circular) orbit with apogee and perigee radii larger than synchronous radius

3) Elliptical orbit with apogee radius larger and perigee radius smaller than synchronous radius

4) Elliptical (or circular) orbit with apogee and perigee radii smaller than synchronous radius

In the presence of launch vehicle injection and apogee motor dispersions, detailed orbit determination results subsequent to the apogee injection are required to define the drift orbit; i.e., drift rate. Should the resulting drift rate be small, the reaction control system will be used to establish a drift rate toward the desired operating station. A typical sequence of events for the drift phase is described in the following sections; however, the detailed velocity correction scheme and the total velocity requirements

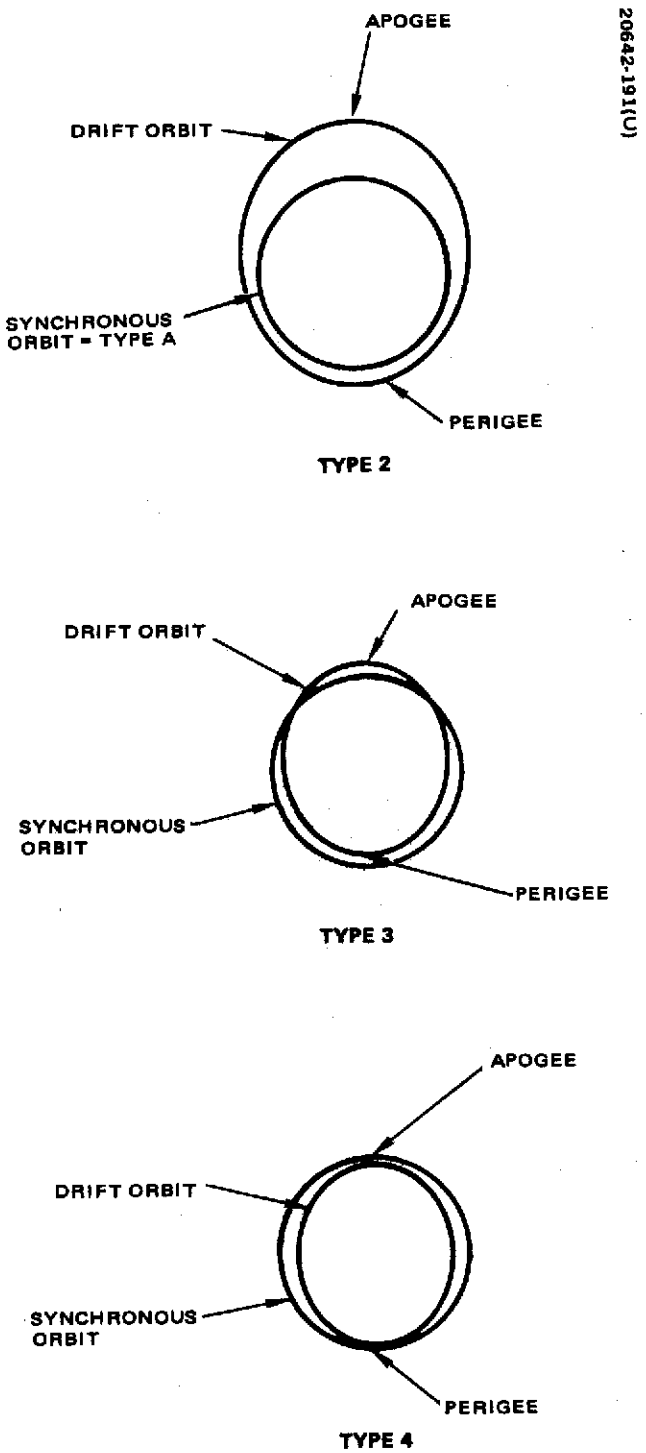

Figure 2-17. Types of Drift Orbits

will depend on the actual dispersions incurred. The following discussion simply forms a background for the analysis and decisions required to achieve the final operating longitude.

Subsequent to the apogee injection, orbit determination will be required to define the drift orbit. Approximately 12 hours of data should define the velocity within 0.915 m/sec (3σ); i.e., 0.3 deg/sec drift rate.

After the apogee injection, the spin axis will nominally be reoriented and kept normal to the orbit plane. The nominal spin axis precession in 65 degrees and is accomplished by the use of the axial thruster in a pulsed mode.

A sequence of circularization maneuvers is required to accomplish the following:

1) Establish an acceptable drift rate toward the operating longitude

2) Reduce the drift rate to about 0.5 deg/day at about 48 hours prior to arrival at the station

3) Synchronize the final orbit with the satellite at the operating longitude

All in-plane velocity maneuvers will nominally be executed with the radial thruster in a pulsed mode with a 60 degree duty cycle per spacecraft revolution.

The maneuvers will be performed either at the apogee or perigee of the drift orbit. A convenient graphic presentation of the maneuvers is depicted in Figure 2-18. In this figure, any orbit is represented as a single point. The maximum drift rates and reaction control requirements to circularize the drift orbits will be bounded by a diamond shape region as shown in the figure. The circularization maneuvers are represented by vertical and horizontal steps. The velocity required for each maneuver is directly proportional to the length of the line representing the maneuver, and any sequence of circularization maneuvers – so long as the steps are directed toward the origin – will require an identical amount of velocity change. The attainable intermediate drift rates will usually dictate the choice of the nominal maneuver sequence.

Nominally, the inclination dispersions will not be immediately corrected; however, such a capability is available by use of the axial thruster in a continuous rather than a pulsed mode. The spacecraft orientation (spin axis normal to the orbit plane) is compatible with the inclination corrections; but the proper node must be chosen due to axial thruster location, which is unidirectional.

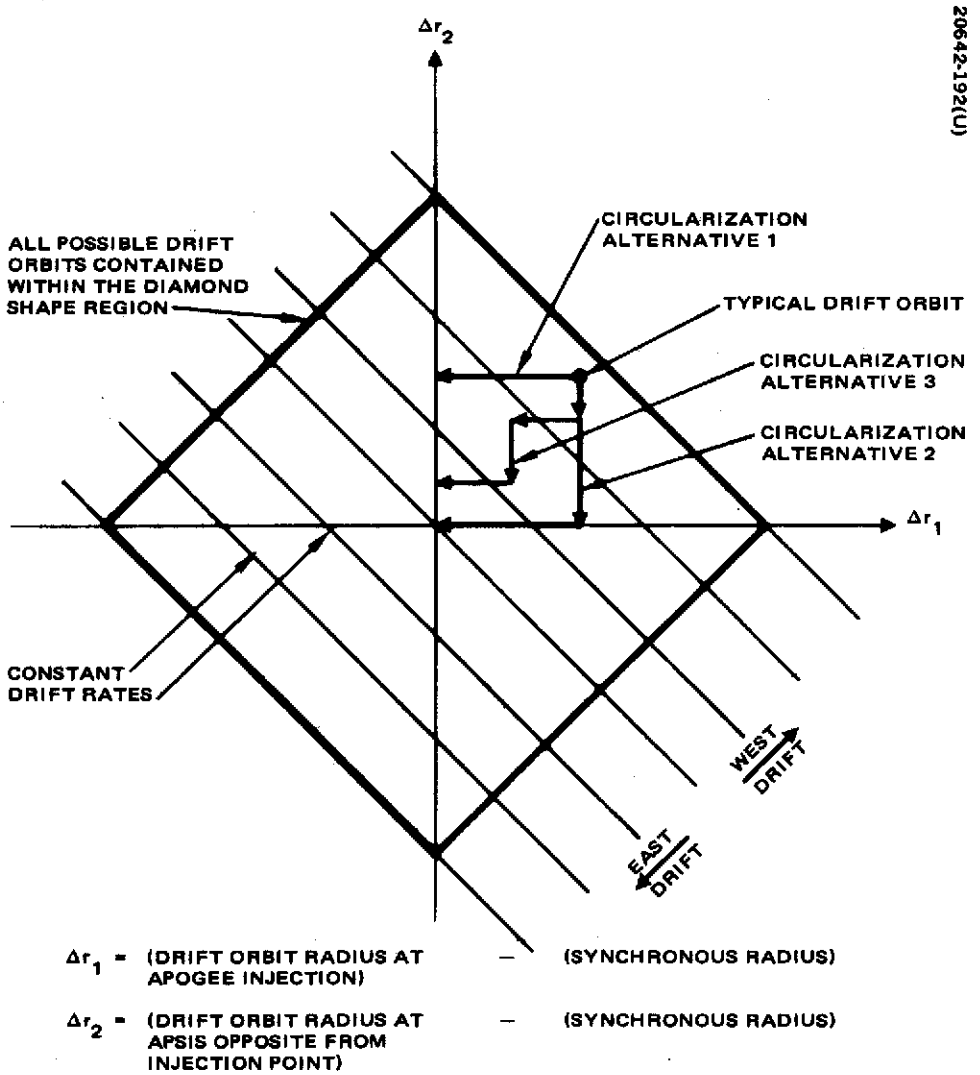

Figure 2-18. Graphic Representation of Nearly Synchronous Orbits

2.2.5 East-West Stationkeeping

A 5 year allowance of 10.7 m/sec has been made for east-west stationkeeping maneuvers at a worst case longitude. For an allowable longitudinal excursion of ±1 degree, the maneuvers will be executed approximately every 100 days. The longitude limit has been dictated by ground station elevation angle constraints of 10 degrees. North-south stationkeeping is eliminated by a combination of inclination biasing and proper nodal selection.

2.2.6 Station Change

A velocity allowance for two station change maneuvers at a drift rate of 4.33 deg/day has been included. This allowance is sufficient to initiate the desired drift rate and, after arrival at the new station location, to terminate the drift.

2.3 TDRS ON-ORBIT CONTROL

The three TDR satellites can be controlled and monitored in a manner very similar to current synchronous satellites; these functions are performed from the TDRS control center (TDRS CC). This control center's assigned functions are as follows:

1) Originate the spacecraft activity plan and coordinate schedules with STDN and other supporting facilities.

2) Direct or monitor all operational support.

3) Receive, process, display, and disseminate spacecraft data.

4) Control, operate, and manipulate the spacecraft.

5) Analyze and evaluate data to determine spacecraft configuration, status, and performance.

6) Compile and maintain operational records and spacecraft data.

7) Assist in special studies involving spacecraft and ground stations.

8) Evaluate overall systems performance include spacecraft and ground support.

The data flow to and from the control center is shown in Figure 2-19. The TDRS CC will make maximum use of the orbital analysis and other capabilities already available at GSFC. Its design assures maximum availability of the TDR satellites for telecommunication service by continuous monitoring of the spacecraft.

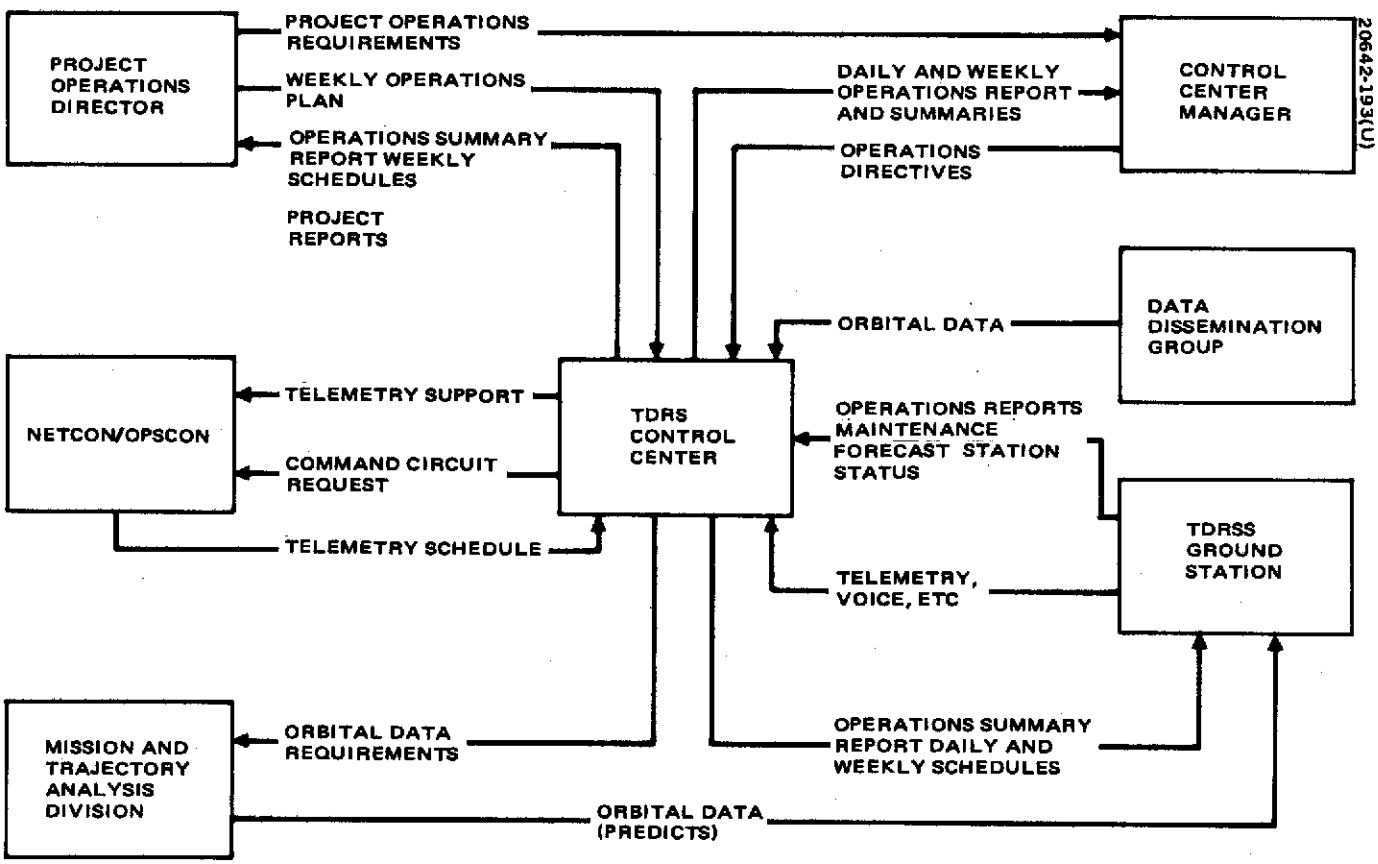

Figure 2-19. TDRSS Data Flow Diagram

A general layout of the TDRS CC is shown in Figure 2-20. The TDRS CC is linked to the ground station by data lines. These lines provide command and telemetry to and from the three on-orbit spacecraft. Voice circuits are also provided for coordination with ground station operations personnel. The received data stream is demultiplexed into three 1 kbps bit streams of the form transmitted by the spacecraft. The telemetry processors perform engineering unit conversion and check each value against established nominal values. Out-of-tolerance alerts are sent directly to the director's console. The data from each processor is displayed on a separate CRT display at the console. The console also contains a command generator including capability for initiating real time execute pulses. A small digital computer routinely generates pointing commands for the spacecraft high gain antennas.

2.3.1 Attitude Stability and Control

During life on-orbit, periodic corrections in the attitude of the satellite will be required to enhance the performance of the communication mission. The attitude errors induced by solar radiation torque require periodic correction (approximately every 2 days). One attitude precession maneuver is nominally required to make the entire correction. Orbit adjustment maneuvers will generally induce errors in spacecraft attitude. These attitude errors must be removed within approximately 1 hour following each orbit adjustment maneuver. One attitude correction will normally be required to correct this type of error.

During the life of the mission, the attitude of the satellite must be determined and predicted as a prerequisite to maneuver planning. The changing solar torque imparted to the satellite throughout the year must be determined to allow accurate planning of attitude correction maneuvers. A preliminary analysis of solar radiation pressure has been performed and the results indicate that a nominal solar torque precession rate of 2.4×10^{-7} deg/sec can be expected. A maximum allowable excursion of 0.25 degree will require attitude corrections approximately every 2 days.

Attitude maneuver planning consists of deciding on a target attitude and setting up a sequence of maneuvers to achieve it. The sequence considers constraints such as satellite position, attitude tolerance, fuel budgeting, fuel performance, attitude precession rate, initial attitude, etc. The sequence also considers the manner in which perturbations on the orbit and attitude affect their motion so as to use this motion to minimize the complexity of the sequence. Crosscoupling between maneuvers is of primary concern since procedures must be devised to cancel the usually unwanted results of coupling.

The general procedure to be followed in the design of attitude maneuvers is to utilize the solar torque precession predictions to select the target attitude for the maneuver. Once the edge of the attitude dead band is reached, the spacecraft spin axis will be repositioned to approximately the other side of the dead band such that the spin axis will subsequently precess

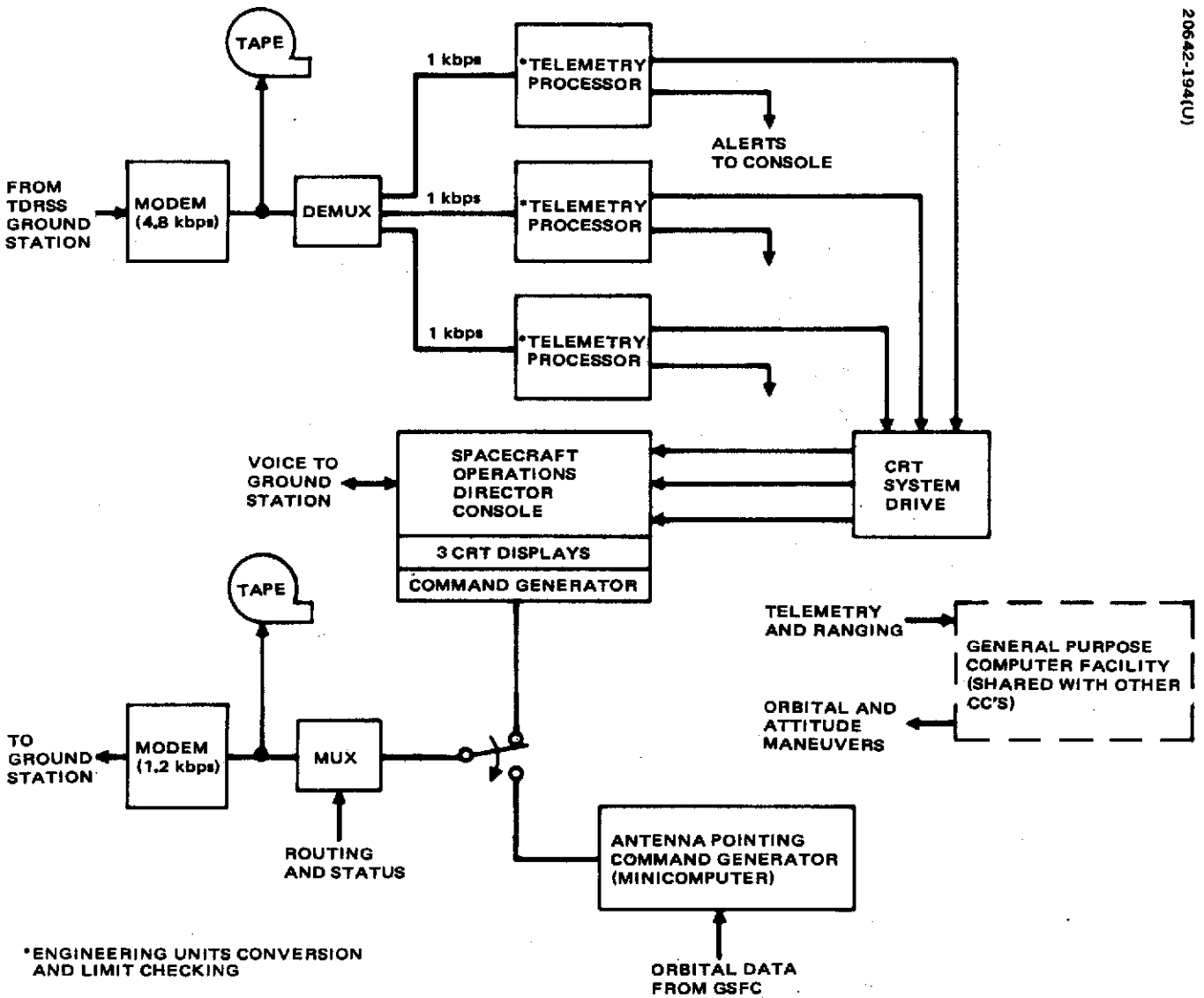

Figure 2-20. TDRS Control Center

through the orbit normal (zero attitude error) and pass on to the edge of the dead band, thus maximizing the time between maneuvers. This procedure will be repeated approximately every 2 days over the 5 year life of the mission. Figure 2-21 presents a typical attitude error history following the above scheme for a synchronous communication satellite with a 1 degree limit on attitude error. In this example, the spin axis passed to within 0.05 degree of the orbit normal.

2.3.2 Stationkeeping

Once on station, the satellite orbit will be affected by a variety of perturbations including solar and lunar gravitational attractions, solar radiation pressure, and higher order terms in the earth's gravitational potential. The longitude-dependent terms of the last type will cause drift acceleration. The primary effect of solar radiation pressure is to cause the eccentricity of the orbit to approach a value of the order of a few parts in 10^5, the value generally being less for satellites of larger size. This effect can be eliminated by a modest expenditure of control fuel and in any case is virtually negligible, although for precise stationkeeping it should be considered in determination of the mean orbital plane, causing inclination increase that results in a daily north-south motion of increasing amplitude.

Since the initial inclination will be biased at 7 degrees, no north-south stationkeeping will be required over the mission life. However, periodic east-west stationkeeping maneuvers will be required to maintain the spacecraft within 1 degree of its nominal operating longitude. The required east-west stationkeeping impulse is about 1.89 m/s/yr for a worst case station longitude.

Once the velocity required to stop and reverse the satellite drift at one end of the dead band is determined, the generation of a maneuver plan follows a fixed procedure. The optimum location in the orbit for the maneuver is established (usually apogee or perigee) and the corresponding time on the day selected for the maneuver is determined. For a given state of the on-board reaction control system; e.g., pressure, temperature, etc., and for a particular jet and pulsewidth, the jet start angle, total number of pulses, execution time, etc., are determined by use of a series of maneuver generating computer programs. Predictions are made as to the effect of the maneuver on spin axis attitude, spin speed, RCS pressure, propellant consumption, etc. The results of a typical east-west stationkeeping maneuver of a synchronous communication satellite are shown in Table 2-5.

2.3.3 Repositioning Maneuvers

Two in-plane velocity maneuvers are required for repositioning of the spacecraft to a new operating longitude. The requirement to drift 65 degrees in 15 days exists, and corresponds to a drift rate of 4.33 degrees per day. The on-board velocity needed to start and stop two such station change maneuvers amounts to approximately 49 m/sec.

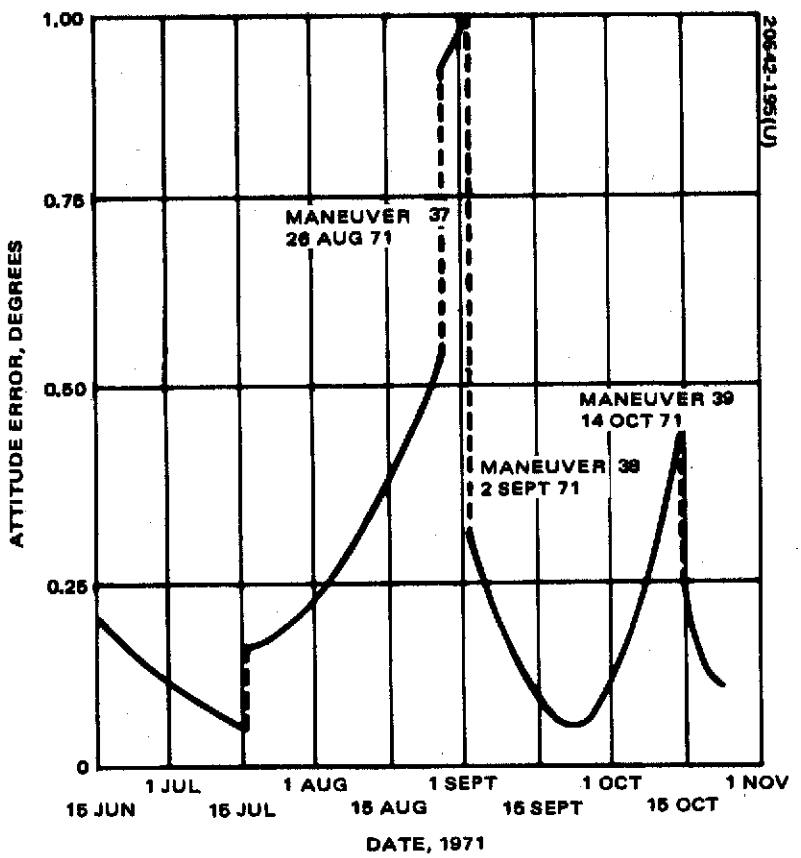

Figure 2-21. Typical Attitude Error History

The procedure to be followed in generating repositioning maneuvers and the execution of these maneuvers will be identical to that required for east-west stationkeeping maneuvers with the exception that the magnitude of the repositioning maneuvers will be considerably larger than that of the stationkeeping maneuvers. Thus, the execution time of the repositioning maneuvers will be also larger.

2.3.4 Antenna Pointing

A primary function of the TDRS CC is to provide commands to point the S band MDR and K band return ground link antennas. A small computer will be required for this function. Continually updated orbital data for the TDRS and MDR users will be sent to the memory of this computer from the GSFC data processing facility. The MDR schedule will then be used to compute the required antenna position which will be converted to the appropriate command. These commands are then sent to the ground station for transmission to the TDR satellites.

After initial system checkout, command transmission delays will be measured and time variations calibrated. This data will be used to command the two antennas in real time.

TABLE 2-5. STATIONKEEPING MANEUVER RESULTS

Characteristic	Before Maneuver	After Maneuver	
		Predicted	Actual
Drift rate, deg/day	0.053 E	0.058 W	0.052 W
Apogee altitude above synchronous, km	±15.0	*	+12.6
Perigee altitude above synchronous, km	-21.5	*	-5.9
Attitude error, degrees	0.02	0.027	0.027
Spin speed, rad/sec	5.68995	5.70147	5.70869

*Changes in these parameters are so slight for a maneuver of this small magnitude that they cannot be predicted accurately.

2.4 TELECOMMUNICATION SERVICE SYSTEM OPERATIONS

The TDRS system consists of five major elements: 1) GSFC communications control and processing facility, subsequently referred to as GSFC; 2) the satellite control centers for the users and the TDR spacecraft; 3) the ground station; 4) the tracking and data relay satellites; and 5) the user spacecraft. The overall functional relationship among these elements is shown in Figure 2-22. Note that GSFC has the responsibility for scheduling the TDRSS communication services and providing most data processing.

Figure 2-23 shows additional details of the functional relationships between the ground elements. Note that the TDRSS becomes an addition to current STDN capability and makes use of existing scheduling, switching, and data processing facilities at GSFC.

The TDRS control center computes commands for the TDR satellites and sends them to the ground station for transmission to the satellites. These commands configure the repeater and point the two steerable antennas as well as produce housekeeping and sybsystem control functions. Each user control center will issue commands to his spacecraft, limited only by the predetermined schedule. Return telemetry will be routed directly to users' offices, if desired, and/or may be processed at GSFC.

The ground station is the interface between the TDRS control center, GSFC, and the TDR satellites. All modulation/demodulation, multiplexing/demultiplexing, and RF transmitting/receiving is performed at this facility.

Before discussing these elements in further detail, a description of the functions required to provide the services will prove helpful.

2.4.1 Low Data Rate (LDR) Service Operations

The LDR service has the capability to provide near real time command of and telemetry from up to 40 user spacecraft. Ground operations should be implemented so as to take advantage of this capability. A two-way voice link is available in addition to, and simultaneous with, command and telemetry. A master schedule for this service will continuously be provided by GSFC.

The LDR service consists of two forward link channels per TDRS and the capability to return telemetry from up to 20 user spacecraft simultaneously per TDRS. The two forward links are identical in capability (30 dBw EIRP) but one can be used only 25 percent of the time due to TDRS power limitations. It is also expected that the time limited channel will be used primarily for voice communication to manned users.

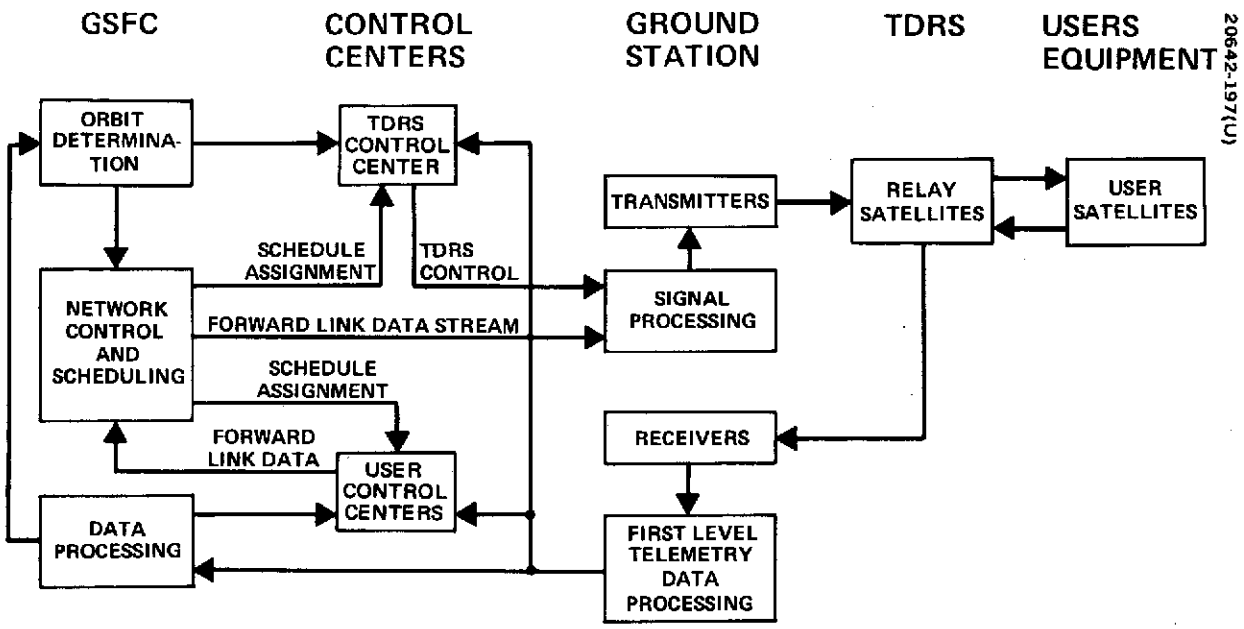

Figure 2-22. TDRSS Functional Operations

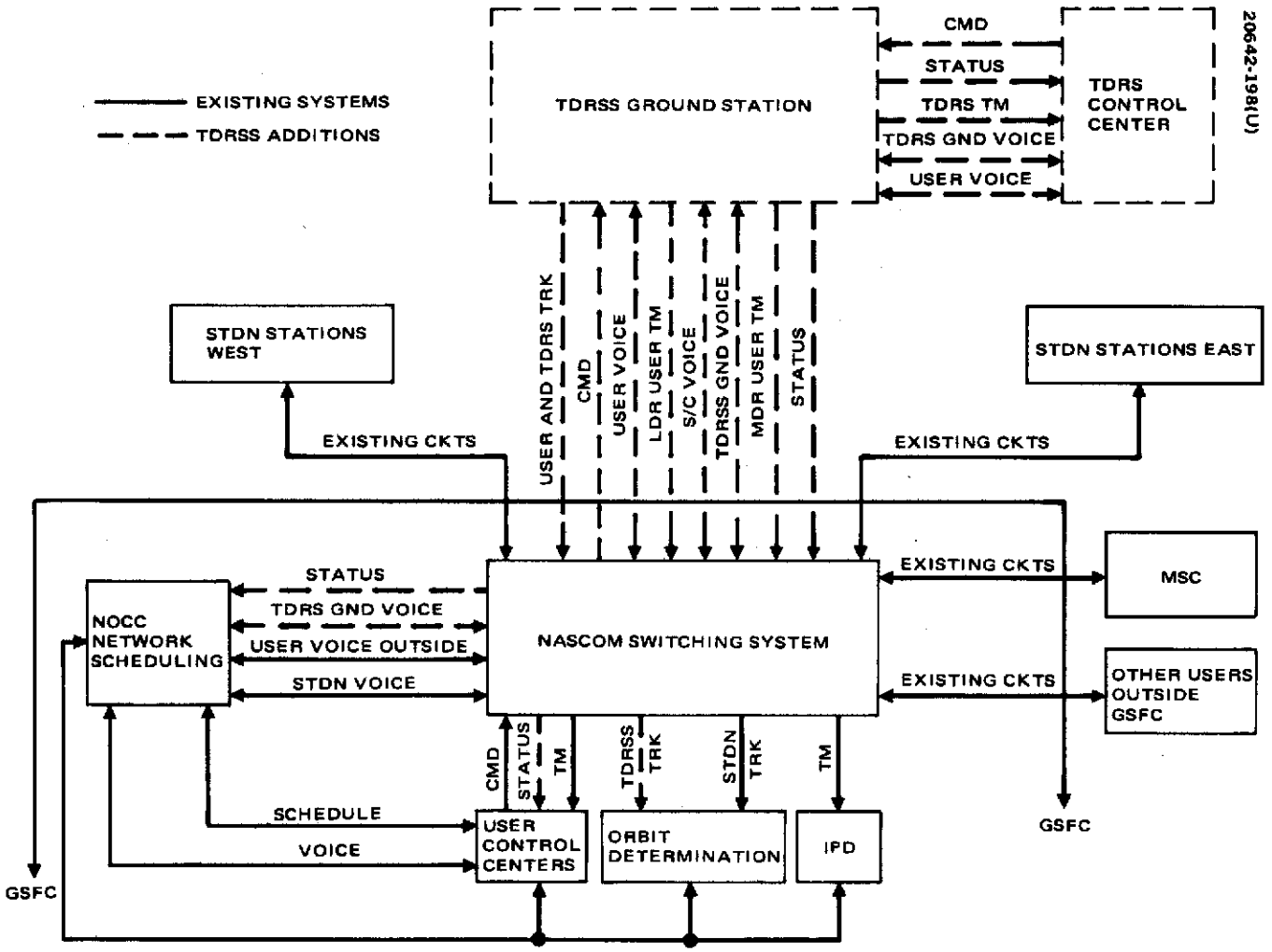

Figure 2-23. TDRSS Ground Elements

2.4.1.1 Telemetry and Command

For return telemetry and command, Figure 2-24 illustrates a typical sequence for LDR service to a user spacecraft. An explanation of this sequence will aid in understanding the LDR control functions.

Position 1 represents the end of an occultation period during which neither TDRS was visible to the user spacecraft. At this point, after a brief period not exceeding 1 minute, the user's receiver will automatically synchronize to the pseudo-noise code modulated signal transmitted at UHF from TDRS E. Following this signal acquisition, the user spacecraft is ready to receive commands. If the user is then commanded to turn his transmitter on, or if it is already on, a ground receiver corresponding to that user's coded telemetry signal must be connected to the output of the antenna/receiver receiving from TDRS E. This receiver will acquire the user's signal in a brief period, less than 1 minute, and then range and range rate measurements may be made simultaneously with telemetry data reception.

Due to the nature of the signal transmitted by TDRS E, each and every user spacecraft becoming visible to TDRS E will automatically synchronize to its signal with no operational procedure required at that time on the ground. Further, commands to a user beyond transmitter activation are not required for tracking; i.e., only the one coded forward link signal per TDRS is used for tracking all users.

In position 2, the user is visible to both spacecraft, and a command is sent to the user via TDRS E to change his receiver code to correspond to the signal from TDRS W, i.e., code 2. This change is followed by automatic acquisition of the signal from TDRS W. Only two receiver codes are required for all users. Finally, in position 4 before occultation, the user is commanded to change his receiver code back to code 1 from TDRS E in preparation for communication following occultation.

Handover times corresponding to positions 2 and 3 of Figure 2-24 will be determined by GSFC based on user ephemerides and relevant RFI data. At handover, commands to a user will be switched from the LDR forward link channel of one TDRS to that of the other. Since the forward link command stream is modulated by a different PN sequence for each TDRS, the user spacecraft must be commanded to change his code prior to handover. Each user control center may send the handover command to its satellite according to the master schedule which will include handover times. However, another option is possible if desired by a user control center. The master scheduling computer could be programmed to provide the handover command and inject it into the forward link channel at the appropriate time. This automatic handover service would be provided only at the request of a user control center.

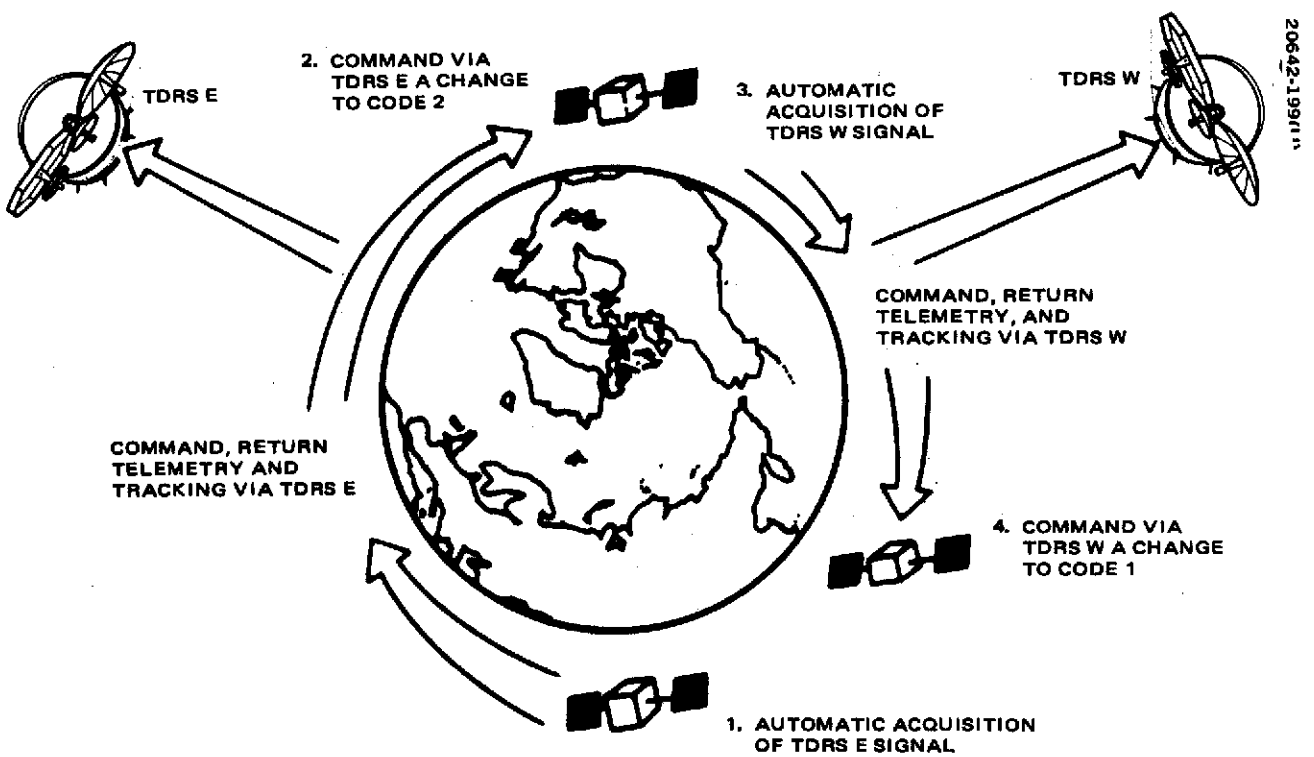

Figure 2-24. Low Data Rate Service Profile

User commands may be transmitted to GSFC in either a block, containing many commands, or one at a time for near real time command. In either case, the commands will be time-tagged to indicate the approximate time that they should be injected into one of the two forward link command channels. Master scheduling and priority control at GSFC will resolve conflicts that may arise. This forward link command stream assembly can be fully automated, employing techniques identical to those of time-sharing computation facilities.

2.4.1.2 Voice

Voice communication is provided by the second LDR link. This service has a usage limitation due to power constraints; each TDRS can provide LDR voice service 25 percent of the time. This is an end of life limitation and greater usage is possible at the beginning of the system life. The manned user spacecraft will be provided with visibility times and a handover schedule; thus, commands to change receiver codes do not need to be transmitted.

Forward link voice will be sent direct to GSFC where it will be converted to a binary waveform and multiplexed with three forward link signals for transmission to the ground station. Likewise, return link voice from the spacecraft will be sent from the ground station to GSFC for distribution.

Due to the nature of the signal design and user receiver operation, the acquisition of a TDRS signal by a user spacecraft is automatic and does not require that the user be sent any special command other than the required handover command discussed above. Signal acquisition means that both time and phase synchronization with the PN modulated signal transmitted by a visible TDRS has been achieved. Acquisition of the return link is not necessarily automatic because all of the users' signals occupy the same frequency in code division multiplex (CDM).

For each transmitting user, a demultiplexer/demodulator must be connected to one of the two ground station receivers. Generally, the receiver to be used for any particular user will correspond to the transmitter as determined by the system schedule based on user ephemerides. That is, both transmission and reception will be via the same TDRS at any given time, and the master schedule will determine when handover will occur for each user.

Return telemetry may be routed directly from the ground station to user control centers via GSFC or may be processed at GSFC prior to distribution.

2.4.2 Medium Data Rate (MDR) Operations

The MDR service differs operationally from the LDR in that only one user spacecraft is in the beam of a TDRS MDR antenna. Thus, during any given period, communication with only one user per TDRS is possible.

Control of the MDR is primarily a matter of scheduling. Mission priorities, together with user ephemerides, will be used by GSFC to determine the schedule. All MDR signals, both forward and return, will be routed through GSFC, and the routing matrix will be enabled according to the MDR schedule. This signal routing will result in only a small delay so that real time two-way communication is possible.

In addition to the high gain steerable S band antenna on each TDRS, a low gain, broad beam order wire receiving antenna is provided. This allows a manned spacecraft in orbit to request the MDR service. Such a request would have top priority and override the predetermined schedule. It is expected that unscheduled service requests via the order wire antenna will be made only under emergency conditions. An order wire request signal will be relayed simultaneously to GSFC, the TDRS control center, and the Manned Spacecraft Center. The TDRS control center will immediately send commands to the appropriate TDRS which will point the S band at the manned spacecraft. GSFC will immediately establish the two-way connection of the MDR channel.

2.4.3 GSFC Operations

All of the TDRSS telecommunication services will be scheduled and controlled by GSFC. Most of these basic functions have been discussed above but are summarized below.

2.4.3.1 LDR Operations

Service Scheduling. The nature of the LDR service is such that under most conditions the schedule would not limit user communications but would merely inform user control centers of visibility periods.

Handover Schedule. This schedule is supplied to user control centers so that they can command their spacecraft to "listen" to the TDRS through which their subsequent commands will be transmitted. This same schedule is used in the GSFC processor which assembles the two forward link command bit streams.

Forward Link Assembly. The flow of commands via each TDRS LDR link is determined at GSFC. Command inputs from user control centers are buffered as required and then inserted into one of the two forward command links based on time tags and predetermined priorities. This operation will be similar to that required for current time-shared computation with a central processor. It is foreseeable that transmission time conflicts will arise resulting in short delays for some commands similar to those delays

that occur during busy periods of time-shared computation. However, due to the rapid interleaving of commands, these delays should be short, presenting little difficulty to effective user spacecraft control.

Return Link Distribution. There will be up to 40 return telemetry signals received simultaneously and sent to GSFC for distribution. If processing by the GSFC TDRSS center is desired by a user, the distribution may be delayed. If a user control center is able to process the raw telemetry data from its spacecraft, then the telemetry can be routed immediately to the user center.

Voice Conversion. The LDR links have been designed for digital signals, thus the voice signal must be converted to binary form for forward link transmission and reconverted from binary to analog form in the return link. Delta modulation is recommended for the analog-to-digital (A/D) conversion.

2.4.3.2 Medium Data Rate Operations

Service Scheduling. Because only one user spacecraft per TDRS can be serviced with the MDR system, scheduling becomes the major function of GSFC operations. User mission priorities and ephemerides will both be used to produce the schedule. Voice service request by a manned spacecraft via the TDRS order wire channel will receive highest priority. The order wire implementation will allow an urgency rating to be transmitted by the manned spacecraft as part of its service request. This rating can be used to determine if the current MDR communication link should be immediately terminated or if service to the manned spacecraft can be delayed for a short period until a more convenient time.

Signal Routing. Based on the MDR schedule, two-way lines from user control centers to one of the two MDR channels will be connected. Thus, user centers will have real time two-way communication with their spacecraft for the duration of their scheduled period. If handover from one TDRS to another occurs during this period, it will be performed automatically by the routing matrix at GSFC in coordination with the TDRS control center and ground station.

Processing/Storage. Some user control centers may require storage and/or processing of both forward and return signals. These functions will be performed by GSFC. For instance, commands may be sent to GSFC in advance of the scheduled user service period. These will be stored and later read into one of the MDR channels.

2.4.3.3 General Operations

Orbit Determination. Range and range rate measurements made at the ground station for each user will be sent to GSFC. The measurements will be used to estimate user orbital parameters which, in turn, will be used to determine the schedules for LDR and MDR services. The orbital parameters will also be sent to user control centers.

Multiplexing/Demultiplexing. Communication between GSFC and the ground station will utilize a minimum number of individual links. At GSFC, the six forward link channels (two LDR and one MDR per TDRS) must be multiplexed for transmission to the ground station. The return link signals may include:

1) Up to 40 simultaneous LDR telemetry signals

2) One LDR voice signal of 20 kbps

3) Two MDR signals with maximum rates of 1 Mbps.

These signals must be demultiplexed and then routed as discussed above.

2.4.4 TDRS Control Center

The TDRS control center is responsible for monitoring the telemetry from the two satellites and for generating commands to be transmitted to them. For telecommunication control, commands are required for each TDRS to accomplish the following:

1) Point the S band antenna

2) Point the K band antenna

3) Select the forward and return MDR frequency bands within the total possible bandwidths

4) Set return link channel gains

Required inputs to the control center include:

1) Orbital parameters of each TDRS from GSFC

2) Schedules for both LDR and MDR services from GSFC

3) Telemetry from each TDRS direct from the ground station

2.4.5 Ground Station Operations

The ground station is the interface between the other ground elements and the TDRS satellites. The ground station must perform the following functions:

1) Ground station antenna pointing

2) Transmitting to and receiving from the TDRSs

3) Demultiplexing the signal from GSFC into the six forward link channels plus additional status, scheduling, and control signals

4) Spreading the spectra of the forward link signals

5) Carrier modulation

6) Filtering as required to separate the received signals and to reduce RFI in the LDR return channels

7) Configuration of demodulation equipment according to the schedule for all services

8) Multiplexing of all return link signals, range and range rate measurements, and status data for transmission to GSFC

9) Internal forward links verification: this verification amounts to comparing what was transmitted to the TDR satellites in each link to the outputs of the forward link demultiplexer. This comparison verifies the integrity of the spectrum spreading, baseband to RF conversion and final multiplexing. The functional processes are illustrated in Figure 2-25.

The LDR return link service is operationally the most difficult because there will be many telemetry signals simultaneously present in the two common channels from each TDRS. The choice of which TDRS channel to connect the demodulation equipment to is made preliminarily at GSFC and may be automated based on the GSFC handover schedule. These functions are illustrated in Figure 2-26. MDR functions are conceptually the same as for the LDR, but only one signal per TDRS at any time will be received. Further, acquisition and demodulation of the MDR signals will be simpler.

More detail on ground station implementaion is presented later in this volume in subsection 3.5.

2.4.6 Command Verification

Verification of the commands sent to user spacecraft via the TDRSS forward links is a necessary and conventional procedure. With the TDRS system several levels of command verification are possible:

1) Internal ground station signal verification: this has been discussed above.

2) GSFC verification of the link between GSFC and the ground station: this verification requires a comparison of the binary signals in each of the forward link channels with the return outputs of the ground station verification system.

3) User command verification: finally, the actual commands must be verified on a per user basis. This requires the return telemetry from the user spacecraft to be monitored and can be performed at either GSFC or the user control centers.

The functional relationship of the TDRSS elements in order to provide these three verifications is shown in Figure 2-27.

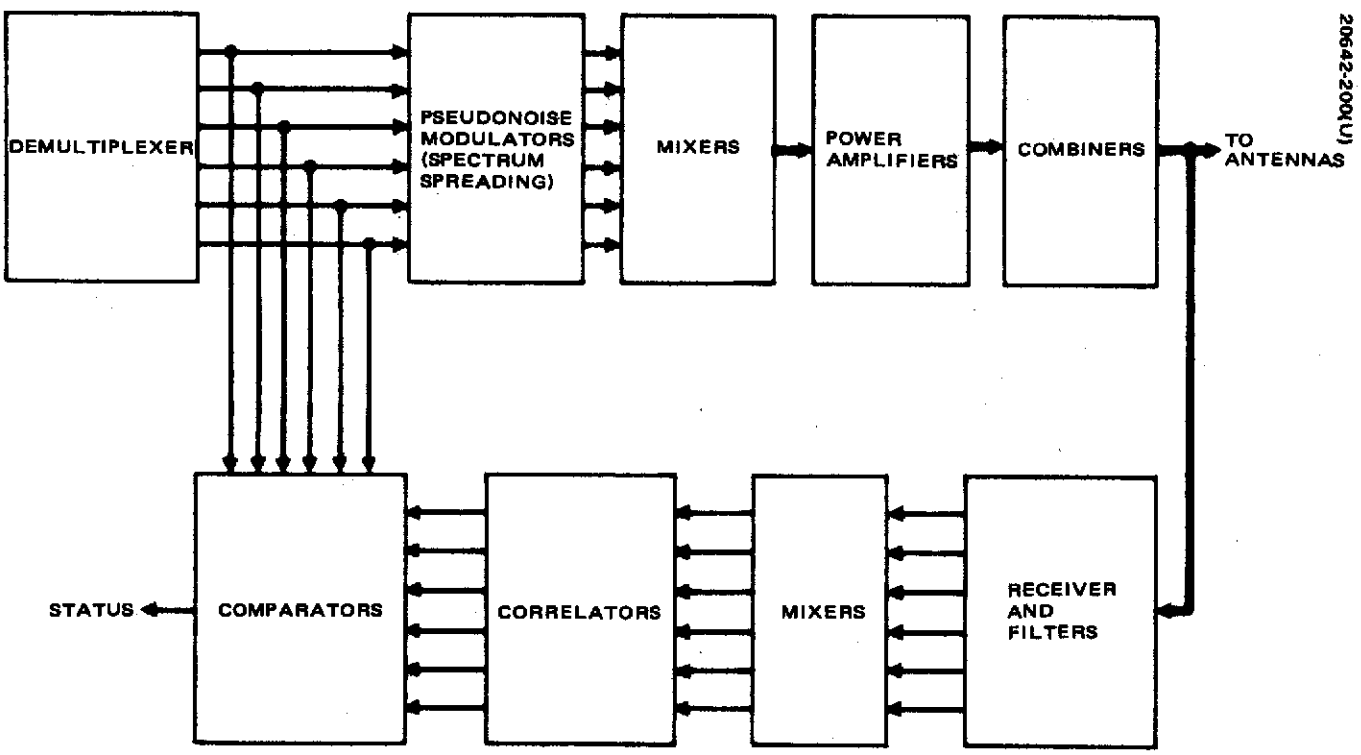

Figure 2-25. Ground Station Forward Link Verification

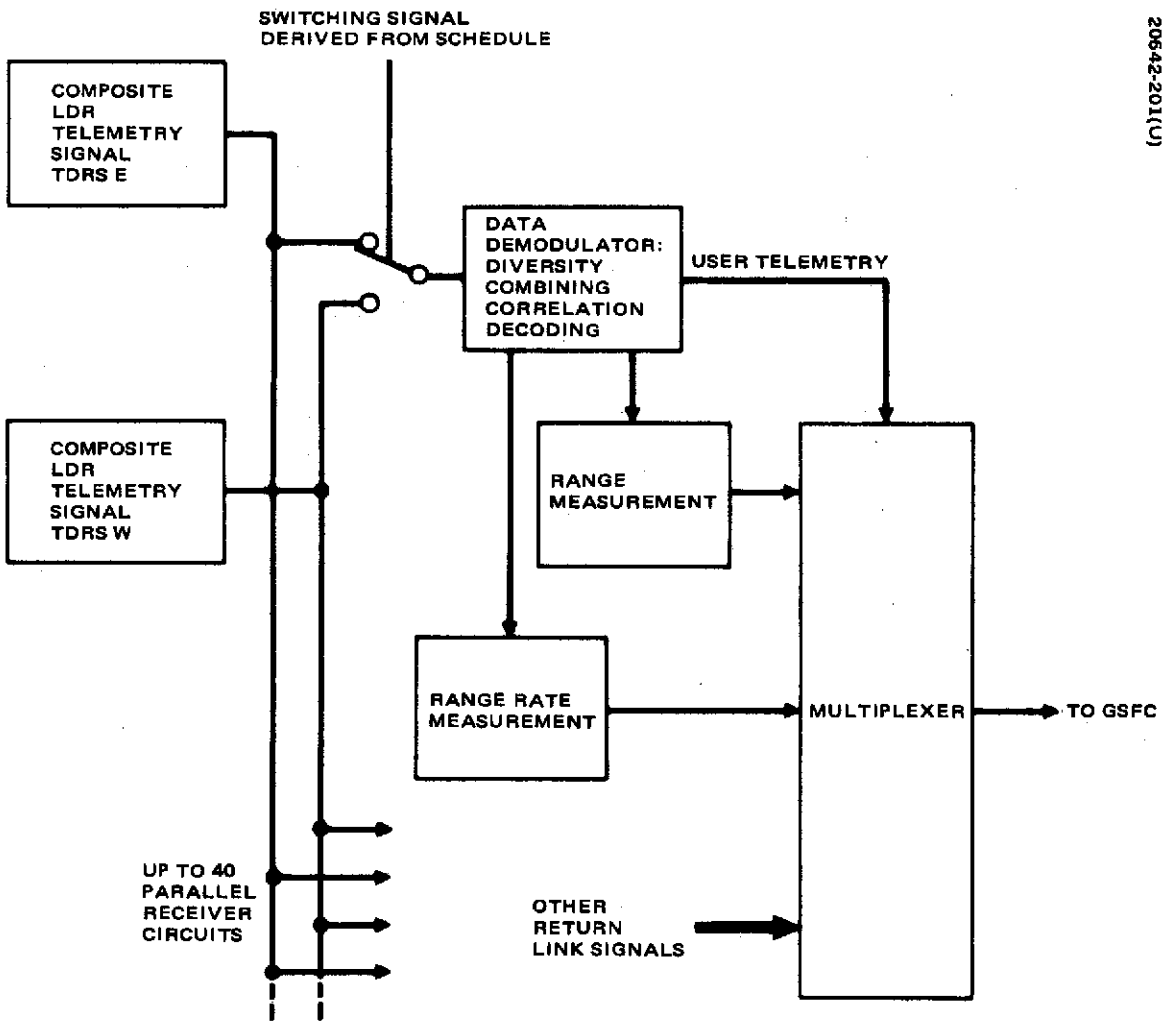

Figure 2-26. Ground Station Functions for Low Data Rate Return Link

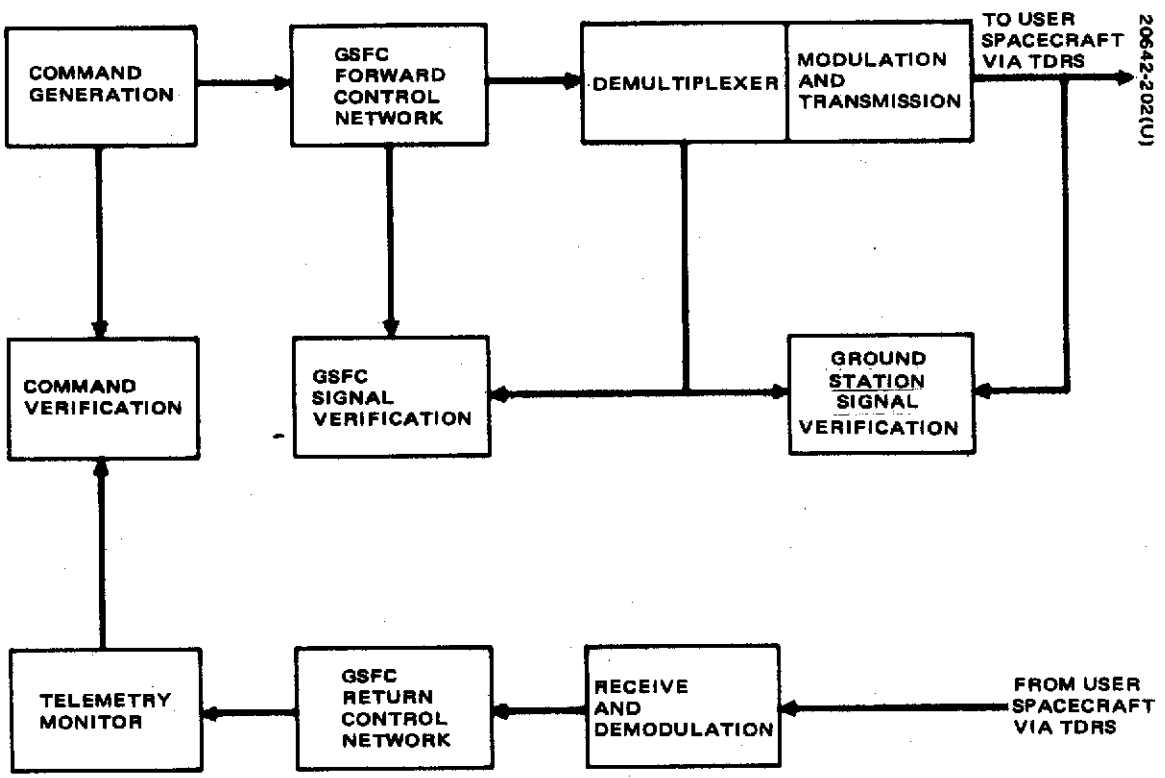

Figure 2-27. Three-Level Signal and Command Verification

3. TELECOMMUNICATION SERVICE SYSTEM

The Telecommunication Service System consists of the communication equipment in the Tracking and Data Relay Satellite (TDRS), user spacecraft, and ground station. The services and their operational aspects have been discussed above and are depicted in Figure 3-1. Forward links are those from the ground station to the user via a TDRS, and return links are those from the user to the ground station via a TDRS. The telecommunication services can be briefly summarized as:

1) Low data rate (LDR) service for command to, telemetry from, and tracking of at least 20 users per TDRS

2) Medium data rate (MDR) service for users requiring higher return data rates up to 1 Mbps

3) Two-way (full-duplex) voice for manned users via both the LDR and MDR services

This section contains both the analysis that led to major conceptual and implementation decisions and descriptions of baseline designs for equipments. First, the requirements and design objectives are discussed in subsection 3.1 followed in subsection 3.2 by a brief summary of the telecommunications service system performance, capability, and major features.

The detailed analysis and tradeoffs for the LDR and MDR space links and the ground link are presented in subsection 3.3. Subsection 3.4 describes the design of the TDRS communication subsystem. The ground station is discussed in subsection 3.5, and, finally, user spacecraft equipment is discussed in subsection 3.6.

3.1 REQUIREMENTS AND OBJECTIVES

The requirements for the TDRSS telecommunications service system fall into two categories: 1) performance requirements on the functions and capabilities of the LDR and MDR services and 2) design requirements that have a direct impact on the RF communication equipment of the TDR satellites, user satellites, and ground station. The objectives can also be separated into two classes: 1) performance objectives and 2) general system design objectives. The former concern user capability and additional system

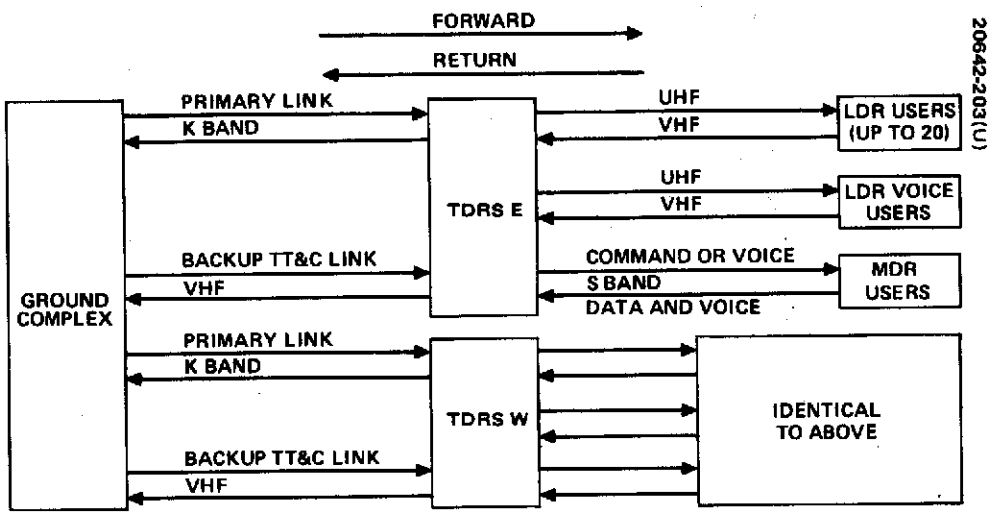

Figure 3-1. Telecommunication Service System

functional capability, while the latter include those objectives that are the general goals of every large system design such as reliability, minimum cost, operational flexibility, and maximizing failure mode capability. Little more can be said about these general objectives at this point, but in the analysis and design discussion to follow, selections between design alternatives, all of which provided the required performance, were made on the basis of these objectives.

3.1.1 Requirements

Performance requirements are summarized in Table 3-1. The required user services range of bit rates and tracking accuracy are taken from the contract statement of work. The required probability of bit error of 10^{-5} and voice duty cycle were a result of mutual agreement between Hughes and the NASA TDRS Program Office. For the forward links it has been assumed that any bit rate in the specified range is satisfactory. The medium data rate return link bit rate range is assumed as a firm requirement, i.e., that the system must have the capability to relay any return telemetry rate from 10 kbps to 1 Mbps. In light of the unknown interference environment of the low data rate return link, the required bit rate range is interpreted as a performance limit; that is, 100 bps per user is an absolute minimum, but system design should maximize the low data rate return rate potential, with no greater than 10 kbps required.

The design requirements are listed in Tables 3-2 and 3-3. The requirements of Table 3-2 primarily concern the TDRS/user spacecraft communication links. The requirements of Table 3-3 apply only to communications between the ground and TDRS, i.e., the ground links. The weather margin requirement of this table was selected by GSFC based on link availability analysis by Hughes during the study.

Referring to Table 3-2, the change in low data rate return link G/T from -14.0 to -16.0 dB/K is noted. This requirement was changed as a result of: 1) antenna size limitations as determined in the mechanical design and 2) analysis showing that in the RFI environment of the low data rate return link, the lower G/T value will result in a negligible reduction of communication capability.

Originally, three potential frequency bands for the medium data rate links were available including the S band frequencies shown in Table 3-2. A trade study was performed to compare the effect of these bands (S, X, and K bands) on TDRS and user weight, the results of which are in subsection 3.3.2.2. However, discussion with GSFC during the course of the study indicated that S band is necessary for support of manned users and hence must be used for medium data rate communication. The two available bands for low data rate forward links required a trade study resulting in the selection of the 400.5 to 401.5 MHz band as discussed in subsection 3.3.1.4.

TABLE 3-1. TELECOMMUNICATION SERVICE SYSTEM PERFORMANCE REQUIREMENTS PER TDRS

		Low Rate User Support		Medium Rate User Support	
		Forward	Return	Forward	Return
General	Service required per TDRS	Two parallel links for simultaneous voice, command, and tracking	Up to 20 parallel links for telemetry and tracking simultaneous with voice	Command (or voice) and tracking to at least one user	Telemetry (or voice) and tracking from at least one user
Communications	Data bit rate per user, bps	100 to 1000	100 to 10,000	100 to 1000	10 kbps to 1 Mbps
	Probability of bit error	10^{-5}	10^{-5}	10^{-5}	10^{-5}
	Voice duty cycle, percent	25	100	25	100
RMS Tracking Uncertainty	Random range, meters	≤15		≤2	
	Systematic range, meters	≤10		≤6	
	Random range rate, cm/sec	10.0 for 1 second integration time 1.0 for 10 seconds integration time		0.60 for 1 second integration time 0.05 for 10 seconds integration time	
	Systematic range rate, cm/sec	0.00		0.00	

TABLE 3-2. DESIGN REQUIREMENTS FOR THE TELECOMMUNICATIONS SERVICE SYSTEM

	Communications			
	Low Rate User Support		Medium Rate User Support	
	Forward	Return	Forward	Return
Number of users or links	Two parallel links for simultaneous voice, command, and tracking	Up to 20 users simultaneously	At least one user	At least one user
Minimum EIRP	For each VHF link: 30.0 dBw within 26 degree cone 28.0 dBw within 30 degree cone	-	41 dBw at S band or 52 dBw at K band within ≥ 1.0 degree beam pointable anywhere within a 30 degree cone	-
Repeater type	Frequency translation (hard limiting permissible)	Linear, separate frequency translation for each channel	Frequency translation (hard limiting permissible)	Frequency translation (hard limiting permissible
Minimum G/T	-	At either polarization: - 16.0 dB/K* within 26 degree cone	-	2.0 dB/K at S band or 12.0 dB/K at K band within ≥ 1.0 degree beam pointable anywhere within a 30 degree cone
Polarization	-	Separate orthogonal receive polarizations with ≥ 20.0 dB isolation between channels	-	Circular polarization
Space link frequency MHz	VHF: 118 to 132 or UHF: 400.5 to 401.5	VHF: 136 to 138	S band: 2035 to 2120	S band: 2200 to 2300
CCIR limit on earth incident flux density $dBw/m^2/4$ kHz	VHF: -144 UHF: -150	-144	-154	-154

*Original Statement of Work Requirement: -14.0 dB/K with 26 degree cone.

Note: Coverage requirement refers to an earth-centered cone.

TABLE 3-3. GROUND LINK REQUIREMENTS

Frequency Plan	
Ground to TDRS (forward)	
Primary Frequency	
Ku Band	13.4 to 14.0 GHz
Backup, user simulation and checkout	
S band	2200 to 2290
Launch phase and backup TDRS command and tracking	
VHF	149 to 150 MHz
TDRS to ground link (return)	
Primary frequency	
Ku band	14.6 to 15.2 GHz
Backup, user simulation and checkout	
S band	2025 to 2110 MHz
Launch phase and backup TDRS command and tracking	
VHF	136 to 138 MHz
Primary link (K band) requirements	
Weather margin:	17.5 dB
Earth incident flux density limit:	-154 dBw/m^2/4 kHz

3.1.2 Objectives

In addition to the requirements discussed above, there are a number of design and performance objectives. One objective is to provide the performance of Table 3-1, with the following user characteristics:

LDR users:

Antenna gain	-3 dB
Antenna polarization	linear
Transmitter RF output power	5 watts

MDR manned users

Antenna gain	0 dB
Antenna polarization	circular
Transmitter RF output power	100 watts
Return link	voice plus 78 kbps data

Other objectives included:

1) For both forward and return medium data rate links, provide a 10 MHz bandwidth channel whose position can be varied anywhere in the available bands (see Table 3-2).

2) Provide order wire capability to allow a service request to be made by the manned spacecraft.

3.2 TELECOMMUNICATIONS SUMMARY

All of the performance requirements and objectives of the previous subsection have been satisfied in the telecommunication service system design. This section summarizes the principal features and parameters associated with the services provided.

3.2.1 Low Data Rate Service

The signaling techniques selected allow 20 unmanned users per TDRS as a minimum for both the forward and return links. The forward link is timed-shared; thus only one user can be commanded at a time per TDRS. However, there is no system limit to the number of users to which commands be sent, since each command will have a user identifying prefix that activates the command decoder of the intended user.

The return user telemetry link capacity is limited primarily by RFI, as discussed later. The number of users transmitting in the common spectrum also has a significant effect on the capacity. However, the exact number of users that may use the return link cannot be identified. It is the nature of the selected wideband code division multiplex (CDM) approach that if a total of 40 users are successfully transmitting return telemetry via the two TDRSs, then 41 or maybe even 50 could also successfully return telemetry. This link is analyzed later in subsection 3.3.1.4.

3.2.1.1 Forward Link

The low data rate service provides two forward links, one of which will be used primarily for command of user spacecraft, and the other primarily for voice communication with a manned user. These two separate channels have been identically designed to provide greater system flexibility and spaceborne electronics reliability and provide a high capability failure mode. Due to TDRS power limitations, the channel used primarily for voice is restricted to 25 percent usage; however, this includes 25 percent of an eclipse period. Both the command and voice services discussed below are provided within a 30 degree conical coverage pattern of the UHF TDRS antenna.

Major selected signaling and multiplexing techniques are:

1) PN coding for both user commands and voice

2) Code division multiplexing of user commands and voice

The use of PN coding is the major signal design characteristic and allows four objectives to be accomplished:

1) Commands and voice can be code division multiplexed.

2) Multipath interference is reduced due to the spectrum spreading.

3) Earth-incident flux density is reduced to meet CCIR requirements.

4) Range measurement accuracy is improved.

Command Channel. The user command channel will be time-shared; that is, only one user can be commanded at a time. However, commands may be sent to many users within a period of 1 minute. All users will receive the TDRS transmitted RF signal; thus each command will have a prefix which will activate the command decoder of the intended user.

Other operational features include:

1)	Automatic user acquisition	User available for command shortly after becoming visible.
2)	Time shared link	Requires synchronized sequencing of user commands.
3)	Fixed timing	User receivers can be standardized; ground operations and equipment can be simplified.
4)	Variable format	Number of bits and their significance in a user command can be different for every user if desired, i.e., command format flexibility.

Analysis of the low data rate links and a study of ground emitters has revealed that RFI is most likely the limiting factor in these links. Figure 3-2 shows how the bit rate is limited by RFI. The parameter chosen to quantify RFI is the average spectral density of the RFI power at the receiver input. The selected baseline bit rate is 300 bps.

Voice Channel. The voice channel employs delta modulation to convert the analog voice signal to a binary wave form. The baseline bit rate is 9.6 Kbps, resulting in high quality transmission. The bit energy-to-noise density is shown in Figure 3-3 as a function of RFI density. It may be noted that the use of convolutional encoding will allow operation at higher levels of RFI and will probably be required.

Signal Parameters. The signal parameters selected for the baseline design are:

1)	Chip (PN code symbol) rate	614 kchips/sec
2)	Command bit rate	300 bps
3)	Command code length	2048

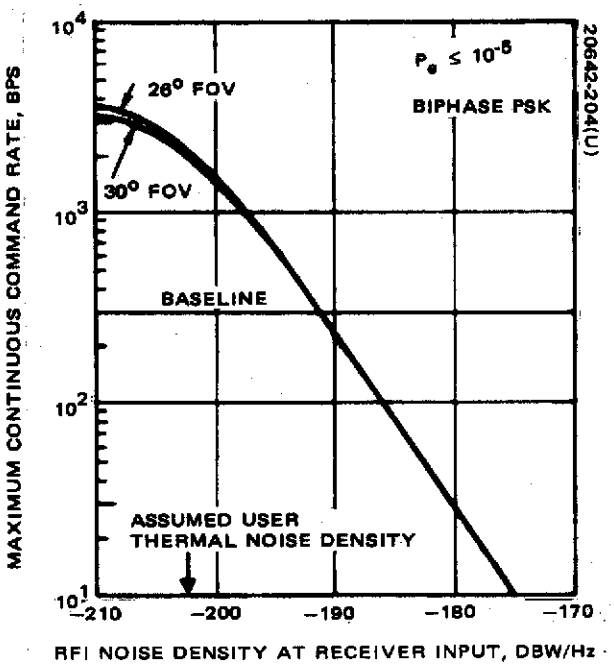

Figure 3-2. Low Data Rate Forward Link Capability

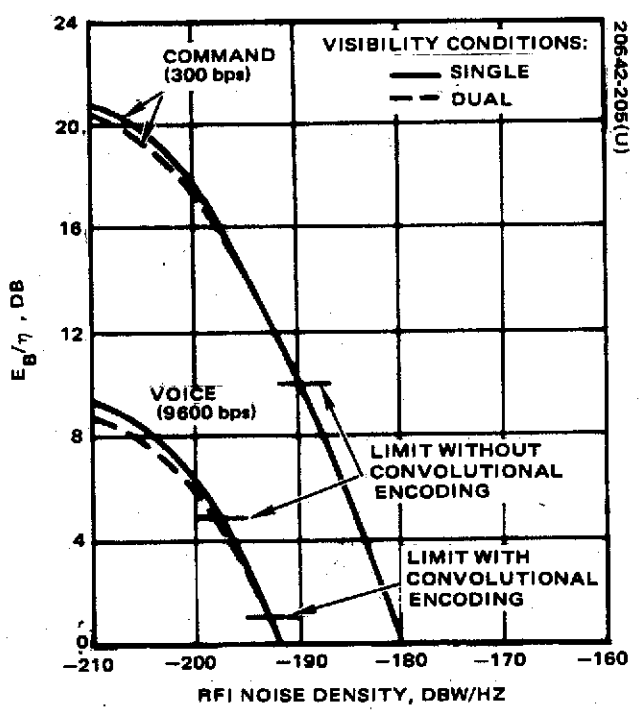

Figure 3-3. UHF Forward Link Signal Concepts; 26 Degrees FOV

4)	Voice bit rate	9.6 Kbps
5)	Voice code length with rate 1/2 convolutional encoding	32

The frequency band chosen is the allocated UHF band 400.5 to 401.5 MHz. This band was selected over a VHF band because 1) more bandwidth is available, 2) RFI is expected to be smaller, and 3) it is a currently internationally allocated band for space use.

Transmit Equipment Parameters. The EIRP and contributory parameters are as follows for each of the two forward links:

	26 degree FOV	30 degree FOV
Antenna gain, dB	12.5	11.8
Radiated power, dBw	17.5	17.5
EIRP, dBw	30	29.3

3.2.1.2 Return Link

The LDR return link allows simultaneous reception from up to at least 20 telemetry transmitting users and one voice user per TDRS. The telemetry channel and voice channel occupy separate frequency bands at 136 to 137 MHz and 137 to 138 MHz, respectively. As with the forward link, the return link service is provided over a 30 degree conical coverage pattern.

The low data rate return link capability per user is a function of the number of active users, their EIRP, and the multipath and RFI environment. Figure 3-4 shows the telemetry link capability per user versus the user EIRP, with the RFI noise density as a parameter. The curves are plotted over a representative set of system parameters and include allocations for various degradations, but do not assume worst case conditions or a link design margin. For a user EIRP of 4 dBw, in the absence of RFI, the system is limited to about 2.5 Kbps, as can be seen from the upper curve. With a more advanced user communications terminal with greater EIRP, the link is limited to 4 Kbps.

The RFI noise density is that which appears at the receiver input. Note the dramatic effect of RFI as it increases above the thermal noise level of -200 dBw/Hz. The higher values of user EIRP may be required to provide desired data capacity in presence of current RFI estimates. The assumptions that were used in producing Figure 3-3 are listed in Table 3-4. The multipath assumption is that for multiple users, the total received multipath power from all users is 6 dB less than the total received direct power. This may also be interpreted as follows: on the average each user's multipath power received by the TDRS is 6 dB less than its direct power.

TABLE 3-4. LOW DATA RATE RETURN TELEMETRY CHANNEL ASSUMPTIONS

- 20 visible users
- Average received power of other users 4 dB more than user of interest
- Average relative multipath per user -6 dB
- RFI noise density measured at TDRS receiver input
- TDRS G/T≥-16 dB/K (edge of coverage)
- Polarization combining 0.5 dB from theoretical
- PN correlator/convolutional decoder operation 2 dB from theoretical
- Ground link signal-to-noise ratio, ≥ 16.5 dB
- Bit error rate, $\leq 10^{-5}$
- RF bandwidth, 1 MHz

Signal Parameters. The selected signaling and multiplexing techniques are:

1) User telemetry and voice occupy separate frequency bands:

Telemetry	136 to 137 MHz
Voice	137 to 138 MHz

2) User telemetry will be PN code modulated to occupy the entire 1 MHz band.

3) Voice signal will PN code modulated as required to meet CCIR requirements.

4) Simultaneous multiple user telemetry signals are code division multiplexed in the 136 to 137 MHz channel; thus, each user's PN code will be different.

5) Convolutional encoding will be employed on user telemetry for bit error correction; link quality is improved significantly with this technique.

The baseline approach assumes that the return bit rate is standardized for all users but this is not a system requirement. With this standardization the baseline parameters are as follows:

1)	Telemetry bit rate	1200 bps
2)	Convolutional encoding rate	1/2
3)	PN code length	511
4)	Chip rate	1.22 Mchips/sec
5)	Voice bit rate (delta modulation)	19.2 Kbps

Receiving Equipment Parameters. The G/T and contributory parameters are as follows for a 30 degree conical field of view:

	26 degree FOV	30 degree FOV
VHF antenna gain, dB	11.2	11.8
Receiver noise figure, dB	3.9	3.9
Receiver noise temperature, K	420	420
Equipment G/T, dB/K	-15.0	-14.4

3.2.1.3 User Tracking

Tracking refers to range and range rate measurements from which user orbital parameters can be derived. The geometry shown in Figure 3-5 shows the four segments that are involved in the required two way transmission. Thus, four transmitters and four receivers are active in this process; two of each are on the TDRS.

Range rate measurement requires the determination of total doppler shift at the ground station, and thus requires phase coherence of the three oscillators in the respective terminals as shown. Measurement of range requires time delay determination in the round trip signal transmission; thus timing synchronization is required. The use of PN codes in the low data rate services automatically provides this synchronization at both user and ground station.

Due to the PN code signaling, user spacecraft receivers automatically acquire and synchronize to the signal transmitted from a TDRS. After the brief acquisition period, range and range rate measurements can be made. However, the user's transmitter must be turned on, and the return signal acquired at the ground station. A particular operational advantage of the signaling concepts used here is that both range and range measurements can be made simultaneous with telemetry reception, and no forward link commands are required.

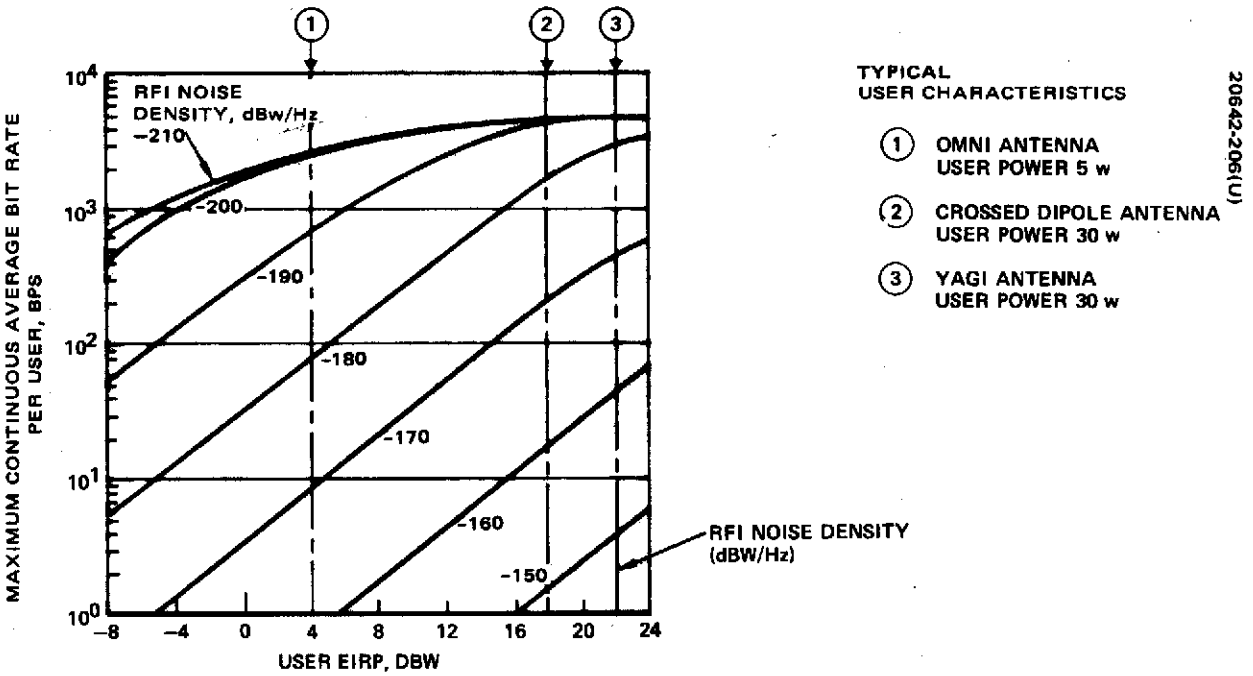

Figure 3-4. Low Data Rate Return Link Capability

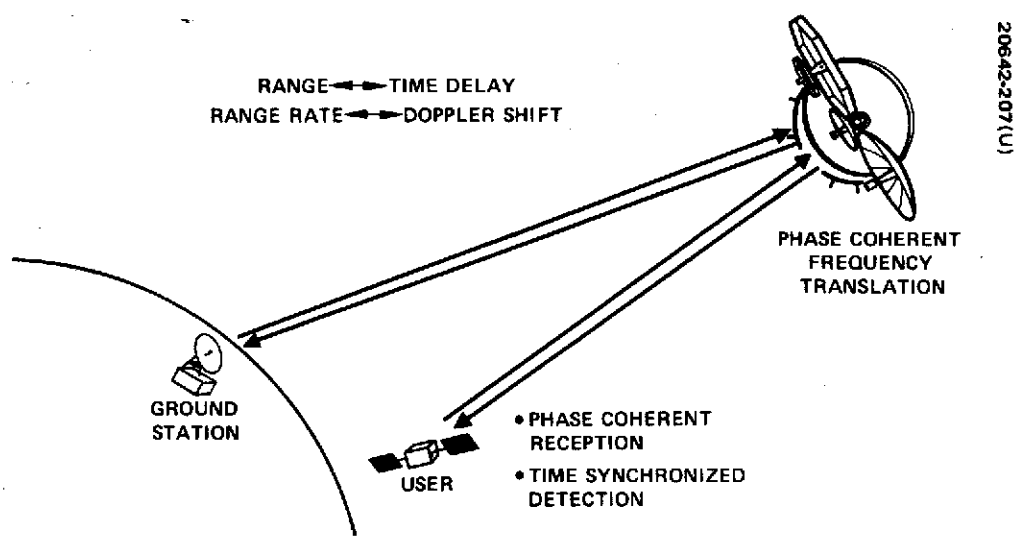

Figure 3-5. User Tracking

The performance limit of the range measurement system is shown in Figure 3-6 as a function of return link RFI noise density. The total rms uncertainty is the sum of the forward and return link uncertainties.

The accuracy of range measurements is limited by thermal noise in the receivers and instability of the three oscillators in the round trip transmission. It can be seen that the low data rate system requirement of 15 meters random uncertainty can be satisfied if RFI power is small for the forward link and limited to less than about -180 dBw/Hz in the return link.

3.2.2 Medium Data Rate (MDR) Service

The medium data rate service requires a high gain antenna on each TDRS. This antenna has the angular freedom to follow user spacecraft in orbits with altitudes up to 5000 km. Because of the narrowbeam antenna pattern, two way communication is possible with only one user spacecraft at a time via each TDRS.

The TDRS repeater has been designed to accommodate a 1 Mbps data rate on the return link.

The wideband (10 MHz) phase coherent repeater allows range and range rate measurements to be made by almost any method preferred by the user. In addition, capability is provided to position the transmit (forward link) 10 MHz band, anywhere in the 2035 to 2120 MHz frequency range and to position the receiver (return link) 10 MHz band anywhere in the 2200 to 2300 MHz range.

The S band transmitter operates at two power levels resulting in two EIRP levels: 47 and 41 dBw. The former is restricted to part-time use due to TDRS power limitations.

The high power mode will allow transmission of 22 Kbps delta modulated voice on the forward link, to accommodate 19.6 Kbps delta modulated voice and 2 Kbps data. The TDRS antenna and receiver design provides for a 100 Kbps combination of voice and data on the return link from a manned user with an omni antenna and 100 watts of RF power.

Flux density calculations indicate that the forward link spectrum must be spread prior to transmission from the ground complex in order to meet CCIR requirements, and probably the return link spectrum will also require spreading.

3.2.2.1 Forward Link

As mentioned above, each TDRS has two transmitter power levels for the MDR forward link. In addition to this variation, the user's antenna gain and receiver quality determine the data rate capacity of the medium data rate forward links. Figure 3-7 shows the maximum possible forward link data rate, assuming no error correction encoding and a receiver system noise temperature of 800 K.

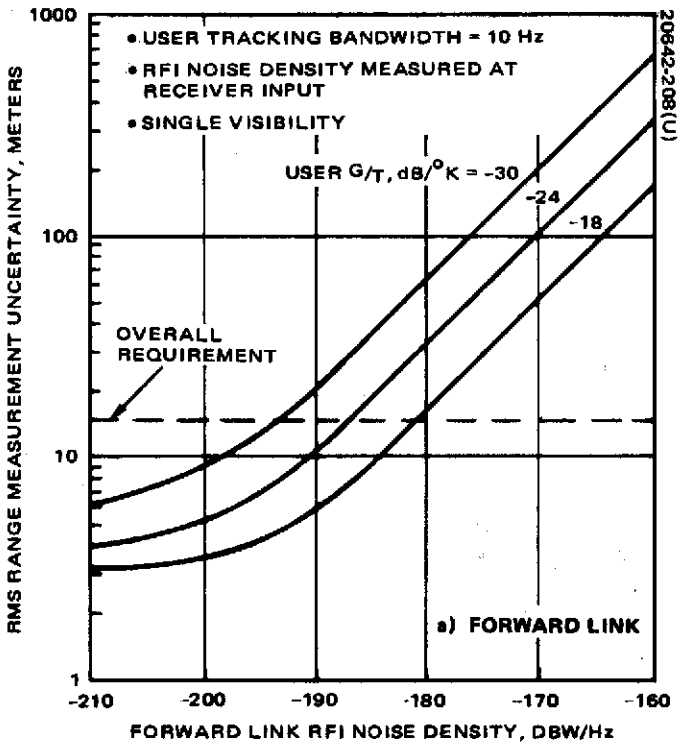

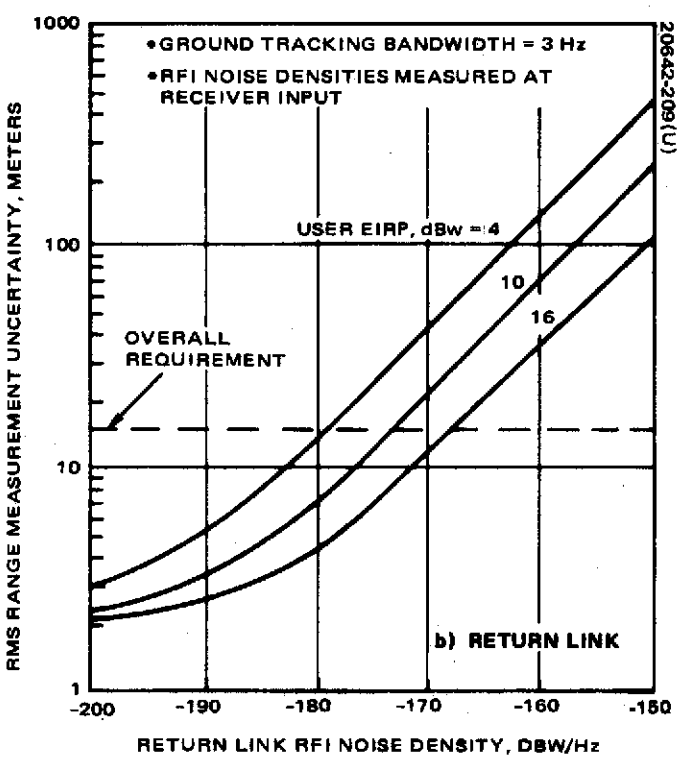

Figure 3-6. RMS Range Measurement Uncertainty

The high power level was determined by the requirement to transmit a 22 Kbps digital voice plus data signal to the Space Shuttle with a 0 dB gain antenna. It can be seen that in the low power mode bit rates greater than 1 Kbps are possible with antenna gains less than 0 dB. Note that even a 20 dB gain requires a relatively small antenna. The TDRS antenna gain for the forward link is 36 dB and the radiated power is 3.2 and 12.5 watts for low and high power modes, respectively.

3.2.2.2 Return Link

The medium data rate return link capability is determined by the TDRS G/T ratio and user EIRP. The TDRS G/T ratio (10.5 dB/K considering receiver noise only) was determined by the requirement to receive data plus voice (approximately 100 Kbps total) from the Space Shuttle with an EIRP of 20 dBw (100 watts). Figure 3-8 relates the maximum possible data rate to user power and antenna gain assuming no error correction encoding. The use of error correction encoding would increase the maximum data rate of both the forward and return links by a factor of up to 7.

The return link system requirement of 1 Mbps can be achieved with a user EIRP of 30 dBw, which might consist of a 20 dB antenna gain and 10 watts of RF power.

3.2.2.3 Tracking

The 10 MHz bandwidth will allow both the range and range rate measurement accuracy requirements to be met with sufficient ground oscillator quality and user communication equipment capability.

3.2.3 Order Wire

An S band antenna has been provided which has a gain of 13.2 dB or greater for orbital altitudes up to 550 km. The repeater channel has been designed so that approximately 1 Kbps can be transmitted to the Ground Station at any time by a manned spacecraft with an omni antenna and 100 watts of radiated RF power. Thus, a request can be made by such a spacecraft for MDR service accompanied by priority level data.

The channel bandwidth is 1 MHz centered at 2250 MHz so that if the manned spacecraft can provide greater EIRP, more data, or even voice, could be relayed via this service.

3.2.4 S Band Transponder

A turnaround S band transponder has been provided to allow accurate TDRS range measurements. The bandwidth is 8 MHz centered at 2010 MHz for receive and 2075 MHz for transmit. The transmitted EIRP is 18 dBW. This transponder will allow trilateration techniques such as those currently being designed for the Synchronous Meteorological Satellite.

For completeness in this section the link power budgets corresponding to TDRS transmission and reception are presented in Tables 3-5 and 3-6, respectively. These power budgets are the basis for much of the following analysis and contain the important link parameters.

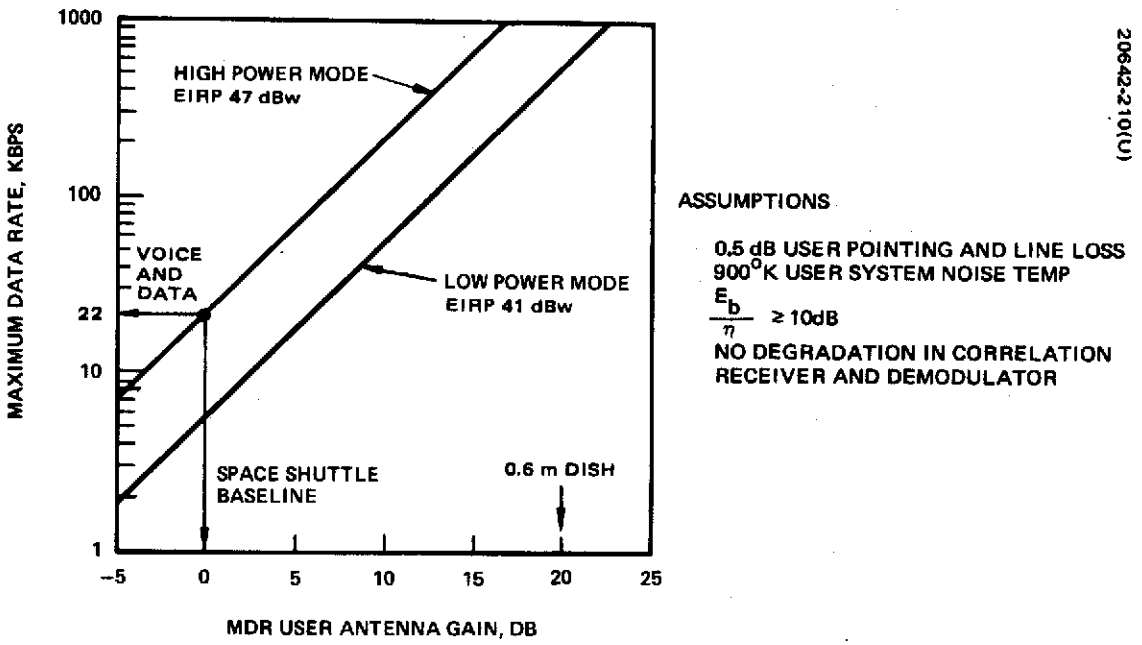

Figure 3-7. Medium Data Rate Forward Link Capability

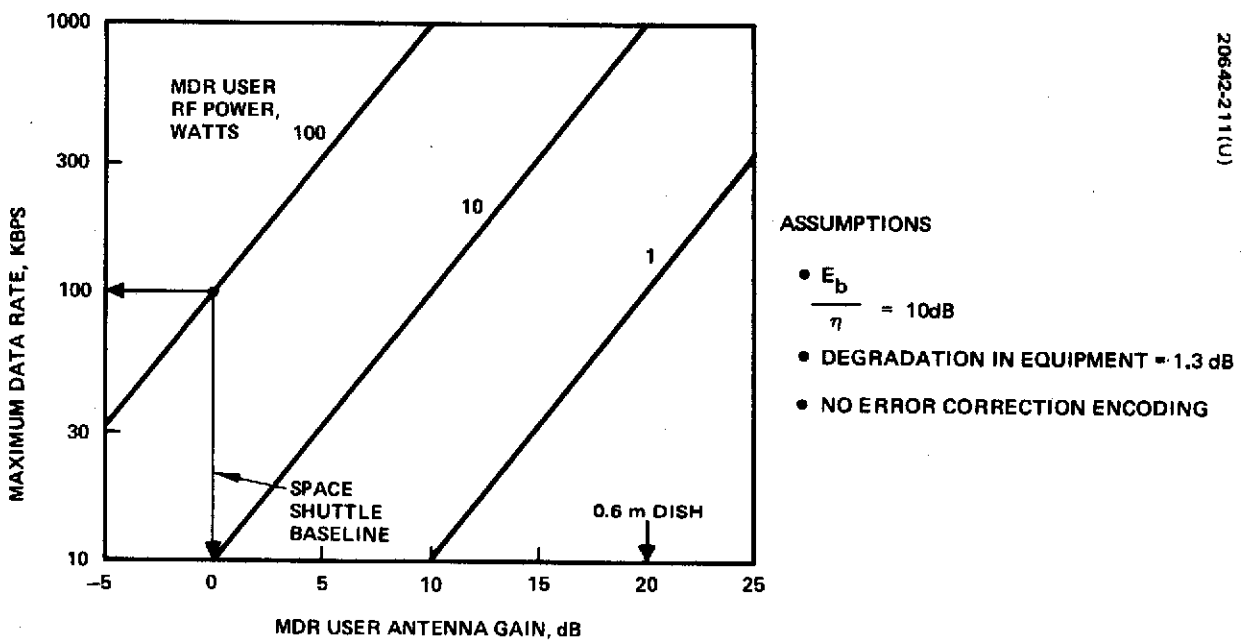

Figure 3-8. Medium Data Rate Return Link Capability

TABLE 3-5. TDRS TRANSMIT LINK BUDGETS

Parameter	LDR Command UHF	Voice UHF	MDR Forward S Band		Ground K Band	S Band Transponder
			High Power	Low Power		
TDRS EIRP	-30.0*	30.0	47.0	41.0	EIRP	18.0
TDRS pointing loss	-	-	-0.5	-0.5	-0.5	-
Space loss	-177.5	-177.5	-192.0	-192.0	-208.4	-192.0
Receive antenna gain	-3.0	-1.0	G_u	G_u	63.0	32.0
Receive pointing loss	-	-	-0.3	-0.3	-0.5	-0.3
Receive line loss	-0.5	-1.0	0	0	-0.3	-1.0
Receive ellipticity loss	-3.0	-1.0	0	0	-0.2	-0.2
Receive power, P_r	-154.0	-150.5	G_u-146	G_u-152	EIRP-146.9	-143.5
Receiver noise figure, dB	3.75	3.75	5.5		3.8	3.8
Receiver noise temperature, K	400	400	750		400	400
Background noise temperature, K	50	50	50		20	50
Total system noise temperature, K	450	450	800		420	450
Noise density, η_T dBw/Hz	-202	-202	-199.5		-202.3	-202.0
Pr/η_T dB-Hz	48	51.5	G_u+53.5	G_u+47.5	EIRP+55.4	58.5

*For 26 degree conical coverage, 29.3 dBw for 30 degree coverage.

TABLE 3-6. TDRS RECEIVE LINK BUDGETS

Parameter	LDR VHF (minimum)	Voice VHF	MDR S Band	Order Wire S Band	Ground K Band
Transmit power	7.0	20		20	P
Transmit antenna gain	-3.0	0	EIRP	0	62
Transmit pointing plus line loss	-	-		-	-3
Space loss	-167.5	-167.5	-192.7	-192.7	-207.5
TDRS antenna gain	11.2*	11.8	36.7	13.2	18.5
TDRS pointing loss	-	-	-0.5	-	-2.0
TDRS line loss	-1.0	-1.0	-2.2	-1.0	-1.0
TDRS ellipticity loss	-0.5	-0.2	0	-0.2	0
Receiver power, PR	-153.8	-136.9	EIRP -158.7	-160.7	P-133
Noise figure, dB	3.9	3.9	3.9	3.9	9
Receiver noise temperature, K	420	420	420	420	2000
Earth noise temperature, K	210	210	300	300	300
Total system noise temperature, K	630	630	720	720	2300
Noise density, η_T, dBw/Hz	-200.6	-200.6	-200	-200	-195
P_r/η_T CB-Hz	46.8	63.7	EIRP +41.3	39.3	P + 62

*For 30 degree conical coverage.

3.3 ANALYSIS

The analysis required for the telecommunications service system design has been separated into three major portions:

1) The low data rate TDRS/user spacecraft links

2) The medium data rate TDRS/user spacecraft links

3) The TDRS/ground station links

Each of these subjects is treated successively in the following three subsections. Subsection 3.3.4 presents a brief summary of the selected techniques and baseline parameters.

Each subsection presents foundational data and alternative concepts which are then followed by representative designs. These are then compared on such quantitative bases as multipath rejection, RFI margin, and bit rate capacity. Other system considerations also were important in baseline design choices; these considerations include operational flexibility, user equipment standardization, and reliability of spaceborne equipment.

3.3.1 Low Data Rate System Analysis

The low data rate analysis and conceptual design is summarized in the following sections. The key engineering trades described in this section are listed in Table 3-7. The link design procedure is illustrated in Figure 3-9.

The anti-multipath technique selection of pseudo-noise (PN) coding was based largely on previous studies for TDRSS. The major alternative, burst transmission, was studied, but was not found to outperform the PN approach. The use of PN coding simultaneously accomplishes the following objectives:

1) Reduces effects of multipath interference

2) Allows accurate range measurement

3) Provides technique for signal multiplexing

4) Spreads the power spectrum to satisfy the CCIR flux density requirements

In addition, PN coding, in conjunction with notch filtering, can also be used for protection against RFI (radio frequency interference). The Electromagnetics Systems Laboratories, Inc. frequency diversity approach was considered against RFI, but it is complex and not readily adaptable for use in ranging. A multielement antenna with signal processing on the ground was another alternative. This would effectively result in directing antenna nulls toward RFI sources and an antenna gain peak toward the user

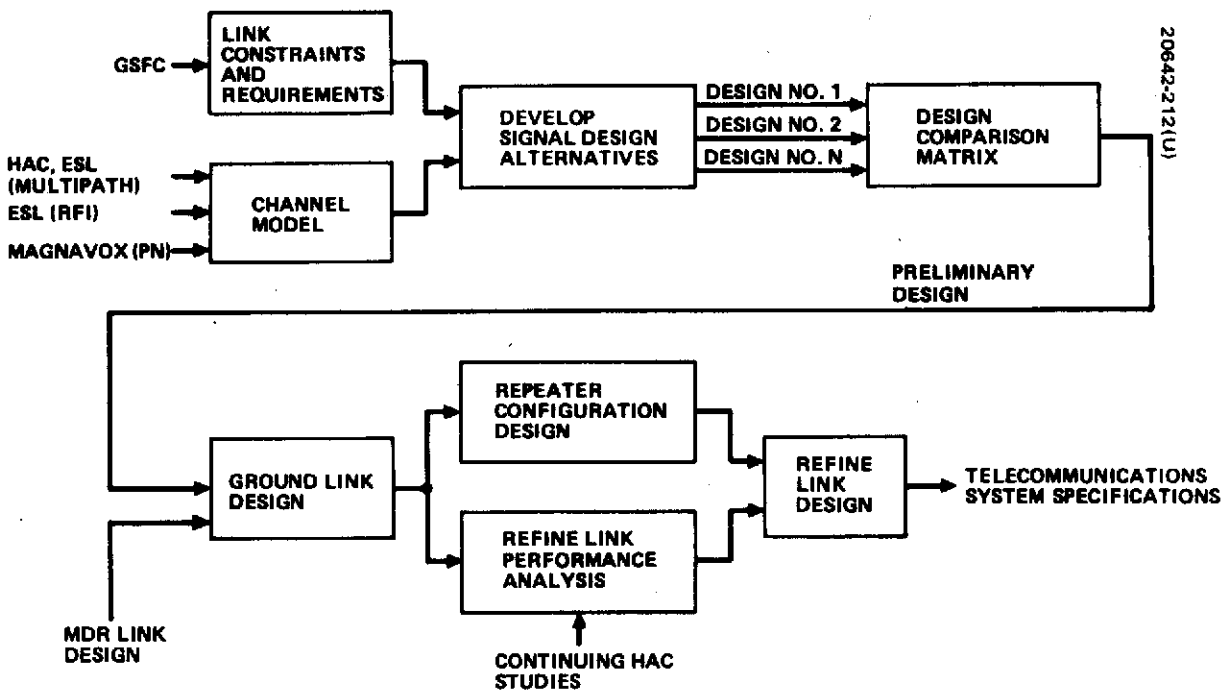

Figure 3-9. Low Data Rate Link Design Procedure

TABLE 3-7. LOW DATA RATE SYSTEM ALTERNATIVES

Trade Topic	Principal Alternatives	Selections
Antimultipath technique	Polarization discrimination* Pseudo noise Burst transmission	Polarization discrimination* Pseudo noise
Anti-RFI technique	Frequency diversity PN with notch filtering Processing antenna	PN with notch filtering
Forward link frequency	VHF: 117.525 MHz UHF: 400.5 to 401.5 MHz	UHF
Voice and data multiplexing	• Separate frequency channels (FDM) • Common channel (CDM)	FDM for return link CDM for forward link
Voice modulation	Delta modulation Vocoding	Delta modulation
Data multiplexing	FDM CDM	CDM (code division muliplex)

*Manned user only

spacecraft. Unfortunately, TDR satellite constraints limit the number of antenna elements and therefore the improvement which can be achieved. If the RFI sources are conveniently located, the processing antenna approach would provide some RFI rejection part of the time, but it provides only slight advantage when the user is above the RFI source. The notch filtering approach was selected because of its simplicity and the fact that its performance will be independent of user location.

The low data rate forward link frequency was selected as UHF primarily because greater bandwidth was available for ranging and voice, and because this band is already allocated to space use.

The principal alternatives for voice and data multiplexing were code division multiplexing (CDM) and frequency division multiplexing (FDM). The FDM approach was selected for the return link to prevent telemetry data degradation by the voice signal. This also permits the addition of power control at the TDRS for the voice or telemetry channels if deemed necessary. Furthermore, it was found that a repeater bandwidth convenient at VHF easily permitted separation of the signals. A baseband CDM approach was selected for the command and voice forward links in order to simplify the

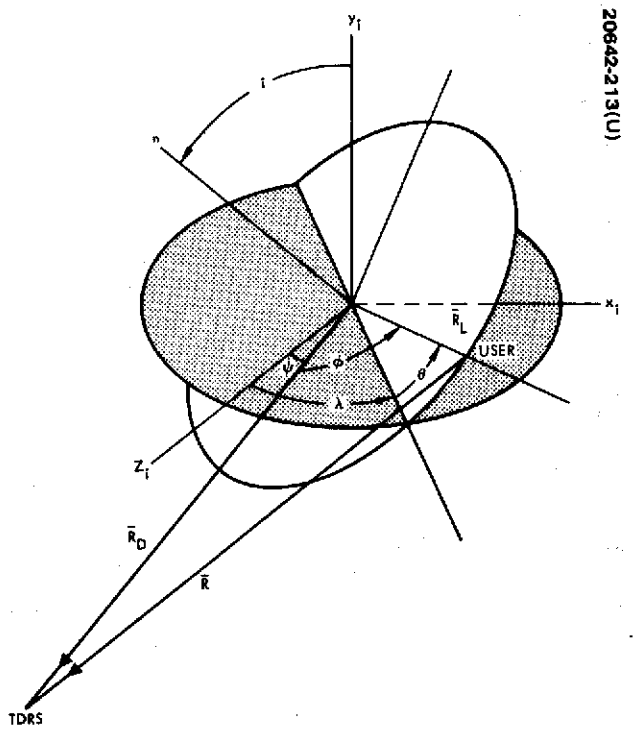

Figure 3-10. Orbital Parameters

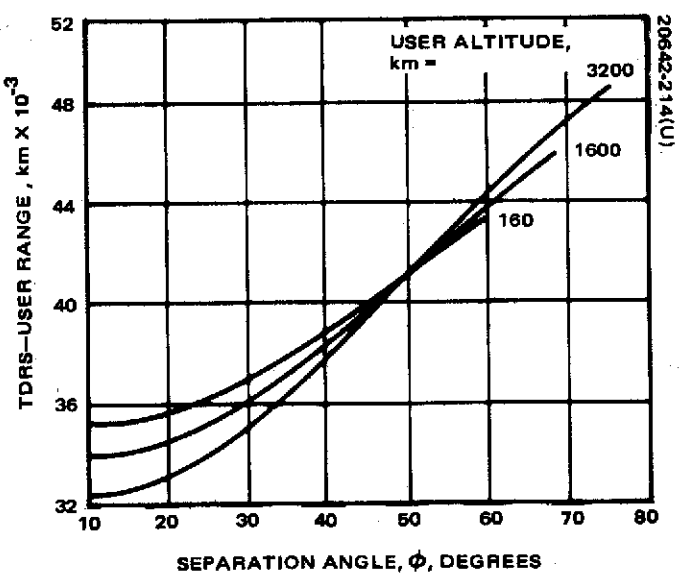

Figure 3-11. Range as Function of Separation Angle

TDR satellite transmitter design. The composite command and voice at RF appears as a single signal in the saturated amplifier. Sufficient bandwidth is available at UHF to minimize crosscorrelation effects.

For TDRS system voice encoding, delta modulation has been selected. An encoding rate of 9.6 Kbps has been selected for the forward link, resulting in very good intelligibility of the demodulated voice on the manned spacecraft. The return link encoding rate is 19.2 Kbps, exactly twice the forward link rate, and gives even better voice reproduction so that astronaut voice inflections due to emotional stress can be distinguished.

For data multiplexing in both the forward and return links, CDM has been selected. This is the most convenient approach when using pseudo noise modulation. Using FDM in the return link would require an allocation for doppler between each of the 40 users. A common channel CDM design requires only one such allocation. Furthermore, all user transceivers will have the same turnaround, input-to-output frequency ratio, allowing a standardization of much, if not all, of every user transceiver.

This section presents the analysis details and the comparison of various link design alternatives. A summary of the selected techniques and the baseline parameters may be found in 3.3.4.

3.3.1.1 Communication Channel Model

The TDRSS low data rate (LDR) service concept requires communication between a synchronous altitude relay spacecraft and multiple low altitude user spacecraft. The user spacecraft are constrained to low transmit power levels and unsophisticated antenna systems. The typical LDR user, for design purposes, transmits 5 watts of VHF power through a -3 dB gain antenna. The user receives commands with an antenna of a similar omnidirectional nature. A low data rate trade study was performed to determine the user's receive frequency as one of two possible bands — one at UHF and one at VHF. Modeling these TDRS/user communications links must include three important considerations:

1) Basic TDRS/user communications geometry

2) Multipath signals which are reflected by the earth's surface

3) RFI noise caused by undesired earthbound emitters.

Basic Communication Geometry. Figure 3-10 shows the basic TDRS/user orbital geometry. The maximum value of the range vector, $\overline{R}$, determines the maximum "space spreading loss" the links will experience. Figure 3-11 shows range as a function of separation angle, ϕ, and user altitude as given by:

$$R^2 = R_D^2 + R_L^2 - 2R_D R_L \cos \phi$$

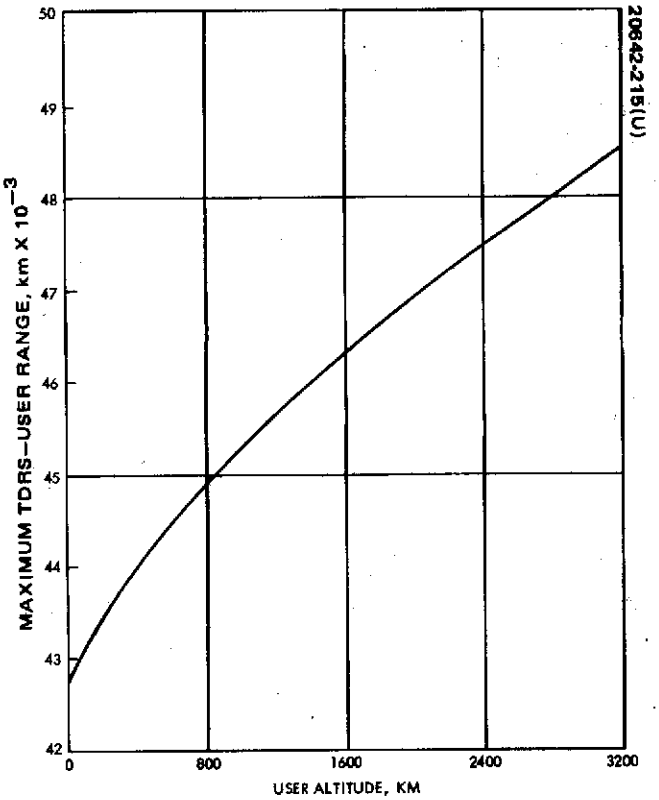

Figure 3-12. Maximum User/TDRS Range

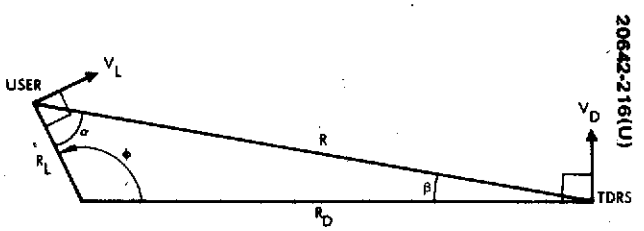

Figure 3-13. Maximum Range Rate Geometry

where

R_D = synchronous radius

R_E = earth's mean radius

$R_L = R_E + h$

h = user altitude

ϕ = geocentric separation angle

For a given user circular orbit altitude, there exists a maximum value for ϕ since the earth occults the user/TDRS line of sight. The maximum range corresponding to these maximum values for ϕ is given in Figure 3-12 as a function of user altitude. The maximum TDRS/user range is also given directly by the expression:

$$R_{max} = \sqrt{R_D^2 - R_E^2} + \sqrt{2R_E h + h^2}$$

Range rate, the component of the relative velocity vector of the two satellites which is parallel to $\bar{R}$, is important from a communication design standpoint since it will cause a received carrier to be shifted in frequency. The doppler shift for a range rate of $\dot{R}$ km/sec and a carrier of f Hertz is given by:

$$\Delta f = \frac{\dot{R}}{C} f$$

when relativistic effects are ignored. The maximum value of Δf fixes the frequency uncertainty that a receiver must search in order to establish a coherent link. The geometry for this condition is planar and is shown in Figure 3-13. From the figure it can be seen that:

$$\dot{R} = V_L \operatorname{Sin} \alpha + V_D \operatorname{Sin} \beta$$

By the law of sines

$$\frac{\operatorname{Sin} \alpha}{R_D} = \frac{\operatorname{Sin} \beta}{R_L} = \frac{\operatorname{Sin} \phi}{|\bar{R}|}$$

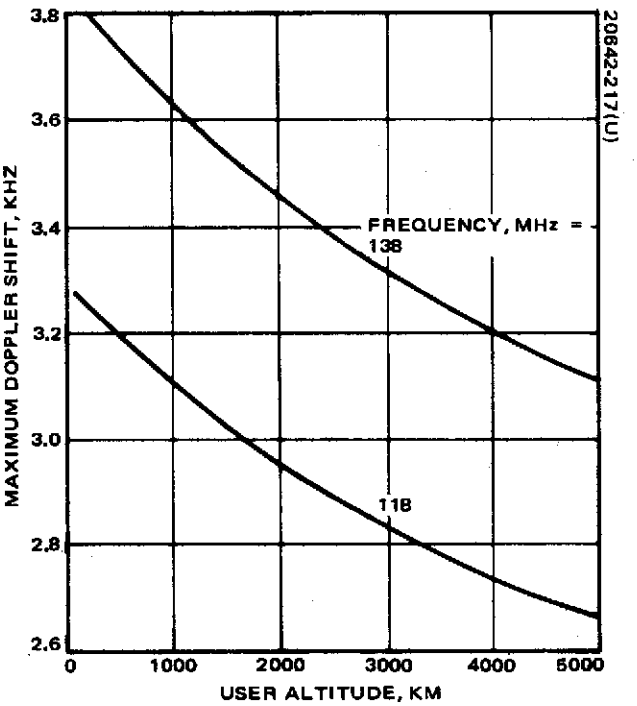

Figure 3-14. Maximum Doppler Shift in Low Data Rate Links at VHF (One-Way Frequency Lock)

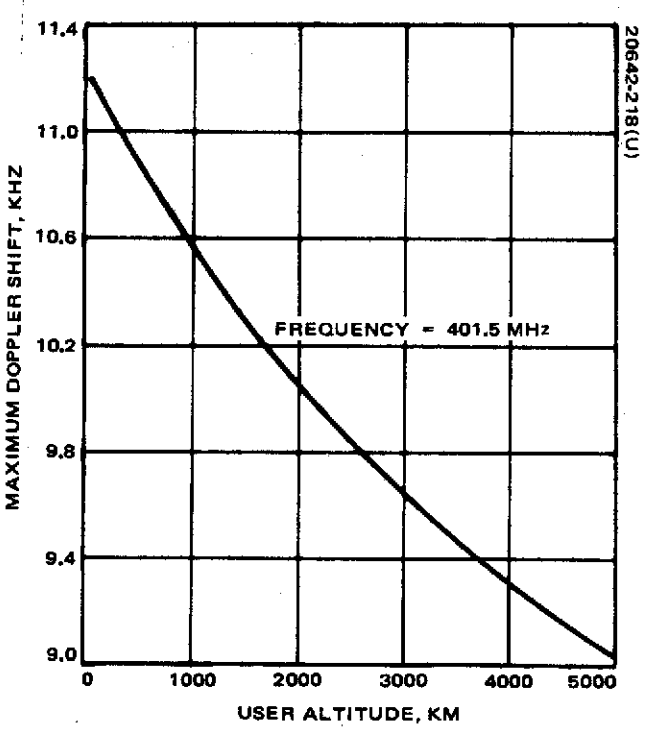

Figure 3-15. Maximum Doppler Shift in Low Data Rate Links at UHF

and

$$\dot{R} = \left(\frac{V_L R_D + V_D R_L}{|\bar{R}|} \right) (\sin \phi)$$

Figures 3-14 and 3-15 show the maximum doppler shift expected at candidate LDR service frequencies. Note that the doppler in the return link at ≅138 MHz will be twice that shown when the system is in two-way lock.

Let the user receive a carrier at a frequency of f_1 which is multiplied to some frequency f_2 for coherent transmission.

$$f_2 = r f_1$$

where r is the turnaround ratio. If f_1' and f_2' denote the doppler shifted frequencies received by the user and TDRS respectively, then

$$f_2 = r f_1'$$

with

$$f_1' = f_1 \left(1 + \frac{\dot{R}}{C} \right)$$

and

$$f_2' = \left[f_2 \right] \left(1 + \frac{\dot{R}}{C} \right)$$

$$f_2' = \left[r f_1 \left(1 + \frac{\dot{R}}{C} \right) \right] \left(1 + \frac{\dot{R}}{C} \right) = f_2 \left(1 + \frac{\dot{R}}{C} \right)^2$$

$$\Delta f_2' = f_2' - f_2 \approx 2 f_2 \frac{\dot{R}}{C}$$

The time-rate-of-change of the doppler shift or doppler rate is also important in communication design since it specifies the frequency tracking characteristics of the receiver. The maximum doppler rate is found by differentiating the previous equation for doppler. Figures 3-16 and 3-17 summarize the pertinent doppler rate data. When in two-way frequency lock, the doppler rate on the return carrier will be exactly twice that shown.

Multipath Environment. The term "multipath" refers to a communication link in which more than one signal propagation path exists between the signal source and the receiver. In TDRSS communication, there are basically two paths between the satellites, as shown in Figure 3-18: a direct path and a path by reflection from the earth's surface. The total reflecting surface may be envisioned as many smaller reflecting surfaces; hence, the overall reflection path is a collection of many reflection paths. The signal received via this reflection path is delayed and distorted with respect to the received, directly transmitted signal. Figure 3-19 shows this effect when the

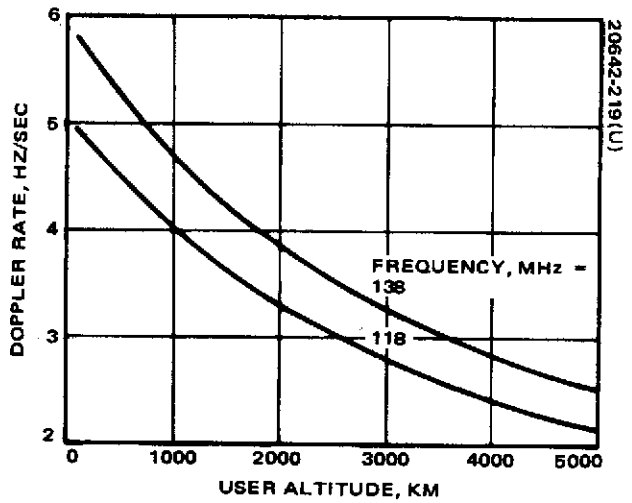

Figure 3-16. Maximum Doppler Rate in Low Data Rate Links at VHF (One-Way Frequency Lock)

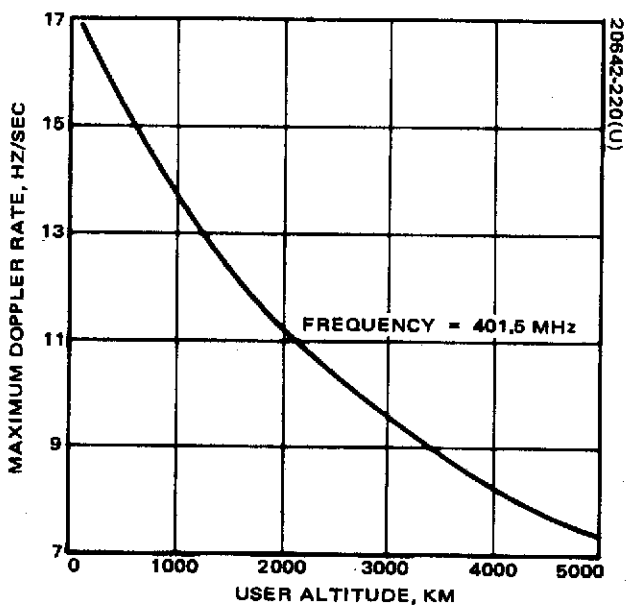

Figure 3-17. Maximum Doppler Rate in Low Data Rate Links at UHF

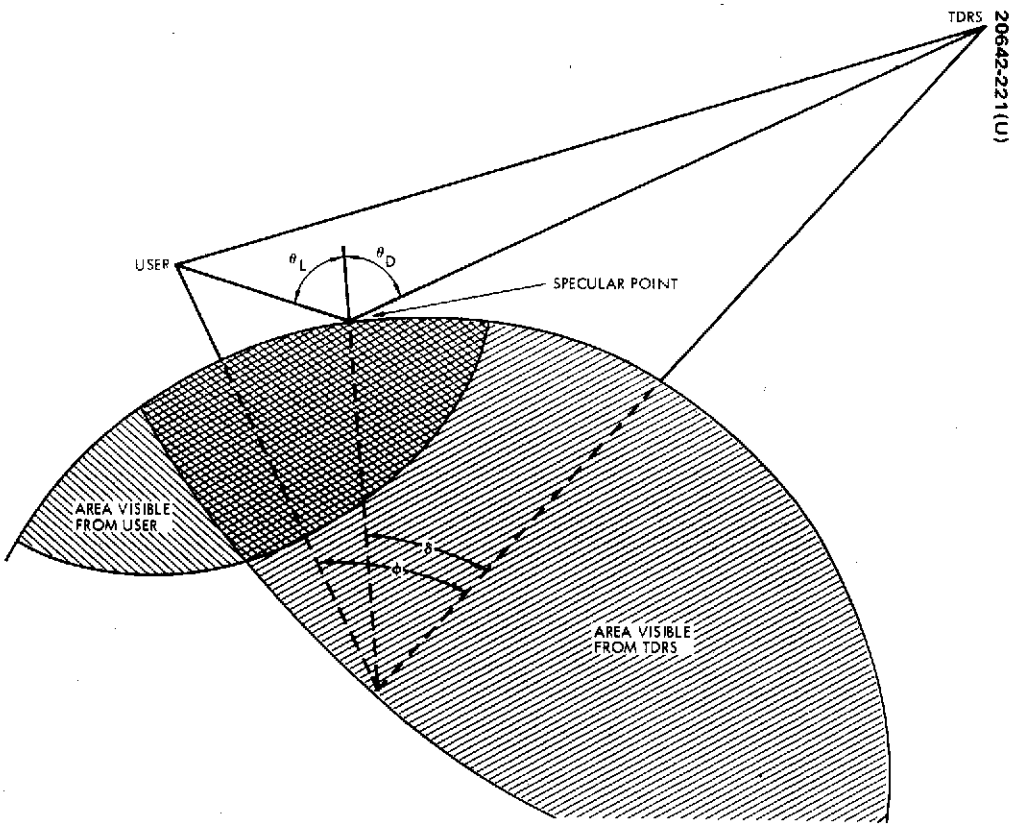

Figure 3-18. TDRS-User Multipath Geometry

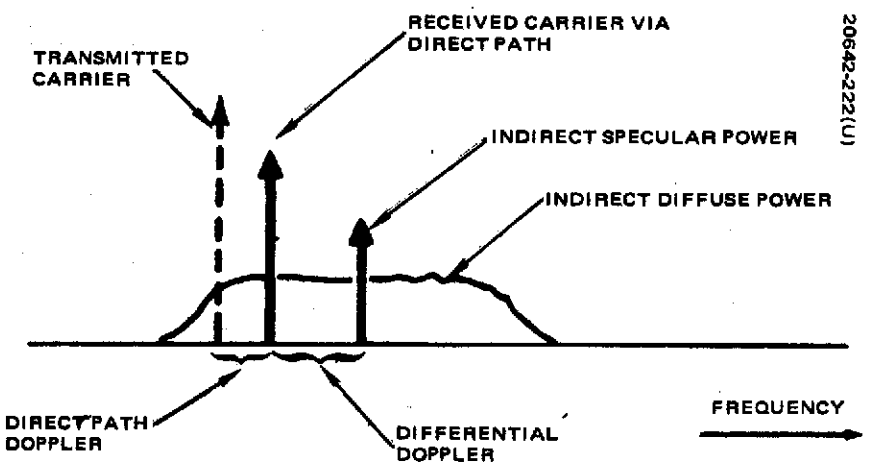

Figure 3-19. Multipath Channel Effects on Transmitted Carrier

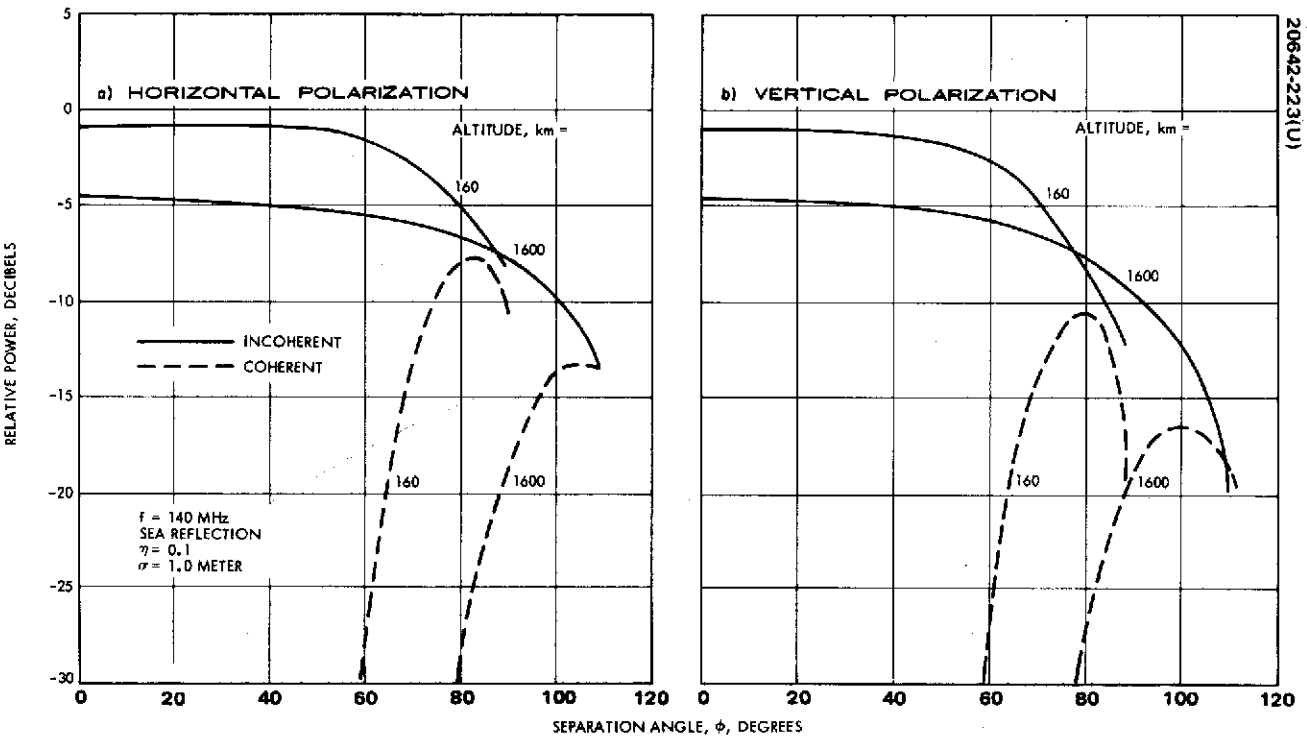

Figure 3-20. Relative Multipath Power

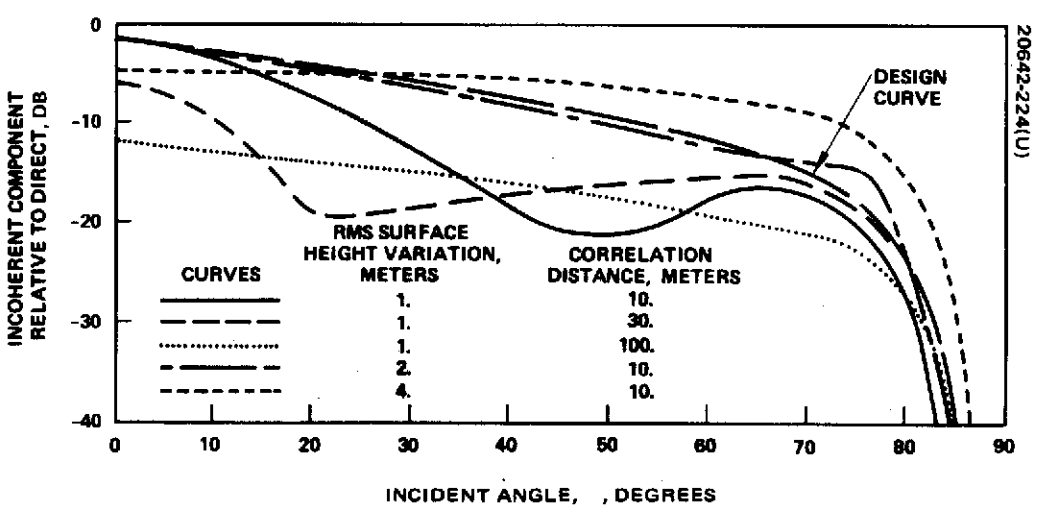

Figure 3-21. Incoherent Multipath Reflected From Sea Water for 550 km User Altitude

transmitted signal is a single carrier. The signal received via the direct path is a doppler shifted version of the original. The multipath or indirect signals are of two different types. The specular power is again a doppler shifted version of the original signal, but the doppler is different since the relative motion of the satellites is different along the indirect path. Most of the time a major portion of the multipath signal can be characterized as diffuse power, incoherent with respect to the direct signal. This signal is composed of multiple reflected signals with different frequencies and randomly varying phases.

Hughes Aircraft Company performed a study of this multipath phenomena for GSFC under contract NAS 5-11602; this work is documented in Reference 1. A similar analytical study was done by Electromagnetics Systems Laboratories (Reference 2).

A quantity useful for evaluating the received reflected power with respect to the received direct power is called the relative power and is defined as the ratio of the two. Figure 3-20 shows an estimate of the relative power as a function of separation angle and altitude. The worst case occurs for low altitudes when the separation angle is zero; i. e., the TDRS is directly above the user. From the figure it can be seen that the incoherent reflected power is only about 1 dB less than the directly received power for this condition and an altitude of 160 km.

Figure 3-21 shows similar curves from the ESL study with the incident angle θ, as the independent variable. Figure 3-22 gives the relationship between ϕ and θ. The previous figure includes a curve labeled "design" which was used during the LDR parametric trades discussed later. It applies to a fairly severe set of conditions that can occur over ocean regions, which constitute 70 percent of the earth's surface. The multipath environment over land is probably less severe, but its statistics are much more complex.

The time response is most conveniently referenced to the specular point reflection, where the specular point is the surface point where θ_R and θ_D of Figure 3-18 are equal. It can be shown that energy reflected from this point is delayed less than that reflected from any other point. Thus, energy reflected from surrounding points will cause a time spreading of a transmitted signal. Figure 3-23 shows impulse response curves normalized to the specular point. Figure 3-24 is the result of a simple calculation to determine the propagation time difference between the direct and specular signals. Comparing these figures, it can be seen that for the majority of geometrical conditions ($\phi \leq 1.4$ radians) the time spreading is at least an order of magnitude less than the specular differential delay.

The doppler shift of the direct signal was discussed above. The spectral characteristics of the reflected signal may be separated into two components as done for the time response:

1) Doppler shift of the specular point reflection

2) Frequency spreading about the specular point reflection

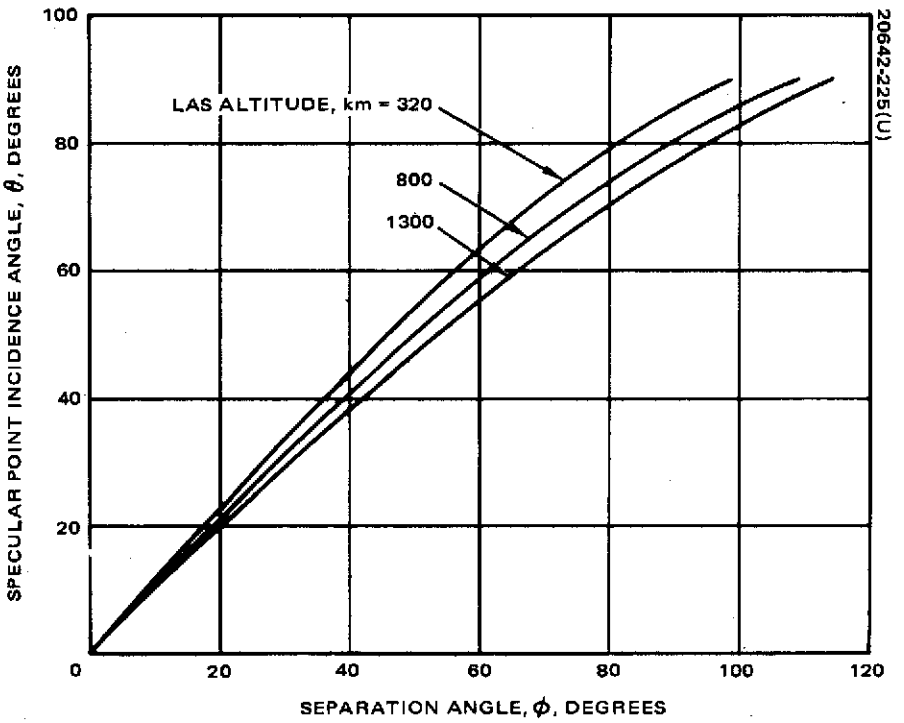

Figure 3-22. Specular Point Incidence Angle Versus Separation Angle

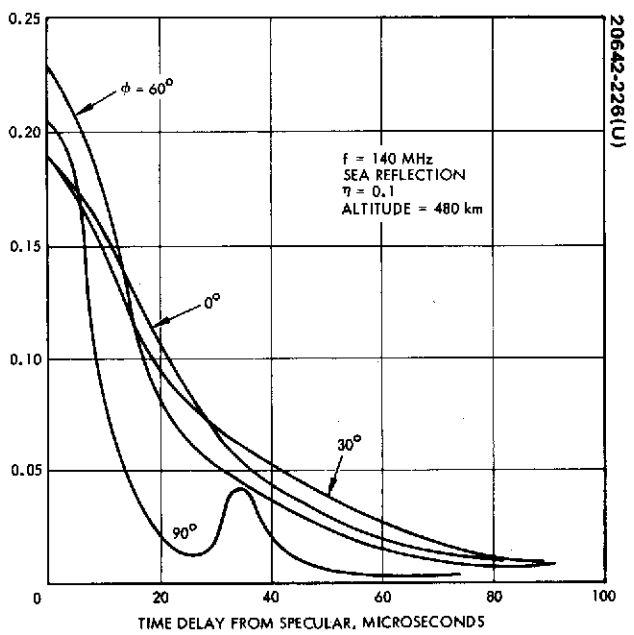

Figure 3-23. Time Response for Horizontal Polarization

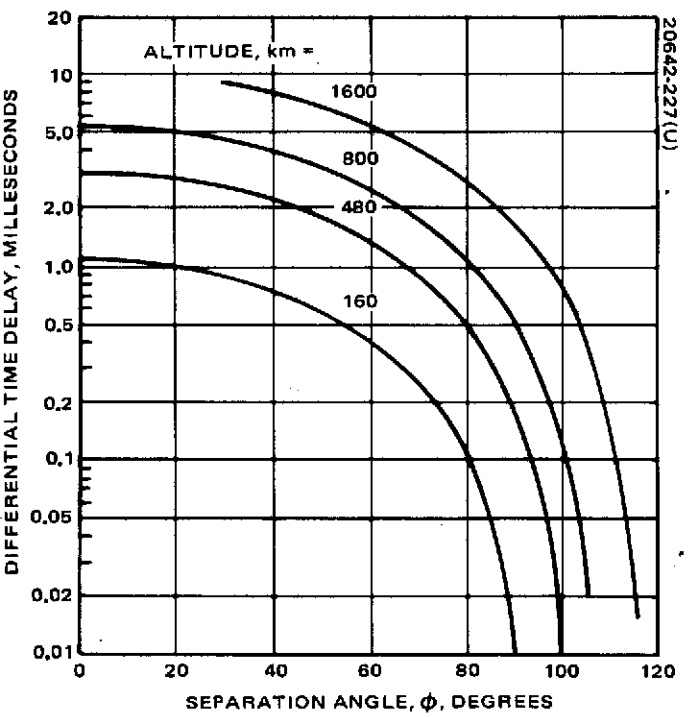

Figure 3-24. Specular Differential Time Delay

As was discussed previously, the doppler shift depends on the relative orientation of the two satellite velocity vectors and the transmission path. Figure 3-25 shows the relative specular doppler shift for a worst case in terms of direct path doppler. Figure 3-26 contains typical reflected signal spectra corresponding to the diffuse reflection geometry. Since the scattering region can be visualized as many small contiguous scattering patches, the reflection path to a given patch will differ from other paths. Consequently, the doppler shift will be different for each patch with a received reflected frequency spectrum for a single transmitted carrier being a composite of the various effects.

If a circularly polarized electromagnetic wave impinges on a perfecting reflecting surface with normal incidence, the reflected wave will be circularly polarized but of the opposite sense. The Hughes multipath model predicts polarization changes for arbitrary angles and for rough earth and smooth earth surface conditions. Figures 3-27 and 3-28 give results from the model in terms of polarization discrimination — that is, the relative multipath power that will be received by an antenna of given ellipticity. In terms of direct signal/indirect signal isolation, the indirect signal essentially reverses polarization under a wide range of conditions. The advantage of circular polarization is recommended later for manned users.

Radio Frequency Interference. Earth based transmitters radiate energy in the VHF and UHF bands of interest with strength sufficient to produce serious interference. The basic geometry of this RFI problem is shown in Figure 3-29. In the return link, the TDRS antenna will receive signals from 40 percent of the earth's surface. The east TDRS with a broad coverage antenna would receive RFI simultaneously from both Europe and the United States. The command link or forward link to the users constitutes a somewhat different problem. The user is much closer to the interfering sources, but much less of the earth's surface is within view. This is shown quantitatively in Figure 3-30. Over the ocean regions, the low altitude user will be shielded from many RFI emitters.

The most detailed estimate of the RFI that will be experienced by synchronous spacecraft has been made by ESL, Inc. (Reference 3). These estimates are based on an emitter library containing the location, antenna pattern, transmitter power, etc., of about 45,000 RFI sources.

For a given synchronous satellite location and a given emitter, the ESL program gives the power at the terminals of an antenna with 16 dB peak gain. When this calculation has been performed for all RFI sources in a given 1 MHz band, the program outputs the total power received by the spacecraft in that band. Figures 3-31 and 3-32 and Table 3-8 summarize the ESL data and indicate the nature of current VHF allocations. These data do not include duty cycle factors for the emitters; therefore the curves may be pessimistic. However, the data may also be optimistic since some transmitters may not be cataloged.

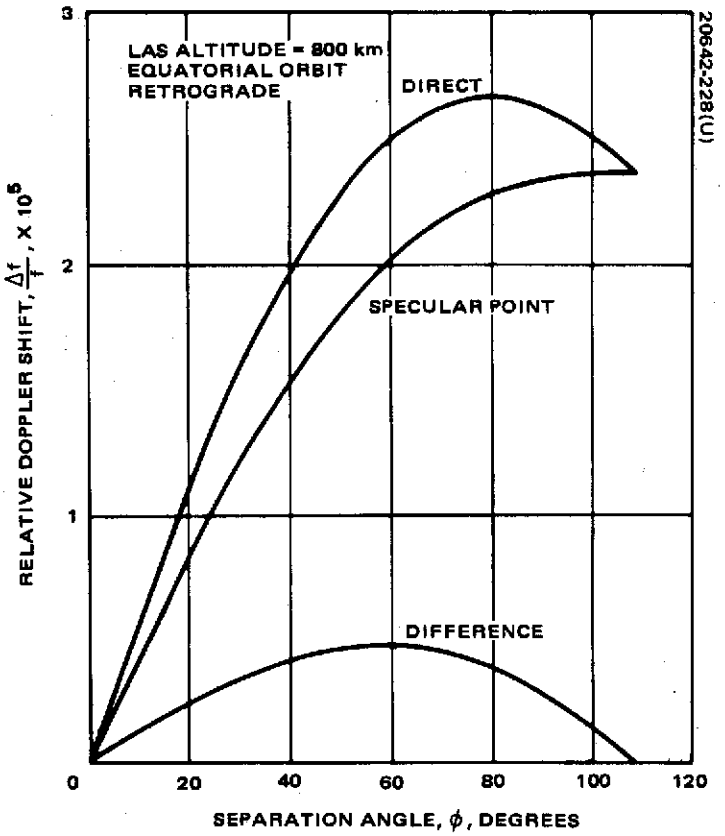

Figure 3-25. Relative Specular Doppler Shift

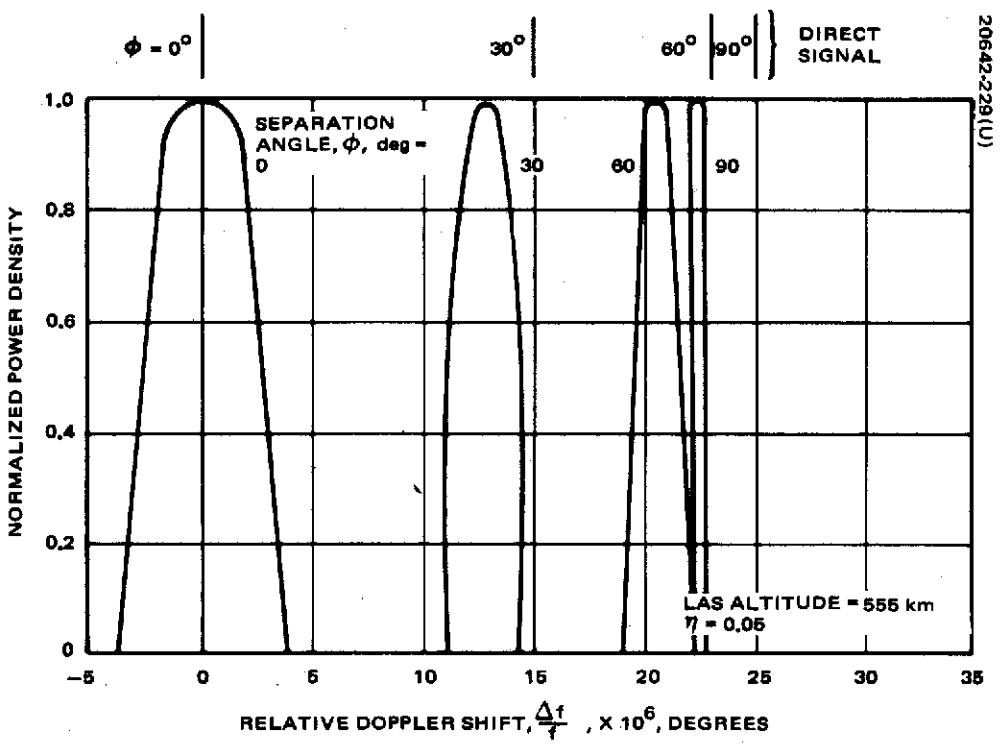

Figure 3-26. Typical Reflected Signal Spectra

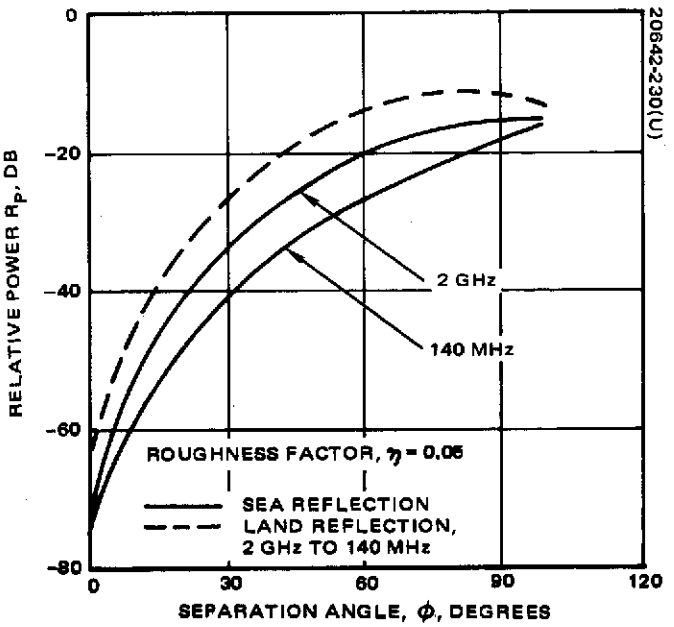

Figure 3-27. Polarization Discrimination for Rough Earth Model User and TDRS Antennas Circularly Polarized

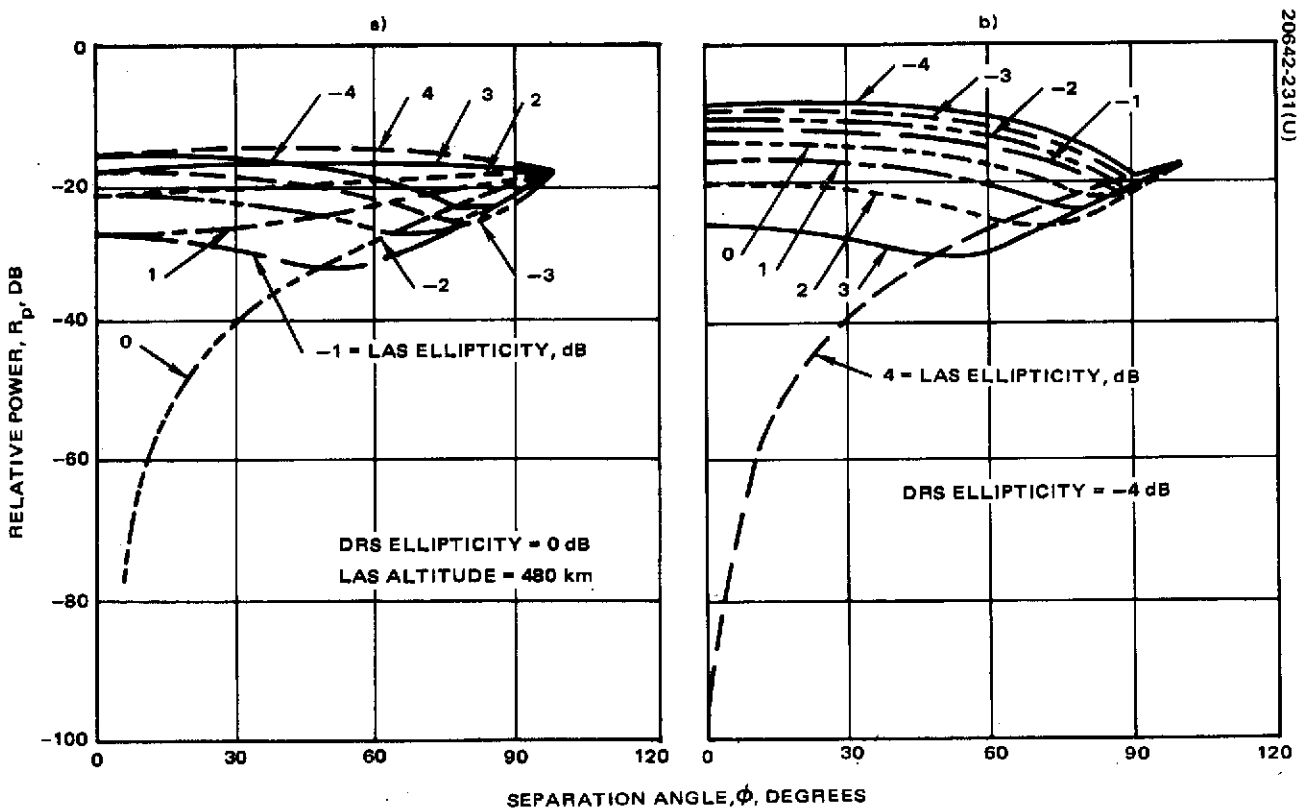

Figure 3-28. Polarization Discrimination for Smooth Earth Model Sea Water Reflection for 140 MHz

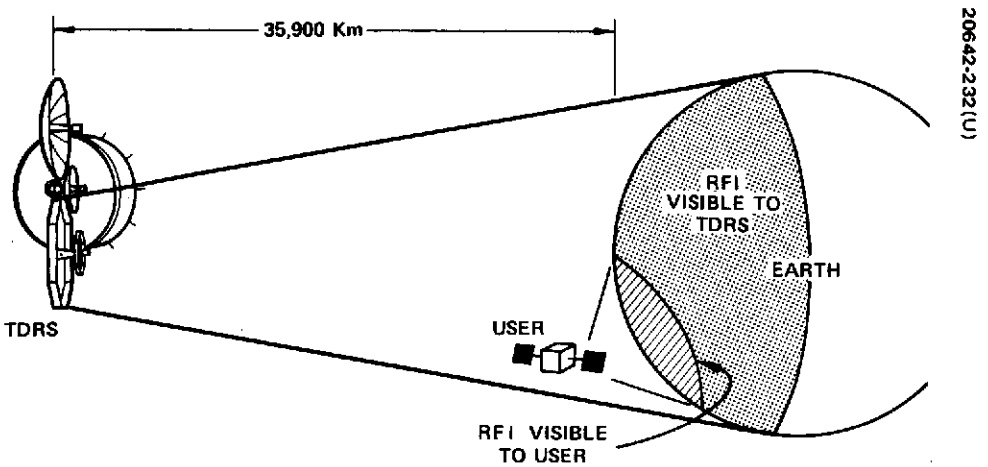

Figure 3-29. RFI Geometry

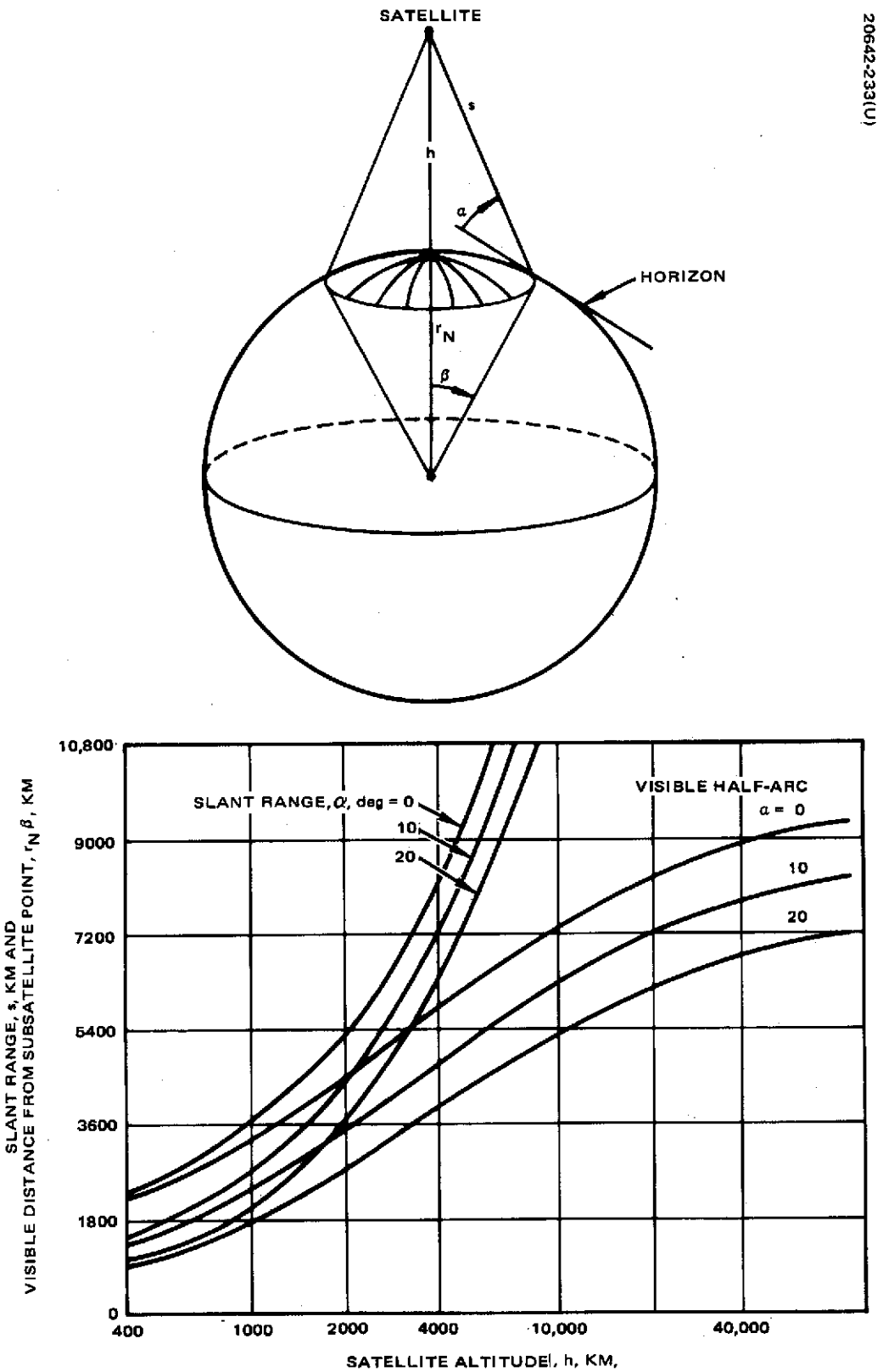

Figure 3-30. Visibility to Potential RFI Sources as Function of User Altitude

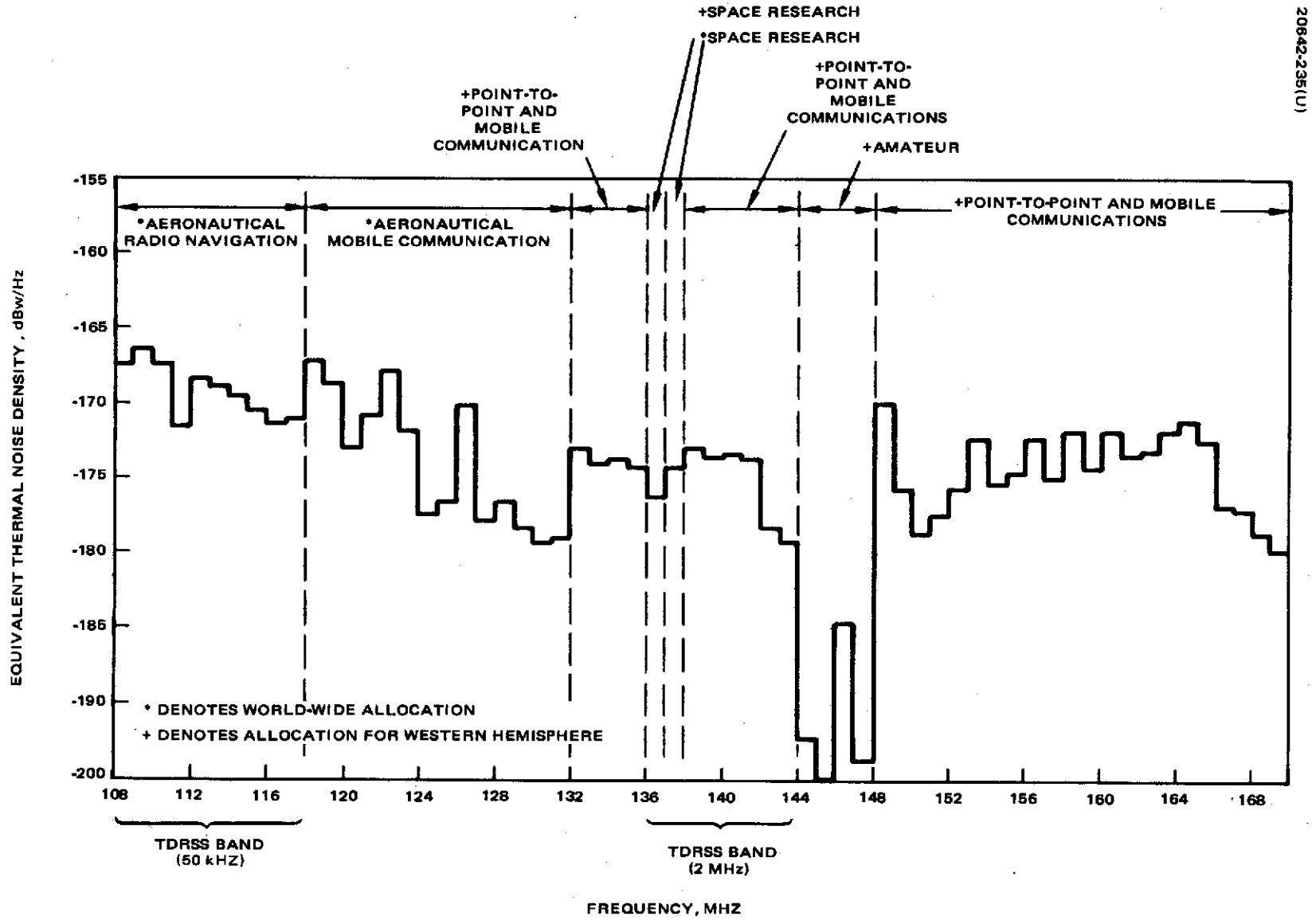

Figure 3-31. ESL, Inc. RFI Prediction for TDRS at 11° W

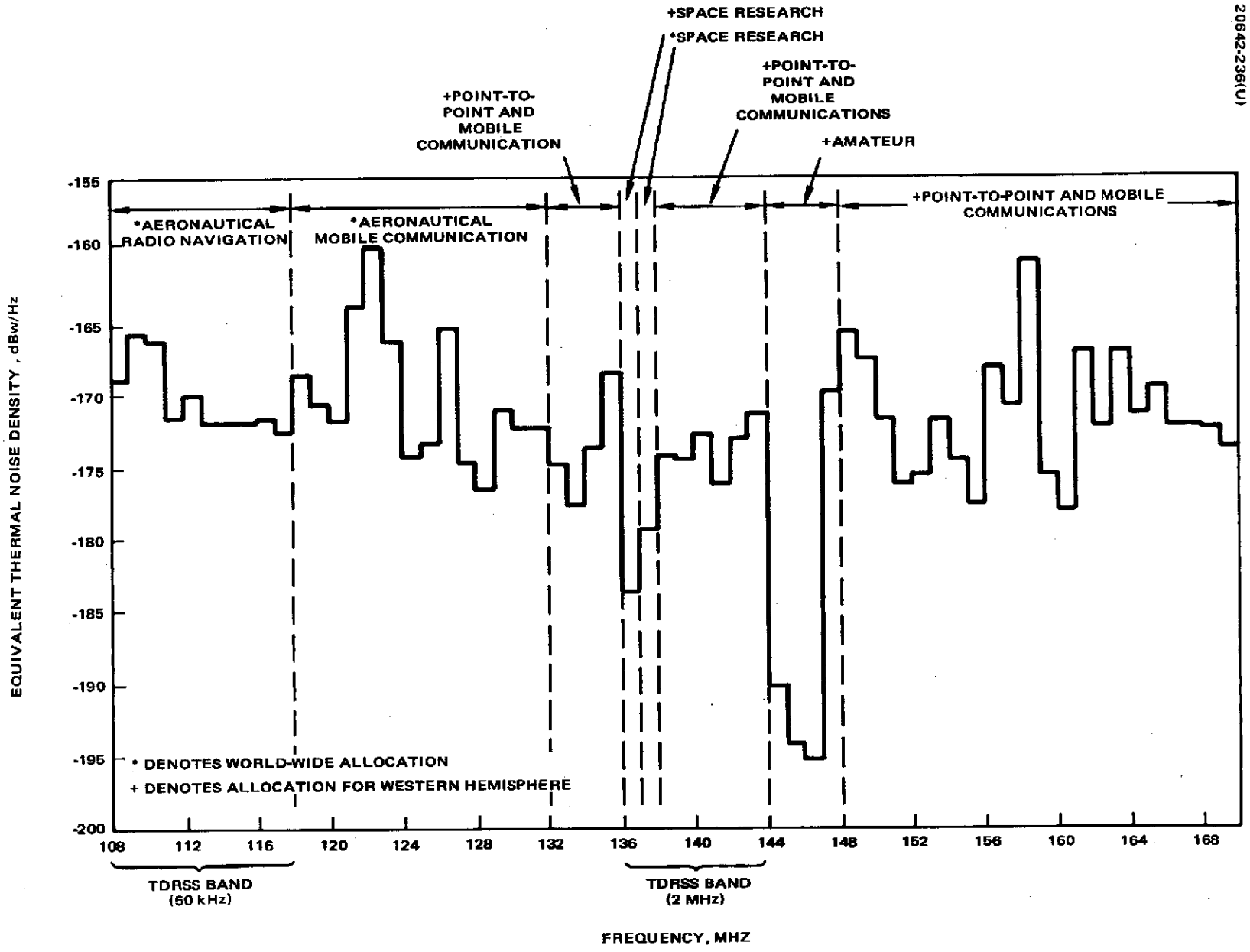

Figure 3-32. ESL, Inc. RFI Prediction for TDRS at 143° W

TABLE 3-8. SUMMARY OF RFI AT NASA FREQUENCIES FROM ESL, INC. PREDICTION PROGRAM

Band	TDRS at 11°W		TDRS at 143°W	
	Noise Density, * dBw/Hz	Number of Emitters	Noise Density, * dBw/Hz	Number of Emitters
136 to 137	-171.3	132	-177.8	56
137 to 138	-169.4	235	-174.8	100
148 to 149	-165.1	114	-160.8	789
149 to 150	-171.0	70	-162.9	852
154 to 155	-170.6	252	-169.9	216

*Equivalent thermal noise level at output ports of 16 dB TDRS antenna (no emitter duty cycle included)

The Statement of Work frequency plan indicated the possibility of a 50 kHz allocation at 117.55 MHz for LDR user command. This service would be located in a band currently reserved worldwide for aeronautical radio navigation which commonly utilizes a phase comparison omnirange VHF omnidirectional radio (VOR) system. Typically, a 30 Hz reference is radiated omnidirectionally as FM on a 9960 Hz subcarrier, and a variable phase 30 Hz signal is radiated as a suppressed carrier AM field rotating at 30 Hz. Assuming an FM modulation index of 5, the required RF bandwidth for VOR is approximately 22 kHz. The VOR transmitters are currently located every 100 kHz in the 108 to 118 MHz band, but plans are underway to double the spectrum utilization by using a 50 kHz separation. The TDRSS could possibly use one of the new locations between 117.50 and 117.60 MHz. The interference noise level at 117.55 MHz would probably be less than that shown in Figures 3-31 and 3-32, since only an average power figure is given for the 117 to 118 MHz band. However, the use of a duty cycle factor is not appropriate since VOR is used day and night worldwide.

The GSFC frequency plan placed the LDR return links in a 2 MHz band between 136 and 144 MHz. The region 136 to 138 MHz is most attractive since it is already allocated to space research, although at 136 to 137 MHz this pertains only to the Western Hemisphere. The ESL report does not

catalog the modulation characteristics of the interfering signals at 136 to 138 MHz, but in the Western Hemisphere many would be NASA or military spacecraft transmissions. These signals or AM voice transmissions would typically be a few kilohertz in bandwidth. Voice transmissions using FM normally require about 40 kHz. Spacecraft ranging signals require much wider bandwidths; the GRARR system uses up to 100 kHz at VHF. A proper characterization of the RFI requires further study of available documentation and also in-orbit measurements. Use of the 136 to 138 MHz band may be quite different in the Eastern Hemisphere. Such a study may also justify a duty cycle factor that will effectively lower the power densities given by ESL.

The LDR user command service may receive an allocation at 400.50 to 401.50 MHz. On a worldwide basis, this UHF region is allocated as follows:

1) 400.05 to 401.00 MHz
   - Meteorological aids
   - Meteorological satellite maintenance telemetry
   - Space research – telemetry and tracking
2) 401.00 to 402.00 MHz
   - Meteorological aids
   - Space telemetering
   - Point-to-point communication
   - Mobile communication except aeronautical

Although the ESL study did not consider these bands, it is believed that, at least in the 400.05 to 401.00 MHz band, international controls are generally adhered to. Even in this band meteorological aids could pose a problem; these include balloon-borne radiosondes.

3.3.1.2 Signal Design and Signal Processing Alternatives

The design effort for the LDR links has involved the end-to-end design of a digital communications system that must provide voice, data, and tracking information from multiple users in a severe channel environment. Figure 3-33 shows the conceptual arrangement of a typical digital communications system. The signal flow of this figure also indicates the logical flow of the following sections. The first section discusses voice encoding techniques for manned users. The second section outlines the primary considerations given to selection of a baseband coding technique for forward error control. The selection of this technique is largely independent of the RF

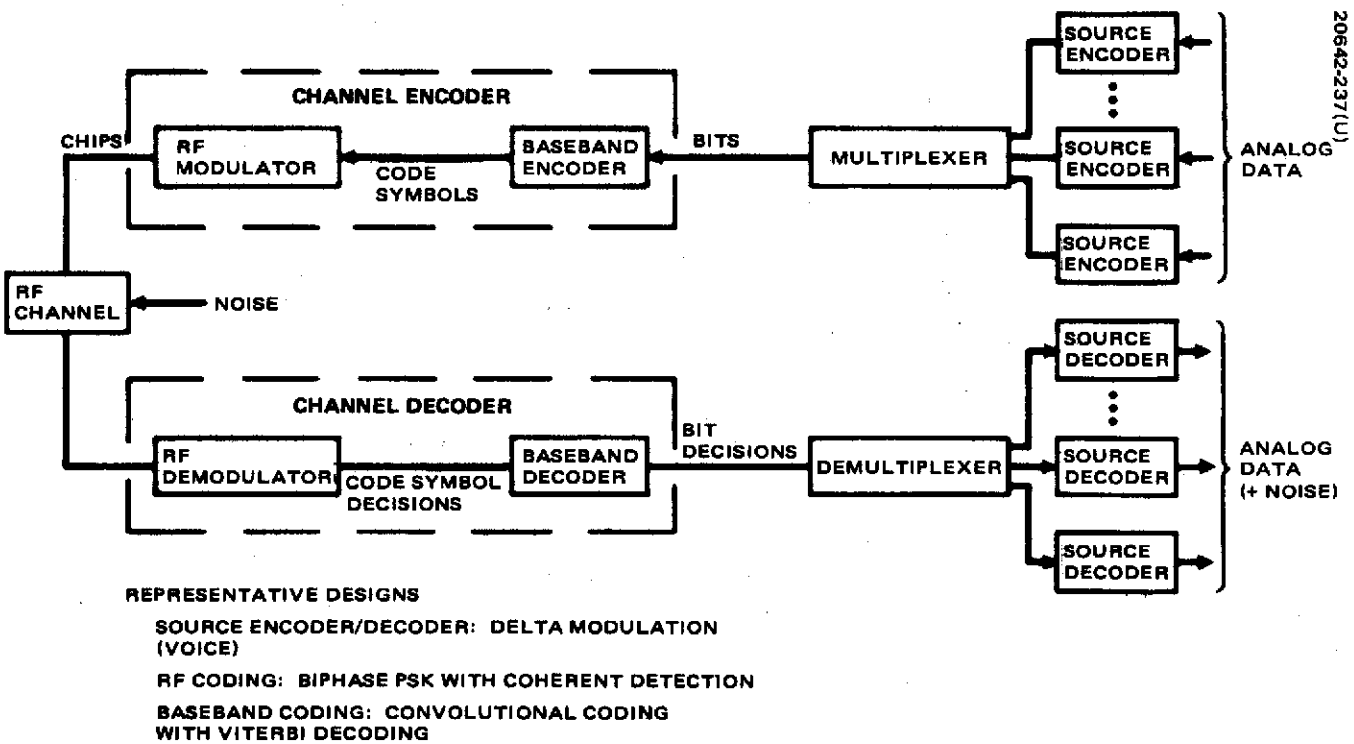

Figure 3-33. Conceptual Arrangement of Typical Digital Communication System

channel characteristics. The major portion of the discussion gives a summary of the techniques available at RF or IF for optimizing system performance. These techniques include antenna design options in addition to signal design.

Source Encoding for Voice. The basic requirement for selection of a voice encoding technique for TDRSS is intelligibility. The requirement set for the Space Shuttle, a potential TDRSS user, is a word intelligibility of 90 percent (Reference 4). Of course, good subjective quality is also desirable. For TDRSS the coding technique must be compatible with data multiplexing, error control coding, anti-multipath schemes, and RF multiple access. Studies of such techniques have been performed by Magnavox for aeronautical applications (Reference 5) and by the Comsat Corporation (Reference 6).

Table 3-9 shows a summary of the Magnavox results. The digital techniques offer ease of compatibility with antimultipath signalling and other schemes. The principal deficiency of the digital techniques is the "threshold" phenomenon where their performance rapidly degrades. The table does indicate that many analog and digital techniques are available that will meet the 90 percent intelligibility condition. In Table 3-9 it is shown that all the techniques have an intelligibility of 95 percent for a bit rate greater than 4.8 Kbps. However, the greater bandwidth techniques such as delta modulation do provide significantly higher fidelity speech reproduction. To account for this effect, a subjective quality rating has been established for the TDRSS study and has been used in preliminary design trades. The rating varies from one to ten. The military's low rate 1.2 Kbps vocoder is assigned a value of 1. The 19.2 Kbps delta modulation technique under study at the Manned Spacecraft Center has been assigned the value of 10. Note that the scale shown in Table 3-10 is such that for low rate techniques, doubling the bandwidth doubles the quality rating. For high rate techniques, an increase in bandwidth produces a much smaller improvement in the rating.

Although less sophisticated modems would be sufficient, it appears that 19.2 Kbps delta modulation would serve TDRSS users with voice of quite good quality. This voice modem has been extensively studied by the Manned Spacecraft Center. The test setup used at MSC is shown in Figure 3-34. A similar 19.2 Kbps delta modulation technique was selected for the tri-service MALLARD communications program. Delta modulation has also been investigated by Bell Telephone Laboratories for commercial service. At MSC, phonetically balanced word intelligibility tests were performed using dual-companding delta and delta-sigma configurations with bit rates of 19.2, 14.4, and 9.6 Kbps. The test setup is shown in Figure 3-34, and the word intelligibility scores are tabulated in Table 3-11.

The principal conclusion of this study is that the intelligibility of delta-modulated voice operated at 19.2 Kbps will be satisfactory if a bit error probability of 10^{-1} (or better) is maintained. However, a subjective evaluation of voice quality at various error rate indicates that an error rate of 10^{-3} or better will provide a channel relatively free of annoying "clicks."

TABLE 3-9. VOICE MODULATION TECHNIQUES

(From Birch and Getzin, Reference 5)

Encoder	Subjective Quality	Intelligibility, percent	Bandwidth, kHz	Performance Threshold, dB Hz	Multiplexing Compatibility	Error Control Compatibility	Antimultipath Compatibility	Multiple Access Compatibility
Source Encoders								
Channel vocoder	Fair	87	2.4	39	Yes	Yes	Yes	Yes
Lincoln Laboratories vocoder	Fair	90	2.4	39	Yes	Yes	Yes	Yes
Predictive coder	Very good	95	2.4 9.6	39 45	Yes	Yes	Yes	Yes
Voice excited vocoder	Very good	95	4.8 9.6	42 45	Yes	Yes	Yes	Yes
Delta modulation	Very good	95	12 20	42 44	Yes	Yes	Yes	Yes
Companded PCM	Very good	95	20	48	Yes	Yes	Yes	Yes
Combined Source and Channel Encoders								
SSB-AM	Very good	?	3	65	F	No	No	F
Ex. Threshold FM	Very good	95	20	40	F	No	No	F
Pulse duration modulation	Very good	95	20	40	F, T, P	No	Yes	Yes

F = frequency
T = time
P = phase

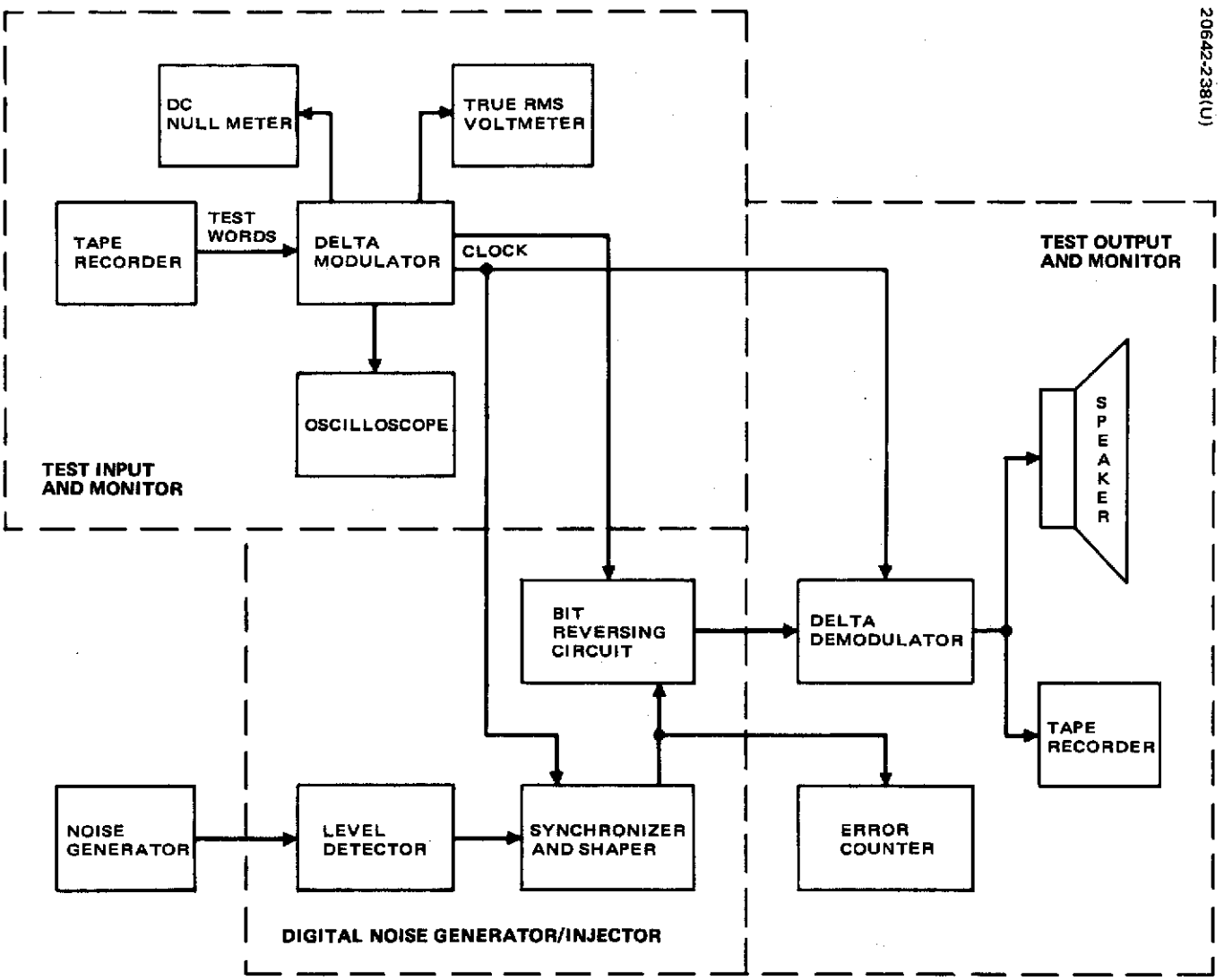

Figure 3-34. Configuration of NASA/MSC Delta Modem Test Setup

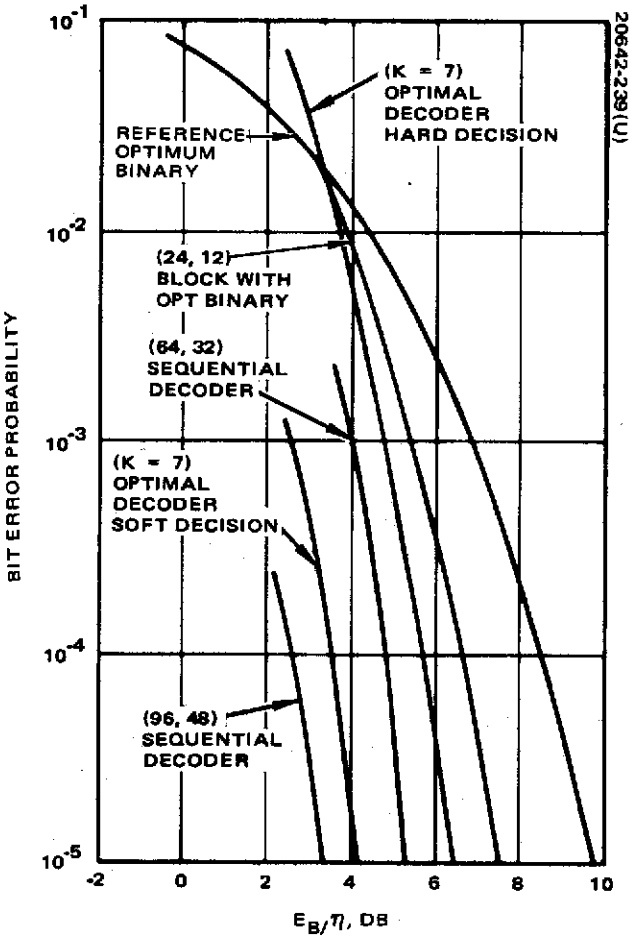

Figure 3-35. Performance of Representative Rate 1/2 Error/ Control Schemes

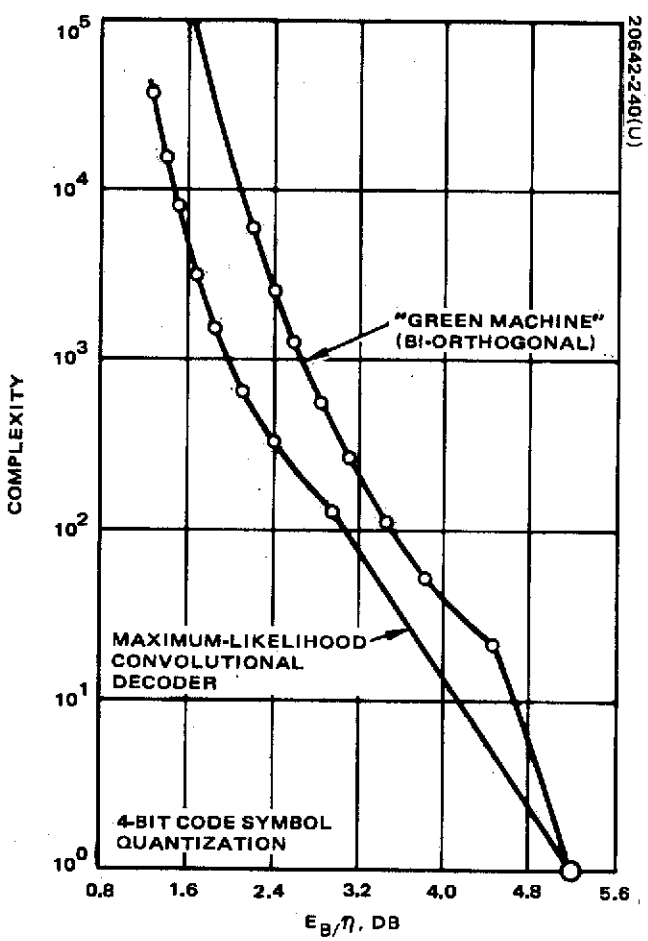

Figure 3-36. Variation of Decoder Complexity With E_b/η Needed to Achieve a 5×10^{-3} Bit/Error Probability (Reference 8)

TABLE 3-10. RATING OF DIGITAL VOICE MODULATION TECHNIQUES

Encoder	Intelligibility, percent	Bandwidth, kHz	Quality Rating
Channel vocoder	?	1.2	1
Lincoln Laboratories vocoder	90	2.4	2
Voice excited vocoder	95	4.8	4
Predictive coder	95	9.6	6
Delta modulation	95	12.	8
Delta modulation	95	20.	10

Baseband Coding Techniques. It is possible that a single baseband coding technique could be found that provides error correction as well as multipath and RFI protection. However, the approach given in the "Multipath/Modulation Study for TDRSS" (Reference 7) is to separate these problems and find optimum solutions for each independently. Although the final design may be sub-optimum, its performance and implementation are much better understood.

Error control codes fall into the two broad categories of block and convolutional. The block codes require block or frame synchronization and are best used with word oriented data streams such as spacecraft command data. In fact, it is recommended that TDRSS users block encode their command data and perform error detection within their command decoders. The user transceiver compatible with TDRSS will output command data with a bit error rate of 10^{-5}, but this may still give an unacceptable false command probability. Although error correction is too complex for the unmanned users, it can be used quite easily in the LDR return link. The user's encoder is quite simple; the rather complex decoder will be located at the TDRSS ground station. For this return telemetry data, convolutional coding is preferred over block coding.

Figure 3-35 shows the performance of several rate 1/2 coding schemes – that is, designs with a bandwidth expansion of two. The (24, 12) code is the only block code shown; several convolutional codes are shown with different decoding algorithms. In general, convolutional codes outperform block codes for a given bandwidth expansion and a given decoder complexity. This type of comparison was performed at the Jet Propulsion Laboratory using biorthogonal block codes with an optimally organized decoder versus convolutional codes with the optimal (Viterbi) decoder (Reference 8). Figure 3-36 shows that the block decoder is from

TABLE 3-11. DELTA MODULATION WORD INTELLIGIBILITY SCORES (PHONETICALLY BALANCED WORD LIST SOURCE TAPE)

Configuration	Transmission Rate, Kbps	Channel Noise, BER	Word Intelligibility Scores, percent
ΔΣ dual comp.	19.2	0.0	96.8 (99.5)*
ΔΣ dual comp.	19.2	10^{-2}	99.1 (99.8)
ΔΣ dual comp.	19.2	5×10^{-2}	97.4 (99.8)
ΔΣ dual comp.	19.2	10^{-1}	91.4 (99.5)
ΔΣ dual comp.	14.4	0.0	98.3 (99.9)
ΔΣ dual comp.	9.6	0.0	94.6 (99.5)
Δ dual comp.	19.2	0.0	98.9 (99.8)
Δ dual comp.	19.2	10^{-2}	99.0 (99.7)
Δ dual comp.	19.2	5×10^{-2}	95.1 (99.4)
Δ dual comp.	19.2	10^{-1}	93.3 (99.7)
Δ dual comp.	14.4	0.0	97.2 (99.3)
Δ dual comp.	9.6	0.0	93.7 (99.5)

*( ): Upper limit performance scores of the source tape. (From Y. S. Kuo, Reference 4).

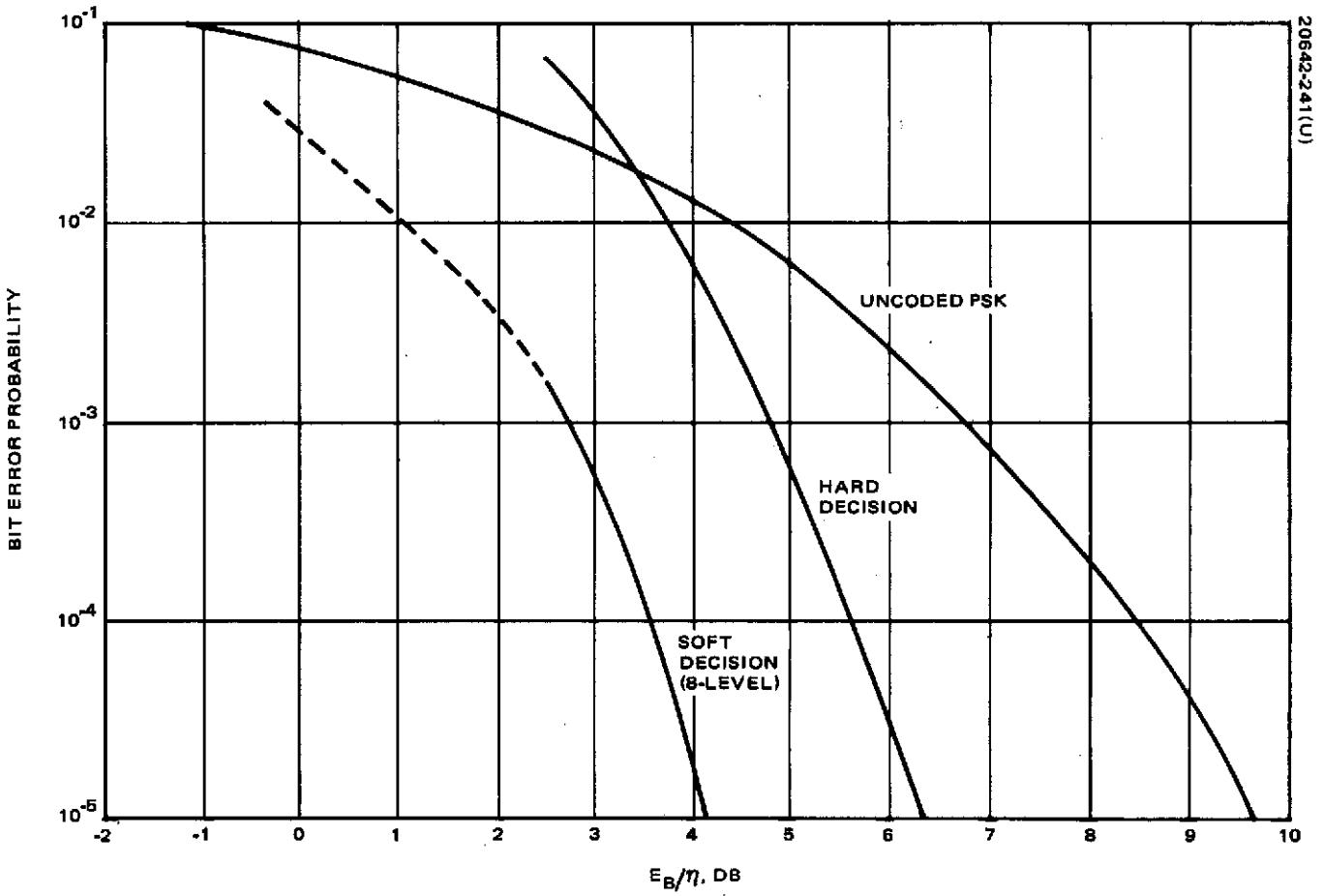

Figure 3-37. Linkabit LV 7026 Convolutional Encoder/Viterbi Decoder Performance

2 to 10 times more complex than the convolutional decoder for the same E_B/η when the required bit error rate is 5×10^{-3}.

Given that convolutional coding is used, two chief alternatives remain as follows:

1) Long constraint length (and therefore powerful) codes with suboptimal sequential decoding

2) Short constraint length codes with optimal decoding

Short constraint length codes must be used with the maximal likelihood decoder since the decoder's complexity increases exponentially with K. It appears that for equivalent complexity this latter alternative is preferred for $P_e \gtrsim 10^{-5}$ (Reference 9). Furthermore, when operating in a burst noise environment like TDRSS, a maximal likelihood decoder requires a much shorter interleaver for error randomization. Figure 3-37 gives performance data for a unit available from Linkabit Corporation. The Hughes link design will be based on these data, but sequential decoding can achieve similar or superior performance. It is not required at this juncture to choose a particular code or decoder. Two points of interest are as follows:

1) $P_e = 10^{-2}$ for voice requires $E_B/\eta = 1.1$ dB

2) $P_e = 10^{-5}$ for data requires $E_B/\eta = 4.1$ dB

RF Design Alternatives. The LDR system design requires consideration of RF design techniques including both signal design and antenna design. This subsection discusses techniques which have been proposed and studied for the LDR system.

Multipath Protection. As discussed in a previous section, the TDRS/user low data rate channel is characterized by severe multipath. For a wide range of geometrical and surface roughness conditions, the average incoherent reflected power will lie between 2 and 10 dB below the direct signal power. Coherent multipath will occur only for large ϕ and will be at least 15 dB down. With no techniques for rejecting multipath, the average signal-to-noise ratios would be limited to 2 to 10 dB without including thermal noise or RFI effects. It is also evident that greater transmitted power will not improve the situation since more power will also be reflected. The applicable techniques for reducing the multipath interference can be placed in two categories: 1) signal processing and 2) antenna discrimination.

Theoretically, appropriate processing could make use of the information contained in the multipath signal. This would ultimately employ a continuum of combiners using correlation techniques to determine the optimum weighting for each branch. The difficulty of implementing this concept led to studies of techniques that avoid the multipath, such as a time hop or burst system, or techniques that effectively reduce the interfering signal by large time-bandwidth correlation. Antimultipath signaling studies have been performed by Hughes (Reference 1), ESL (References 2, 10), Magnavox (Reference 7),

and Hekemian Laboratories (Reference 11). These studies have considered the following:

1) Frequency diversity

2) Pseudorandom time or frequency hopped signal

3) Random access/discrete address

   - Small address system (FH/TH hybrid)
   - Large address system

4) Pseudo noise modulation

   - Narrowband pseudo noise (possible frequency agile)
   - Wideband pseudo noise

5) Programmed systems

   - Time hopped programmed system and adaptive system
   - Frequency hopped programmed system and adaptive system
   - Frequency hopped/time hopped programmed system for all orbits and all data relay satellites

6) Adaptive burst communication

At the start of the TDRS System Study, only pseudo-noise modulation and adaptive burst communication survived analytical scrutiny. A review of these alternatives during the study led to the following conclusions:

1) Both will work and provide satisfactory reduction of multipath interference.

2) Both require complex processing to provide initial time synchronization of receivers to the incoming signal, i.e., signal acquisition.

3) Neither technique by itself results in a significant reduction of RFI

However, consideration of system and implementation aspects revealed some disadvantages of the burst transmission technique that the spread spectrum technique does not have:

1) For reliable communication, each transmitter must operate in a separate frequency band. In order to accommodate all users

in the portion of the available VHF band which is quietest in terms of RFI, the channels must be approximately 50 kHz or less which will severely limit the range measurement accuracy.

2) The forward link repeater may be unconventional in order to provide high peak power levels while requiring the same average power as for a conventional repeater.

3) All other things being equal, the link capacity will be somewhat smaller due to the rise time required for transmitters used in a pulsed mode.

4) Signal timing parameters are determined by the orbital geometry and thus a single forward link timing format would not be as good for one orbit as for another. (See Figure 3-38.)

From the above considerations, it appears that the spread spectrum approach is more attractive and will result in better system performance with lower costs.

Pseudo noise modulation protects against both diffuse and specular multipath. If the former is such that its characteristics approach that of Gaussian noise, the PN coding gain is R_c/R_b where R_c is the chip rate and R_b is the bit rate. The specular multipath is defined to be a delayed replica of the direct signal. Here the protection is enhanced since the reference PN waveform is correlated against the received (multipath) waveform and provides a $(R_c/R_b)^2$ gain in terms of power. This assumes the perfect autocorrelation shown in Figure 3-39 and that the differential time delay is not a multiple of the code time.

There are two basic single aperture, antenna discrimination techniques: 1) directivity and 2) circular polarization. Since the TDRS antenna is circularly polarized for transmission and the gain is fixed by the coverage requirements, these techniques only apply to users. However, current requirements include omnidirectional antennas on both manned and unmanned users. The only remaining option is circular polarization for the user antenna. This may be difficult for small unmanned users where whip arrays are attractive, but for a manned user such as the Space Station, circular polarization is a reasonable alternative. Hughes has suggested a VHF array in Reference 12 which would allow circular polarization and omnidirectional coverage. Its basic characteristics are given in Table 3-12 and Figure 3-40. A similar array could be designed for the Space Shuttle with cavity backed dipole elements. However, surface area utilization would limit the number of elements and therefore the pattern uniformity and ellipticity. Figure 3-41 shows the ellipticity is 4 dB at 60 degrees off axis for a crossed dipole.

Polarization discrimination is based on the fact that during reflection the sense of rotation of the E vector is reversed if the angle of incidence is smaller than the pseudo Brewster angle. An estimate of the effect of circular polarization is shown in Figure 3-42 and is repeated from 3. 3. 1. 1.

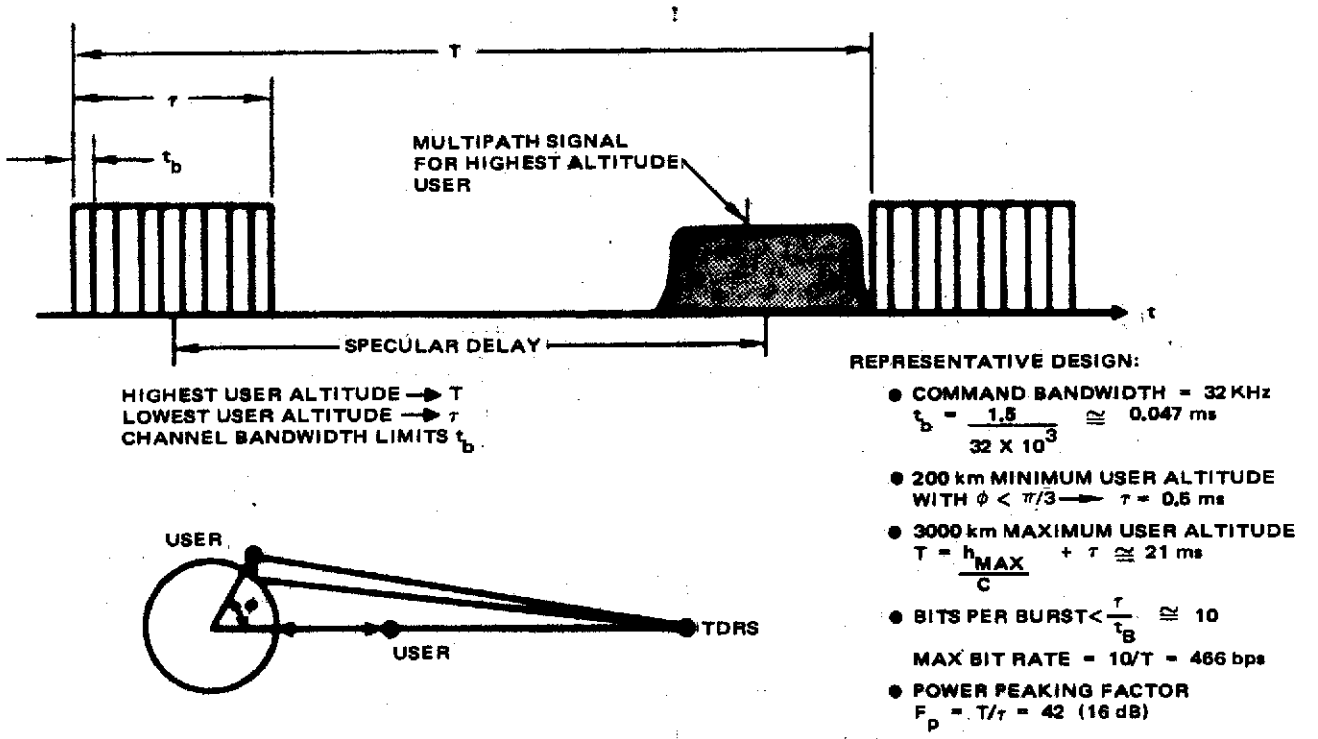

Figure 3-38. Burst Transmission: Common Command Format

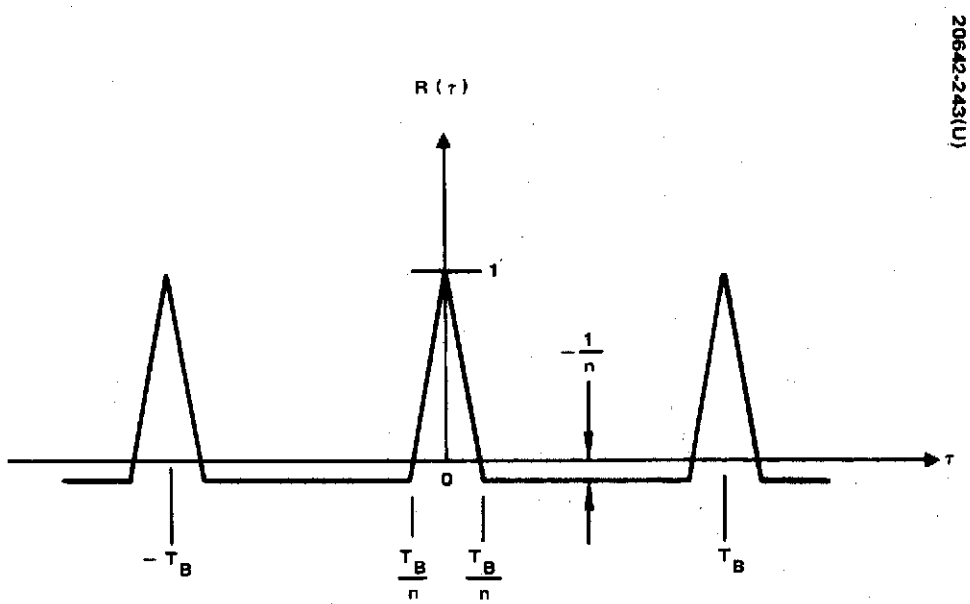

Figure 3-39. Autocorrelation Function of PN Sequence

TABLE 3-12. PERFORMANCE OF VHF ARRAYS FOR MANNED SPACE STATION

Circumferential Array*			Axial Array**	
Degrees Off Axis	G	Ellipticity, dB	G	Ellipticity, dB
0	+0.5	1	+2.5	1
10	+0.1		+2.2	
20	-0.5		+1.5	
30	-1.6		+0.5	
40	-3.0		-1.1	
45	-4.0	5	-2.0	5
50	-5.0		-3.0	
60	-7.5	10	-5.5	10
70	-10.5		-8.5	
80	-14.5		-12.5	

*Ripple = ±1 dB at 0 degree, ohmic loss = 1.5 dB.
**Ohmic loss (per element) = 0.4 dB.

It can be seen that the average multipath power will be at least 12 dB below the direct signal with circular polarization and a user ellipticity of 4 dB. As mentioned above, this corresponds to 60 degrees off-axis for a typical crossed dipole element.

RFI Protection. Both signal design and signal processing techniques can possibly provide protection against RFI. In the broad sense of signal processing, antenna design at both the user and TDR satellite is included. For any of these design approaches to be successful, a characterization of the RFI environment is required. An RFI analytical model is unavailable at this time. Experimental data from in-orbit measurements should be the basis for future TDRS system design decisions.

If many broadband emitters are present in the LDR telemetry or command bands, the resultant interference can be modeled by white Gaussian noise. Protection against Gaussian noise is only provided by error control coding such as the convolutional coding which was selected above. The use

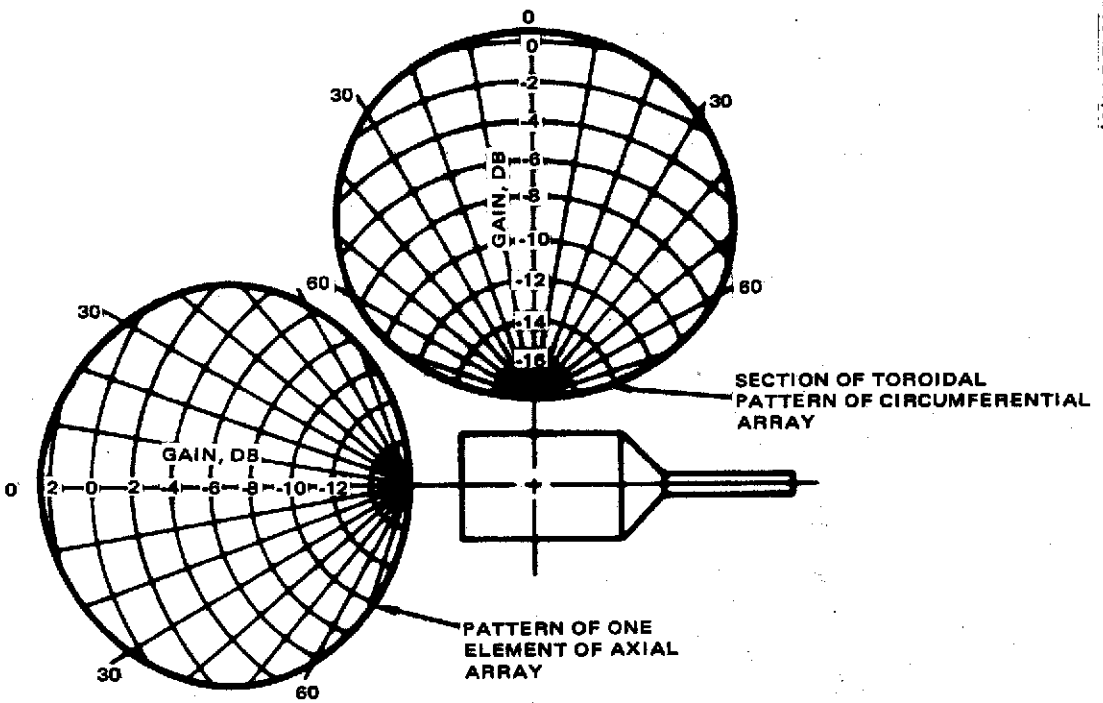

Figure 3-40. Gain Patterns of VHF Arrays

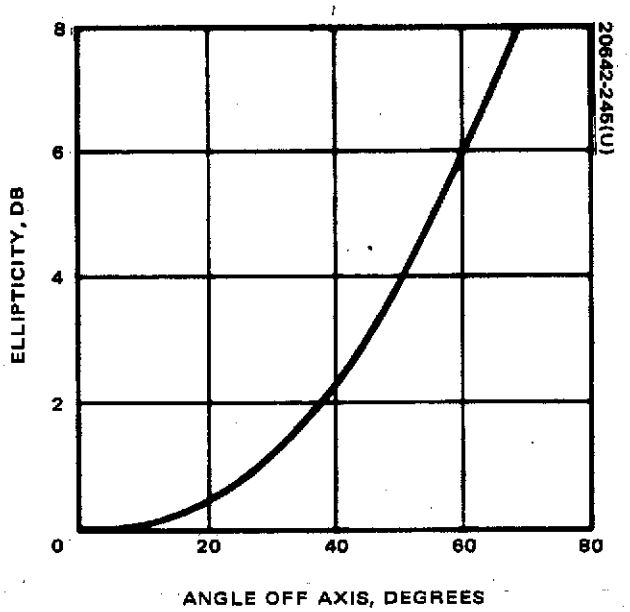

Figure 3-41. Ellipticity Off Axis for Crossed Dipole Antenna

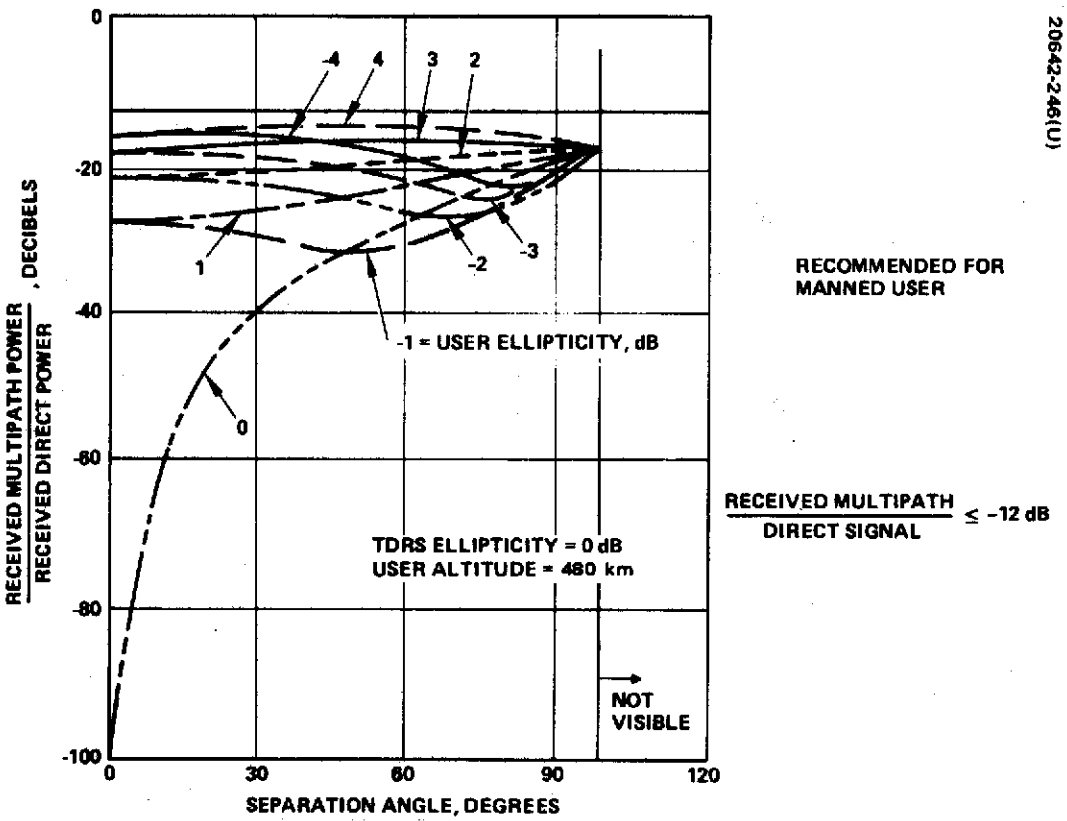

Figure 3-42. Circular Polarization Discrimination

of PN or other spread spectrum modulation techniques does not improve the system performance against Gaussian noise above that available with convolutional coding. However, if it is assumed that some of the emitters are narrowband, certain other techniques are attractive. The ESL, Inc. Study (Reference 3) recommended a hybrid modulation system which permits avoidance of bands with high RFI levels, but also has a 10 dB spread factor against multipath. This system would use dual-diversity in the best 400 kHz of the 136 to 138 MHz band, quad-diversity in the next best 800 kHz, and would not utilize the worst 800 kHz at all. Although attractive, this approach does not appear compatible with the TDRSS requirement for ranging. Spread spectrum modulation techniques do not avoid narrowband RFI in this manner, but they do permit filtering at the receiver. Notch filter schemes permit suppressing signals in about 10 kHz or 1 percent of the received spectrum by 30 dB with a degradation in the desired signal of less than 0.5 dB (Reference 13). This data is given in Figure 3-43. Hughes Ground Systems Group has built a device with 18 automatic tracking notch filters in three sequential banks. For the LDR return link such filters would be nominally located at 50 or 100 kHz intervals since frequency assignments are given at this spacing. Even without filtering, narrowband signals appear to be attenuated in a pseudo noise system by a factor n, where n is the code length, and are further suppressed by the coherent receiving process. An interfering carrier at $\Delta\omega$ from the desired carrier is attenuated by

$$\left| \frac{\sin \Delta\omega \frac{T_B}{2}}{\Delta\omega \frac{T_B}{2}} \right| \cos \phi$$

where $\phi = \theta - \Delta\omega T_B/2$ and θ is random.

As in the case of multipath, the most desirable antenna technique is to maximize the receive gain in the desired signal's direction and minimize the gain in the direction of the interference. For the relatively unsophisticated user this is quite difficult, but the forward link RFI can be circumvented operationally by commanding the users only over RFI free regions. Return link RFI is a more difficult problem since the TDRS antenna coverage requirement includes the entire earth. One possible technique would be to use a TDRS antenna with multiple elements. The signals from the antenna could be processed on the ground for each user separately to maximize the signal-to-noise. This would amount to producing nulls in the direction of the emitters and a gain peak in the direction of the user. The principal difficulty with this technique is that with a reasonable number of elements the shape of the effective pattern is quite limited, and the RFI emitters may not be situated in one of the required geographical arrangements. The technique also offers only a small advantage when the user is over a region with many RFI sources. Either onboard storage would be required or data would be lost. There also exist potential implementation problems. The relative gain and phase of the

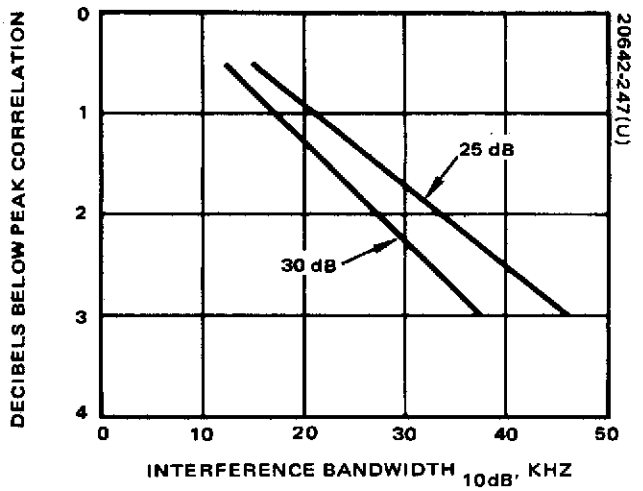

Figure 3-43. Correlation Drop Versus Bandwidth of Interfering Signal for 25 and 30 dB Suppression ($f_o = f_c$)

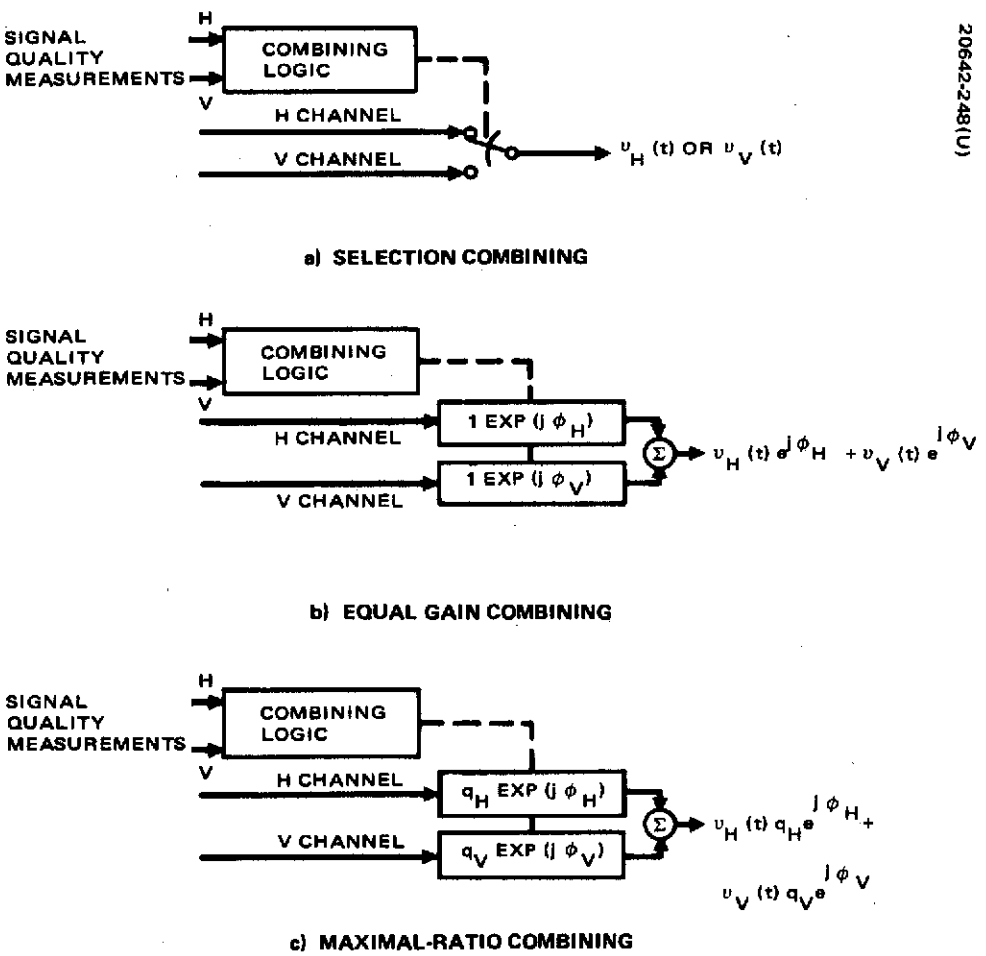

Figure 3-44. Linear Combining Alternatives

communication channels used for the output of each antenna element must be carefully controlled. Furthermore, the complex weighting factors used before the channels are summed must be calculated a priori or determined by previous system operation; any single user's PN signal can not be singled out at IF. This multiple element antenna technique warrants further investigation if studies indicate that RFI sources are distributed geographically such that the performance gain is significant.

Polarization Combining. The polarization combining required at the TDRSS ground station is similar to the processing described above. The low data rate user satellites of the TDRS system utilize relatively unsophisticated linearly polarized antennas. Since the orientation of these antennas will vary with respect to the receiving antenna of the TDRS, the TDRS design includes independent reception at horizontal and vertical polarizations. These H and V channels are transmitted to the ground independently for processing. During the study various forms of diversity combining were considered. Figure 3-44 shows three basic schemes commonly employed; the first two techniques are special cases of the third. The use of a circularly polarized antenna at the spacecraft is essentially a special case of technique B in which the two channels are summed after one is phase-shifted 90 degrees. Any polarization diversity schemes considered should be compared to this very simple, but effective alternative.

The TDRSS application is unique only in that at IF a given user's signal cannot be identified. A correlation receiver is required to remove a user's signal from the signals of the other users, the multipath, and the RFI and thermal noise. Figure 3-45a shows a scheme in which the α_i are derived from the strengths of the carrier of two separate correlation receivers. The "recovered" carrier signals are used since they have high SNRs; it is assumed the noise level is the same in each channel. The complex weighting factors (α_i) are used to weight the signals in the H and V channels before processing by the convolutional decoder. The approach of Figure 3-45a is straightforward, but it has two difficulties. Performance will be degraded since a convolutional code symbol decision is made by the correlation receivers before combining. Even if the correlators output a digital word rather than a hard decision, some "thresholding" will occur. This approach also requires the use of two correlators operating in parallel. Figure 3-45b shows a predetection scheme in which the α_i are stepped sequentially until the correlation receiver achieves lock. Acquisition of a given user's signal now involves a search in "polarization" in addition to frequency and code time. It might be possible to simplify this procedure by the use of a priori information, but the approach could be difficult to implement. It is required that multiple selectable phase characteristics be available at IF and that compensation for different transfer characteristics in the H and V channels is provided.

Theoretically, once the correlation receiver is in lock, the performance of either pre- or postcorrelation combining will be the same. Figure 3-46 shows the performance of the three basic combining techniques assuming both coherent and incoherent noise in the two channels. An assumption of coherent noise may be the better model for an RFI limited

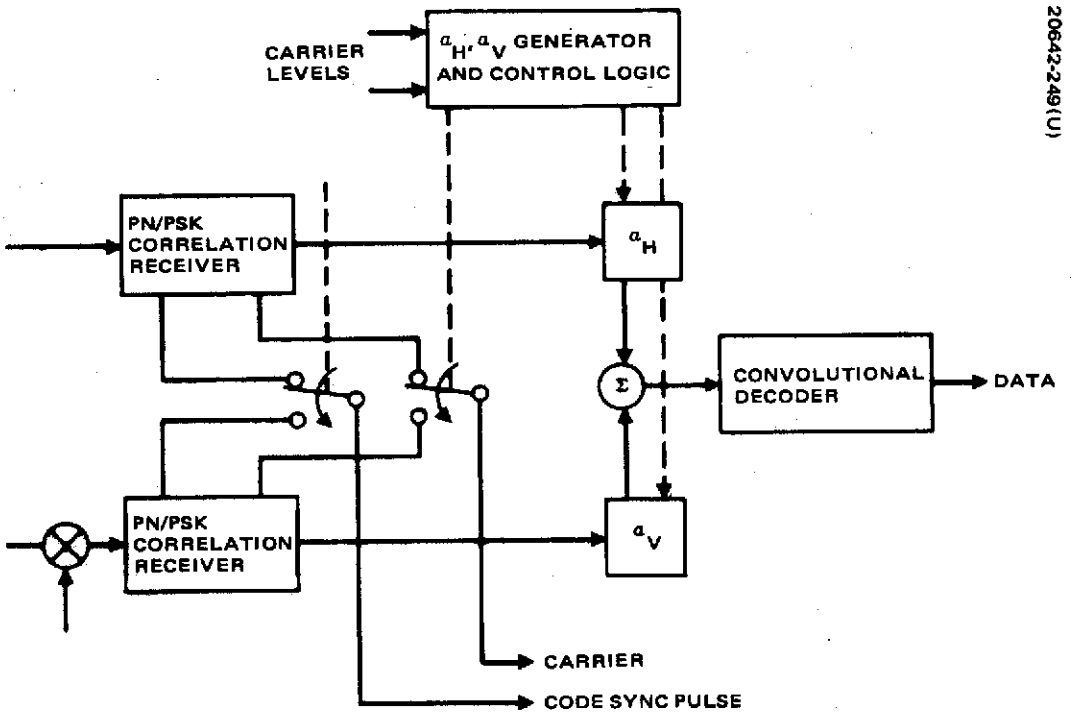

a) POSTCORRELATION COMBINING

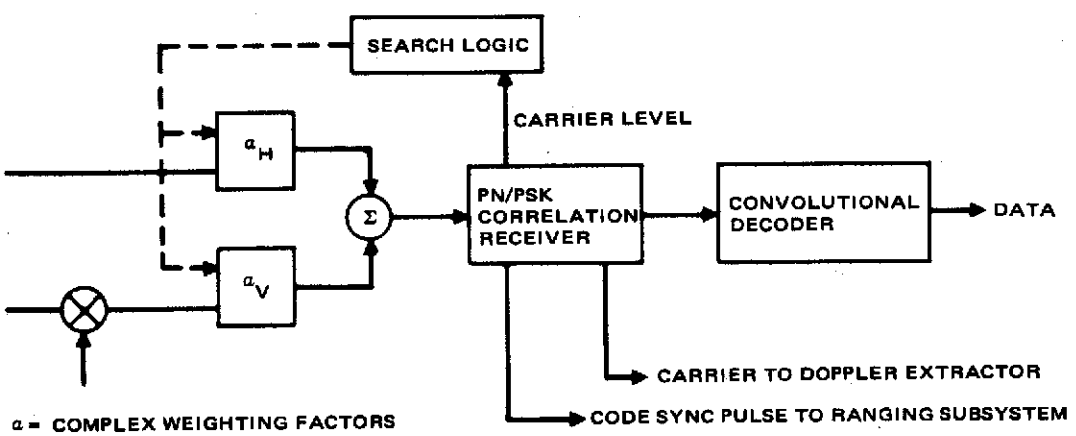

b) PRECORRELATION COMBINING

Figure 3-45. Precorrelation Versus Postcorrelation Diversity Combining

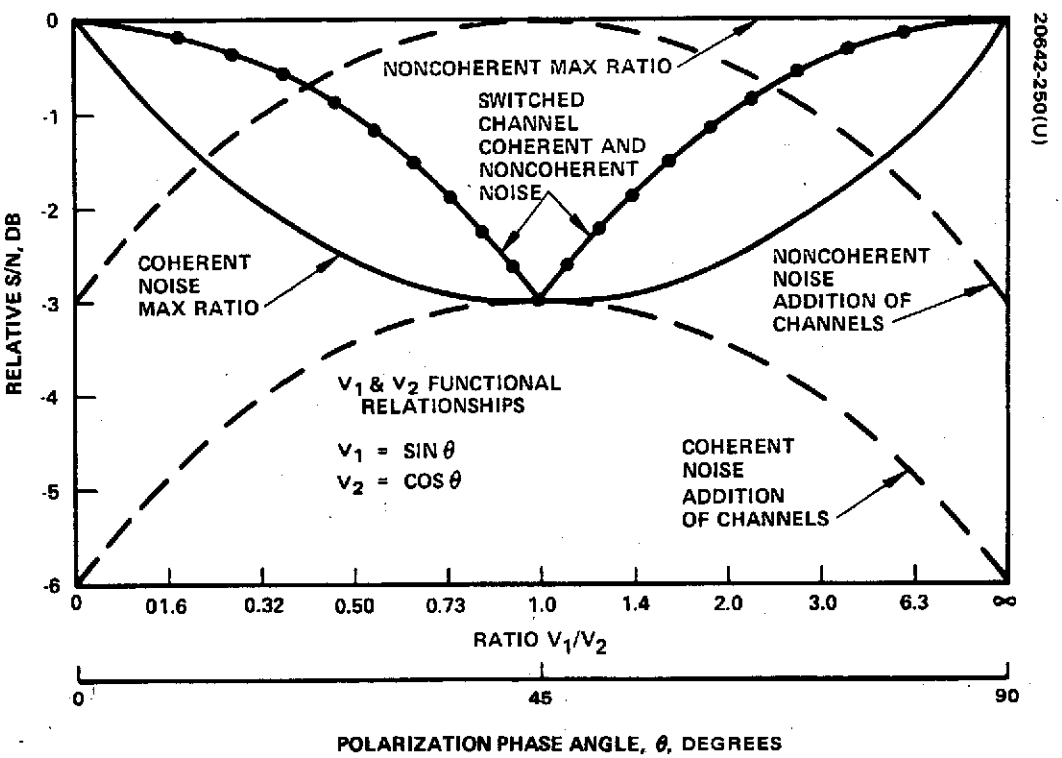

Figure 3-46. Baseband Combining Techniques

system, but data are unavailable. It has been decided to implement a maximal-ratio combiner at the ground station, but if the noise is coherent it can be used as a selection combiner. Figures 3-47 and 3-48 aid in specifying the characteristics of the downlink channels carrying the H and V signals. The first figure shows the degradation in output SNR when one channel has a gain variation with respect to the other. When a majority of the signal power is in the H channel – that is, when θ is small – emphasis of the V channel causes an SNR degradation. The combiner is relatively insensitive to differential gain variations because an AGC circuit is used at the combiner output. A gain variation or gain error of 4 dB will produce a degradation less than 0.25 dB. Figure 3-48 shows that for differential phase errors of 0.26 radians or less the degradation in the SNR is essentially negligible. When the signals are of equal strength and out of phase by $\pi/2$ radians, the degradation will of course be 3 dB.

RF Multiplexing. Both the forward and return link portions of the LDR service system require multiplexing of signals at RF. The forward link requires the multiplexing of command signals from the two relays when users are in the dual coverage region. Forward link voice may also be present. The return link specification requires capability for voice from one user and telemetry from twenty simultaneously per TDRS. The alternatives normally considered for such satellite applications are TDM (time division multiplex), FDM (frequency division multiplex), and CDM (code division multiplex). Time division multiplex was quickly dismissed for the return link because of the timing problem for users whose range is constantly changing. The FDM approach is the most commonly used and was studied as an alternative during the system design. The CDM approach is relatively new and requires discussion.

In a CDM system where each user has the same nominal carrier frequency, a given user is distinguished by a digital code. The pseudo noise codes already considered for ranging and multipath have optimal autocorrelation properties and, by a careful selection process, classes of sequences can be constructed which have good crosscorrelation properties as well. Pseudo-noise – or more precisely, maximal length linear shift register sequences – are, of course, not random because they are completely specified by the characteristic polynomial and initial conditions which describe the linear shift register and feedback connections. Although they do have certain randomness properties, the characteristics of these codes which are of interest to TDRS are as follows:

1) Each has a period p if p is the smallest positive integer for which the associated characteristic polynomial divides the polynomial $1 - x^P$.

2) Each has a correlation function of the form shown in Figure 3-49.

If the M-sequences (maximal length or PN sequences) are members of special families called maximal connected sets, they also have good crosscorrelation properties. That is, they will cause minimal interference when used as the

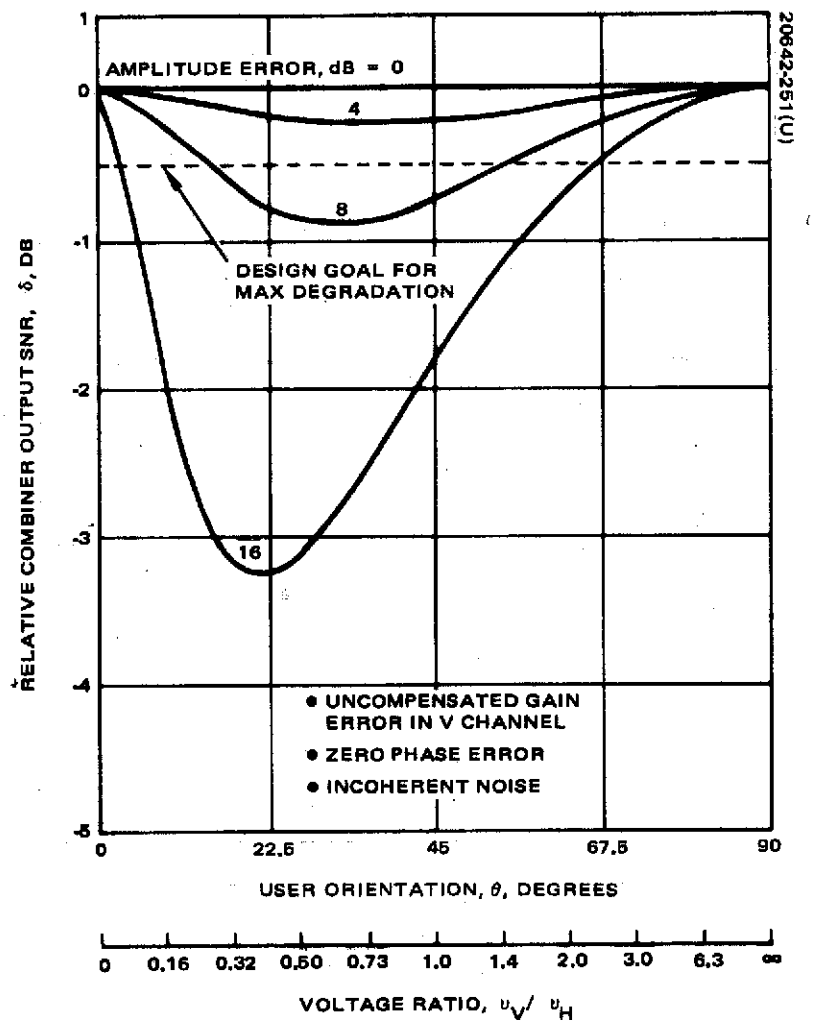

Figure 3-47. Maximal Ratio Combiner Sensitivity to Phase Errors

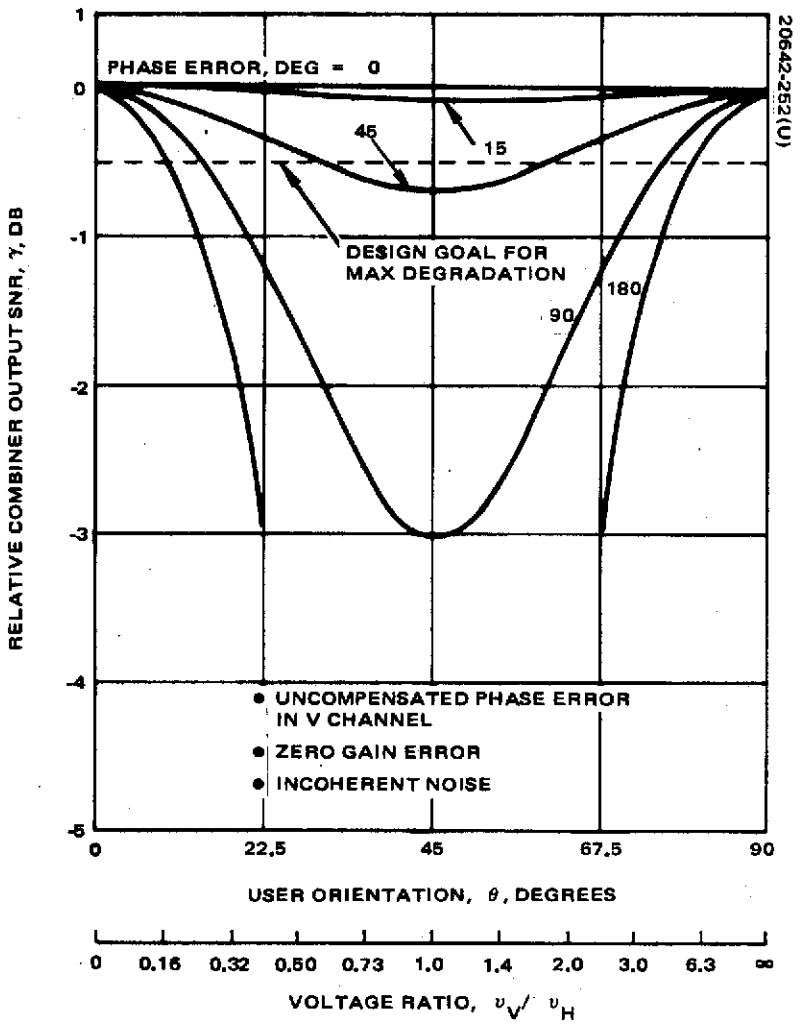

Figure 3-48. Maximal Ratio Combiner Sensitivity to Phase Errors

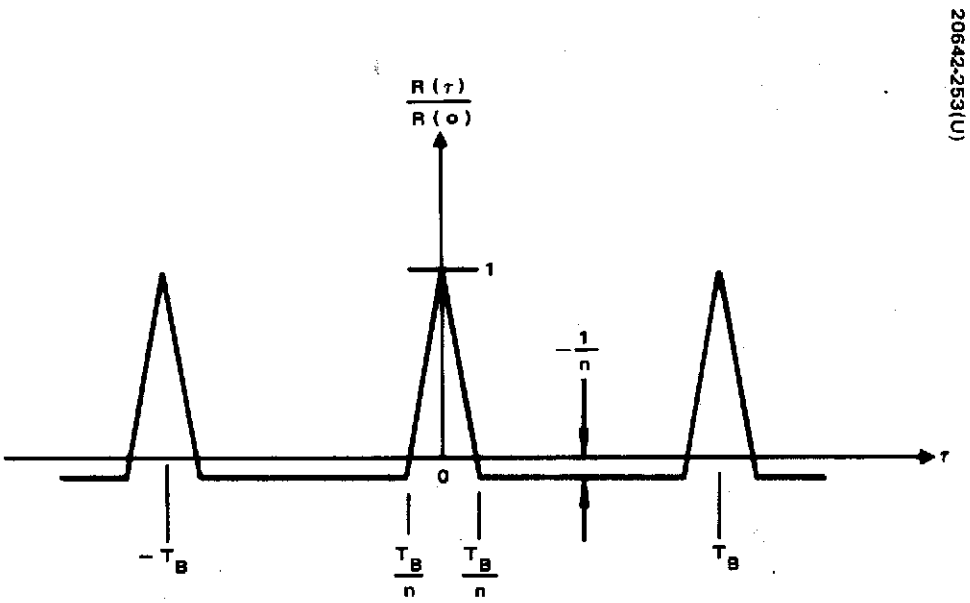

Figure 3-49. Autocorrelation Function of Pseudo Noise Sequence

TABLE 3-13. SUMMARY OF M-SEQUENCES AVAILABLE FOR CDM SYSTEMS

Register Length, n	Code Period, P	Size of Set (Number of Sequences)	Bound on Unnormalized Crosscorrelation, $\theta_{maximum}$	$^{*}(N_o/E_s)_{eff}$
5	31	3	9	19.010^{-3}
6	63	2	17	11.210^{-3}
7	127	6	17	6.0010^{-3}
8	255	0	--	—
9	511	2	33	1.3210^{-3}
10	1023	3	65	0.6610^{-3}
11	2047	4	65	0.3210^{-3}
12	4095	0	--	--
13	8191	4	129	?

*Typical value for the mean-square crosscorrelation to data symbol energy ratio for two codes based on computer simulation.

identifying codes in a CDM system. If such codes exist for a given register length, n, the crosscorrelation for synchronous CDM will be limited to -1, $-2^{(n+2)/2}$, and $2^{(n+2/2)} - 1$ as illustrated in Figure 3-50. Gold and Kopitzke (Reference 14) have experimentally determined the maximal connected sets for $n \leq 13$; Table 3-13 summarizes these results. The last column of the table is based on a computer study by Hughes which includes crosscorrelation effects for asynchronous CDM too complex to be computed algebraically. This study is summarized in Appendices A, B, and C.

Figure 3-51 illustrates the problem of crosscorrelation in an asynchronous CDM system. Partial correlation occurs when data modulation causes a code inversion in the middle of one user's code period with respect to the code period of interest. The Case I condition of full correlation has been bounded or computed analytically for many codes. A histogram of the full correlations for the 2047 code selected for the forward link is given in Figure 3-52; note that it is three-valued. Figure 3-53 gives a partial crosscorrelation histogram which has been computer generated by varying the window W from 1 to 2047. Much larger values for $|\theta|$ are shown in the second figure than in the first, but their frequency of occurrence is also much less. The analysis of Appendix C essentially computes the variance of the crosscorrelation function and hence an effective crosscorrelation noise density-to-data symbol ratio.

The N_o/E_s values of Table 3-13 decrease linearly with n; i.e., the bandwidth expansion, to a very good approximation.

$$\left(\frac{N_o}{E_s}\right)_{eff} = 12. \times 10^{-3}\,\frac{63}{n} \qquad \text{for } n \leq 63$$

Since the correlation process is linear, the interference noise level will also vary linearly with the power of the interfering users.

$$\therefore \left(\frac{N_o}{E_s}\right)_{eff} = \frac{0.76}{n} \sum_{i=2}^{K} \frac{P_i}{P_1}$$

where P_i is the power of one of (K - 1) interfering users. With $R_c = nR_s$ and a time-bandwidth product of $b = B_{RF}\,T_c = B_{RF}/R_c$, we have that

$$R_s = \frac{R_c}{n} = \frac{B_{RF}}{nb}.$$

From above,

$$\left(N_o\right)_{eff} = \frac{P_1}{R_s} \frac{0.76}{n} \sum_{i=2}^{K} \frac{P_i}{P_1}$$

$$= \frac{nb}{B_{RF}} \frac{0.76}{n} P_1 \sum_{i=2}^{K} \frac{P_i}{P_1}$$

$$= 0.76 \frac{b}{B_{RF}} \sum_{i=2}^{K} P_i$$

Other studies have shown that b should be in the region of 1.0 (see Appendix E). Therefore, the effective crosscorrelation noise density for $n \leq 63$ is given by

$$\left(N_o\right)_{eff} = 0.76 \sum_{i=2}^{K} \frac{P_i}{B_{RF}}$$

The interference power of each user is spread across the RF bandwidth and is attenuated by 1.2 dB. This result roughly agrees with that given in Reference 7 although the analysis approach is quite different.

The above results show that PN codes will function quite well in asynchronous CDM if the bandwidth expansion is sufficient. Unfortunately, 40 PN codes or M-sequences of appropriate lengths with good crosscorrelation properties are not available. A related class of codes called Gold codes will be used for the return telemetry link. Although their autocorrelations are not optimum, it has been shown during the study that their crosscorrelation performance is nearly equal that of M-sequences. Figure 3-54 shows the LDR return link degradation due to CDM using Gold codes. The crosscorrelation between any two codes was assumed to be representative worst case number taken from the several codes investigated.

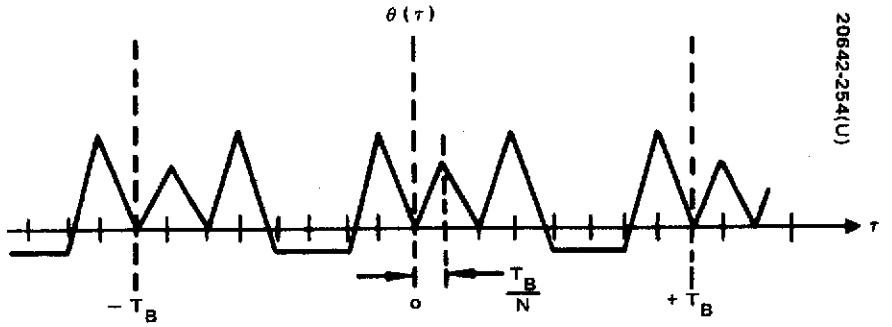

Figure 3-50. Illustrative Three Valued Crosscorrelation Function

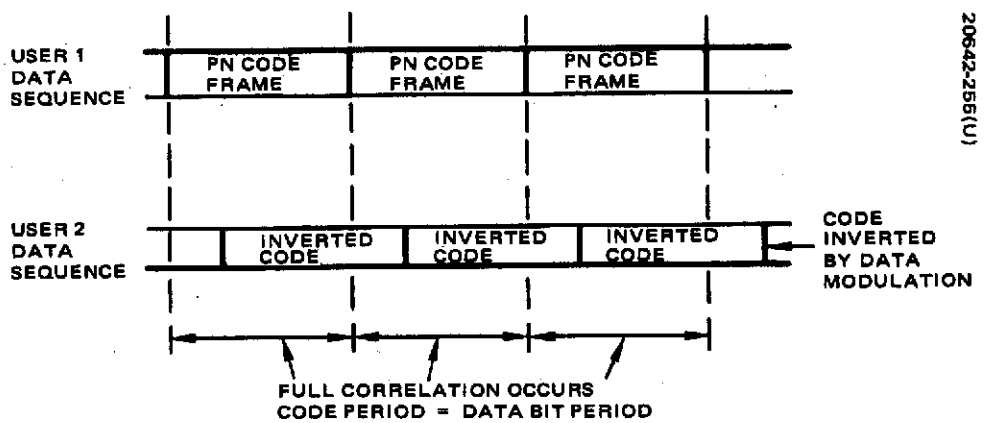

a) CASE I FULL CROSSCORRELATION

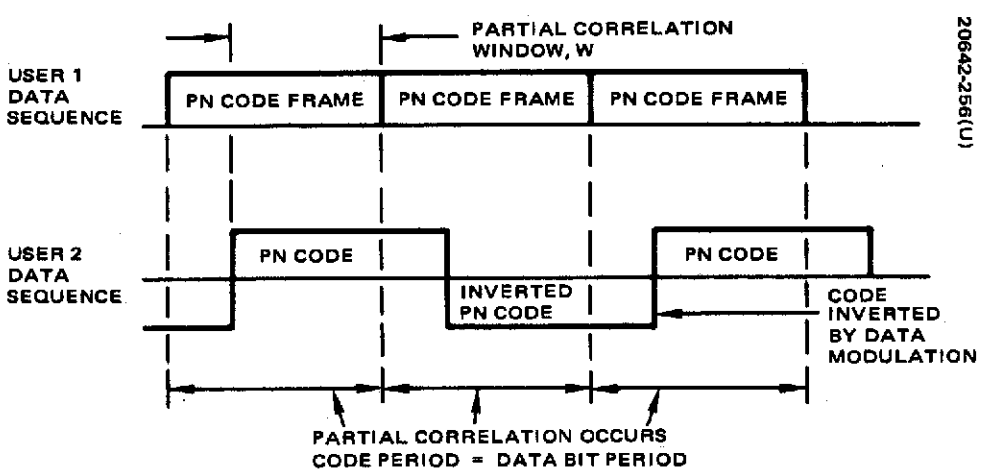

b) CASE II PARTIAL CROSSCORRELATION

Figure 3-51. Crosscorrelation in Asynchronous Code Division Multiplex

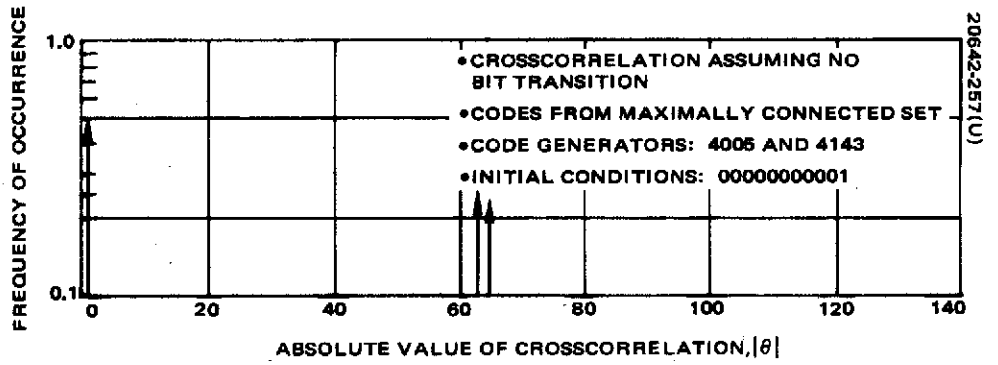

Figure 3-52. Histogram of Full Crosscorrelations for Typical 2047 Length Pseudo Noise Code

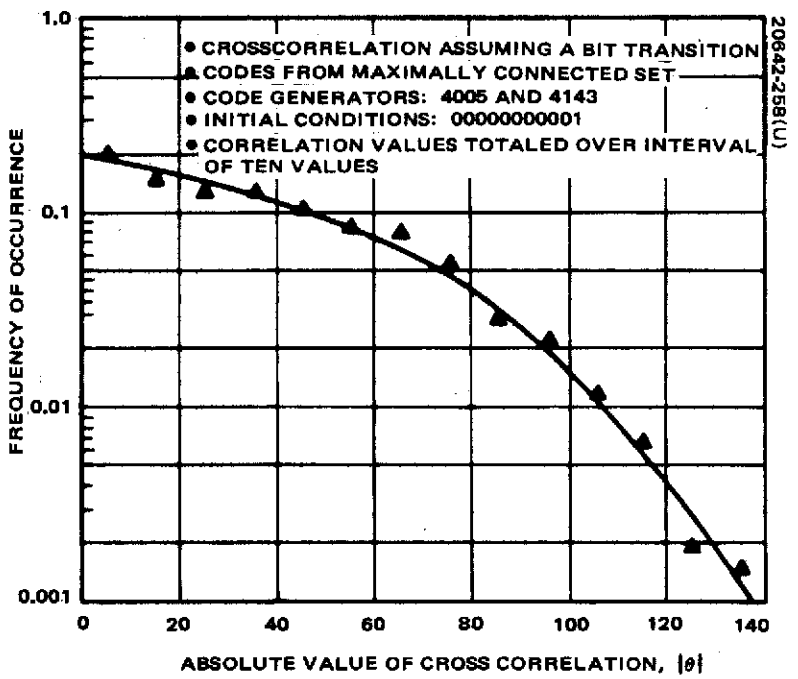

Figure 3-53. Histogram of Partial Crosscorrelations for Typical 2047 Length Pseudo Noise Code

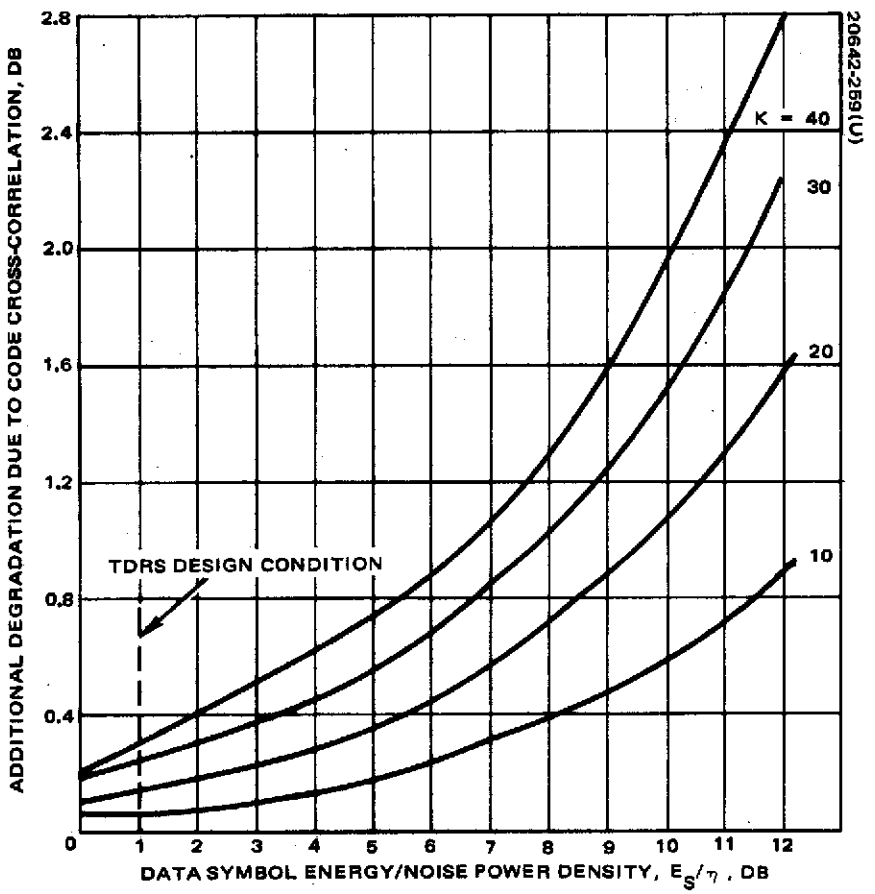

Figure 3-54. Crosscorrelation Degradation With Gold Codes of Length 511

3.3.1.3 Low Data Rate Forward Link Design

The LDR forward link service must be capable of sending command data and voice to users simultaneously. Two frequency bands have been specified as possibilities: 1) a 50 kHz band at 117.55 MHz (VHF) and 2) the 1 MHz band at 400.5 to 401.5 MHz (UHF). The design challenge in the VHF band is in providing the required multipath rejection and dual signal capability both within 50 kHz. In addition, range measurement accuracy is limited by this bandwidth. At UHF the use of fixed gain antennas, i.e., TDRS earth coverage and user omni, results in a space spreading loss approximately 10 times greater than at VHF. An additional problem with UHF is the antenna and/or feed requirements in combination with those for the return link at VHF (136 to 144 MHz).

The approach to the forward link design was to develop first a preferred concept at VHF and then do the same for the UHF band. The two concepts were then compared on communication and tracking performance, link margin, susceptibility to multipath and RFI interference greater than that assumed in the design and on the impact on TDRS and user weight and configuration.

Spread Spectrum Link Analysis. For a spread spectrum forward link, the bit energy-to-noise density ratio after correlation is given by

$$\frac{E}{\eta} = \frac{P_1 \, d/R_b}{\eta_T + \eta_{RFI} + \dfrac{\sum_{i=1}^{K} m_i P_i + 0.76 \sum_{i=2}^{K} P_i}{R_c}}$$

where

P = received signal power

d = factor accounting for bandlimiting effects

R_b = bit rate

R_c = chip rate

η_T = thermal noise density in receiver system

η_{RFI} = interference noise density due to earth based sources

m_i = multipath power ratio due to earth reflection of TDRS transmitted power

The lack of available bandwidth at VHF led to a study of PN system performance with bandlimiting (see Appendices D and E). This analysis of the correlation process has led to Figure 3-55 which shows that the processing gain is limited by the RF bandwidth and, specifically, that increasing the chip rate beyond a value of twice the bandwidth produces no additional gain. Figure 3-56 shows the effect of the ratio of RF bandwidth and chip rate on the range measurement error. For a sharp cutoff filter in the receiver, a value of B_{RF}/R_c of 1.0 is again satisfactory. Increasing B_{RF}/R_c above 1.0 will increase the equipment complexity, but give little improvement against multipath; performance against thermal noise would be reduced. The value of d is shown in Figure 3-57 as a function of the ratio, B_{RF}/R_c. Appendix E shows that d is the decrease in the peak correlation function.

In order to minimize partial correlations and simplify the electronics, a command bit will be made to coincide with an integer multiple, k, of code of lengths, n.

$$\therefore R_c = knR_b$$

Tracking Accuracy. The rms range measurement uncertainty σ_R, which is called "ranging error" for convenience, is given by the following expression:

$$\sigma_R = \frac{\alpha_t c}{R_c (S/N)^{1/2}}$$

where

c = speed of light

R_c = chip rate

S/N = signal-to-noise ratio in the tracking bandwidth, $2B_t$

α_t = factor which accounts for bandlimiting effects.

Figure 3-58 shows α_t at a function of the ratio B_{RF}/R_c (RF bandwidth to chip rate). With no bandlimiting $\alpha_t = \sqrt{2}/2 = 0.707$; this is also its approximate value over a wide range of the parameter, B_{RF}/R_c. Figure 3-59 shows the ranging error, σ_R, as a function of R_c and S/N for $\alpha_t = 0.7$. S/N is given by

$$\frac{S}{N} = \left(\frac{Pd}{\eta}\right) \frac{1}{B_t}$$

where B_t is the code tracking loop bandwidth.

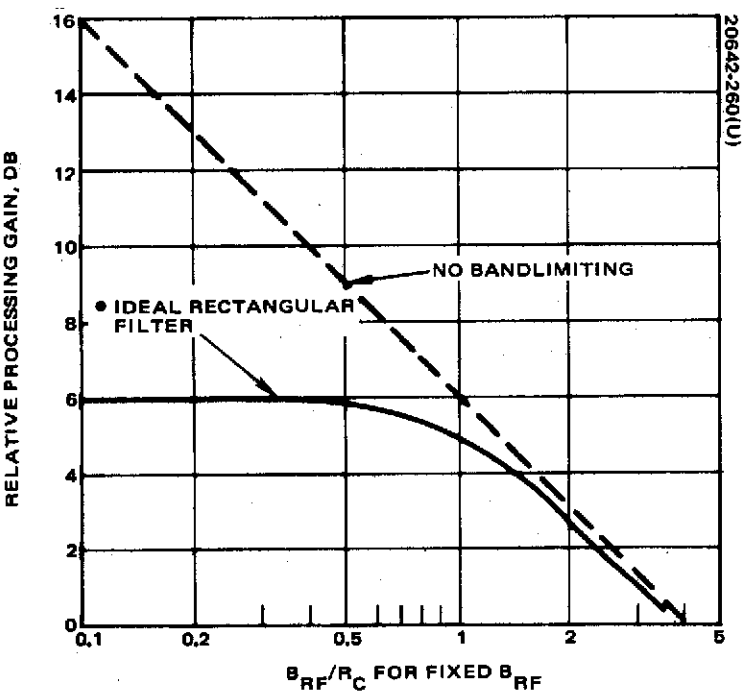

Figure 3-55. Processing Gain Against Diffuse Multipath for Fixed Bandwidth

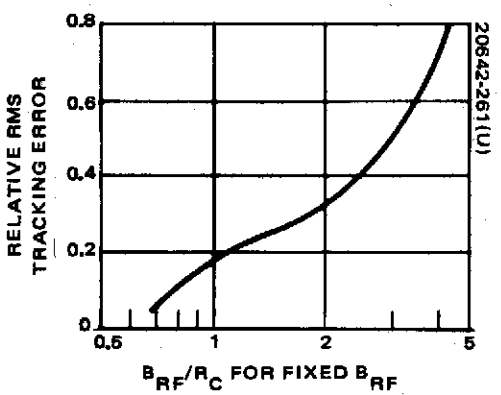

Figure 3-56. Relative RMS Tracking Error for Fixed Bandwidth

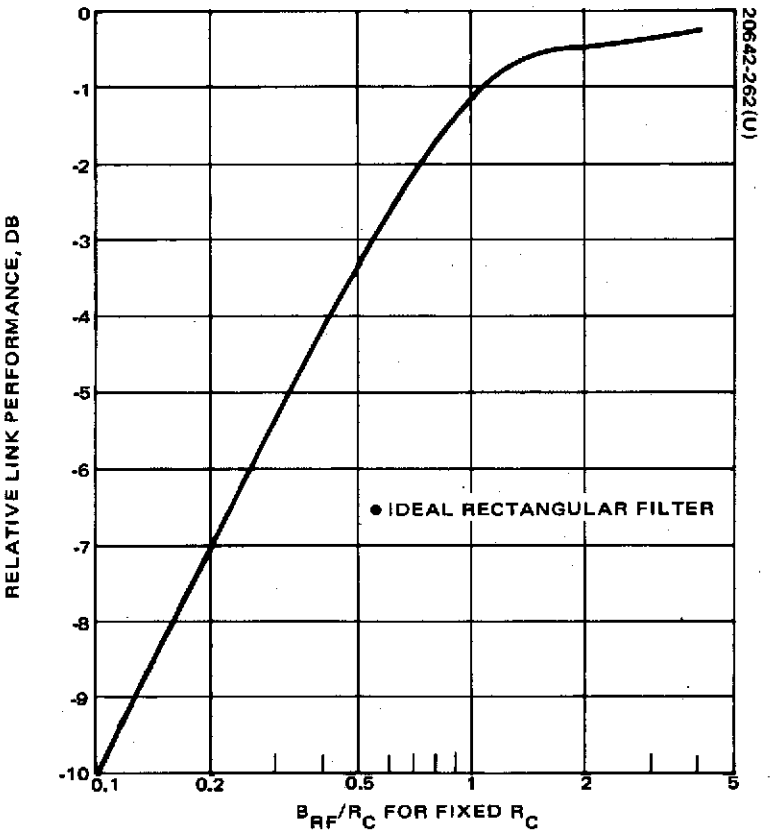

Figure 3-57. Bandlimiting Degradation as a Function of B_{RF}/R_c

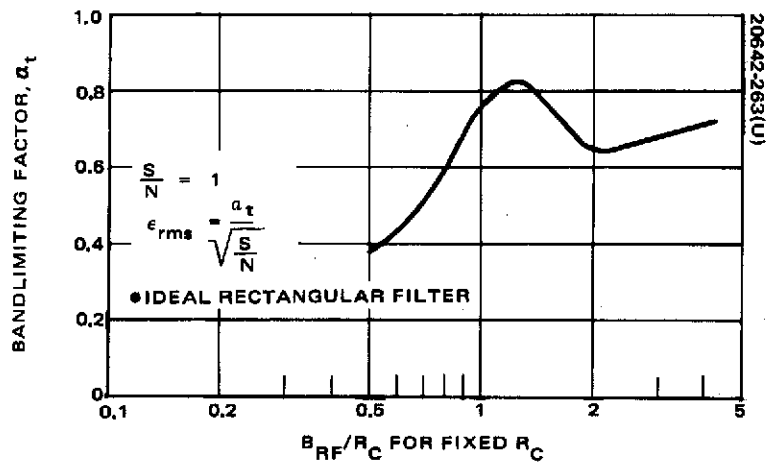

Figure 3-58. Bandlimiting Degradation as a Function of B_{RF}/R_c

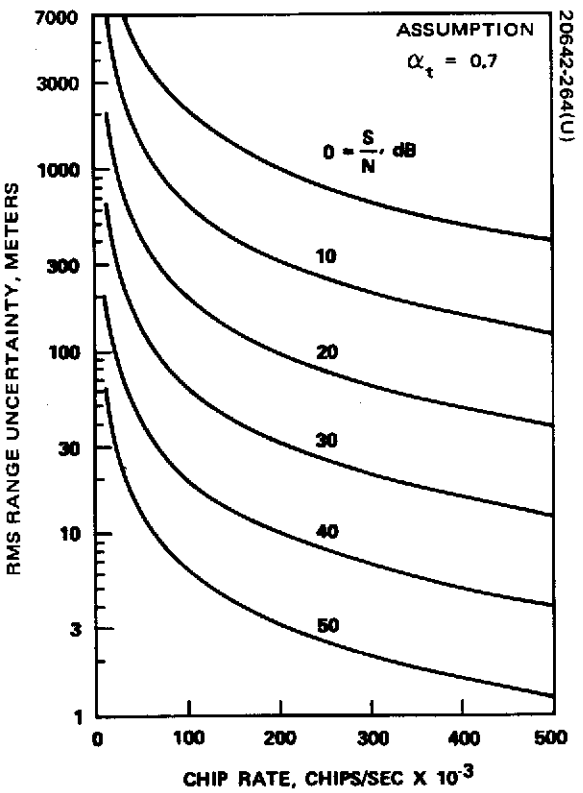

Figure 3-59. Range Measurement Uncertainty

Link Concepts. Both voice and command signals must be transmitted simultaneously; thus when both TDRSs are visible to a user, four signals could be received by the user. The voice signal can be scheduled to be transmitted through one TDRS or the other, and, if this is done, there are effectively three signals to be multiplexed into the forward link spectrum as shown in Figure 3-60.

There are three basic multiplexing methods: 1) frequency division multiplexing (FDM), 2) time division multiplexing (TDM), and 3) code division multiplexing (CDM). It has been concluded that the time varying distances between the users and TDRSs make TDM impractical but both FDM and CDM are viable candidates. The correlation process in spread spectrum reception is identical with code division multiplexing as defined here. Because the codes employed in both spectrum spreading and CDM are modulated by command and/or voice data, partial correlations will occur between signals in the same spectrum. This phenomenon has been discussed in 3.3.1.2 and is not severe for large bandwidth expansion ratios. The CDM is an attractive alternative for the forward link, since baseband multiplexing is possible. However, there is a preference to separate the command signals and voice signal spectra when there is sufficient bandwidth to do so because of the basically different services involved. The 1 MHz band at UHF will allow frequency separation of voice and command signals while still permitting wide variation of the signal parameters. In the 50 kHz band at VHF, this FDM is not as easy to achieve.

The approach to forward link design taken here is to develop several signalling concepts both VHF and UHF. These concepts, covering a range of applicable techniques and parameters, are then compared on the basis of link margin, RFI susceptibility, voice quality, and tracking performance. Link power budgets for both UHF and VHF are fundamental data in beginning the analysis; Table 3-14 presents these budgets.

Table 3-15 presents the signal parameters and multipath associated with the voice and command signals for each concept. The rationale employed in selecting them is described briefly in the following.

VHF CDM System. In this concept, the command and voice from both TDRSs share the same 50 kHz spectrum. Since the command and voice from a given TDRS will originate at the same point, this concept assumes CDM at baseband or IF on the same carrier. To allow for doppler shift, 3 kHz guard bands will be provided on each side of the band leaving 44 kHz for signals. In order to provide adequate code separation of the voice signal from the command signals, the number of code chips per voice bit should be as large as possible. Thus, in order to achieve a chip rate near the 44 kHz usable bandwidth, a low rate digital voice encoding method is required. Table 3-10 listed several voice transmission techniques from which it appears that one of the 2.4 kbps techniques will be required in this concept. The correlation properties of maximum length sequences called PN codes are desirable. These codes have symbol (chip) lengths of $n = 2^P - 1$ where P is an integer, for $P = 5$, $n = 31$. This code length combined with 2.4 kbps data produces a chip rate of 76.6 kchips/sec.

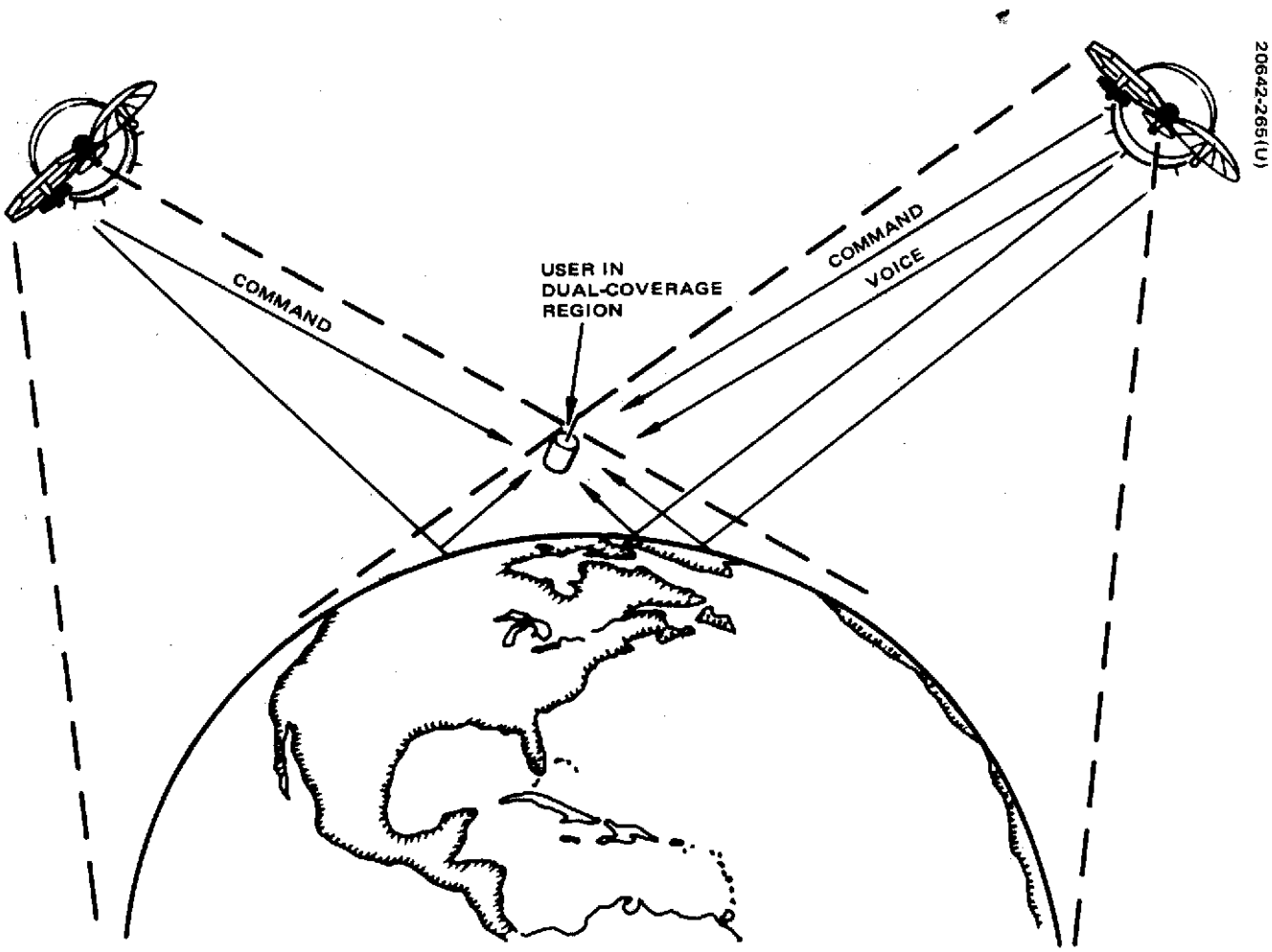

Figure 3-60. Low Data Rate Forward Link Multiplexing

TABLE 3-14. PRELIMINARY LINK BUDGET TDRS TO MANNED/UNMANNED USER

TDRS to Unmanned User	VHF	UHF
TDRS EIRP, dBw	30.0	30.0
Space loss, dB	-167.0	-177.5
Receive losses, dB		
Antenna gain	-3.0	-3.0
Ellipticity	-3.0	-3.0
Line loss	-0.5	-0.5
Received power, P_r, dBw	-143.5	-154.0
Receiver noise temperature, K	400.0	400.0
Earth noise temperature, K	50.0	50.0
Total system noise temperature, K	450.0	450.0
Thermal noise density, η_T, dBw/Hz	-202.0	-202.0
P_r/η_t, dB-Hz	58.5	48.0
Required E_b/η_o, dB	10.0	10.0
Thermal noise bit rate limit, kbps	70.0	6.3
TDRS to Manned User		
TDRS EIRP, dBw	30.0	30.0
Space loss, dB	-167.0	-177.5
Receive losses, dB		
Antenna gain	-1.0	-1.0
Ellipticity	-1.0	-1.0
Line loss	-1.0	-1.0
Received power, P_r, dBw	-140.0	-150.5
Receiver noise temperature, K	400.0	400.0
Earth noise temperature, K	50.0	50.0
Total system noise temperature, K	450.0	450.0
Thermal noise density, η_T, dBw/Hz	-202.0	-202.0
P_r/η_T, dB-Hz	62.0	51.5
Required E_b/η_o, dB	5.0	5.0
Thermal noise bit rate limit, kbps	500.0	40.0

TABLE 3-15. SIGNAL PARAMETERS FOR FORWARD LINK CONCEPTS

System	R_b, bits/sec	R_c, kchips/sec	B_{RF}, kHz	d	n	k	m_i		K	
							Single Visibility	Dual Visibility	Single Visibility	Dual Visibility
VHF CDM										
Command	400	76	44	0.53	31	6	0.63	0.16	2	3
Voice	2.4K	76	44	0.53	31	1	0.063	0.063	2	3
VHF FDM										
Command	340	43	32	0.63	127	1	0.63	0.16	1	2
Voice	12K	12	9	1.0	1	1	0.063	0.063	1	1
UHF CDM										
Command	300	600	600	0.80	2047	1	0.63	0.16	2	3
Voice*	9.6K	600	600	0.80	31	2	0.063	0.063	2	3
VHF FDM										
Command	300	600	600	0.80	2047	1	0.63	0.16	1	2
Voice*	9.6K	600	600	0.80	31	2	0.063	0.063	1	1

*Assumes rate one-half convolutional coding.

Since the unmanned satellite will not utilize polarization discrimination for multipath protection, its multipath factor, m, will be larger and to compensate, the processing gain must also be larger. Using 6 lengths of a 31 code (plus an additional symbol to produce an even length) per bit will provide good correlation and processing gain, but the timing and chip rates will be identical to the voice link.

$$R_b = \frac{76.6 \text{ kchips/sec}}{6\,(32) \text{ chips/bit}} = 400 \text{ bps}$$

Multipath interference depends on the orbital geometry and number of signals. For single visibility, i.e., one TDRS visible to the user, a worst case multipath is 2 dB below the direct signal ($m_i = 0.63$). However, since one voice and one command signal may be present, this number will effectively be twice as great. For dual visibility, there are three signals but each is approximately 8 dB below the direct signal. Figures 3-61 through 3-64 show E/η as a function of η_{RFI}, and Figure 3-65 shows the rms ranging error as a function of RFI for all the link concepts.

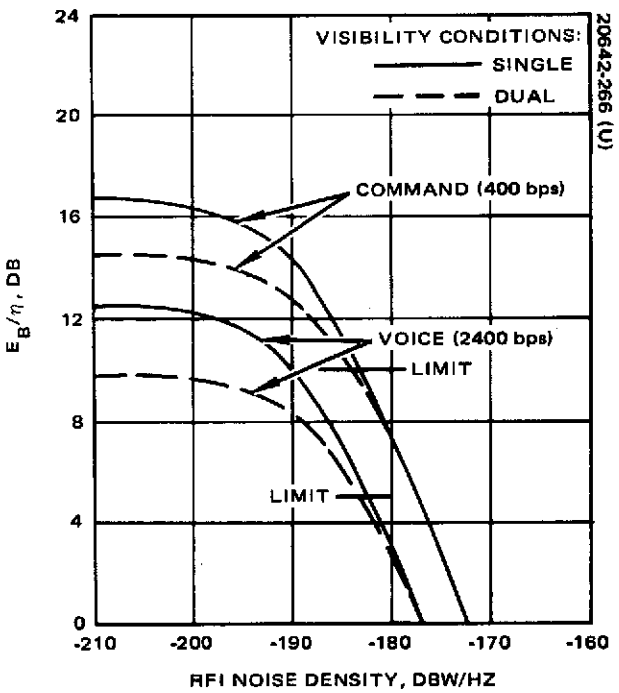

Figure 3-61. VHF Code Division Multiplex System

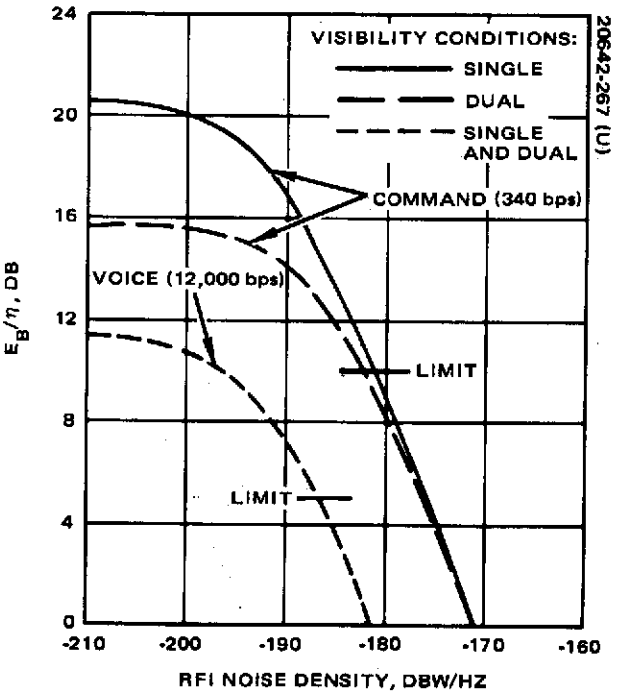

Figure 3-62. VHF Frequency Division Multiplex System

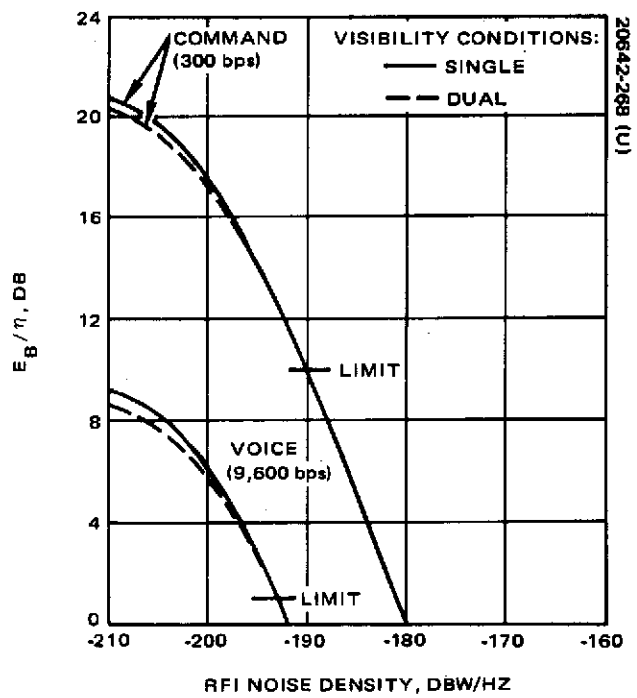

Figure 3-63. UHF Code Division Multiplex System

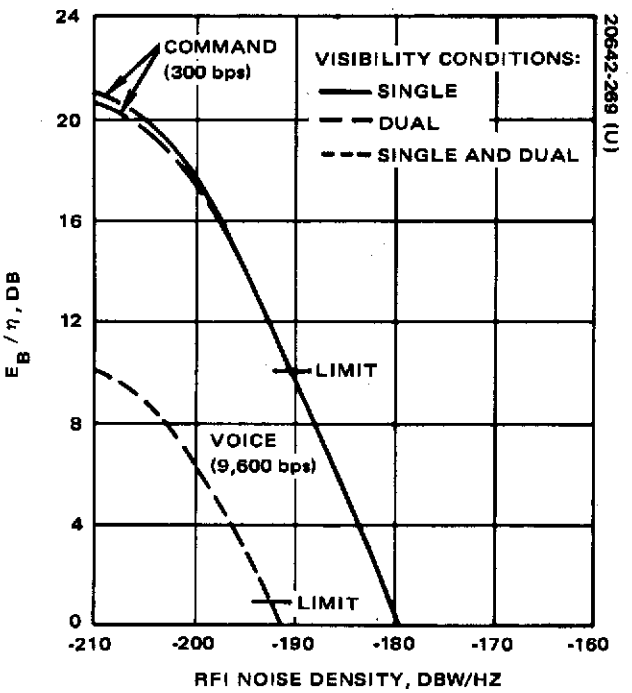

Figure 3-64. UHF Frequency Division Multiplex System

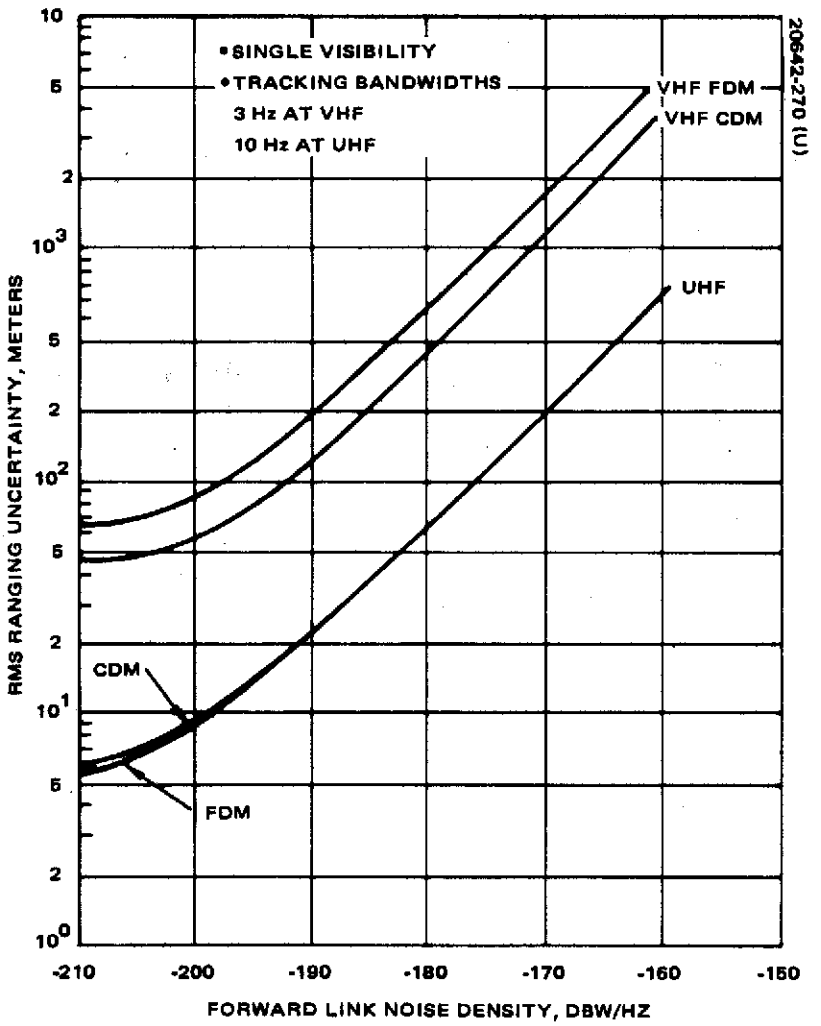

Figure 3-65. RMS Ranging Error as Function of RFI

VHF FDM System. In this system, the voice occupies a separate portion of the 50 kHz spectrum. A 3 kHz guard band is required between the voice and command spectra. Since the manned user rejects multipath with circular polarization, no spreading of the voice spectrum is required; thus an attractive modulation technique is 12 Kbps delta modulation with four phase PSK carrier modulation. The required RF bandwidth is approximately 9 kHz, and with a total of 9 kHz for guard bands, 32 kHz remains for the command channel. For a processing gain and bit rate similar to that for the CDM design R_c = 340 bps x 127 bits/chip = 43 kchips/sec.

Since the voice occupies a separate channel and is not PN code modulated, there is no crosscorrelation. With polarization discrimination, the multipath is assumed to never be larger than 12 dB below the direct signal, i.e., $m_i \leq 0.063$. For single visibility in the command channel, the worst case multipath is 2 dB below the direct signal, i.e., $m_i = 0.63$ and there is no other signal. For dual visibility, the effective multipath is again twice as great.

UHF FDM. The 1 MHz band at UHF will allow frequency separation of the voice and command channels without difficulty, and therefore their respective signal designs can be relatively independent. Considering the command link first, it should be noted from Table 3-14 that about 10.5 dB less power will be received at UHF than at VHF. In addition, the tracking bandwidth required by doppler rate will be about three times larger resulting in a signal-to-noise ratio in the tracking loop 15.3 dB less than for VHF. In order to achieve the same ranging accuracy, the chip rate must be approximately 6 times larger than with the VHF system. Thus, the UHF command chip rate must be greater than 300 kchips/sec to achieve ranging accuracy comparable to the VHF systems. Choosing a chip rate on the order of 600 kchips/sec is possible because of the greater available bandwidth. Thus, let the command bit rate be 300 bps and the PN code length n = 2047. Then, R_c = 614.1 kchips/sec and for a total RF bandwidth allocation of 600 kHz allowing for two 10 kHz guard band requires filtering to an RF signal bandwidth of 580 MHz. Then $B_{RF}/R_c = 0.945$ and, from Figure 3-57, d = 0.76.

For the voice link, the available bandwidth will allow spectrum spreading to provide multipath rejection beyond that provided by circular polarization. Another link improvement technique is convolutional encoding for error correction which at the same time will provide an additional 3 dB reduction in diffuse multipath interference. With these considerations, the following voice link design was proposed:

9.6 Kbps delta modulation

PN code length, n = 31 chips

One code per voice bit

R_c = 600 kchips/sec

B_{RF} = 600 kHz

d = 0.80

UHF CDM. Although ample bandwidth is available at UHF to separate command and voice in frequency, spacecraft design studies indicated a possible advantage to the use of CDM. Code division multiplex at baseband or IF for the voice and data permits maximum transmitter efficiency, because there is only one carrier allowing a single saturated power amplifier. The design is similar to the VHF CDM design, except that more bandwidth is available:

R_c = 614.4 kchips/sec

Command code length = 2048

Command bit rate = 300 bps

Voice PN code length = 32 with rate one-half convolutional coding

Voice bit rate = 9.6 Kbps

In the dual visibility region the signals present are as follows:

1) Signals from TDRS No. 1: Voice and data in synchronous CDM

2) Signals from TDRS No. 2: Data in asynchronous CDM with the signals from TDRS No. 1

System Concept Comparison. To aid in comparing the above systems, Table 3-16 was prepared. Line 1 lists the command bit rate for each concept. The rates were purposely made comparable so that comparisons could be made based on more essential characteristics. Line 2 lists the link margin if there is no RFI. Note that the two UHF systems have the largest margins since the available bandwidth permits the multipath and crosscorrelation effects to be essentially eliminated.

Line 3 shows the RFI noise density where the margin is zero, i.e., where the command bit energy to noise density is 10 dB, the assumed minimum operating level. The VHF FDM is significantly superior in its ability to operate in the presence of RFI. Line 4 contains the estimated rms ranging error contribution due to forward link timing uncertainty caused by system thermal noise and multipath. Note that the UHF system allows much better ranging accuracy. This is due to the much larger bandwidth available, allowing a higher chip rate. The VHF FDM system is the poorest because it has the smallest chip rate.

Voice signal concept parameters are on lines 5 through 9. Line 7 contains the subjective quality rating introduced in subsection 3.3.1.2 for the voice modulation method employed in each concept. This rating is nearly

TABLE 3-16. FORWARD LINK CONCEPTUAL DESIGN COMPARISON

Parameter	VHF		UHF	
	CDM	FDM	CDM	FDM
Command rate, bps	400	340	300	300
Margin for no RFI, dB	2	6	11	12
RFI limit, dBw/Hz	-184	-182	-190	-190
RMS ranging error for no RFI, meters	47	63	6	6
Voice technique	Vo coding	Delta module	Delta module	Delta module
Bit rate, Kbps	2.4	12.0	9.6	9.6
Quality rating	2	8	6	6
Margin for no RFI, dB	7	6	8*	10*
RFI limit, dBw/Hz	-183	-187	-193	-192

*Assumes convolutional coding.

proportional to the bit rate of the baseband digital voice signal. Thus, 2.4 Kbps techniques have a rating of 2, while 12 Kbps delta modulation is given an 8 rating.

The importance of link margin is hard to determine at this point in system design. Normally, margin beyond 5 or 6 dB is unnecessary. The uncertainty of the actual RFI level also makes a selection difficult. The VHF systems provide communication with a higher level of RFI than at UHF, but RFI at UHF will probably be lower. However, a clear VHF channel may be available; in which case, the RFI operating limits are not important and excessive margin beyond 5 or 6 dB is not required. In this case, voice quality and ranging error become major parameters in system selection.

The UHF command system is clearly superior for ranging accuracy, and 9.6 Kbps delta modulated voice can be used also. The UHF scheme with code division multiplex permits high ranging accuracy and high quality voice. Although the voice margins are slightly reduced from the FDM case, the scheme is advantageous since the TDRS transmitter configuration is greatly simplified.

Concept Recommendation. Based on the previously discussed considerations, it is recommended that the UHF band be used for the forward link. A CDM command signaling design similar to that presented above and a voice signaling design employing delta modulation and convolutional encoding are recommended. The reasons are as follows:

1) The UHF band has sufficient bandwidth to allow flexibility in the design.

2) The UHF band is currently allocated for space applications. No new international allocation is required, and RFI should be low.

3) The larger bandwidth allows better ranging accuracy and a higher quality voice.

4) Hardware components are smaller at UHF than at VHF.

5) CDM simplifies TDRS repeater design.

Before a final choice was made between VHF and UHF, the impact on antenna configuration was assessed. Since the TDRS must receive at VHF in the 136 to 144 MHz band, transmitting at 401 MHz significantly affects both TDRS and user antenna design. The resultant TDRS configuration has proved satisfactory, however.

3.3.1.4 Low Data Rate Return Link Design

TDRS must relay telemetry data and ranging signals from up to 40 unmanned users and also provide for the relay of good quality voice from one manned user. The basic constraints and requirements influencing the design of these links are summarized in Section 3.1. As in the forward link, multipath and RFI are severe interferences. As mentioned previously, it has been estimated that the average multipath power will vary between -2 and -10 dB relative to the directly received power for a wide range of orbital and surface roughness conditions. In the return link, however, RFI is received from nearly one-half of the earth's surface; thus, there are no operational procedures for communicating during low RFI conditions as in the forward link where user visibility is more restricted due to its low altitude. Thus, RFI remains an important unknown parameter in return link design. Current estimates have been discussed above.

The TDRS coverage requirements limit peak antenna gain to approximately 16 dB. The final Hughes TDRS configuration provides a $G/T \cong -15$ dBw/K including only receiver thermal noise effects. The baseline TDRS receives both horizontally and vertically polarized signals and relays them in separate channels. This permits polarization combining at the ground station with an improvement of somewhat less than 3 dB. Combining is discussed in subsection 3.3.1.2.

Voice Link. The return voice relay design is different from the telemetry and ranging relay service in that the manned user can easily generate an order of magnitude greater RF power – perhaps 100 watts. This user can also utilize a circularly polarized antenna which provides an estimated 12 dB of multipath protection by polarization discrimination as discussed previously.

Since the voice power is significantly greater than the unmanned user power, the combination of these two signal classes in a single code division multiplex system will produce relatively high correlation noise with respect to the user telemetry signals. Also the manned user does not require

PN codes for ranging although spectrum spreading may be a necessity in meeting CCIR incident flux density requirements. Furthermore, the basically different operational characteristics of the manned and unmanned users support the conclusion that these links should operate in frequency multiplex. During the spacecraft design effort it was found that design of a VHF receiver with a bandwidth less than 2 MHz was difficult. This permits allocation of 1 MHz to the telemetry service and 1 MHz to the voice service. The full 1 MHz is not required for voice, except in the event of spectrum spreading by the user.

Voice encoding for the return and forward link was discussed in subsection 3.3.1.2. The voice technique for previously discussed reasons is 19.2 kbps delta modulation, which requires a bit error rate less than 10^{-2}. Three different RF/code modulation techniques were considered:

1) Biphase PSK with no coding.

2) Biphase PSK with a length 7 PN code for multipath protection.

3) Biphase PSK with a rate one-half convolutional code to lower the E_b/η requirement and to provide a slightly spread spectrum.

Multiphase modulation schemes were not considered because bandwidth was not a constraint.

Table 3-17 shows the basic link power budget. Note that 100 watts of RF power was assumed. Figure 3-66 shows the performance of the three designs under worst case multipath as a function of RFI noise density. Multipath is not critical with any of the designs because of the 12 dB polarization discrimination. All designs work quite well if the $\eta_{RFI} < -190$ dBw/Hz. When the link is RFI limited, the convolutional coding system is 3 dB better than the others because of its lower E_b/η requirement.

Telemetry Link. A detailed design of the return telemetry link must consider the problems of multiple access design for 40 users and compatibility with the command link because coherent turnaround must be provided for range and range rate measurements. Three basic alternatives were considered and design concepts for each were developed. These three concepts and their basic characteristics are listed in Table 3-18. The performance of each is nearly the same. With x FDM channels, the number of interfering users per channel varies as 1/x, but the bandwidth available for "processing gain" also varies as 1/x plus 7 kHz guardbands per channel for doppler. Figure 3-67 illustrates this effect in terms of the crosscorrelation noise due to multiple users in a channel. The abscissa is the number of interfering users; the ordinate gives the E_b/η required with respect to all other noise sources such that the final E_b/η = 10 dB. For the wideband design with 40 users in a common channel with processing gain, G = 1000, the required E_b/η is essentially that of a narrowband system with five users per channel where the processing gain $\cong$ 1/8 that of the wideband design. These results are based on the following previously discussed formula.

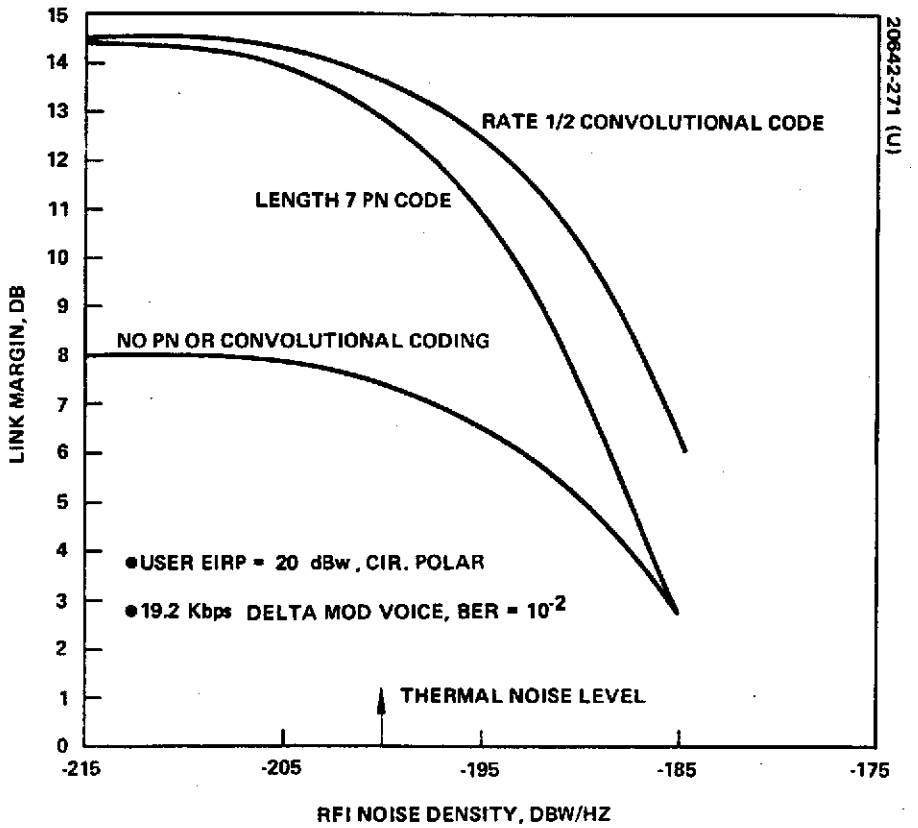

Figure 3-66. Manned User to TDRS at VHF

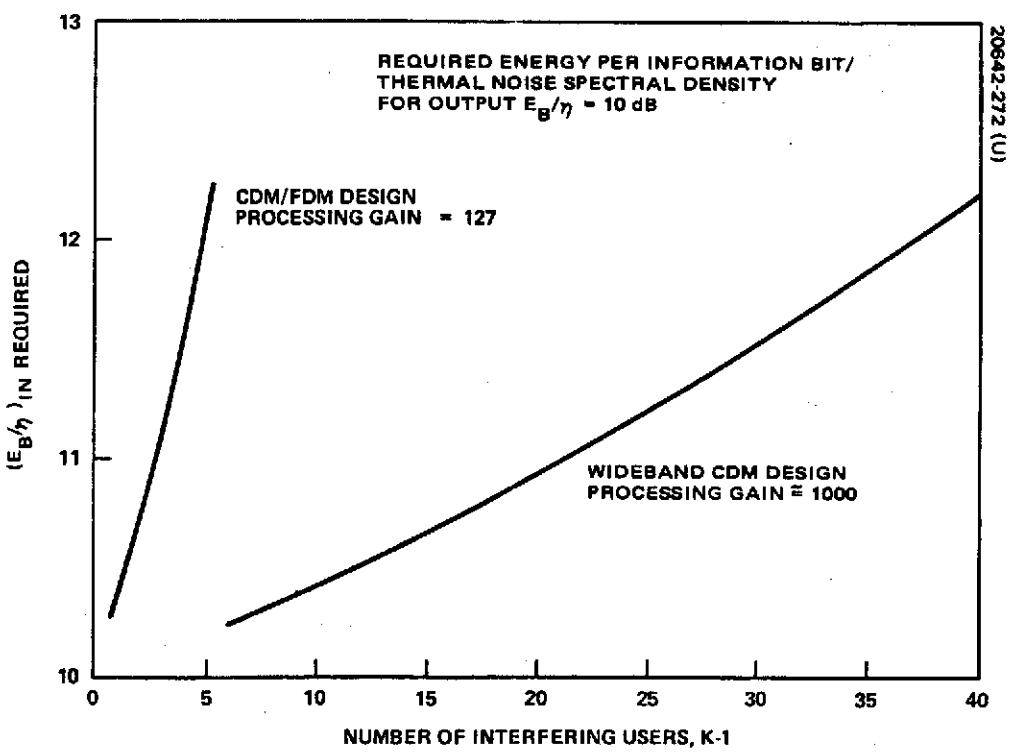

Figure 3-67. Effective Noise Due to Other Users in a Pseudo Noise Code Division Multiplex Systems

TABLE 3-17. PRELIMINARY VHF RETURN LINK POWER SUMMARY FOR VOICE

User transmit power	+20.0 dBw
User antenna gain	0.0 dB
Space loss	-167.5 dB
TDRS gain	11.8 dB
Ellipticity loss	-0.2 dB
Line losses	-1.0 dB
Received power P_r =	-136.9 dBw

For T_s^* = 630 K, η_T = 200.6 dBw/Hz

P_R/η_T = 63.7 dB-Hz

*Receiver noise temperature = 420 K, earth noise = 210 K.

TABLE 3-18. VHF RETURN LINK ALTERNATIVES

Telemetry and Ranging		
Wideband CDM	CDM/FDM	FDM
All 40 users in common PN multiplexed channel.	Seven FDM channels with six users each in PN multiplex.	Forty FDM channels.
• 1200 bps data rate	• 1200 bps data rate	• 1200 bps data rate
• 1.22 Mchips/sec	• 152 kchips/sec	• 18 kchips/sec
• 1 MHz total bandwidth	• 1.1 MHz total bandwidth	• 1.0 MHz total bandwidth
• Gold sequences	• Optimum M-sequences	• Use of single M-sequence

$$\left(\frac{E_b}{\eta}\right)_{OUT} = \frac{\left(\frac{E_b}{\eta}\right)_{IN}}{1 + \left(\frac{E_b}{\eta}\right)_{IN} \frac{0.76\,(K-1)\,R_s}{R_c}}$$

For reasons discussed later, the wideband CDM concept is preferred. The basic performance of the system is shown in Figure 3-68 based on the link power budget of Table 3-19. In the presence of a nominal multipath environment, a very sophisticated design will support nearly 10 Kbps per user. However, if the RFI noise density is roughly -190 dBw/Hz, only about 700 bps can be supported continuously. The figure also shows that convolutional coding gives a 5.5 dB improvement, and that polarization combining gives about 2.5 dB. Figure 3-69 shows that with a 1 MHz RF bandwidth, multipath interference is virtually eliminated. With a 1200 bps data rate and a 1 megachip/sec chip rate, each user has approximately a 30 dB protection against multipath. Under worst case multipath, the baseline design with coding and polarization combining has zero margin at an RFI noise density ten times the thermal noise.

Concept Comparison and Recommendations. The performance of the various designs are summarized in Table 3-20. A final design selection must include qualitative factors in addition to these quantitative ones. In the recommended design, the voice link operates in FDM with the telemetry and ranging. If the voice user can generate 100 watts of RF power, no coding is required, and the added complexity is not justified unless additional RFI protection is deemed necessary. A biphase PSK carrier modulation at 19.2 Kbps will require about 30 kHz RF bandwidth; the VHF band at 136 to 137 MHz is preferable, but this 1 MHz has been assigned to the more RFI sensitive telemetry links and the 137 to 138 MHz band is selected for voice.

The summary table (Table 3-20) shows that the three telemetry and ranging schemes have the same data rate and link margin performance. The only significant advantage of one system over another is the tracking performance of the wideband CDM approach.

The principal advantage of the FDM approach is that it permits full channelization of the repeater, if feasible, for power control and RFI immunity. Under RFI jamming, a given channel could easily be eliminated, but that user would require the ability to move to another channel. This implies user transceiver capable of generating multiple turnaround frequency ratios.

The CDM/FDM approach is truly a compromise between the full FDM and full CDM designs. The six users per FDM channel configuration were chosen because groups of six M-sequences are known with good (small) crosscorrelation and optimum autocorrelation properties. It has been

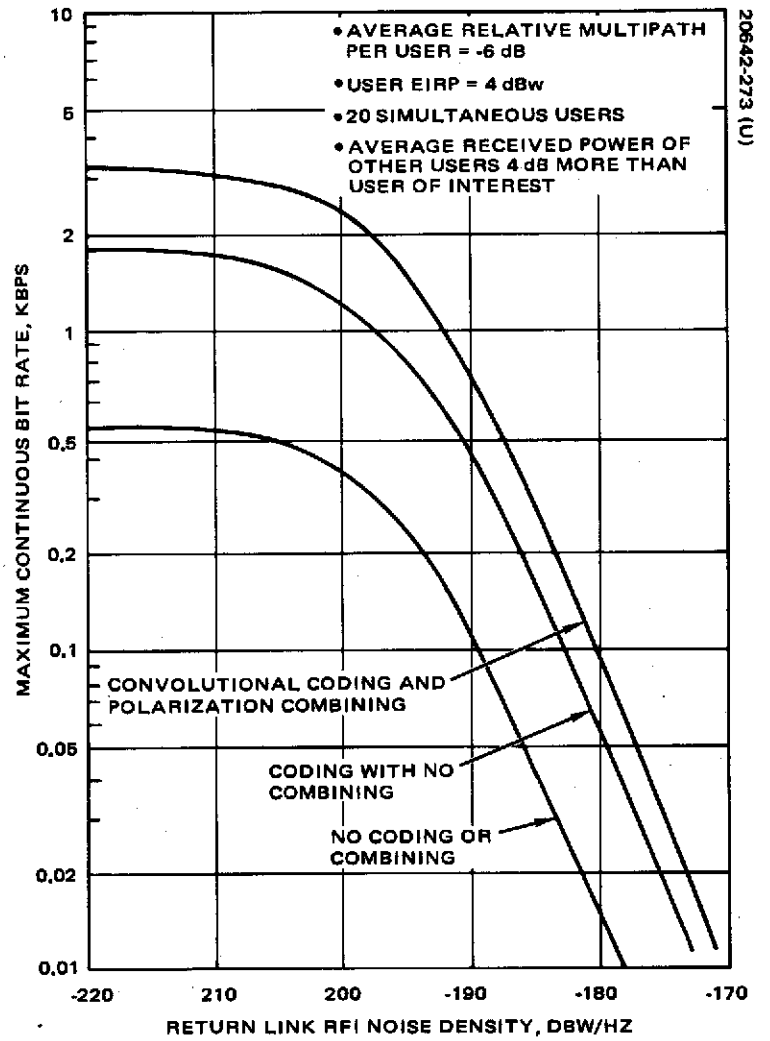

Figure 3-68. Telemetry Bit Rate Versus RFI Noise Density For Wideband DCM Design

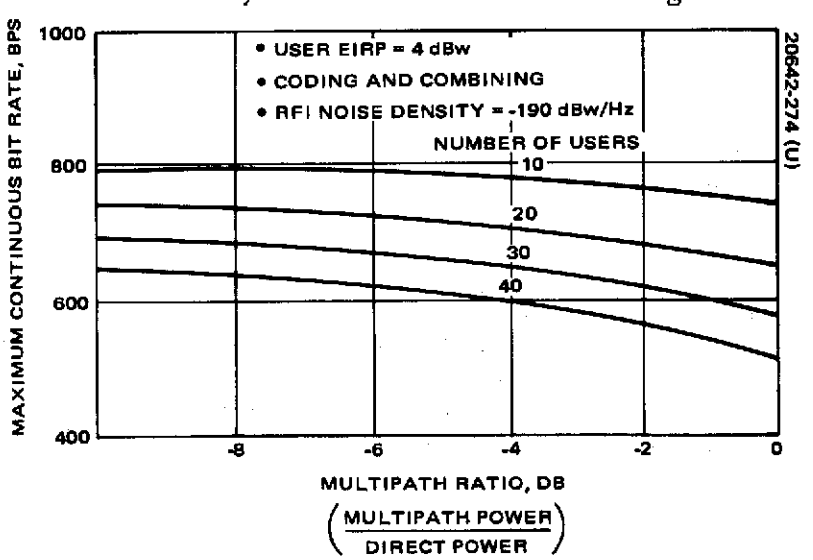

Figure 3-69. Telemetry Bit Rate Versus Multipath Ratio for Wideband CDM Design

TABLE 3-19. PRELIMINARY VHF RETURN LINK POWER BUDGET FOR TELEMETRY

User transmit power	7.0 dBw
User antenna gain	-3.0 dB
Space loss	-167.5 dB
TDRS gain	11.2 dB
Ellipticity loss	-0.5 dB
Line losses	-0.6 dB
Received power, P_i =	-153.8 dBw

For T_s^* = 630 K, η_T = -200.0 dBw/Hz

$$P_i/\eta_T = 46.8 \text{ dB-Hz}$$

$$\frac{E_b}{\eta} = \frac{\frac{P_i}{R_b} d}{\eta_T + \eta_{RFI} + \frac{\sum_{i=1}^{K} m_i P_i + 0.76 \sum_{i=1}^{K-1} P_i}{R_c}}$$

d = bandlimiting factor, R_c = chip rate

*Receiver noise temperature = 420 K, earth noise temperature = 210 K

concluded that these optimum autocorrelation properties are not really necessary, although they would enhance code acquisition. In any code division multiple access system, the user correlation receivers must be able to reject false synchronization on other users. They can, therefore, also reject false sync on the side peaks of the autocorrelation function. The optimal autocorrelation is also not required to reject specular multipath; studies show that specular multipath is virtually nonexistent.

TABLE 3-20. QUANTITATIVE PERFORMANCE OF VHF TELEMETRY RETURN LINK ALTERNATIVES

a. Telemetry and Ranging Performance*

	Wideband CDM	CDM/FDM	FDM
Telemetry			
Rate, bps	1200.0	1200	1200
Margin for RFI = 0, dB	8.0	9	10
RFI limit, dBw/Hz	-188.0	-187	-186
Ranging			
RMS error for RFI = 0, meters	4.8	28	210

*Assumes 30 users with R_P = -6 dB with convolutional coding and diversity combining. Tracking bandwidth of 10 Hz. No downlink degradation.

b. Voice Performance with 19.2 kbps Delta Modulation

	No Coding	PN Coding	Convolutional Coding
Margin for RFI = 0, dB	8	14	14
RFI limit, dBw/Hz	-183	-183	-180

The full CDM scheme is the easiest to implement since all users have identical transceivers except for their identifying PN code. The system has greater flexibility in terms of scheduling and growth. It also is more efficient in terms of spectrum utilization since a doppler guardband is required only once. The system can provide protection against narrowband RFI by the use of one or more notch filters by the TDRS or at the ground. A CDM design is therefore selected for a baseline.

If a fixed data rate is selected for all users, then a PN code period should be set equal to a convolutional code symbol time. At a bit rate of 1200 bps, the 511 Gold codes and rate one-half convolutional coding would give a chip rate of

$$R_c = 1200 \times 511 \times 2 = 1.22 \text{ Mchips/sec}$$

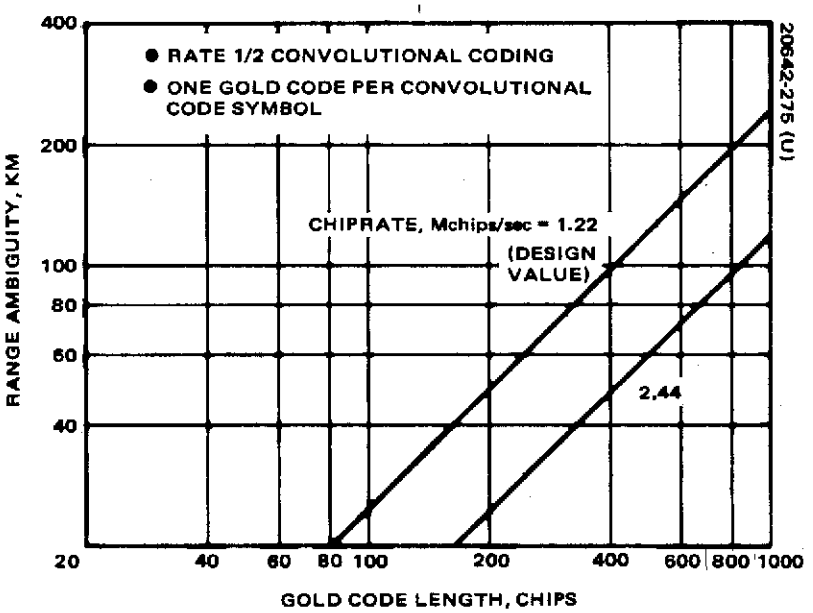

Figure 3-70. Low Data Rate Return Link Range Ambiguity

The range ambiguity provided by this design is the propagation time corresponding to 1/(1200 x 2) sec or about 125 km. The system can also be designed to accommodate multiple user bit rates by the use of multiple code lengths per code symbol – for example, the use of 8 codes of length 63 for the 1200 bps rate. At 10 Kbps or 8 x 1.2 Kbps the user transceiver would use only one length 63 code per bit. The range ambiguity resolution is reduced to 15 km as shown in Figure 3-70.

3.3.2 Medium Data Rate Links

The medium data rate service allows return telemetry rates up to 1.0 Mbps. The following subsections describe the analysis and design performed for this telecommunications service. The principal trade performed was that of frequency selection. It was concluded that K band was slightly superior in terms of the minimum user weight penalty. However, discussion with GSFC indicated that S band provided the least overall user impact and it was selected as the MDR frequency.

3.3.2.1 Communications Channel Model

Basic Communications Geometry. The basic communications geometry for the MDR links is identical to that for the LDR links. Figures 3-71 through 3-76 give the doppler shift and doppler rate values which are appropriate at the three potential MDR frequencies.

Noise Environment. The noise environment for the majority of MDR users is far less complex than that for the LDR users. The directive antennas of the user and the TDR satellites will essentially eliminate the multipath and RFI problems. Multipath will only be a problem if TDRS/user communication is maintained to the edge of the horizon where the earth would be included within the antenna sidelobes or perhaps the main beam. This same condition will also have design impact from the standpoint of CCIR requirements on incident flux density as illustrated in Figure 3-77. These problems can be eliminated by spread spectrum techniques or by operational constraints. Spread spectrum was discussed in connection with the LDR design. Figure 3-78 illustrates that either problem can be considered operationally as a limit on the communications horizon. Normally the altitude h_a is fixed by earth surface features or an effective atmosphere height.

The multipath and RFI problems are less severe for the MDR user with omni antennas than for the LDR user with omnis. The former can use circular polarization for antenna discrimination. At S band, an antenna capable of transmitting or receiving a circularly polarized wave requires very little surface area. Suitable antenna designs applicable to the Space Shuttle have been developed for guided missile S band telemetry systems. Multipath effects will also be reduced in the MDR system since the TDRS antenna is relatively narrow beam.

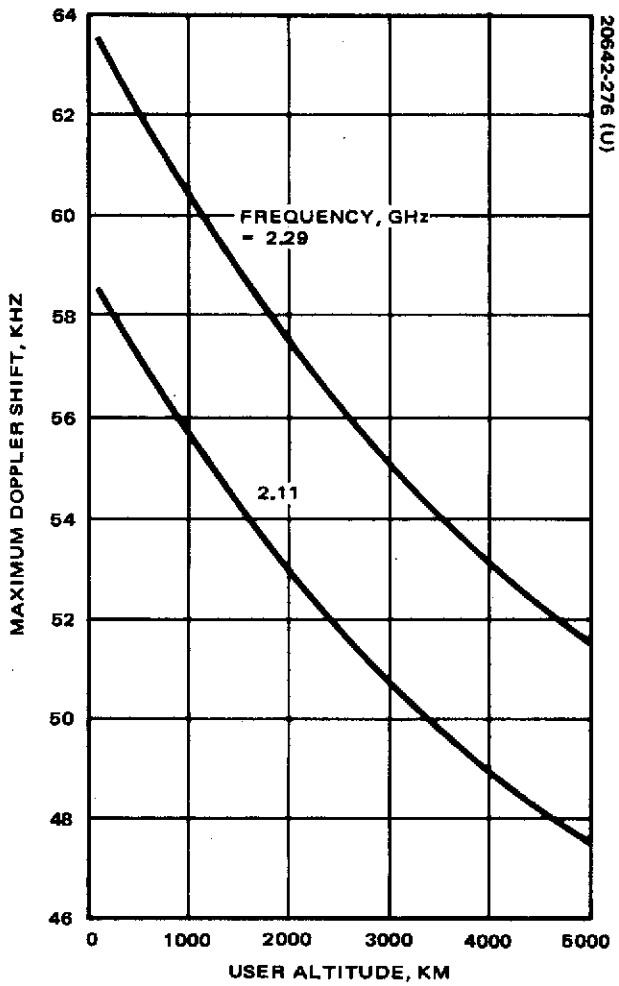

Figure 3-71. Maximum Doppler Shift in Medium Data Rate Links at S Band (One-Way Frequency Lock)

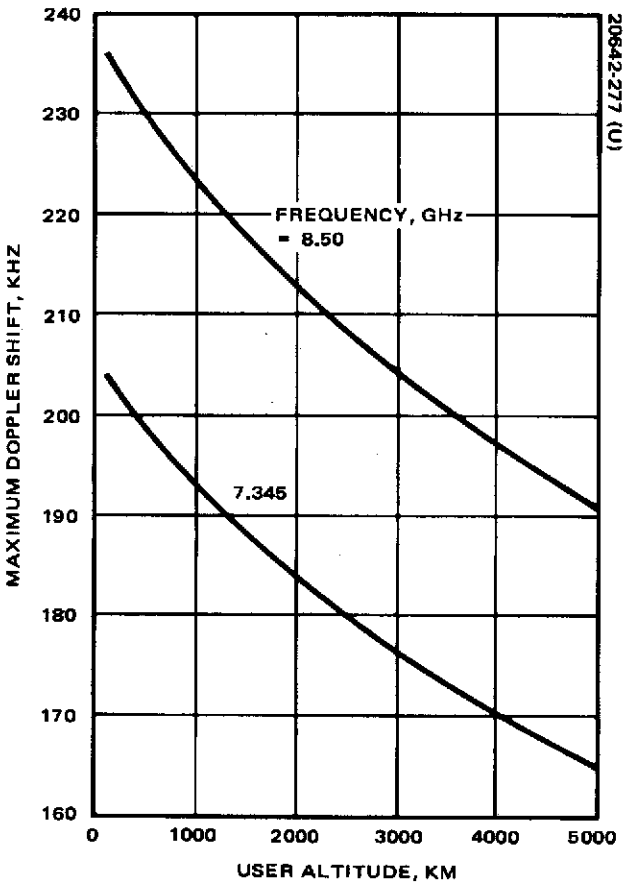

Figure 3-72. Maximum Doppler Shift in Medium Data Rate Links at X Band (One-Way Frequency Lock)

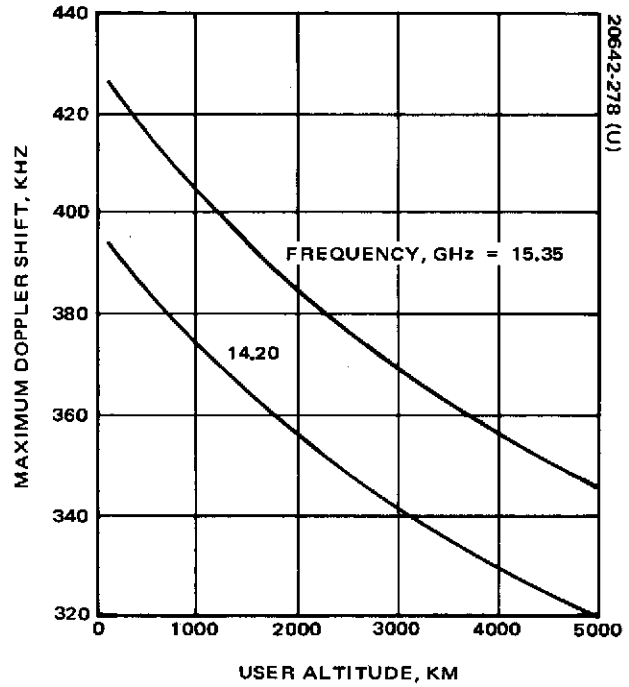

Figure 3-73. Maximum Doppler Shift in Medium Data Rate Links at K Band (One-Way Frequency Lock)

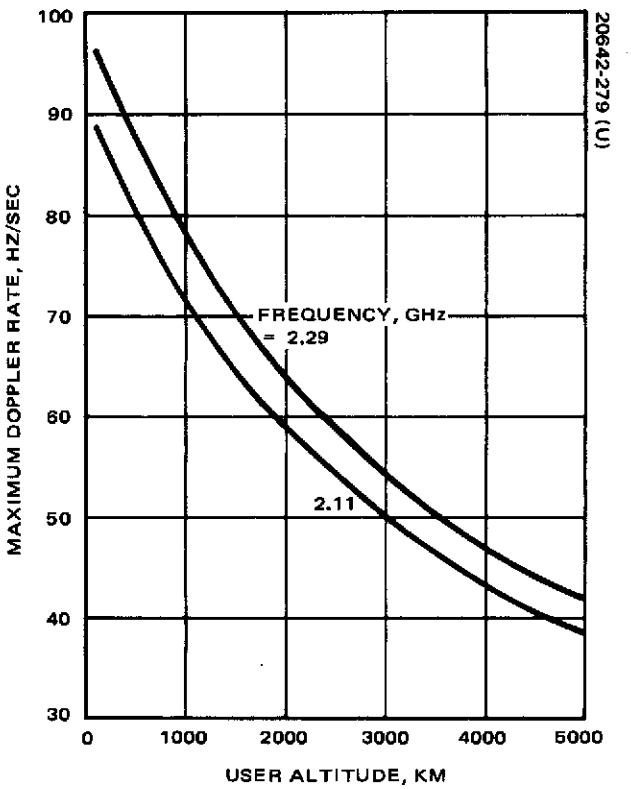

Figure 3-74. Maximum Doppler Rate in Medium Data Rate Links at S Band (One-Way Frequency Lock)

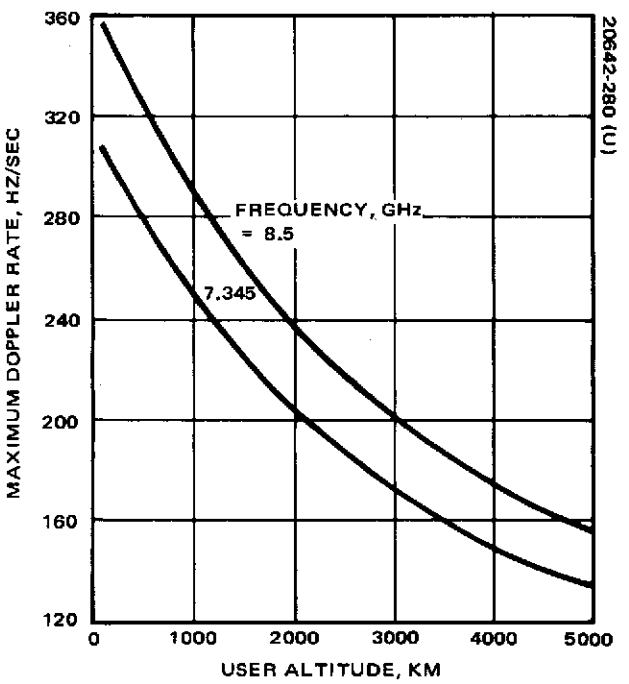

Figure 3-75. Maximum Doppler Rate in Low Data Rate Links at X Band (One-Way Frequency Lock)

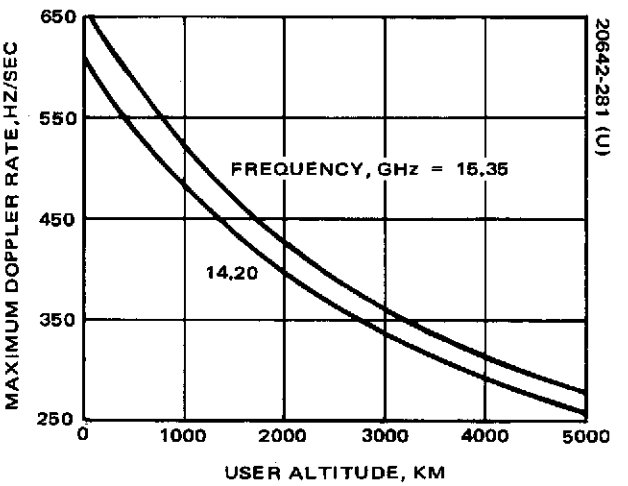

Figure 3-76. Maximum Doppler Rate in Medium Data Rate Links at K Band (One-Way Frequency Lock)

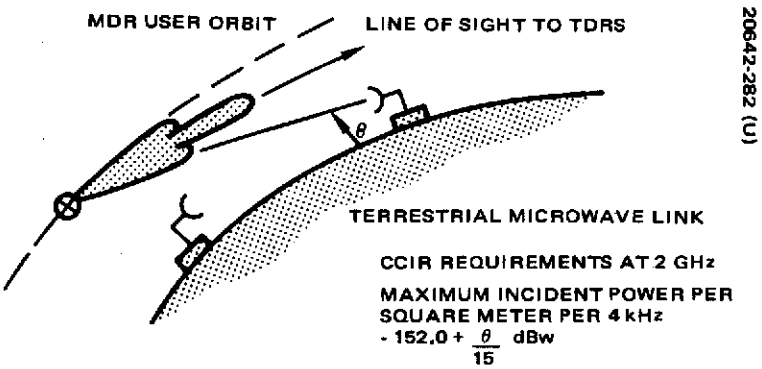

Figure 3-77. CCIR Requirements Due to Frequency Sharing at S Band

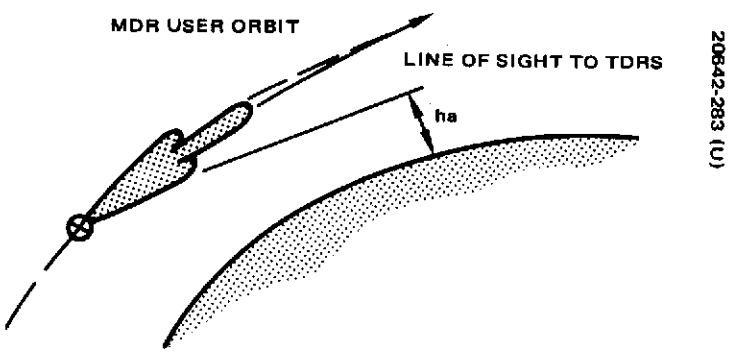

Figure 3-78. Effect of Multipath and CCIR Requirements on Parameter h_a

3.3.2.2 Frequency Selection

The TDRS is expected to service many user satellites with a medium date rate RF link with capacity up to 1 Mbps. Three frequency bands have been considered for this link: S band, X band, and K band. These bands have user transmit frequencies of 2.2 to 2.29 GHz, 7.145 to 7.345 GHz, and 13.25 to 14.2 GHz, respectively. The user satellites are not specified and therefore their weight, power, and space availability are not known. Since the communications transponder and the antenna system added to the user satellite may be a significant contributor to the user satellite weight, a minimum weight criteria was used to aid in the comparison of the potential data link frequencies. The analysis and results given in this report indicate that K band or X band are slightly preferable to S band in terms of minimum weight. However, the use of S band will minimize overall user impact in terms of cost and development risk.

Weight Optimization Procedure. Communication systems hardware placed on the user satellite is compared on the basis of weight for each frequency, with the lightest system capable of transmitting the required data defined as the "best". Since there are three frequencies to compare, it is necessary to compare the lightest K band system with the lightest X band system, with the lightest S band system to obtain a true comparison among the three frequency bands.

The individual communication system weights depend upon the relative choice of transmitted power and transmitter antenna size, with an optimum choice of these two parameters determining a minimum weight system. The minimum communications weights were determined based upon work done for NASA/GSFC under contract NAS 5-9637 which produced the COPS Communication OPtimization System computer program. In this method of optimization, a performance constraint is set (e.g. SNR equal a constant) and all the hardware components of the communications transponder are modeled to relate their weight to a key communication system parameter. The two parameters used in this analysis were transmit antenna diameter and transmitted power. Table 3-21 indicates the communication system modeling and the dependence upon transmitted power, P_T, or transmit antenna diameter, d_T. The analytical problem is to take the three general equations given in the table and from them determine the minimum weight of the total communications system. Rather than develop the equations in this report (Reference 15) a simple model will be described which illustrates how a minimum weight system may be determined.

Figure 3-79 is a three dimensional sketch having as independent axes transmitted power, P_T, and transmitter antenna diameter, d_T, and as the dependent axis, weight. A weight model of the antenna is shown in the d_T-weight plane and a weight model of the transmitter is shown in the P_T-weight plane. The sum of these two models is a sheet in the three dimensional space. The performance criteria is shown in the d_T-P_T plane. It is not restricted in the weight dimension and therefore is a vertical sheet which intersects the "weight" sheet. On the line of intersection there is a minimum

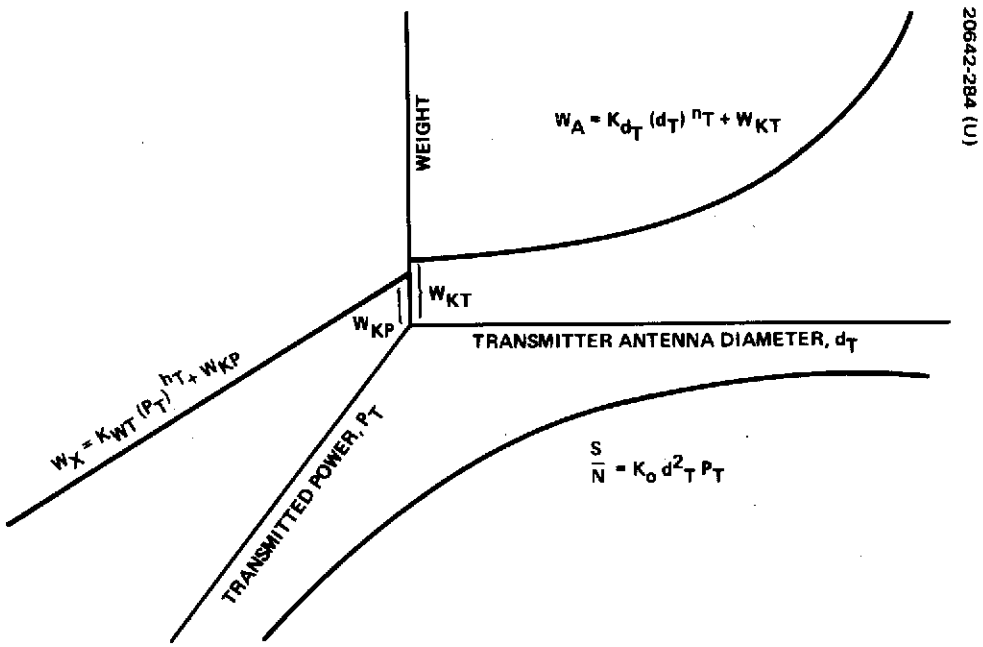

Figure 3-79. Performance and Weight Functions

TABLE 3-21. OPTIMIZATION PROCEDURE

- Performance constraint: S/N = constant
- Weight modeling
  - Antenna (d_T)
  - Acquisition and tracking (d_T)
  - Transponder (P_T)
  - Heat exchanger (P_T)
  - Power supply
    - Transponder (P_T)
    - Acquisition and tracking (d_T)
    - Power efficiency (P_T)
- Key equations
  - $\frac{S}{N} = F_1(d_T, P_T)$ (1)
  - $W_X = F_2(P_T)$ (2)
  - $W_A = F_3(d_T)$ (3)
  - Find minimum ($W_X + W_A$) which meets Equation 1

weight value. The values of d_T and P_T which correspond to this minimum then become the optimum design values. The analysis to determine the minimum weight system was completed and implemented into a computer program. All the values presented in subsequent graphs are optimized in this sense.

This analysis approach can be illustrated by an example at the TDRSS S band frequency. The performance criteria of signal-to-noise ratio specifies the EIRP per unit bandwidth as given in Table 3-22. If, for instance, a 2 MHz bandwidth is required for the S band link, the required EIRP will be -26.4

TABLE 3-22. PERFORMANCE CRITERIA FOR SPACE-TO-SPACE LINK

Signal-to-noise ratio	13 dB
Path attenuation (2.25 GHz, 42159.5 km)	-192.0 dB
Transmitting antenna pointing loss	-0.1 dB
Receiving antenna gain (diameter = 183 cm)	30.1 dB
Transmit and receive RF losses	-1.0 dB
Receiver noise density (temperature = 420K)	-202.4 dB (w/Hz)
(Transmit power) (antenna gain)/(bandwidth)	-26.4 dB (w/Hz)

dBw/Hz + 63 dB (Hz) or 36.6 dBw. All the links are calculated for synchronous altitude ranges, for a 6 foot receiving diameter on the TDRS, and for low noise, transistor RF amplifiers for the TDRS receiver. All antenna gains use 55 percent efficiency and have tracking feeds.

The modeling has been done for each frequency based upon state of the art hardware. The standard model is in the form of:

$$Y = K_1 + K_2 X^{K_3}$$

where

Y = dependent variable (weight, total power or efficiency)

X = transmitted power or the antenna diameter K_1, K_2, and K_3 constants

To determine the constants, values of "Y" were determined for three values of "X" for each frequency. The constants K_1, K_2, and K_3 were then determined by a curve-fitting computer program.

The weight models for the two S band power amplifier configurations are given in Table 3-23. This modeling is based upon actual hardware for both a solid state S band power amplifier and a TWT S band power amplifier. There are three significant differences between these two cases. First, the solid state "transponder weight" is less than the corresponding TWT value. Second, the "transponder efficiency" is different for the two

TABLE 3-23. S BAND WEIGHT MODELING

NOTE: Weights are in pounds; power is in watts; diameter is in meters

Solid State Weight Modeling

Antenna weight, WDT = 6.56156 D ↑ 2.01861 + 1.28077

Acquisition and track weight, WQT = 15 + 0.13 [WDT]

Transponder weight, WT = 4.53531 E-2 [PT] ↑ 0.84219 + 7.08465

Transponder efficiency, KE = 0.5287 + 0.3647 * PT ↑ -0.34

Heat exchanger weight, WH = 0.22 * [(1-KE)/KE] * PT + 0

Transponder input power, PPT = PT/KE

Acquisition and track power, PQT = 2 [15 + 0.13 * 6.56165 * D ↑ 2.01861]

Power supply weight, WST = 0.32 [PPT + PQT] + 1

TWT Weight Modeling

Antenna weight, WDT = 6.56165 D ↑ 2.01861 + 1.28077

Acquisition and track weight, WQT = 15 + 0.13 [WDT]

Transponder weight, WT = 0.330847 [PT] ↑ 0.86613 + 10.0692

Heat exchanger weight, WH = 0.22 [PT/KE] + 0

Transponder efficiency, KE = -0.240931 + 0.300931 * PT ↑ 0.26263

Transponder input power, PPT = PT/KE

Acquisition and track power, PQT = 2 [15 + 0.13 * 6.56165 * D ↑ 2.01861]

Power supply weight, WST = 0.32 [PPT + PQT] + 1

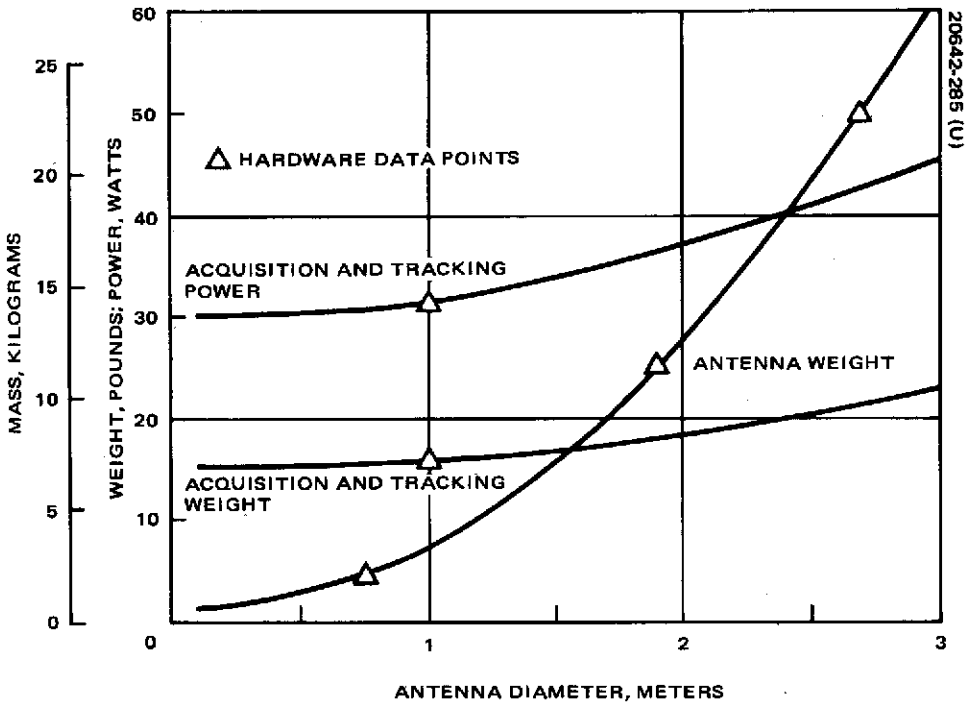

Figure 3-80. Weight Modeling for Parameters Dependent Upon Antenna Diameter

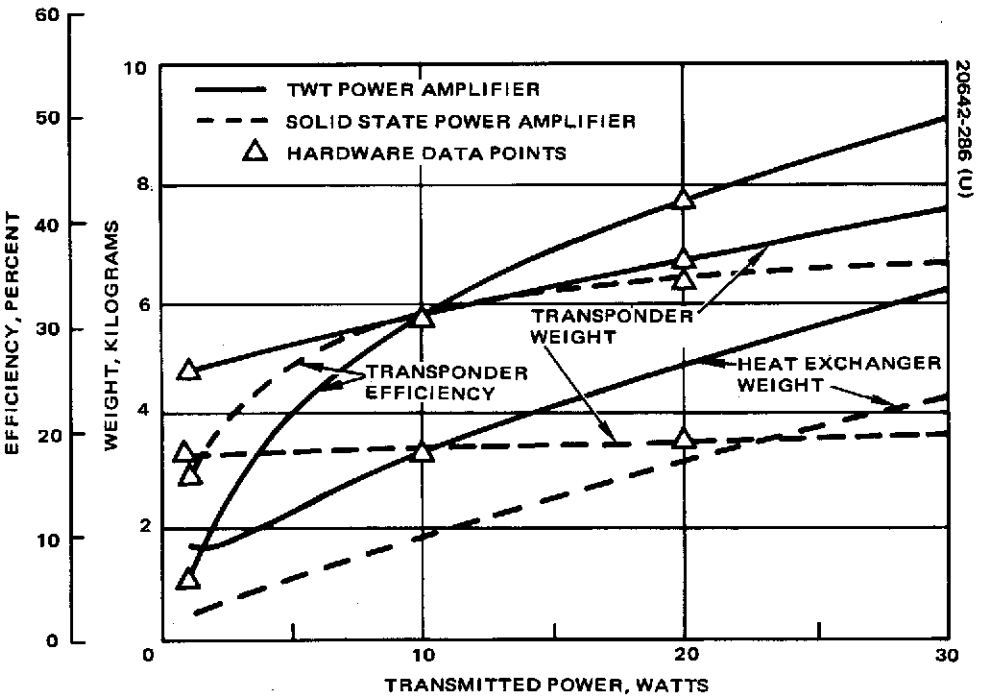

Figure 3-81. Weight Modeling for Parameters Dependent Upon Transmitted Power

cases*. Third, the power dissipation, and therefore heat exchanger weight, is different. The power dissipation is different since the maximum power that can be dissipated in a TWT is the total input power, occurring when there is no drive power. In a solid state, Class C power amplifier, the maximum dissipation occurs at maximum input drive and is equal to the dc input power less the RF output power. This difference in maximum dissipation in the two types of power amplifiers affects the heat exchanger weight, as may be seen by comparing the form of the heat exchanger weight equation for the two cases.

Figures 3-80 and 3-81 plot the key curves given by the equations in Table 3-23. The modeling of parameters dependent upon antenna diameter is given in Figure 3-80 and applies to both types of power amplifiers. The weights dependent upon the transmitted power are shown in Figure 3-81. These illustrate the difference in transponder weight, heat exchanger weight, and transponder efficiency.** Especially noteworthy is the relatively high efficiency displayed by the solid state amplifiers at low power output levels.

Analysis Results. The next step of the analysis of the sample problem is to combine the performance criteria with the weight criteria and determine an optimum set of values for the transmitted power and the transmitter antenna diameter. The optimum values are defined as the ones that yield a minimum weight system for a given data rate. Figures 3-82 through 3-85 give the optimized values as a function of the receiver noise bandwidth and compare these values to the K band and X band data. Figures 3-86 through 3-89 indicate the effects of varying the TDRS receiving antenna upon the user transmitter weight power and parameter values.

Figure 3-82 indicates that the S band solid state power amplifier configuration is 8 to 10 pounds lighter than the S band TWT power amplifier configuration over a wide range of bandwidths. This weight difference is largely due to the differences in the transponder weights and in the heat exchanger weights. This may be seen in Table 3-24 which lists the individual weights of the communications subsystem components.

At low data bandwidths, the S band solid state transmitter is lighter than the K band and X band systems but is heavier at the 2 MHz, medium data rate point. Figure 3-83 indicates that the dc power requirement follows the same pattern as the overall weight, with less power required for the solid state power amplifier than for the TWT power amplifier.

---

*A significant factor in this type of evaluation is accounting for the variation of transponder (transmitter and receiver) efficiency as a function of output power. A seven to one variation is typical for a wide range of output powers when a TWT is used.

**The heat exchanger weight is due only to the heat dissipation from the transponder. The required heat exchanger weight for the acquisition and tracking power dissipation is included in the acquisition and tracking weight.

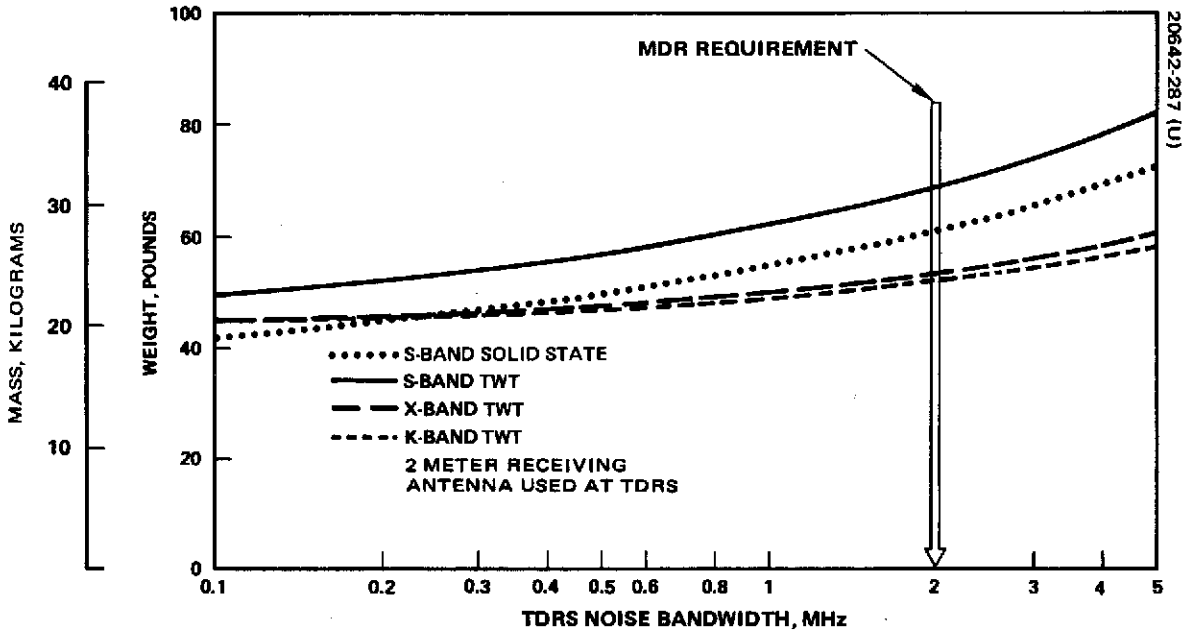

Figure 3-82. Communication Subsystem Weight for Weight Optimized Design as Function of Noise Bandwidth

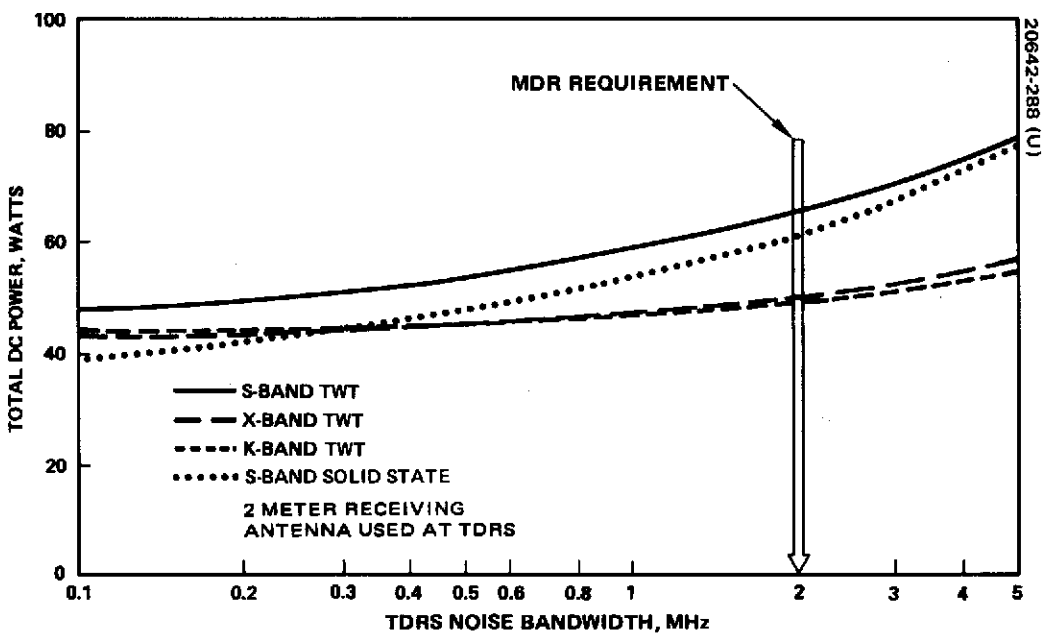

Figure 3-83. Communication Subsystem Power for Weight Optimized Design as Function of Noise Bandwidth

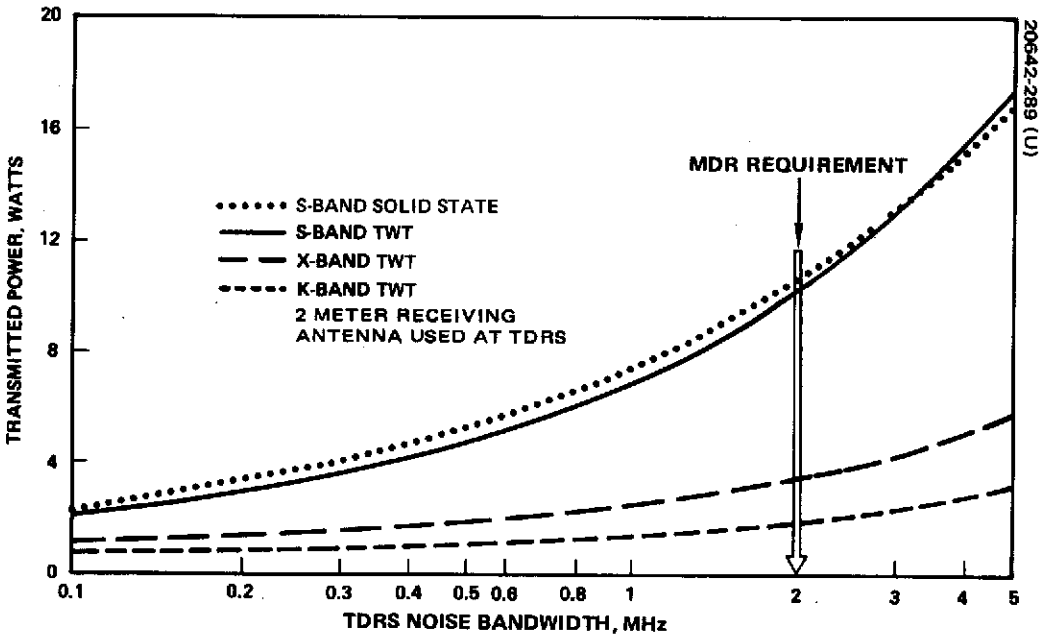

Figure 3-84. Transmitted Power for Weight Otpimized Design as Function of Noise Bandwidth

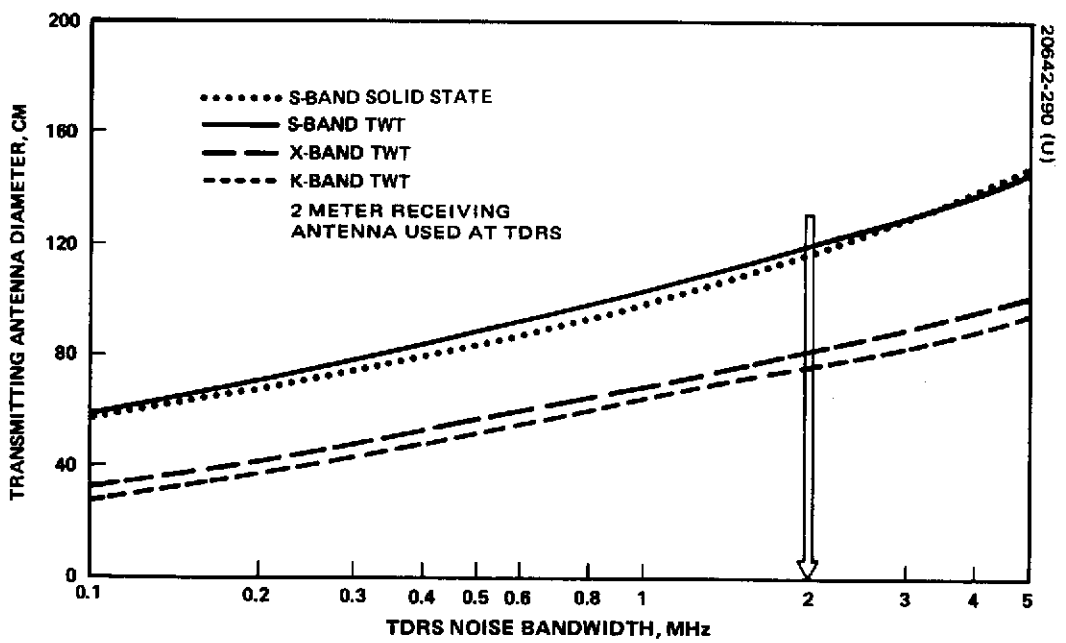

Figure 3-85. Transmitting Antenna Diameter for Weight Optimized Design as Function of Noise Bandwidth

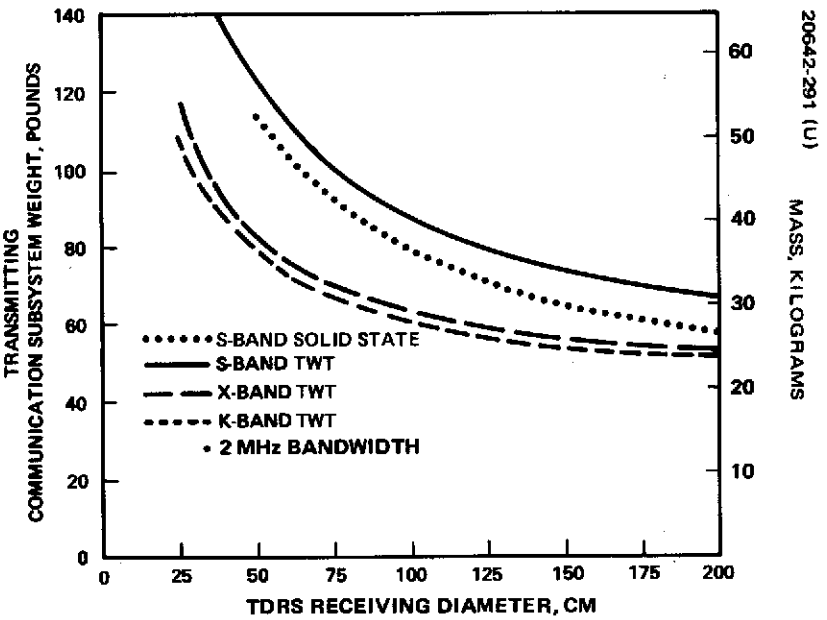

Figure 3-86. Communication Subsystem Weight Optimized Design as Function of TDRS Antenna Diameter.

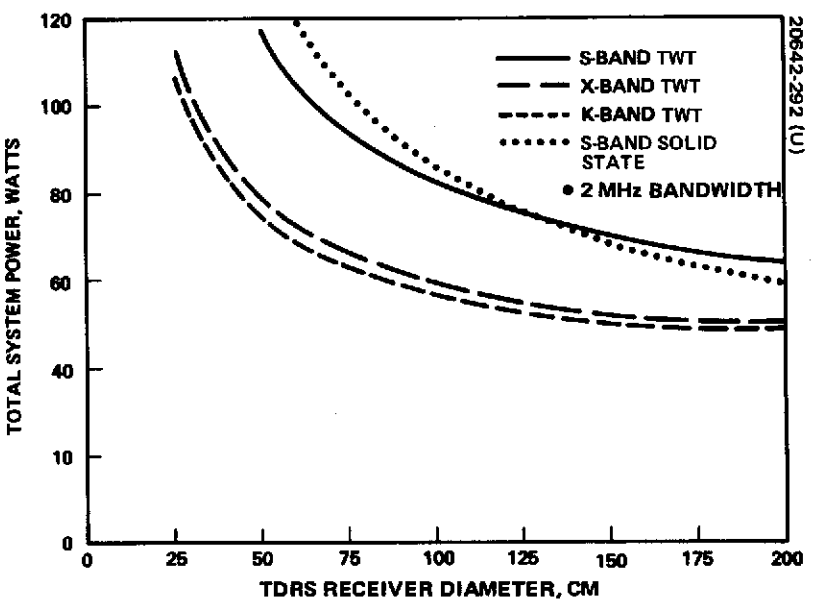

Figure 3-87. Total System Power for Weight Optimized Design as Function of TDRS Antenna Diameter

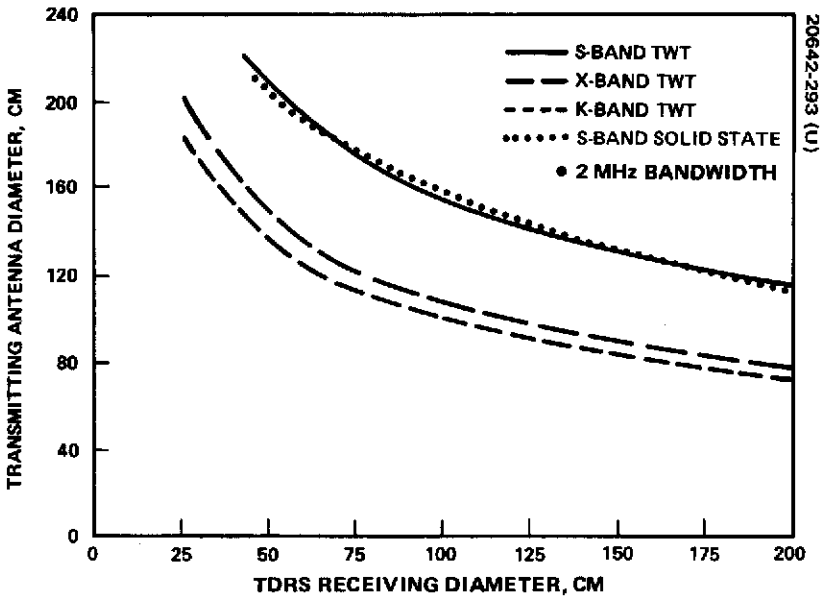

Figure 3-88. User Antenna Diameter for Weight Optimized Design as Function of TDRS Antenna Diameter

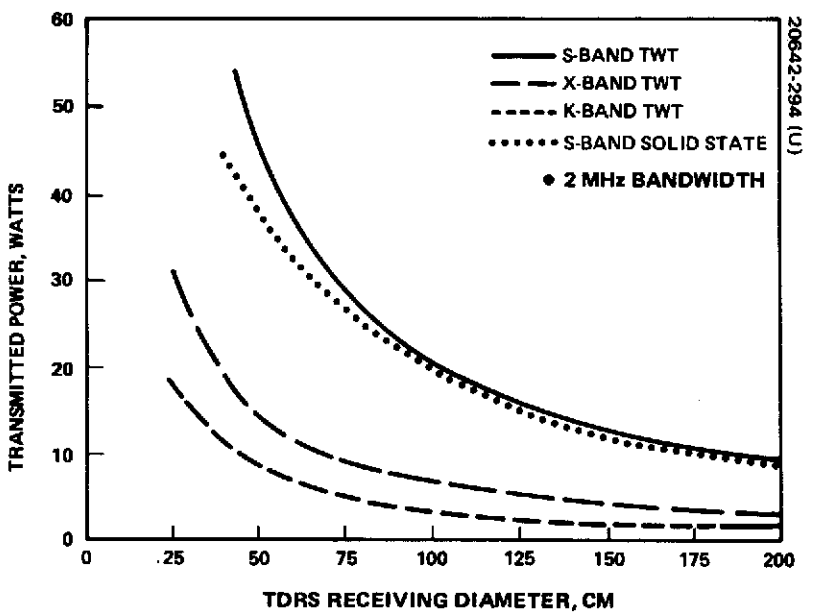

Figure 3-89. Transmitted Power for Weight Optimized Design as Function of TDRS Antenna Diameter

TABLE 3-24. PARAMETER VALUES, WEIGHTS, AND POWERS FOR WEIGHT OPTIMIZED S BAND COMMUNICATIONS SYSTEMS WITH 2 MHz NOISE BANDWIDTH

TWT Weight Modeling		
Antenna diameter	120.5 cm	
Antenna weight	4.91	
Acquisition and track weight	7.46	
Transponder weight	5.72	
Weight subtotal	18.09 kg	
Prime power supply weight	9.95	
Heat exchanger weight	3.27	
Total weight		31.31 kg
Transponder input power	32.9	
Acquisition and track power	32.5	
Total DC power		65.4 watts
Transponder efficiency	31.5 percent	
Transmitted power	10.4 watts	
Solid State Weight Modeling		
Antenna diameter	118.6 cm	
Antenna weight	4.77	
Acquisition and track weight	7.46	
Transponder weight	3.36	
Weight Subtotal	15.59 kg	
Prime power supply weight	9.40	
Heat exchanger weight	1.86	
Total Weight		26.85 kg
Transponder input power	29.3	
Acquisition and track power	32.4	
Total dc power		61.7 watts
Transponder efficiency	36.6 percent	
Transmitter power	10.7 watts	

Figures 3-84 and 3-85 indicate that the transmitted power and antenna diameter are about the same for both configurations. However, at low power levels, where the solid state power is cheaper in terms of weight than the TWT power, the optimum solid state configuration has a higher output power than the optimum TWT configuration. The antenna diameters shown in Figure 3-85 have the opposite relative values as compared to the output power to match the EIRP performance criteria.

Figures 3-86 through 3-89 use as a parameter the receiving antenna diameter of the TDRS. The total system weight, plotted in Figure 3-86, shows a marked improvement for the solid state S band system as compared to the TWT S band system. However, the K band and X band systems are still lighter for a 2 MHz noise bandwidth system.

The power variation between the two S band systems shown in Figure 3-87 is a function of the two efficiencies, transponder weights, and heat exchanger requirements. Figures 3-88 and 3-89 plot the two communication parameters, transmitter antenna diameter and transmitted power. Since the EIRP requirements are identical for the two S band systems, the values of those parameters is about the same for the solid state and TWT S band configurations.

At a medium data rate requiring a noise bandwidth of 2 MHz, a K band communication system is the lightest of the four considered. However, the advantage of the K band system over the solid state S band system is considerably less than the corresponding advantage of the K band system over the TWT S band system and, from Figure 3-82, this weight difference is approximately 4.5 kg.

3.3.2.3 Link Analysis

With the selection of S band as the MDR frequency, the design of the forward and return links is straightforward. The TDRS EIRP and G/T requirements are determined by the assumed manned user characteristics as listed in 3.1. The link power budget indicates that in order to transmit a 20 kbps voice signal to a manned user with a circularly polarized, omnidirectional antenna the TDRS must have an EIRP of 47 dBw. In order to relay a 100 kbps signal consisting of voice and data, the TDRS G/T must be approximately 7 dB/K or greater. This is 5 dB larger than the SOW requirements as listed in Table 3-25. With a receiver noise figure of 3.9 dB and an assumed earth temperature of 300 K, the system noise temperature will be about 720K. The minimum required antenna gain is 35.6 dB which requires a 3.66 meter antenna diameter with a 50 percent efficiency.

Antenna Size and Transmitter Power. A parametric study was made to determine the combination of antenna size and transmitter RF power which produces the required EIRP of 47 dBw but results in minimum spacecraft weight. Figure 3-90 shows the minimum weight combination of antenna size and transmitter power for a given product of power and antenna gain. When the transmission losses and pointing loss are included, the product of transmitter power and antenna gain must be slightly greater than 50 dB in order

TABLE 3-25. MEDIUM DATA RATE SERVICE POWER BUDGETS

Forward Link

Parameter	MDR Forward S Band	
	High Power	Low Power
TDRS EIRP	47.0	41.0
TRDS pointing loss	-0.5	-0.5
Space loss	-192.0	-192.0
Receive antenna gain	G_u	G_u
Receive pointing loss	-0.3	-0.3
Receive line loss	0	0
Receive ellipticity loss	0	0
Receive power, P_r	G_u-146	G_u-152
Receiver noise figure, dB	5.5	
Receiver noise temperature, K	750	
Background noise temperature, K	50	
Total system noise temperature, K	800	
Noise density, η_T, dBw/Hz	-199.5	
P_r/η_T dB-Hz	G_u+53	G_u+47

Return Link

Parameter	MDR S Band	Order Wire S Band
Transmit power		20
Transmit antenna gain	EIRP	0
Transmit pointing plus line loss	—	—
Space loss	-192.7	-192.7
TDRS antenna gain	36.7	13.2
TDRS pointing loss	-0.5	—
TDRS line loss	-2.2	-1.0
TDRS ellipticity loss	0	-0.2
Received power P_R	EIRP -158.7	-160.7
Noise figure, dB	3.9	3.9
Receiver noise temperature, K	420	420
Earth noise temperature, K	300	300
Total system noise temperature, K	720	720
Noise density, η_T, dBw/Hz	-200	-200
P_r/dB-Hz	EIRP + 41.3	39.3

to provide 47 dBw EIRP. This design value is indicated on the graph. Such an optimum design would require a transmitter power of 20 watts and an antenna diameter of 4.15 meters. However, an antenna diameter of 3.82 meters (12.5 feet) was selected because a current design can be used with some modification. The corresponding required RF power is 24.5 watts. Figure 3-91 shows the effect on TDRS weight of choosing a nonoptimum antenna size. Note that the selected size results in less than a 1 kg penalty relative to the optimum size. Included in the S band subsystem are the transmitters, the receivers, the prorated value of the spacecraft power supply, the prorated value of the spacecraft heat exchanger, the antenna weight, and the acquisition and tracking weight. This small increase in weight due to nonoptimum antenna size is not felt to be a serious deviation from an optimum design in view of the desirability of using an S band antenna that is well advanced in its development cycle.

The selected antenna size of 3.82 meters also satisfies the return link G/T requirement. The original SOW EIRP requirement of 41 dBw can be accommodated in a low power mode.

Link Capability. For these TDRS characteristics, Table 3-25 presents the link power budgets for both forward and return links. The user EIRP and antenna gain remain as parameters in this table and the effect of user characteristics on the data rate capacity is shown in Figures 3-92 and 3-93 for the forward and return links respectively.

Flux Density. The power flux density, D, is given by D = EIRP - 162 dBw/m^2. The required minimum signal bandwidth, B, to ensure that the CCIR requirement of -154 dBw/m^2/4 kHz is given by 10 log B $\geq$ D - CCIR Req. + 36. For the high power mode with 47 dBw EIRP, D = -115 dBw/m^2 and log B $\geq$ 7.5 and hence B $\geq$ 32 MHz. The repeater design is limited to 10 MHz; thus, there will be a 5 dB violation of the CCIR requirement. This violation is a direct result of the requirement to transmit voice to a manned spacecraft which has an omnidirectional antenna.

3.3.3 Ground Link Analysis

The ground link is defined as the RF communication link between the TDRS and the ground station. As previously defined, communication from the TDRS to the ground is called the return link and has been allocated the frequency band 14.4 to 15.35 GHz. Signals sent from the ground station to a TDRS comprise the forward link and the allocated band is 13.4 to 14.0 GHz. These K band frequencies were selected over available allocations at S band and X band because of the greater total bandwidth available. This greater bandwidth will allow growth to larger link capacity and greater flexibility in signal multiplexing.

The objective of ground link design is to parametrically relate the major link parameters of both the TDRS and ground station RF equipment and then to choose a combination of transmitters, receivers, and antennas that meet these requirements while at the same time satisfing limitations on or minimizing cost, TDRS weight, and size. The major emphasis is on the

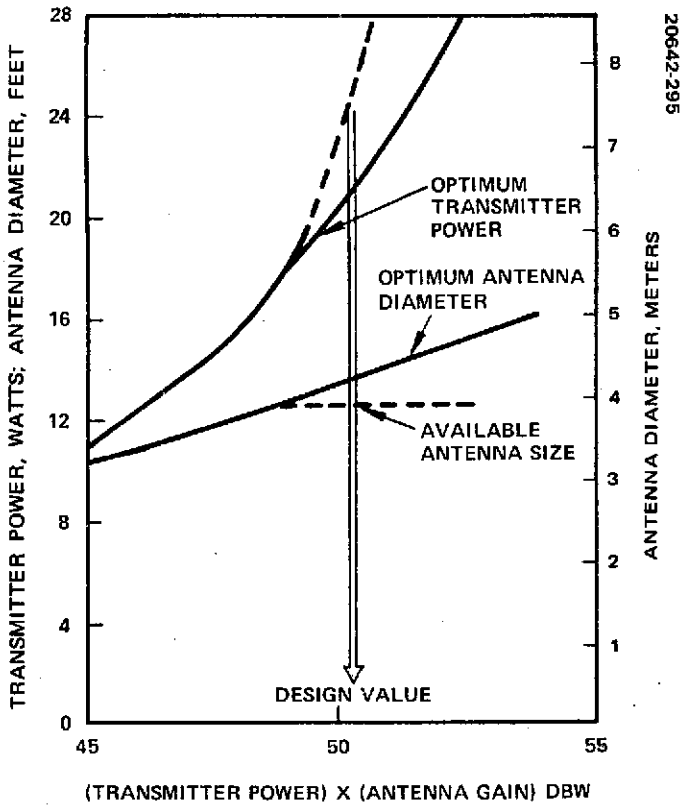

Figure 3-90. S Band Transmitting Parameters

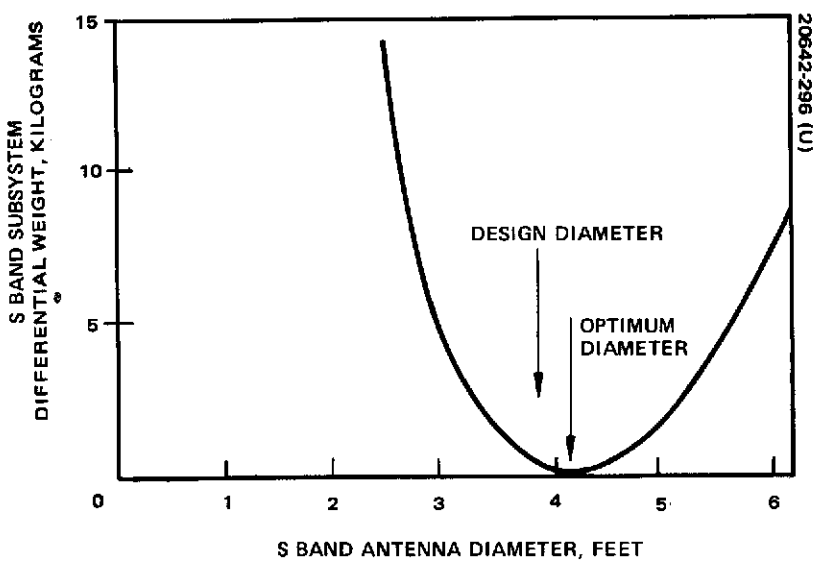

Figure 3-91. Effect of Antenna Diameter Choice Upon Subsystem Weight

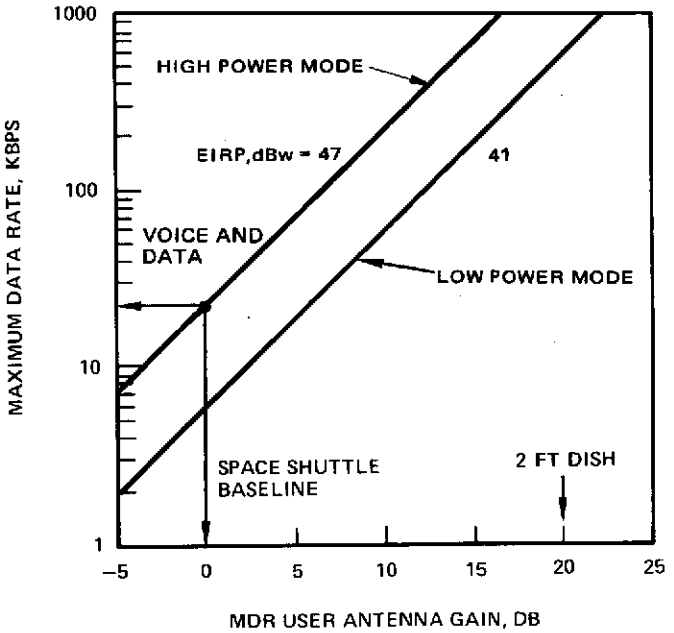

20642-297 (U)

ASSUMPTIONS

0.5 dB USER POINTING AND LINE LOSS
900°K USER SYSTEM NOISE TEMP
$\frac{E_b}{\eta} \geq 10dB$
NO DEGRADATION IN CORRELATION RECEIVER AND DEMODULATOR

Figure 3-92. Medium Data Rate Forward Link Capability

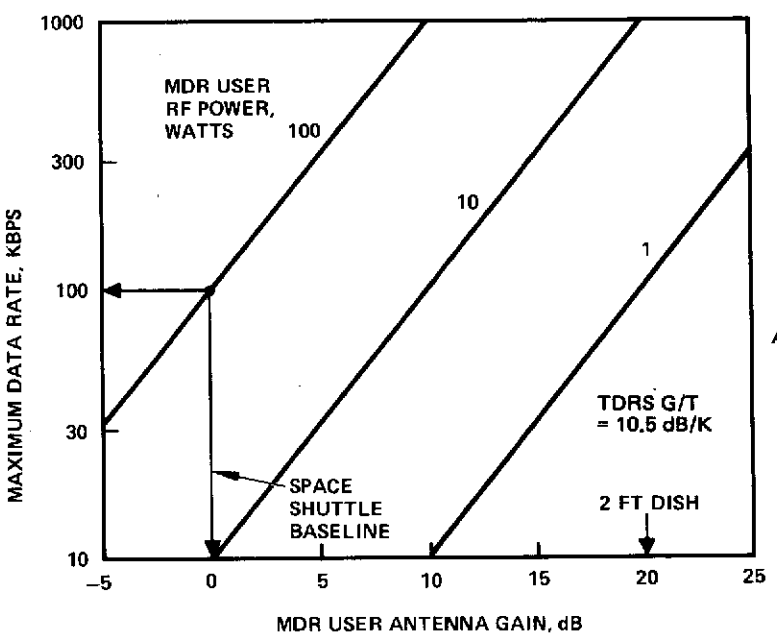

20642-298 (U)

ASSUMPTIONS

$\frac{E_b}{\eta} = 10dB$

DEGRADATION IN EQUIPMENT = 1.3 dB

NO ERROR CORRECTION ENCODING

Figure 3-93. Medium Data Rate Return Link Capability

return link which employs a K band transmitter on the TDRS where power is limited. Also, the size of the TDRS and ground antennas is important. The TDRS antenna has an impact on mechanical design while the ground antenna cost is monotonically related to its size.

The requirements and constraints imposed on the ground link are summarized in Table 3-26. The baseline parameters chosen as a result of the analysis are as follows:

1) Ground station antenna diameter = 12.8 meters

2) TDRS single power amplifier saturation power = 8 watts

3) TDRS K band antenna diameter = 1.43 meters

4) Minimum power backoff = 5 dB

3.3.3.1 Return Link

The return link design approach is depicted in Figure 3-94. First an investigation of potential ground receivers and their noise characteristics allows a preliminary choice and establishes the noise density contributed by the ground receiver. Next the effects of weather in the Washington D.C. area establish a relationship between required link margin and link availability. Turning to the repeater configuration, there are several types of signals being relayed from user spacecraft to the ground via a TDRS. This signal variety plus the requirement for linearity of the low data rate telemetry channels leads to three possible frequency translation alternatives for final power amplification.

The linearity requirement also involves a consideration of TWT backoff and gain from input to output for each return channel. Following the input/output analysis, a power amplifier configuration can be selected on the basis of required saturation power (which determines the bus power requirements) and complexity. Finally, trades between ground antenna size and TDRS EIRP, and consequently weight, can be made allowing a selection of TDRS antenna size, TWT saturation power, and ground antenna size.

Ground Station Parameters. The ground station performance improves with an increase in antenna gain, G, or with a decrease in receiving system temperature, T. The gain increases with the square of the diameter, but the antenna structural difficulties vary roughly as D^3. Furthermore, for very large apertures, surface variations and structural distortions can reduce the achievable gain. A trade exists between increased surface accuracy and increased diameter in attaining a desired gain. The cost of the TDRSS ground antennas will be minimized by use of designs already available. Numerous antennas have been built at 12.2, 12.8, 18.3, 25.9, and 29.6 meters although few have been used at K band.

Ground receiver quality will lie between that of an uncooled parametric amplifier (paramp) with noise temperature, T_R, of about 420 K and a

TABLE 3-26. CONSTRAINTS AND REQUIREMENTS FOR TDRSS GROUND LINKS

GENERAL

1) Minimum ground antenna elevation angle = 10 degrees
2) Ground station at GSFC
3) 17.5 dB weather margin
4) Linear power amplification of LDR return link channels

RETURN LINK

1) Frequency band 14.40 to 15.35 GHz
2) Services

Signal	No. of Users	Date Rate Per User, kbps	Probability of Bit Error
LDR telemetry	20	1.2	10^{-5}
LDR voice	1	20.0	10^{-2}
MDR telemetry	1	1000.0	10^{-5}
Order wire	1	0.5	10^{-5}
TDRS telemetry	-	1.0	10^{-6}

FORWARD LINK

1) Frequency band 13.25 to 14.2 GHz
2) Services

Signal	No. of Users	Data Rate, bps	Probability of Bit Error
LDR channel 1	1	300	10^{-5}
LDR channel 2 (primarily voice)	1	9,600	10^{-2}
MDR	1	20,000	10^{-5}
TDRS command	-	500	10^{-5}

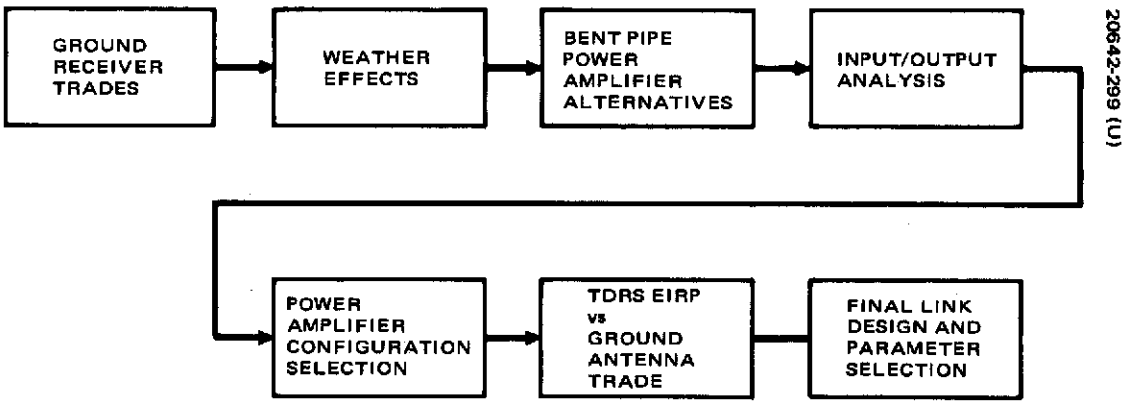

Figure 3-94. Return Ground Link Design Flow

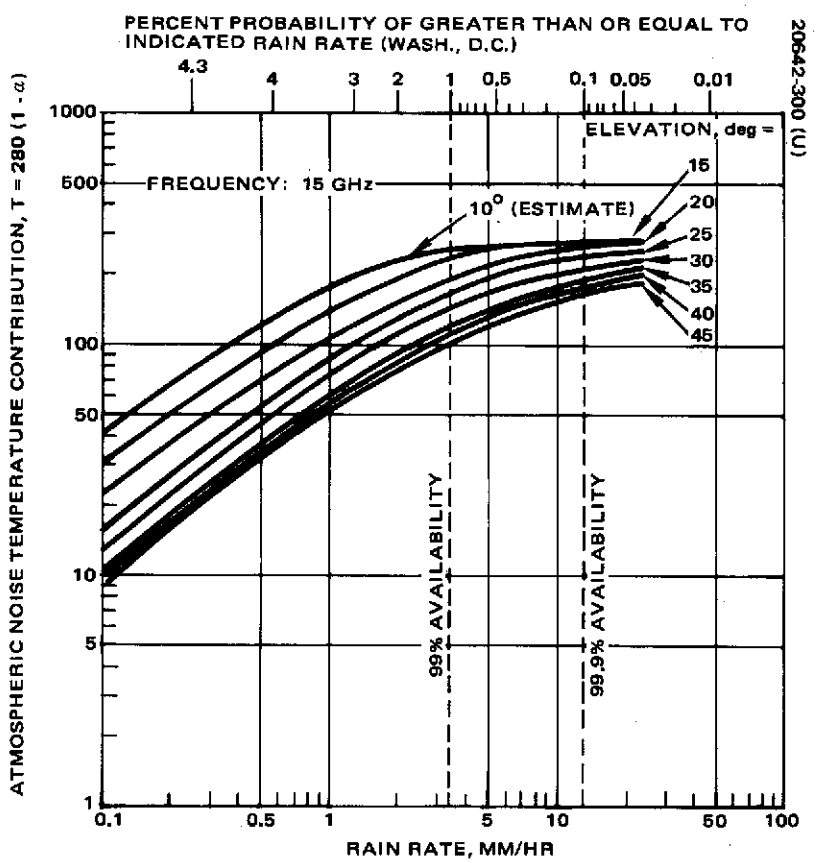

Figure 3-95. Sky Noise Temperature Versus Rain Rate (From Deerkoski, "Ku Band TDRS Ground Antenna Study")

state of the art maser with T_R = 50 K. The 9.2 dB advantage is reduced during periods of heavy rainfall. Figure 3-95 shows the additional effective noise temperature due to rain. Note that at Washington D.C. this sky noise temperature will be as large as 280 K approximately 1 percent of the time. Since the ground link must be designed for at least 99 percent availability, this additional noise temperature contribution must be included. The advantage of the maser over the paramp then becomes

$$10 \log \left(\frac{420 + 280}{50 + 280} \right) = 3.4 \text{ dB}$$

The much greater complexity of the maser does not appear justified, and for the following analysis it will be assumed that a paramp with T_R = 420 K will be employed. This is consistent with the ground station implementation of a high quality uncooled paramp (see subsection 3.5.1).

The results of the analysis to follow show that if a maser were employed, one or a combination of the following would be possible:

1) TDRS K band equipment weight could be decreased by possibly 12 kg.

2) Link availability would be increased a few hours per year.

3) The ground antenna could be smaller in size.

Although the effect on the TDRS is significant, the cost complexity and maintenance problems associated with a maser do not appear warranted. Reducing the ground antenna size from the selected value will not reduce the cost significantly due to a compensating increase in power amplifier cost.

Weather Effects at K Band. For clear sky conditions, the effects of the atmosphere on propagation at 15 GHz are quite minimal. However, signal attenuation due to absorption increases to significant levels under conditions of heavy cloud cover or precipitation. The atmospheric constituents which attentuate the signal also absorp radiant energy and re-emit the energy as noise. Thus atmospheric moisture can attentuate the communications signal and increase the receiver system noise. Finally, even for clear sky conditions, atmospheric scintillations can limit the bandwidth available for coherent communications. In Reference 1 it is shown that the latter effect can be ignored but that the other effects are quite important. A comparison of the GSFC attenuation model (Reference 2) and the Hughes model (Reference 3) shows that they give similar predictions for attenuation as a function of rain rate although the GSFC model is somewhat more conservative. The two models are also consistent with the experimental data available from the ATS-5 Millimeter Wave Experiment (Reference 4). Because the GSFC model is more conservative, it was used in the analysis. This raw data was used to produce Figure 3-96, showing the effect of both antenna elevation angle and link availability for a ground station near GSFC.

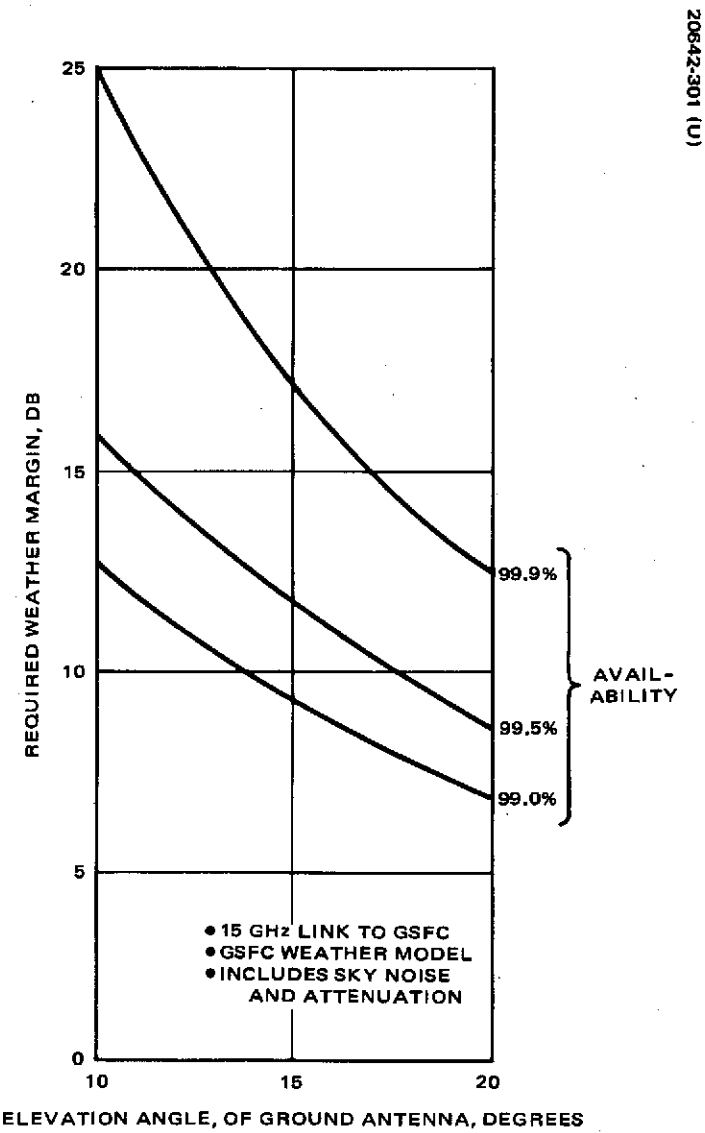

Figure 3-96. Weather Margin Versus Elevation Angle

Total TDRS system visibility increases as the angular separation between TDRSs increases, and hence ground antenna elevation angle decreases. The lower limit on this angle has been specified as 10 degrees (0.175 rad), and so link design will be based on this value. Figure 3-97 shows the relationship between link availability and required weather margin for this elevation angle.

During the course of the study, a required weather margin of 17.5 dB was selected by the TDRS Program Office at GSFC. Note from Figure 3-97 that if the ground station were near GSFC the link availability would be 99.65 percent.

Power Amplifier Alternatives. There are two requirements in the Statement of Work which have a major impact on the design of the return link K band power amplifier:

1) The repeater shall be of the frequency translation type.

2) The LDR telemetry signals shall be amplified linearly.

The first requirement eliminates the commonly considered technique known as FDM/FM whereby the return link channels are frequency multiplexed and this combined signal used to frequency modulate the K band carrier. The second requirement is not defined quantitatively in the SOW, but linearity is generally understood to imply that the effect of remaining nonlinearity results in negligible degradation to link performance.

The four types of signals being relayed by the TDRS to the ground are:

1) Medium data rate return data

2) Voice

3) Low data rate return telemetry from up 20 users all in a common channel.

4) Order wire data

The situation is further complicated by the polarization separation of the signals from the VHF antenna, both of which contain a portion of the LDR telemetry and voice signals.

The linear amplification requirement applies only to the LDR return telemetry channel which is split into two separate signals at the antenna as just mentioned. Thus, one repeater configuration alternative would require the voice to be filtered from the output of the two VHF receivers with subsequent multiplexing and amplifying of the remaining LDR telemetry signals in a separate power amplifier providing linearity. The voice would be combined with the MDR signal and this combination transmitted via another power amplifier operating near saturation for greater power efficiency. The complexity involved in filtering the voice signal out of the two VHF receiver

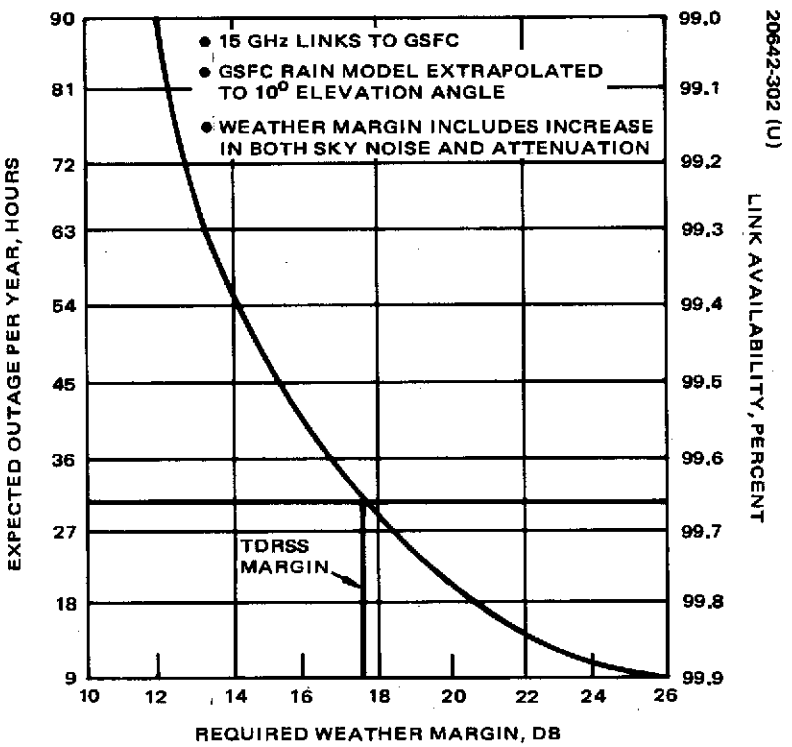

Figure 3-97. Weather Margin Versus Availability

outputs is undesirable and hence a second alternative would eliminate this: multiplexing both VHF received signals at IF (containing both LDR telemetry and voice) and providing a linear power amplifier for this combination. The MDR channel would be amplified in a second saturated TWT. Both methods require two power amplifiers followed by an RF combining circuit.

A third alternative employs only one power amplifier operated below its saturation value, providing linear amplification not only to the VHF receiver outputs, which contain both user telemetry and the voice signal, but to the MDR return link signal as well. Thus, all signals receive linear amplification.

In all the above implementations, ground controlled attenuators are desirable in all channels leading to a linear power amplifier in order to compensate for changes in interference levels, variation in user transmitter power levels, and equipment variation. The three alternatives discussed above are listed briefly in Table 3-27.

Input/Output Analyses. The procedure for this portion of the return link analysis is to

1) Determine the required EIRP per signal the TDRS must generate,

2) Examine the VHF input in order to determine its variation, and then

3) Determine required power amplifier saturation levels considering linearity and backoff requirements.

Table 3-28 presents a simplified link budget where the TDRS EIRP and ground antenna gain have been left as parameters. The 420 K noise temperature receiver corresponds to a good quality parametric amplifier as mentioned above. The equation at the bottom of Table 3-28 was used to

TABLE 3-27. RETURN REPEATER CONFIGURATION ALTERNATIVES

1) One linear power amplifier (PA)
2) Two power amplifiers
a) LDR telemetry and voice in linear (PA)
Medium rate data in saturated PA
b) LDR telemetry in linear PA
Medium rate data and voice in other PA

TABLE 3-28. TDRS-TO-GROUND LINK BUDGET – K-BAND 14.2 TO 15.35 GHz

TDRS EIRP	EIRP
Ground antenna gain	G
Space loss	-208.4
Pointing loss	-1.0
Ground received power, P_r = EIRP + G	-209.4 dBw
Noise temperature (420 K)	+26.3
Boltzmann's constant	-228.6
Thermal noise density, η_T =	-202.3 dBw/Hz

$$\frac{P_r}{\eta_T} = \text{EIRP} + G - 7.1 \text{ dB-Hz}$$

derive the required TDRS EIRP + G per signal in the right hand column 6 of Table 3-29. Column 5 was derived from the following equation:

$$\frac{P}{\eta} = \left(\frac{E_b}{\eta}\right) \quad R_b M_w \tag{1}$$

where E_b/η is the required bit energy to noise density resulting from the ground link alone, R_b is the bit rate per user, and M_w is the weather margin. Column 4 of Table 3-29 shows the 17.5 dB weather margin for all signals except the TDRS housekeeping telemetry which was assigned a 20 dB weather margin. Column 3 lists the design data rate for the respective return link service. The values of E_b/η for each link were chosen so that less than 0.5 dB degradation would occur in the overall signal-to-noise due to the ground link. Note that the dominant value of EIRP + G in column 6 of Table 3-28 corresponds to the MDR signal when 1 Mbps is being returned. Before using the values of Table 3-28 to determine a saturation EIRP, the variation in the VHF input must be examined and a backoff factor selected to provide linearity.

Table 3-30 presents a link budget with potential variations for the LDR return telemetry link. These link power variations were used to produce Figure 3-98 relating VHF power received by the TDRS to the number of visible, transmitting users. The principal assumption in this analysis is that the average user radiated power is 5 watts through an omnidirectional

TABLE 3-29. GROUND LINK SIGNAL PARAMETERS

1 Return Service	2 Minimum Ground Link E_b/η, dB	3 Maximum Data Rate per user, kbps	4 Minimum Weather Margin, dB	5 Minimum P_r/η, dB-Hz	6 Minimum Required EIRP + G, dBw
Low rate telemetry	14	1.2	17.5	62.3	69.4
Voice	14	20	17.5	74.5	81.6
Medium rate data	20	1000	17.5	97.5	104.6
TDRS telemetry	15	1	20	65	72.1
Order wire	15	1	20	65	72.1

TABLE 3-30. VHF TELEMETRY LINK POWER VARIATIONS
(sum of both H and V channels)

	Minimum Value	Tolerance
User transmit power	7.0 dBW	+1.0 dB
User antenna gain	-3.0 dB	+6.0 dB
Space loss	-167.5 dB	+1.5 dB
TDRS gain	11.2[(1)] dB	+3.0[(2)] dB
Ellipticity loss	-0.5 dB	+0.5 dB
Line losses	-1.0 dB	+0.6 dB
Received power	-153.8	+12.0 dB

[(1)] Edge of 30 degree coverage zone.
[(2)] Center of coverage zone.

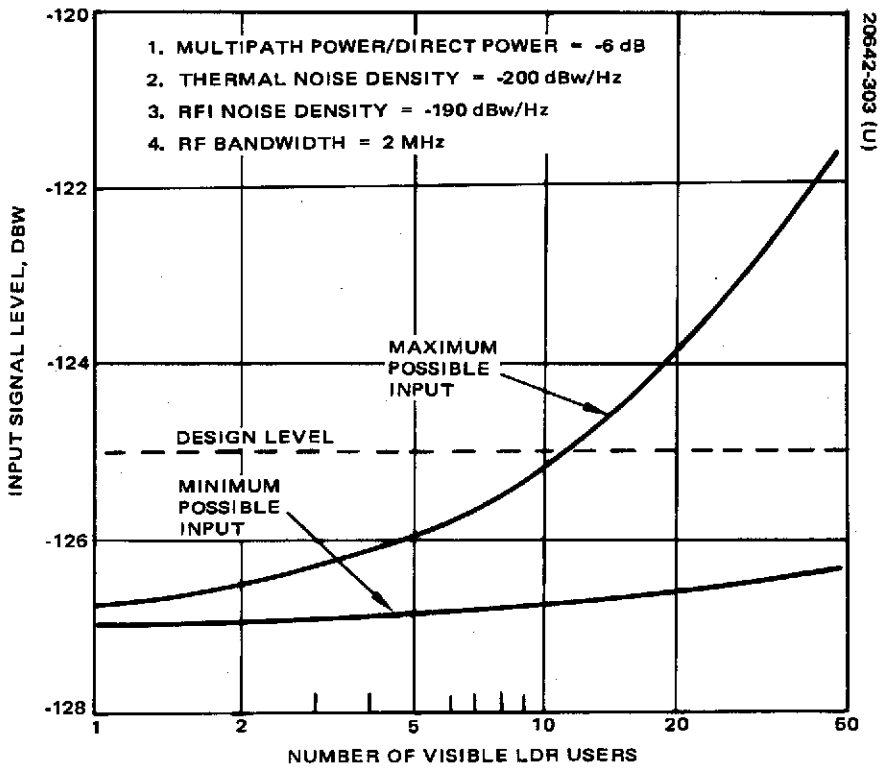

Figure 3-98. Input Signal Level in VHF Receiver From Low Data Rate Telemetry Users, RFI, and Thermal Noise

antenna. The analysis of 3.2.1 has shown that an RFI noise density of -190 dBw/Hz will limit the average LDR return telemetry to less than 1 kbps with these user transmitter characteristics. However, for purposes of analysis this level was assumed primarily because current estimates are even larger than this value.

Referring to Figure 3-98, the difference between the minimum and maximum curves corresponds to variation in TDRS antenna gain over the coverage region, variation in user EIRP, and variation in distance between the spacecraft. The ordinate represents the total power out of the two transmission lines from the VHF antenna due to LDR users and RFI plus thermal noise, but not including the voice signal. The amount of power in each signal depends on many factors, but since both signals will be amplified in the same power output amplifier it is not necessary to know the level of each separately. Assuming a worst case design condition of 30 visible users, an averaging of the variational effects will occur. Cursory analysis indicates that the averaging will result in at least a 2 dB reduction from the maximum input conditions. Thus for design purposes, the input level was taken as -125 dBw.

A variational analysis of the return voice link budget indicates that the maximum VHF receiver input voice power will be -130 dBw. Thus, the total maximum VHF receiver input signal level is -123.5 dBw.

From Table 3-29, the required TDRS EIRP for a single user signal must be 69.4-G dBw and from Table 3-30 the minimum single user input level is -153.8. Thus the LDR return link channel must have a gain of 223.2-G dB. The total input of -123.5 dBw is 30.3 dB greater than the minimum single user signal. But the amplification must remain linear, and hence provide the additional 30.3 dBw output containing the amplified signals of 30 other users, RFI, and the VHF return voice signal. Thus, the EIRP + G required for transmission to the ground of LDR return telemetry and voice is 99.7 dBw and the power amplifier must be operating in a linear region of its gain characteristic.

A link power budget for the MDR return link shows that the reoeived input power for 1 Mbps data rate must be about -128.7 dBw. The estimated MDR receiver noise density is -200 dBw/Hz and the channel bandwidth is 10 MHz, resulting in a noise power of -130 dBw. If this channel were to receive linear amplification in a single power amplifier, the K band signal output EIRP + G must be 104.6 dBw (see Table 3-29); the additional noise output will be 103.3 dBw for a total channel output of 107.0 dBw.

The order wire channel has a maximum capacity of about 1 kbps if a 100 watt transmitter is employed on the manned user. However, the bandwidth of the channel in the TDRS repeater cannot easily be made less than 1 MHz without more complex filters or undesirable additional frequency translations and more complex frequency synthesizer. A link budget indicates a received signal power level of -160.7 dBw, but with a noise density of -200 dBw/Hz, the noise power is -140 dBw, 100 times greater. Filtering at the ground station will produce a satisfactory signal-to-noise ratio, but

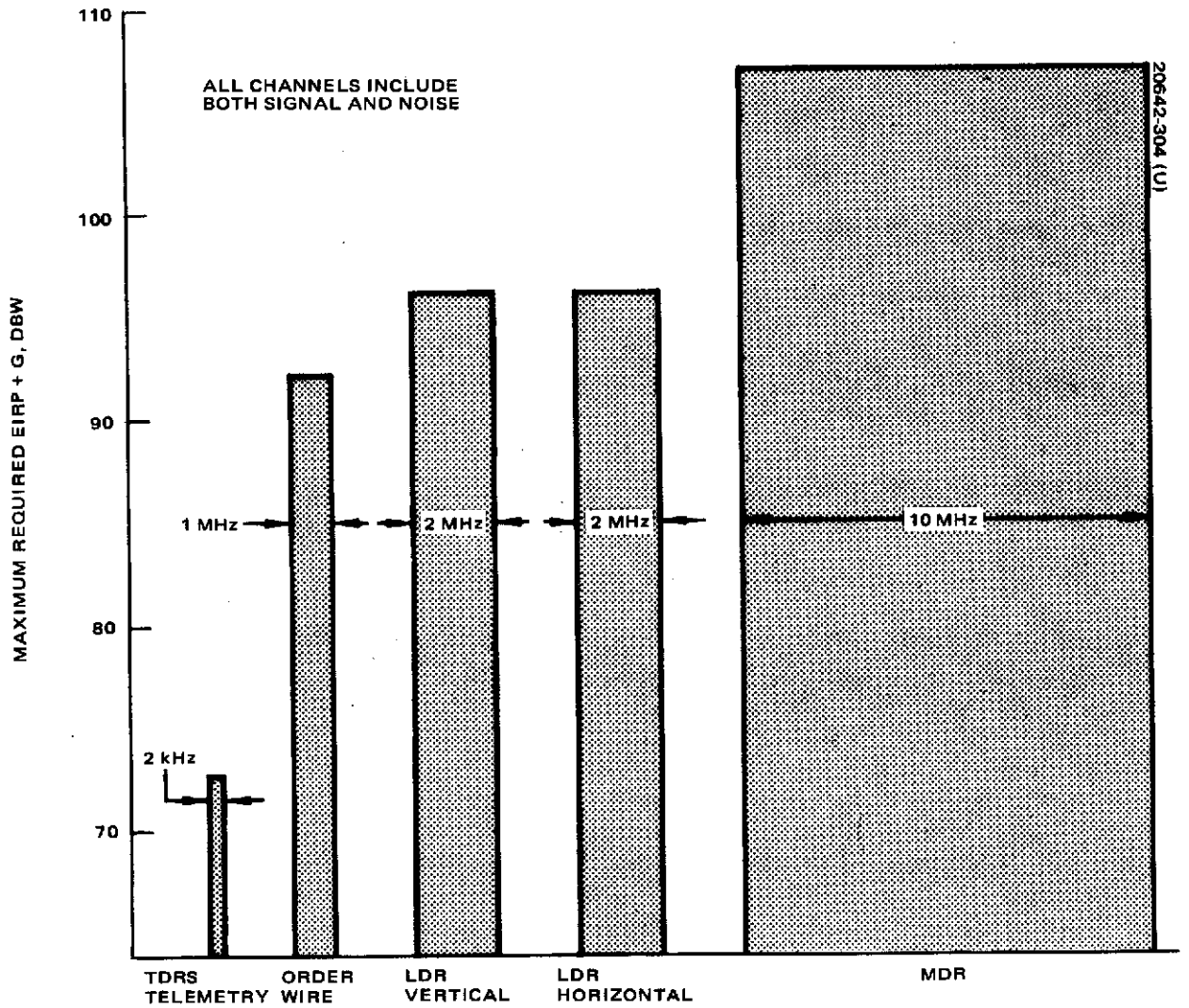

Figure 3-99. Relative Return Link Signal Levels

it is clear that this signal should be amplified linearly to avoid signal suppression, and the required EIRP + G is 72.1 + 20 = 92.1 dBw, most of which is noise power.

Figure 3-99 illustrates the return signal channels and shows their bandwidth and required K band EIRP + G. This set of signals can be visualized, very loosely, as five carriers with varying amounts of modulation. Figure 3-99 assumes linear amplification of all channels, so the noise in both the MDR and order wire channels produce significant outputs. The maximum EIRP + G for the LDR signals has been split equally between the vertically and horizontally polarized inputs.

Linear amplification is generally described in a negative or converse manner. That is, when the effects on the signals due to nonlinearities are small enough so that performance is not significantly affected, an amplifier is said to be linear. The principal nonlinear effects include 1) intermodulation products, 2) AM to PM conversion, and 3) phase distortion. The usual approach is to operate the final amplification stage significantly below its maximum power capability, ensuring that the most nonlinear operating conditions near amplifier saturation are avoided. However, operating below saturation imposes a power penalty on the spacecraft.

For the K band power amplifier, a TWT is recommended and the nature of these devices is such that the dc or bus power required is independent of the operating point, i.e., the RF output power. The required dc power is the same whether the output power is maximum or at a lower level. Thus, not operating at saturation (maximum output) results in an effective power penalty. To minimize this penalty requires that the output power be as near to saturation as possible without serious degradation due to the amplitude non-linearity.

Figure 3-100, taken from Reference 16, shows the effect on undesirable intermodulation power of operating below saturation, i.e., backed off. These curves are the result of measurements, but the inputs were equal magnitude carriers. However, if the TDRS return link spectrum is considered as five narrowband signals, these results will be an approximation. Thus, if the TDRS spectrum is comparable to between 4 and 8 carriers, 5 dB backoff will result in total intermodulation power more than 18 dB below the total output power. This could conceivably degrade the lower power TDRS telemetry and order wire channels, but these could be placed in the band where intermodulation power is not present. This was not done in the baseline design of the return link repeater channels but should present no difficulty if required.

From Figure 3-100 and Hughes experience, it appears that 5 dB backoff will provide sufficient linearity.

Power Amplifier Configuration. If a single power amplifier is used, then the maximum total output power must be 5 dB less than the saturation value. Almost all the power will be in the LDR and MDR channels with the order wire channel power being more than ten times less and the TDRS

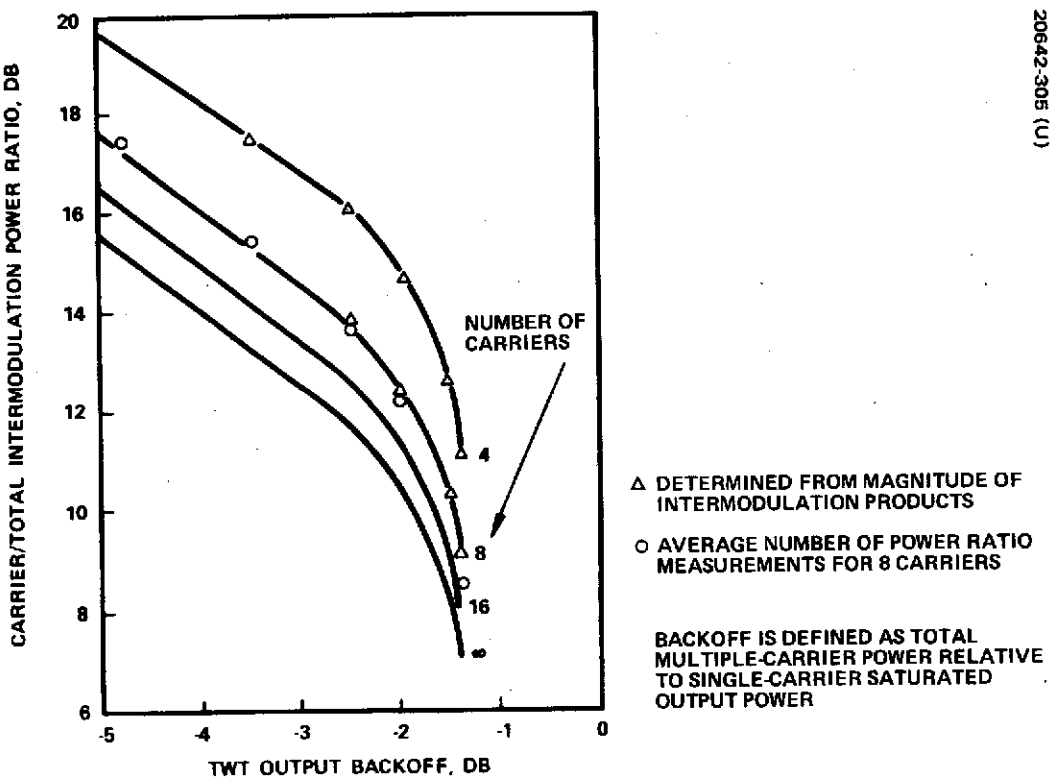

Figure 3-100. TWT Backoff Versus Intermodulation Power

telemetry signal much less than this. The total required EIRP + G is 107.8 dBw and if this power level is 5 dB below saturation, the saturation EIRP + G must be 112.8 dBw.

With the MDR channel amplified through a saturated TWT and all the other signals in a linear TWT with 5 dB backoff, the combined saturation EIRP + G of both outputs is 109.1 dBw, a reduction of 3.7 dB or approximately a factor of 2.4, most of which could be reflected in a reduction of dc power. If the voice is filtered from the LDR channel and amplified in the same output stage as the MDA, some backoff will be required in this output amplifier. The total saturation EIRP + G for this case is estimated to be at least 110 dBw which is greater than the case above.

Using a saturation power amplifier for the MDR channel may result in signal degradation when user power is less than that required for 1 Mbps. For instance, if a user's data rate is only 100 Kbps, then his required EIRP is 20 dBw. The signal-to-noise ratio in the 10 MHz receiver band is -8.7 dB and the output signal-to-noise ratio will be even less due to the "small signal suppression" effect of saturated amplifiers. This additional suppression will degrade the signal so that even after filtering and processing at the ground station, the performance may be unacceptable. It is possible to employ a variable bandwidth filter on the TDRS to eliminate the signal suppression, but the repeater becomes more complex and return link spectrum spreading may not be acceptable.

Combining both MDR and voice in the same output amplifier requires the most complex electronics and gives no advantage over the above two-power amplifier approach where the MDR channel is amplified in one saturated TWT and all other signals are linearly amplified in another.

A single power amplifier (alternative 1, Table 3-31) remains linear, allowing filtering at the ground and eliminating the need for a variable bandwidth filter in the MDR channel, but requireing instead variable gain or attenuation. With a single power amplifier to transmit all signals, the overall complexity is less for providing redundancy, and greater flexibility is possible to accommodate later system requirements and the operation of the telecommunication services. The disadvantage of the single power amplifier approach is that a greater total saturation EIRP is required — approximately 3.7 dB greater. However, at K band, TWT efficiency increases with power level. Considering all factors, the single power amplifier approach will result in only slightly greater TDRS weight while allowing a simpler design with greater flexibility. Therefore, a single power amplifier configuration was selected as the preferable approach for the return link transmitter. The required saturation K band EIRP is 112.8-G as computed above.

Parameter Selection. The minimum required saturation EIRP for a single power amplifier approach is shown in Figure 3-101 as a function of ground antenna gain. The EIRP is the combination of radiated RF power and antenna gain in the direction of the ground antenna. If there are line losses or antenna pointing is imperfect, the

TABLE 3-31. RETURN REPEATER CONFIGURATION COMPARISON

Alternative	Minimum Required EIRP + G	Advantages	Disadvantages
1) One linear power amplifier (PA)	113.9	• Simplest • Most flexible • No voice filtering	• 6 Variable attenuators • Most power required
2) Two power amplifiers TMT and voice in linear PA MDR in saturated PA	110.8	• Less total TDRS EIRP required	• 4 Variable attenuators • More complex
3) Two power amplifiers Telemetry in linear PA MDR + voice in other	112	• Less power than single PA	• Variable attenuators • Mixing of voice required • Most complex

product of antenna gain and power amplifier output power must be greater than the EIRP. Figure 3-102 relates the product of K-band transmitter power and peak gain of the antenna which is defined as the antenna gain to the ground antenna diameter and shows the effect of transmission losses.

The next step is to relate the TDRS power-gain product to TDRS weight and the ground antenna diameter to cost. Figure 3-103 presents the result of an optimization study showing the minimum TDRS K band system weight as a function of ground antenna diameter where it has been assumed that 2.5 dB loss is incurred due to line loss and antenna pointing error. This minimum weight requires the use of the optimum combination of TDRS antenna size and transmitted power and takes into account 1) power amplifiers, 2) drivers, 3) receivers, 4) antenna and gimbaling system, and 5) prorated power supply and heat exchanger.

Forward link power from ground station power amplifiers must be considered in estimating the variation of cost as a function of antenna diameter. However, preliminary estimates indicate a possible saving of nearly $500,000 between 10.3 and 25.9 meter diameter antennas and an additional $250,000 reduction with a 12.2 meter diameter.

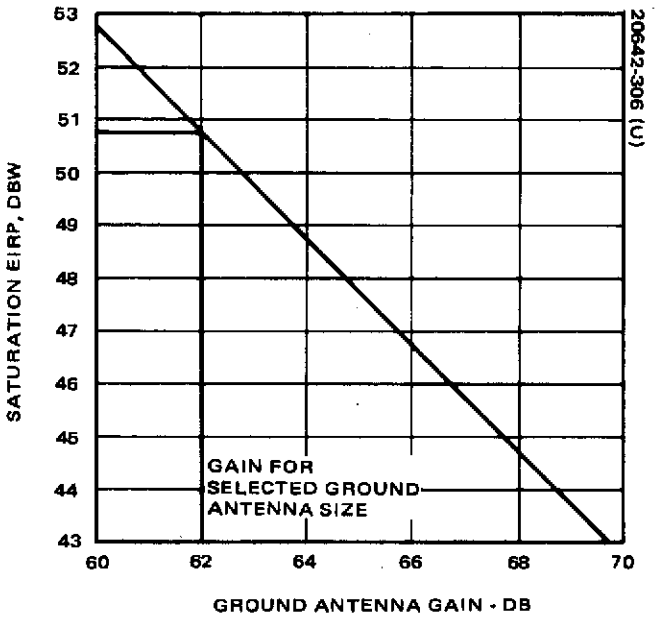

Figure 3-101. Saturation EIRP Versus Ground Antenna Gain

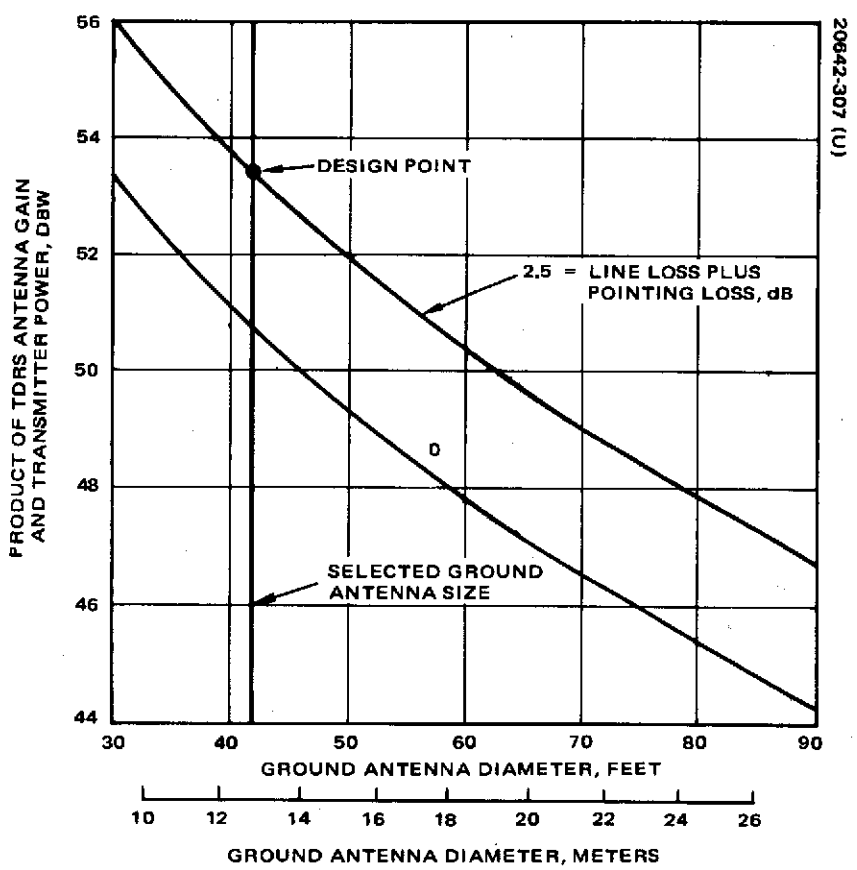

Figure 3-102. TDRS K Band Power-Gain Versus Ground Antenna Size

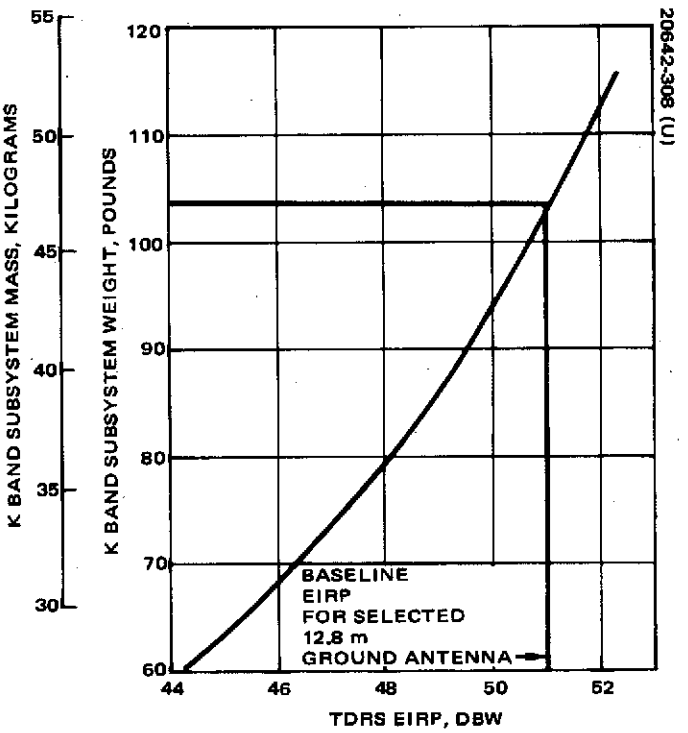

Figure 3-103. Minimum K Band Subsystem Weight

Figure 3-104 resolves the TDRS K band power-gain product into optimum transmitter power and antenna diameter corresponding to the minimum system weight of Figure 3-103. Also shown in Figure 3-104 is the 1.43 meter mechanical limit on the antenna diameter if the antenna is to be nondeployable. Corresponding to this limit is the nonoptimum transmitter power required.

Considering Figures 3-102, 3-103, and 3-104 in an attempt to minimize ground station costs, a ground antenna diameter of 12.8 meters (42 feet) was selected. This size corresponds to a current design, which will aid in reducing engineering costs. Referring to Figure 3-102, the required power gain product is 53.5 dBw including the assumed 2.5 dB line and pointing losses. Figure 3-103 indicates that the minimum K band system weight is 47 kg. It may be noted from Figure 3-103 that increasing the ground antenna size from 12.8 meters to 18.3 meters (60 feet) will allow a TDRS weight reduction of about 12 kg. The choice of the 12.8 meter diameter was made because this additional TDRS weight will allow a considerable saving in the cost of the ground station antenna systems.

Figure 3-105 shows the effect on TDRS weight of the nonoptimum transmitter power and TDRS antenna size selected due to the limitation on antenna diameter. Note that the additional weight due to the size limitation is only about 0.5 kg.

3.3.3.2 Forward Link

The power required at the ground station depends principally on 1) the required (S/N) in the TDRS receiver, 2) channel bandwidth, 3) weather margin, 4) antenna gains, and 5) receiver noise figure. The link power budget of Table 3-32 accounts for the antenna gains and receiver noise figure. Redundant northern hemisphere coverage K band antennas have been chosen for forward link reception on the TDRS. The minimum gain of these antennas is 18.5 dB at 13.3 GHz. A receiver of good quality has been selected with a noise figure of 9 dB, and the gain of the 12.8 meter ground antenna is approximately 62 dB. The link power budget of the table leads to the following result for the ratio of the signal power to noise density:

$$\frac{P}{\eta_T} = P + 62 \text{ dB-Hz} \qquad (1)$$

The required P/η_T is the product of the required ground link $(S/N)_g$, channel bandwidth, B, and weather margin, M_W. If all of these quantities are expressed in decibel units, i.e., 10 log( ),then the required ground station power amplifier output per channel is given by:

$$P = (S/N)_g + B + M_w - 62 \qquad (2)$$

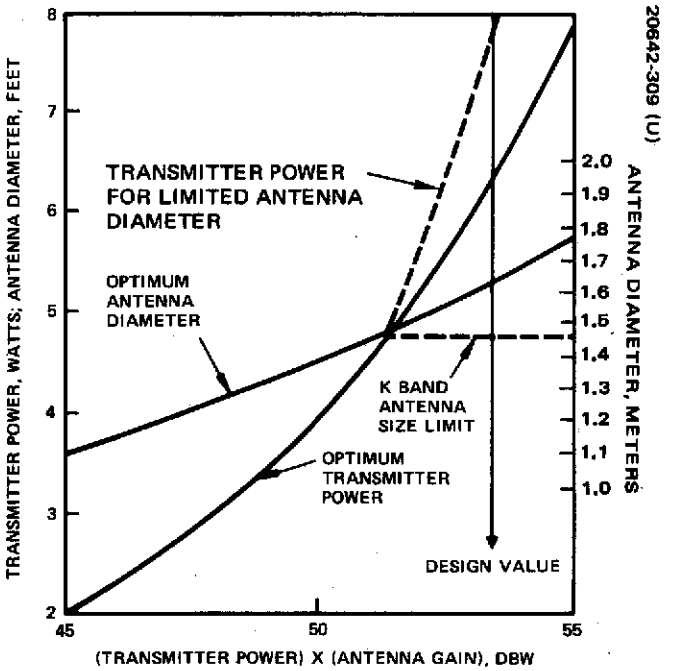

Figure 3-104. TDRS K Band Antenna Diameter and Transmitter Power

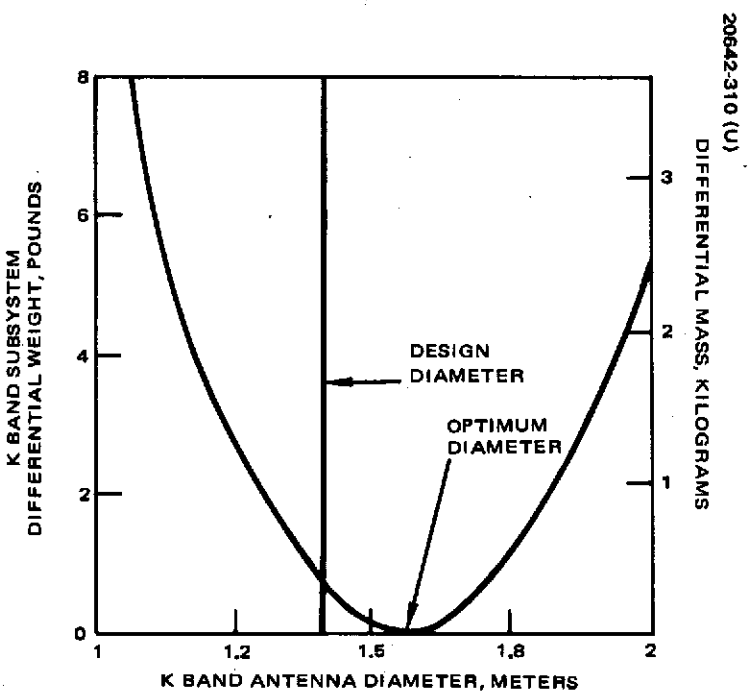

Figure 3-105. Effect of Antenna Diameter Limitation on K Band Subsystem Weight

TABLE 3-32. FORWARD GROUND LINK POWER BUDGET

Link Parameter	Value, dB
Transmit power	P
Transmit antenna gain	61.5
Transmit line and pointing losses	-3.0
Space loss	-207.0
TDRS antenna gain	18.5
TDRS pointing loss	-2.0
TDRS line loss	-1.0
Polarization ellipticity loss	0
RECEIVED POWER, P_r	P - 133
Noise figure	9.0
Thermal noise density, η_T*	-195.0
P/η dB-Hz	P + 62

*Receiver noise temperature = 2000 K, earth noise temperature = 300 K

The weather margin for the MDR and LDR services has been set at 17.5 dB, and the forward link bandwidths are 10 MHz and 1 MHz, respectively, as determined in the above analysis. The ground link S/N must be large enough not to degrade the overall link.

Although the forward link amplification in the repeater is not linear an approximation to the overall S/N can be obtained from the formula for linear amplification given by:

$$(S/N)_o = \frac{(S/N)_g \ (S/N)_s}{(S/N)_g + (S/N)_s + 1} \qquad (3)$$

The subscripts o, g, and s refer to the overall link, ground link, and space link respectively. Due to spectrum spreading, $(S/N)_s$ will be small – less than unity. For instance if the bit energy to noise density, E_b/η, = 10 then on the forward link where the spectrum is spread by a factor of 2000 (33 dB), $(S/N)_s$ = -23 dB = 0.005. It can be seen from Equation 3 that if the ground link is not to significantly degrade the overall link, $(S/N)_g$ must be greater than unity.

If for the LDR link, $(S/N)_g = 20$ (13 dB) then

$$\frac{(S/N)_o}{(S/N)_s} = \frac{(S/N)_g}{(S/N)_g + (S/N)_s + 1} = \frac{20}{21.005} = -0.222 \text{ dB}$$

and thus the overall S/N is degraded by only 0.222 dB due to the ground link.

For the MDR link when 20 kbps voice is transmitted with the spectrum spread to 10 MHz the design EIRP of $E_b/\eta = 10$ results in $(S/N)_s = 0.02$. Thus if $(S/N)_g = 4$ (6 dB)

$$\frac{(S/N)_o}{(S/N)_s} = \frac{4}{5.02} = -0.834 \text{ dB}$$

and hence the overall $(E_b/\eta)_o \approx 9.16$ dB.

Table 3-33 lists the channel parameters from which the required P/η is derived as shown in column 4. Column 5 contains the required ground radiated RF power for the respective channels as determined from Equation 2.

TABLE 3-33. POWER REQUIREMENTS FOR GROUND STATION

	1	2	3	4	5
Channel	Channel Bandwidth, MHz	S/N, dB	Weather Margin, dB	Required P/η_T, dB	Required Power With 12.8m Dish, watts
LDR	1.0	13	17.5	90.5	710
MDR	10.0	6	17.5	93.5	1500
TDRS command	0.001	20	25.0	75.0	20
Beacon	0.001	20	25.0	75.0	20

3.3.4 Analysis Summary

The purpose of this subsection is to summarize concisely the major conceptual design and baseline parameter choices resulting from the analysis of the preceding three subsections.

3.3.4.1 LDR System

Forward Link. The selected signaling and multiplexing techniques are:

1) PN coding for both user commands and voice

2) Code division multiplexing of user commands and voice

The use of PN coding is the major signal design characteristic and allows four objectives to be accomplished:

1) Commands and voice can be code division multiplexed.

2) Multipath interference is reduced due to the spectrum spreading.

3) Earth-incident flux density is reduced to meet CCIR requirements.

4) Range measurement accuracy is improved.

The user command channel will be time-shared; that is, only one user can be commanded at a time. However, commands may be sent to many users within a period of 1 minute. All users will receive the TDRS transmitted RF signal; thus each command will have a prefix which will activate the command decoder of the intended user.

The baseline signaling parameters are:

Chip (PN code symbol) rate	614 kchips/sec
Command bit rate	300 bps
Command code length	2048
Voice bit rate	9.6 kbps
Voice code length with rate 1/2 convolutional encoding	32

The frequency band chosen is the allocated UHF band 400.5 to 401.5 MHz. This band was selected over a VHF band because: 1) more bandwidth is available, 2) RFI is expected to be smaller, and 3) it is a currently internationally allocated band for space use.

Circular antenna polarization is recommended for the manned voice user to provide additional multipath rejection. This is not necessary with the PN CDM signaling approach, but the spectrum is only spread by a factor of 64 compared to 2048 for user commands, and so additional multipath rejection will improve the link.

Return Link. The selected signaling and multiplexing techniques are:

1) User telemetry and voice occupy separate frequency bands

Telemetry	136 to 137 MHz
Voice	137 to 138 MHz

2) User telemetry will be PN code modulated to occupy the entire 1 MHz band.

3) Voice signal will PN code modulated as required to meet CCIR requirements.

4) Simultaneous multiple user telemetry signals are code division multiplexed in the 136 to 137 MHz channel; thus, each user's PN code will be different.

5) Convolutional encoding will be employed on user telemetry for bit error correction; link quality is improved significantly with this technique.

The baseline approach assumes that the return bit rate is standardized for all users but this is not a system requirement. With this standardization the baseline parameters are as follows:

Telemetry bit rate	1200 bps
Convolutional encoding rate	1/2
PN code length	511
Chip rate	1.22 Mchips/sec

3.3.4.2 MDR System

The following selections were made as a result of MDR system analysis:

1) S band frequency allocations shall be used

Forward	2035 to 2120 MHz
Return	2200 to 2300 MHz

2) Required EIRP for forward voice transmission is 47 dBw.

3) S band antenna size 3.89 meters

4) Radiated power 23.5 watts

5) The channel bandwidth shall be 10 MHz to allow spectrum spreading in order to meet CCIR requirements.

3.3.4.3 Ground Link

This link is defined as that between the ground station and a TDRS. A number of parameters important to both TDRS and ground station design resulted from the analysis of 3.3.3.

1) Frequency band - K band

Forward	13.4 to 14.0 GHz
Return	14.4 to 15.35 GHz

2) Ground station antenna Diameter = 12.8 meters. This size reduces ground station costs but does not greatly burden the TDRS.

3) All four return channels are amplified in a single linear power amplifier

4) Required TDRS power amplifier backoff = 5 dB

5) Required TDRS Saturation EIRP = 51 dB

6) TDRS return ground link antenna diameter = 1.43 meters; the Corresponding K band gain is 44.0 dB.

7) TDRS power amplifier saturation output = 8 watts.

8) TDRS forward link K band receiver noise figure = 9 dB

9) Required ground station power amplifier output per forward channel:

LDR	710 watts
MDR	1500 watts
Beacon	20 watts
TDRS command	20 watts

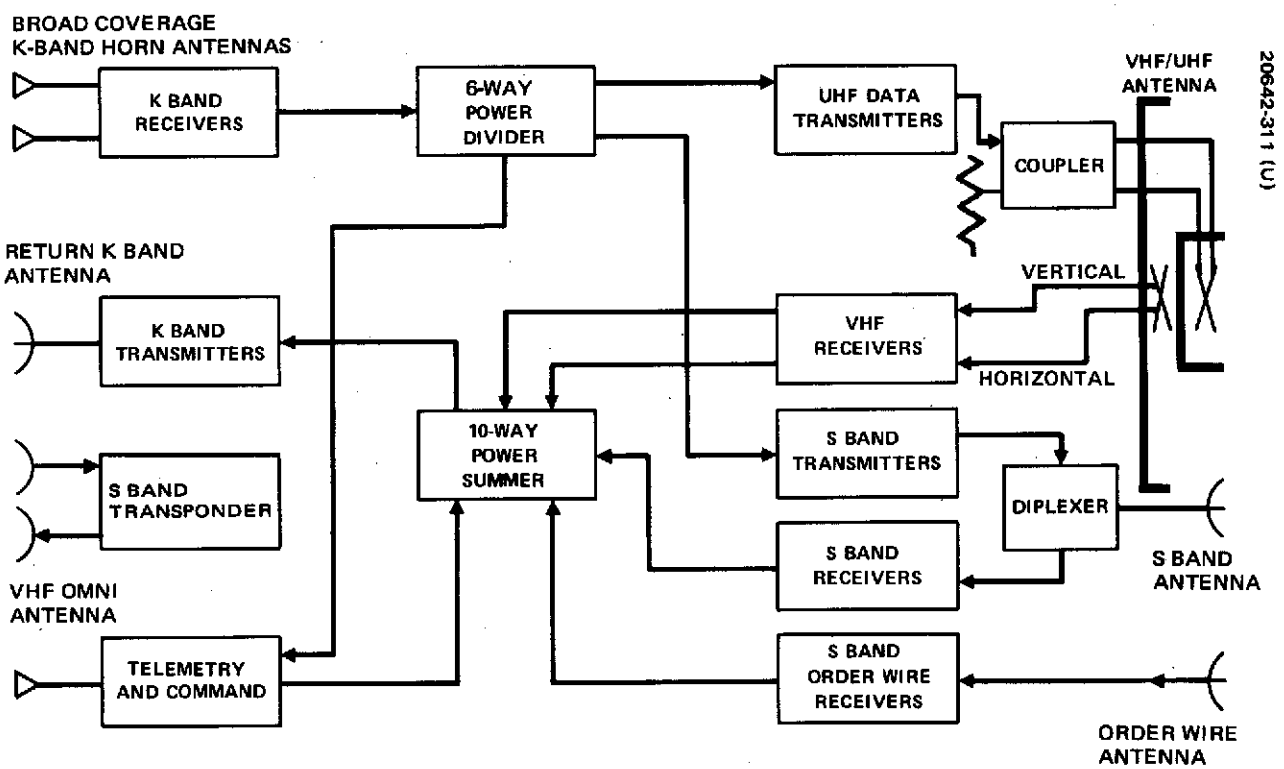

Figure 3-106. TDRS Communication Subsystem

3.4 TDRS COMMUNICATION SUBSYSTEM

The TDRS communication subsystem (Figure 3-106) has been designed not only to satisfy all of the statement of work requirements, but also to allow two way voice and/or data communication with the Space Shuttle. The communication subsystem interfaces with the Ground Station at K band and with the users both in the VHF/UHF bands and at S band. The K band interface to the ground station has four forward channels and five return channels.

The low data rate service employs both UHF and VHF frequencies. The TDRS VHF/UHF subsystem transmits voice and commands at UHF and receives user's telemetry signals at VHF. Up to 20 users' signals are simultaneously amplified through the VHF receiver. Further, the VHF antenna resolves the incoming signals into vertically and horizontally polarized components that are amplified separately.

The TDRS S band system transmits within the 2035 and 2120 MHz band. A single user is serviced by the S band transmitter and receiver. The receiver operates in the 2200 to 2300 MHz band. Both the transmitter and receiver may be tuned in 1 MHz steps, and each has a 10 MHz bandwidth. Thus the S band system is capable of operating at any frequency within the assigned frequency bands, and in effect provides a "bent-pipe" system.

In addition to the S band transmitter and receiver for data transmission and reception, there is an S band "order wire" receiver and turnaround transponder. The order wire receiver uses an earth coverage antenna and is capable of receiving from any user in near-earth orbit. The purpose of the order wire receiver is to provide an "always available" channel from a manned spacecraft through the TDRS to the ground station for requesting medium data rate service. The transponder allows trilateral ranging.

Voice capability is provided by two transmitters-UHF and S band. In the case of the UHF transmitter, a push-to-talk feature is employed.

A backup telemetry and command subsystem is provided for the primary link K band telemetry channel. The two VHF telemetry receivers are on continuously, while only one of the K band receivers is on at a given time.

Although the communication subsystem includes the antennas, their design is greatly influenced by deployment techniques and storage requirements. The details of antenna design are discussed in Volume 3, subsection 4.3. The following discussion primarily treats the repeater design, i.e., the electronics design. However, a brief discussion of antenna size selection is given.

3.4.1 Requirements

The requirements for the telecommunications service system are presented in subsection 2.3.1. The general requirements as they apply to the TDRS communication subsystem are summarized in Table 3-34. In addition to these, two other transmitter requirements have been derived in subsections 3.3.2 and 3.3.3. To allow voice communication at S band with a manned spacecraft that has an omnidirectional antenna, a TDRS EIRP of 47 dBw is required. The ground link analysis resulted in a required saturation EIRP at K band of 51 dBw.

EIRP is split between RF power and antenna gain, thus antennas must be selected before transmitters can be designed. The selection of the medium data rate S band antenna and return ground link K band antenna is discussed in subsection 3.3.2 and 3.3.3. The S band order wire order antenna size was chosen to provide broad coverage, but with sufficient gain, without severely impacting the weight and mechanical design of the spacecraft. The VHF antenna size was chosen to provide the required coverage and G/T and to fit into the volume available for storage. The UHF antenna size was chosen to provide the required coverage for forward link command and voice. The two redundant K band receiving horns were chosen to allow broad, northern hemisphere coverage and uplink reliability with low weight. The antenna parameters are summarized in Table 3-35.

TABLE 3-34. TDRS COMMUNICATION SUBSYSTEM REQUIREMENTS

Low data rate service	
• Forward link	
User command EIRP	30 dBw
Voice EIRP	30 dBw
• Return link	
G/T	-16 dB/K within conical coverage of 26 degrees
Linear amplification	
Separation of orthogonal linear polarizations	
Medium data rate service	
• Forward link EIRP at S band	-41 dBw
• Return link G/T at S band	2 dB/K
General	
• Repeater shall be of the frequency translation type	
• Coherent frequency translation	

TABLE 3-35. TDRS ANTENNA PARAMETERS

Link	Antenna Frequency, MHz	Antenna Diameter, meters	Minimum Antenna Gain, dB
Low data rate forward	UHF	1.43	12.5
Low data rate return	UHF	3.82	11.8
Medium data rate forward	S band	3.82	36.0
Medium data rate return	S band		13.6
Order wire	S band	0.267	13.1
TDRS/ground	K band	1.43	44.0
Ground/TDRS	K band	Horns	18.5

Receiver characteristics are those of current state of the art equipment. Table 3-36 summarizes the receiver noise figures.

A preliminary design determined the transmission losses and the EIRP requirements. The antenna gains of Table 3-35, together with these losses determines the required transmitter power amplifier outputs. The determination of these power levels is summarized in Tables 3-37, 3-38, and 3-39 for the UHF, S band, and K band transmitters. The required

TABLE 3-36. RECEIVER NOISE FIGURES

Receiver Band	Noise Figure, dB
VHF	3.9
S band	
Voice/data	3.9
Orderwire	3.9
K band	9.0

TABLE 3-37. UHF EIRP FOR LOW POWER MODE – COMMAND ONLY, dB

Antenna gain	12.5
Cable (6.1 m) and connectors loss	-0.44
Hybrid loss	-0.16
Low pass filter loss	-0.4
Required RF power, minimum	18.5 dBw (71 watts)
EIRP	30.0 dBw

TABLE 3-38. S BAND EIRP

Parameter	Low Power, dB	High Power, dB
Antenna gain	36.0	36.0
Cable loss	-1.2	-1.2
Diplexer loss	-0.8	-0.8
Switch loss	-0.2	-0.2
Isolator loss	-0.2	-0.2
Summer loss	--	-0.25
Switch loss	-0.2	--
RF power, minimum	8.0 dBw (6.3 watts)	13.7 dBw (23.5 watts)
EIRP	41.4 dBw	47.0 dBw

TABLE 3-39. K BAND EIRP, dB

Antenna gain	44.0
Waveguide loss	-1.0
Rotary joints loss	-0.5
Switch loss	-0.2
Filter loss	-0.3
Transmitter power	9.0 dBw
	51.0 dBw

power of Table 3-37 must be doubled when both voice and command are transmitted. The RF power requirements are summarized below:

Transmitter	Required Power Amplifier Output, watts
UHF	
Low power mode	71
High power mode	142
S band	
Low power mode	6.3
High power mode	23.5
K band Saturation Power	8

3.4.2 Repeater Design

The TDRS repeater is completely redundant. Interface is maintained between the earth and TDRS with a K band link. UHF and VHF are used to communicate with low data rate users and S band is used to communicate with medium data rate users. The K band receivers simultaneously receive four different carrier frequencies. These carrier frequencies are shifted to a low IF, amplified, and divided in a power divider to the various points

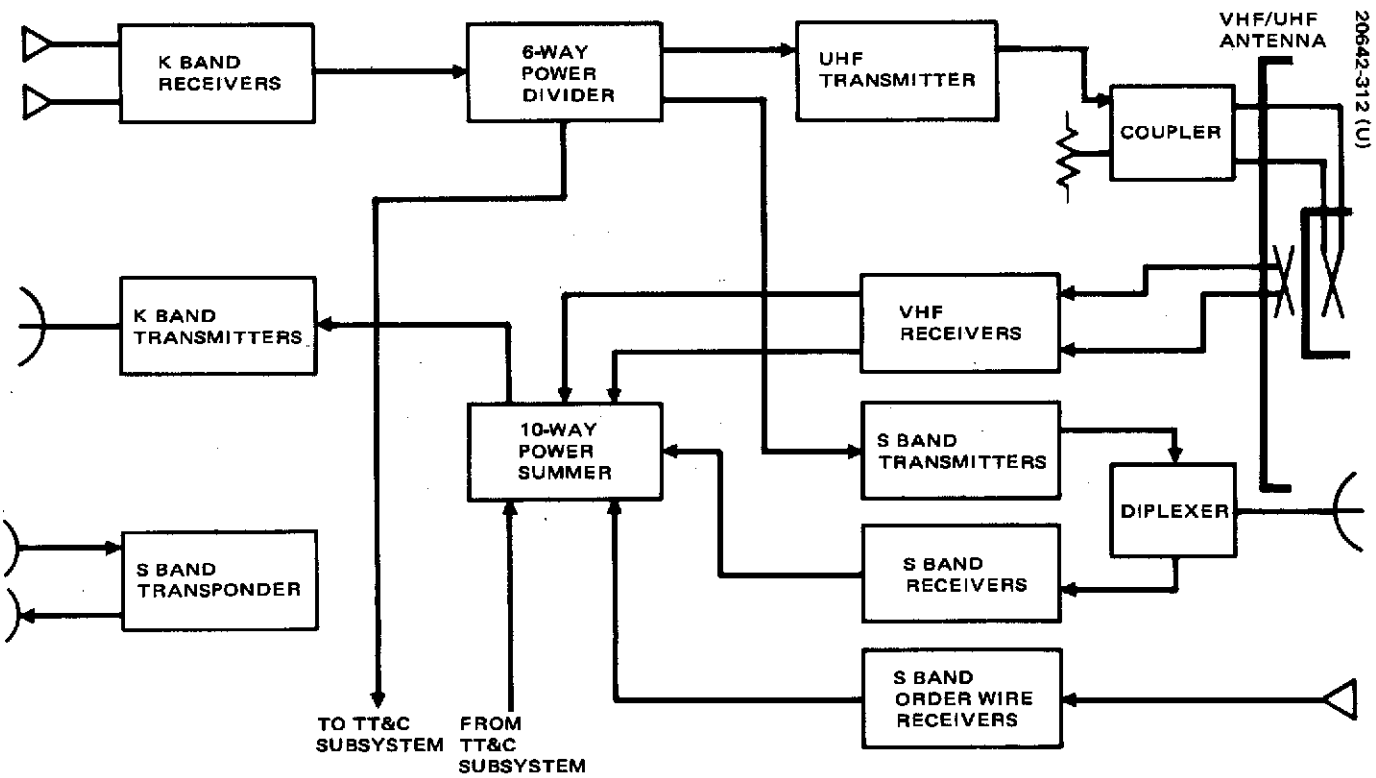

Figure 3-107. TDRS Repeater

of data reception within the TDRS. Table 3-107 illustrates the relationship between the major repeater elements.

The output of the six way power divider supplies the UHF transmitters, the S band transmitters, and the command subsystem. One additional signal, the beacon signal, is received by the K band receiver, which phase locks its local oscillator to this reference. The local oscillator signal then drives the frequency synthesizer to provide coherent translation of all frequencies within the communication subsystem.

The received signals from the VHF receivers, the S band receivers, and the S band order wire receivers are each shifted to a unique IF frequency before being summed in the 10 way power summer. The output of the power summer provides the input to the K band transmitters.

In addition to the signals coming from the various receivers on the TDRS, the TDRS telemetry is sent through the K band transmitter.

Table 3-40 lists the weights of the repeater components, which total to 55.1 kg. There are six power modes possible corresponding to high or low UHF transmitter power and the S band transmitter high, low, or off. However, it has been tacitly assumed that for TDRS design, operation of both transmitters in their high power modes should not be considered. This is because the high power modes are for voice transmission and only one or

TABLE 3-40. REPEATER MASS SUMMARY

	Mass, kg
K band receivers	2.6
K band transmitters	4.1
K band upconverter	0.8
Frequency synthesizers	8.2
S band transmitters	7.3
S band receivers	1.4
S band order wire receivers	1.9
S band transponder	7.6
UHF transmitters	17.2
VHF receivers	4.0
Total	55.1

the other system will be used, not both simultaneously. Further, the case where the S band transmitter is off and the UHF power is low presents little useful design information. A power summary for the other four modes is presented in Table 3-41.

The frequency spectra for each link is shown in Figures 3-108, 3-109, and 3-110. Ground link frequency selections within the allocated bands were somewhat arbitrary, but simplicity of the repeater, and particularly of the frequency synthesizer, was a primary objective. Note that the medium data rate forward link and return link occupy fixed frequency positions in the K band spectrum. However, the TDRS shifts these spectra appropriately in order to match the user requirements and to provide the bent pipe operation for the medium data rate user. Further, the earth station may transmit at any frequency within the provided 10 MHz bandwidth. Thus, any frequency in the allocated S band may be used.

TABLE 3-41. REPEATER POWER SUMMARY

	Unit Power	Telecommunication Mode			
		UHF High		UHF Low	
		S Band Low	S Band Off	S Band High	S Band Low
K band receiver	1.8	1.8	1.8	1.8	1.8
K band transmitter	31	31	31	31	31
K band upconverter	0.8	0.8	0.8	0.8	0.8
Frequency synthesizer	7.3	7.3	7.3	7.3	7.3
S band receiver	0.9	0.9	--	0.9	0.9
Order wire S band receiver	0.9	0.9	0.9	0.9	0.9
S band transmitter	21 or 88	21	--	88	20
S band transponder	21	21	21	21	21
UHF transmitter	141 or 280	280	280	141	141
VHF receiver	2.1	2.1	2.1	2.1	2.1

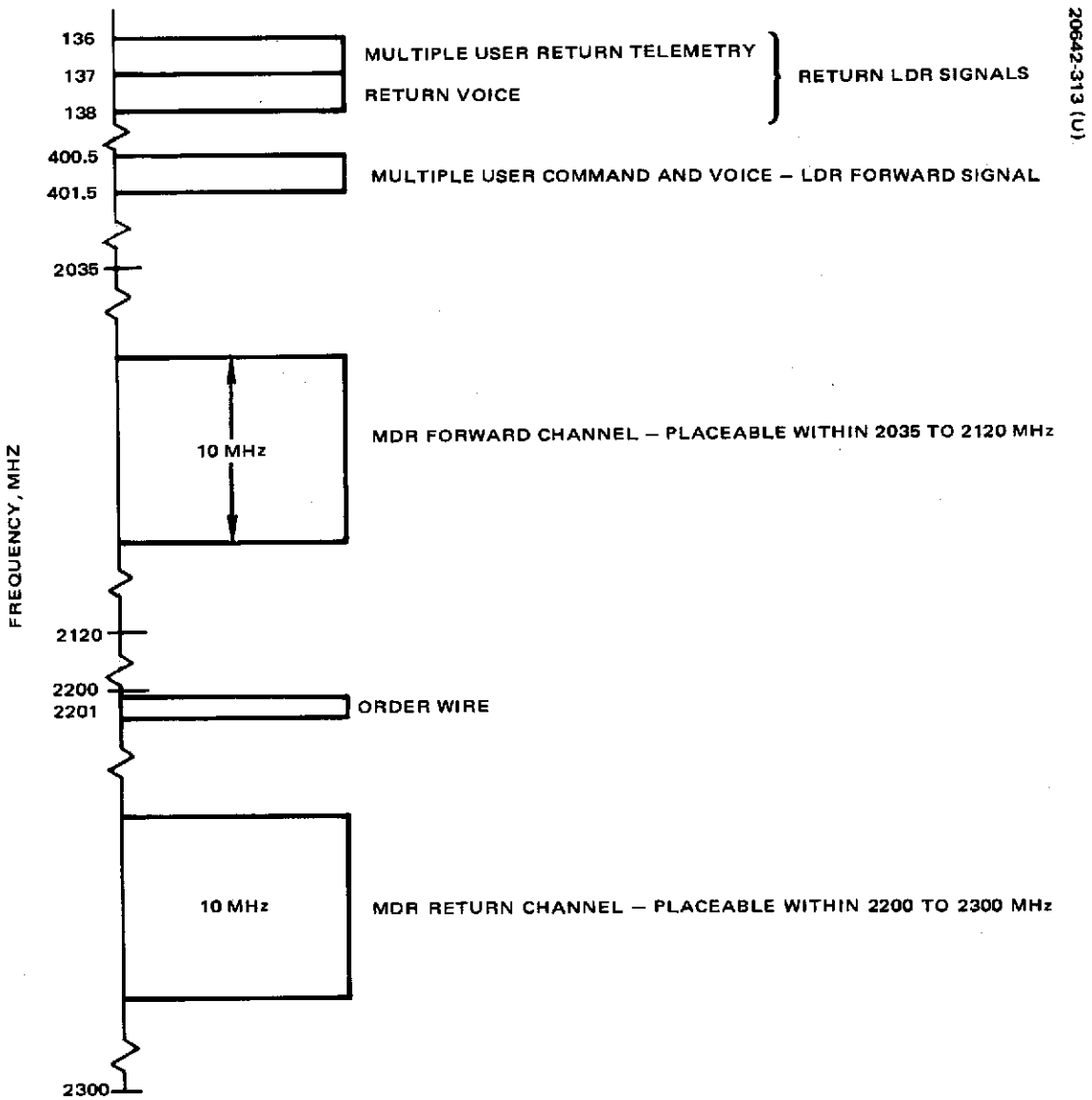

Figure 3-108. TDRS Space Link Spectra

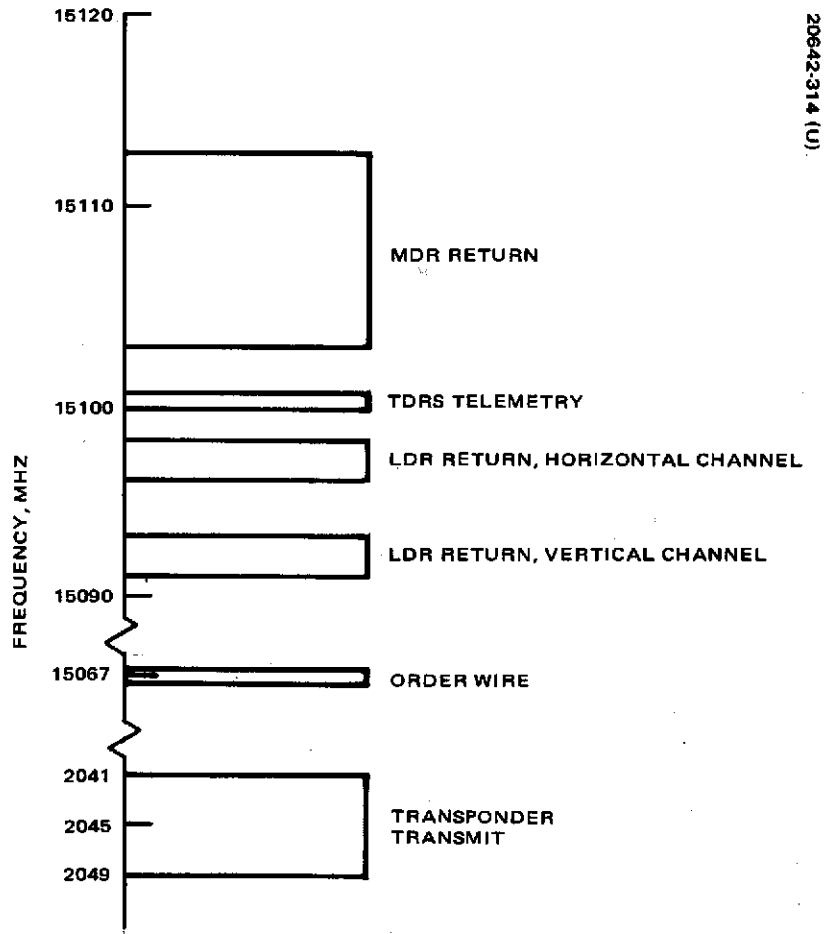

Figure 3-109. Return Ground Link Spectra

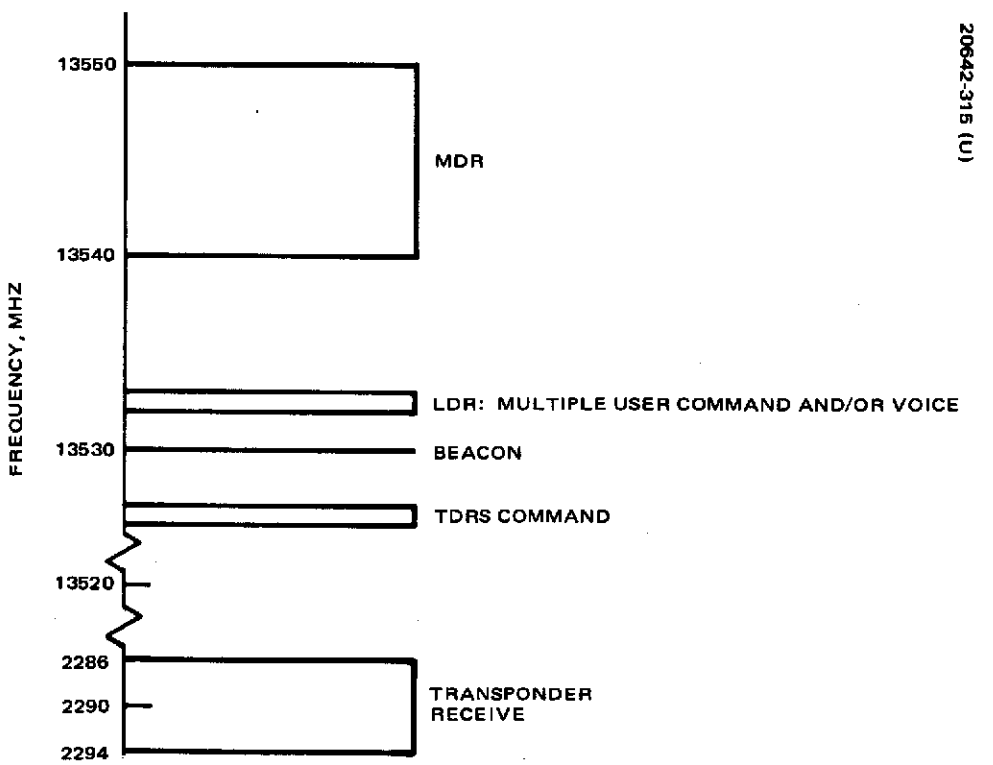

Figure 3-110. Forward Ground Link Spectra

3.4.2.1 K Band Receiver

Redundant K band receivers are used. The design is shown in Figure 3-111. The four input signals are doubly converted to a low IF frequency where they drive the various transmitters and telemetry within the spacecraft. In addition, the reference beacon signal is detected in a phase locked loop, which is part of the K band receiver. When this loop is locked, the locked reference signal drives the frequency synthesizer to provide a coherent reference for all spacecraft frequency translations. The K band receiver also contains sensing circuitry to determine when the phase detector is locked.

The K band receiver IF amplifiers contain AGC circuits to accommodate the K band input signal levels which will vary with weather conditions.

The K band receiver has a noise figure of 9 dB. It operates with an input frequency of 13,526 to 13,550 MHz. Its output frequency is 26 to 50 MHz with a bandwidth of 24 MHz. The total dc input power is 1.76 watts from a bus of 24.5 volts. The overall receiver gain is 65 dB. The weight for two receivers in the redundant set os 2.64 kg. Table 3-42 lists the major parameters.

3.4.2.2 Frequency Synthesizer

The frequency synthesizer has two references. The first is the voltage controlled crystal oscillator, which is part of the phase-locked loop in the K band receiver, and the second is a standby crystal oscillator operating at the same nominal frequency (20 MHz). When the K band receiver is locked to the incoming pilot tone, the 20 MHz receiver voltage controlled crystal oscillator signal provides a coherent frequency reference for the frequency synthesizer. When the K band receiver is not locked to the pilot tone, the standby 20 MHz crystal oscillator is used. All reference signals are coherently related to these 20 MHz signals. Figure 3-112 illustrates the major aspects of the frequency synthesizer.

TABLE 3-42. K BAND RECEIVER PARAMETERS

Noise figure	9 dB
Input frequency	13,526 to 13,550 MHz
Output frequency	26 to 50 MHz
Bandwidth	24 MHz
Input power	1.76 watts
Gain	65 dB
Weight (two receivers)	2.64 kg

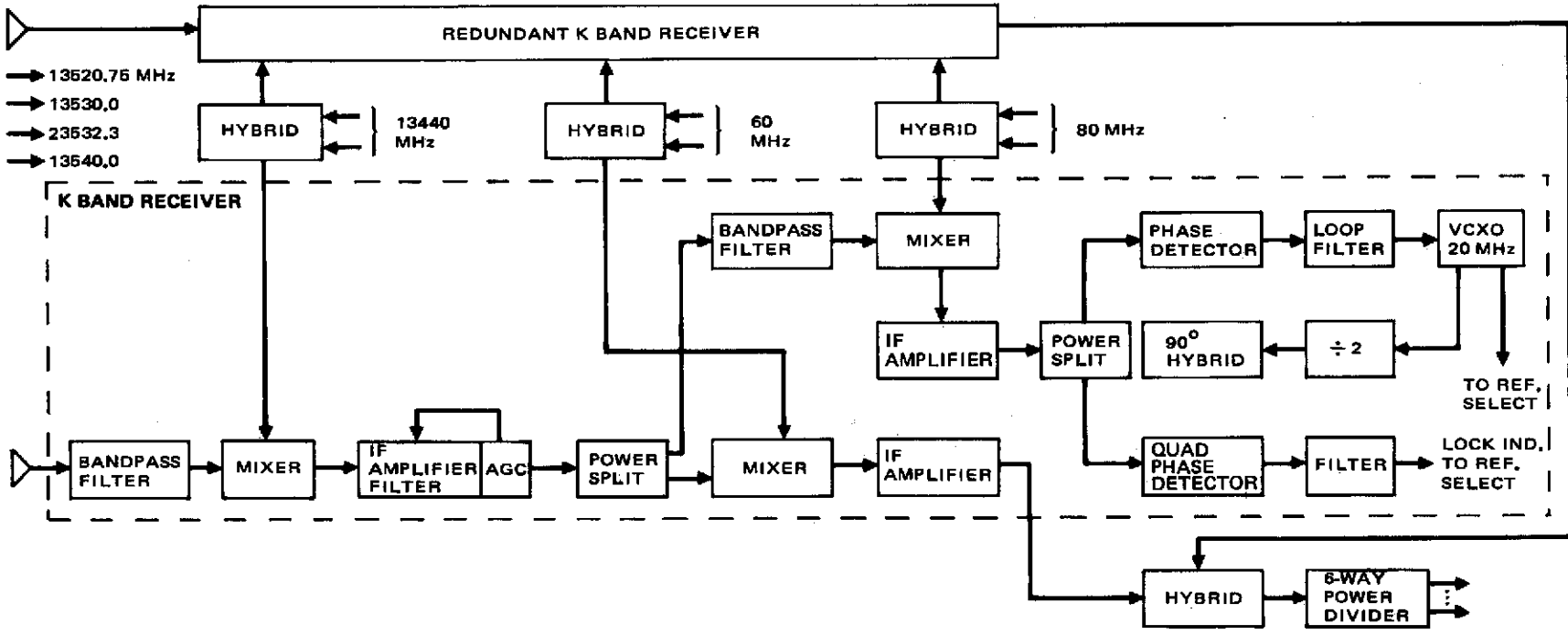

Figure 3-111. K Band Receiver

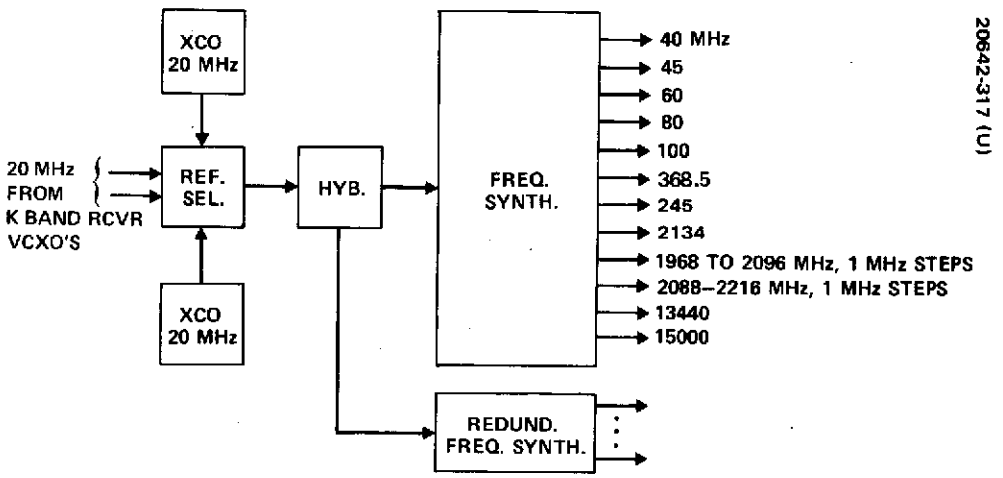

Figure 3-112. Frequency Synthesizer

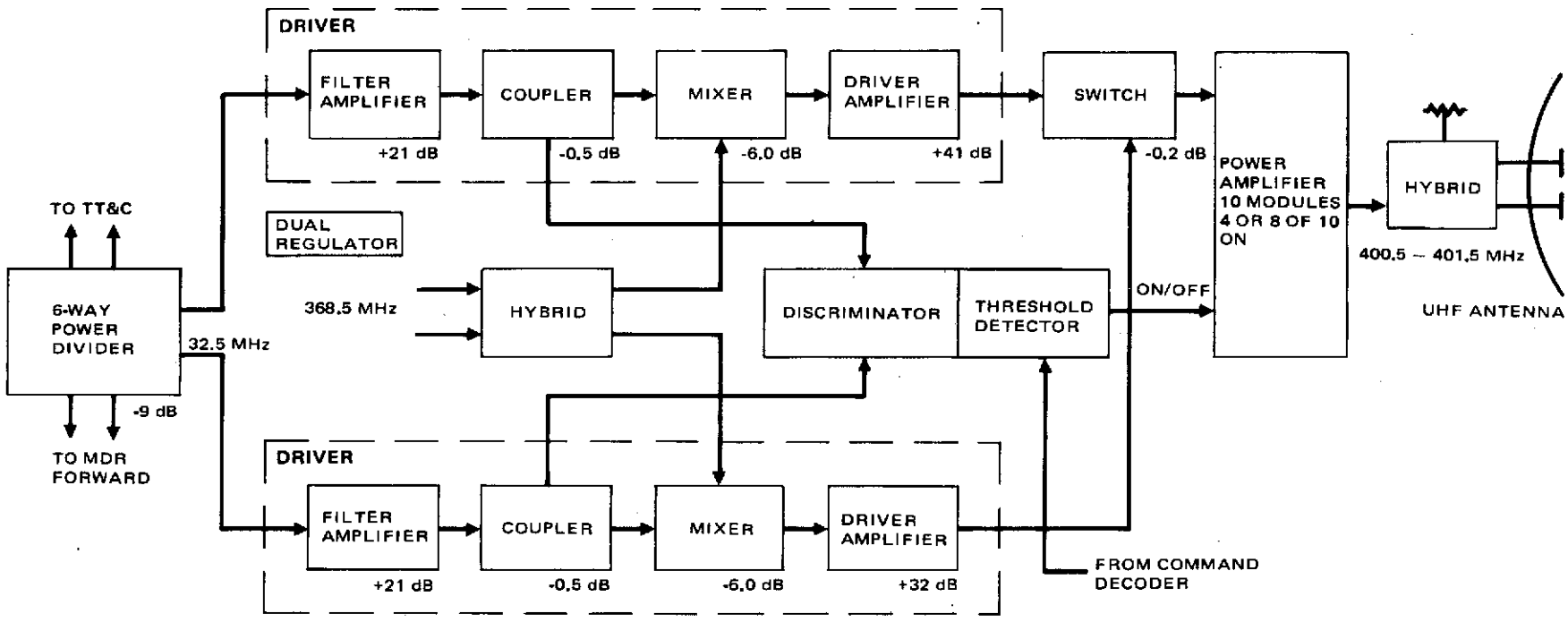

Figure 3-113. UHF Transmitter

The frequency synthesizer provides 12 different output frequencies. Ten of these frequencies are fixed and two are stepped in 1 MHz steps. These two S band signals are used to tune the S band receiver and transmitter over the entire S band ranges in 1 MHz steps. The total power required of the frequency synthesizer is 7.3 watts from a 24.5 volt bus. The weight required is 8.23 kg.

3.4.2.3 UHF Transmitter

The UHF transmitter is configured to operate with maximum flexibility in two power modes for transmitting commands to unmanned users and voice to a manned user. The above two signals can be sent simultaneously or either one separately. The configuration, shown in Figure 3-113, is a result of the use of code division multiplexing of voice and commands, and, in fact, influenced the selection of this multiplexing technique. The digital multiplexing of the two signals at baseband or IF in the ground station allows a single RF carrier frequency to be transmitted, whether command alone or command plus voice are transmitted. Thus only one common passband and power amplifier is required on the TDRS. However, when both signals are in the UHF forward link channel, the transmitter power is divided equally between the signals and so more transmitter power is required to maintain link margins equivalent to the case where each signal has its own frequency channel.

The total power amplifier consists of ten sections. Any four sections generate 71 watts, which result in the required 30 dBw EIRP from the antenna. A push-to-talk feature has been incorporated whereby a subcarrier frequency is sensed when voice has been multiplexed into the channel. This sensing is performed by a discriminator/threshold circuit which activates an additional three sections of the power amplifier. This effectively provides 30 dBw EIRP to both the command and voice signals as required (see Table 3-2).

The additional two sections provide redundancy, and by ground command the configuration will be adjusted so that in case of the failure of any section, three will always operate for command and three will be switched on and off by the threshold circuit. The outputs of all ten sections are summed as was done on TACSAT. The combined signal power is sent to a hybrid coupler where it is split equally into two signals, each of which is used to excite orthogonal elements of the antenna. The resultant antenna radiation is circularly polarized.

A redundant driver stage is provided, and the power amplifier redundancy provided by the two spare sections results in high reliability for the total transmitter with a minimum of complexity. Note also in Figure 3-113 that the additional voice power can be turned on by ground command if the automatic switch circuit should fail. With four sections on, the UHF transmitter provides a power output of 56 watts at the antenna achieved by generating 71 watts at the power amplifier. The input center frequency for the

UHF transmitter driver stage is 32.50 MHz and the output frequency is 401.00 MHz with a bandwidth of 1.0 MHz. The total input power for the transmitter is 141 watts from a 24.50 volt bus, and the overall gain is 67 dB. With eight sections active, the frequencies remain the same, but the power and power gain is doubled. Table 3-43 lists the major transmitter parameters.

3.4.2.4 VHF Receivers

There are two active VHF receivers. Each receiver has a 2 MHz passband from 136 to 138 MHz, which includes both the user telemetry in the 136 to 137 MHz band and, at times, a voice signal in the 137 to 138 MHz band. The total UHF signal is resolved into two components by the VHF antenna corresponding to orthogonal senses of linear polarization. These two VHF signal components are the separate inputs to the two active receivers which use different frequency synthesizer outputs in their mixers, thus translating the two components to separate frequency channels. There

TABLE 3-43. UHF TRANSMITTER PARAMETERS

Output power at the antenna	
High power mode/two links	112 watts
Low power mode/one link	56 watts
Output center frequency	401.0 MHz
Bandwidth	1.0 MHz
Input power	
High power mode	280 watts
Low power mode	141 watts
Input center frequency	32.5 MHz
Gain	
High power mode	70 dB
Low power mode	67 dB
Total weight	17.2 kg

is a redundant receiver for each antenna output. Both AGC and step attenuators are provided in each receiver. The AGC maintains a nominal level, while the step attenuator provides the ability to change the power mix in the K band transmitter, modifying the transmitted spectrum in accordance with the TDRS communications traffic. Figure 3-114 illustrates the receiver design. All receivers have a noise figure of 3.9 dB. The two output 2 MHz channels are centered at IF frequencies of 92.0 and 97.0 MHz. The RF bandwidth of the VHF receiver is 2.0 MHz providing adequate bandwidth amplification for the low data rate telemetry data and voice signals. The output power of the receiver is 3.1 watts and the overall gain is 58 ±6 dB. The weight for two receivers is 3.5 kg. Table 3-44 lists the major receiver characteristics.

3.4.2.5 S Band Transmitter and Receiver

The S band transmitter and receiver are capable of transmitting and receiving at any frequency within the designated bands. Thus a "bent pipe" capability is provided. The instantaneous transmit and receive bandwidths are limited to 10 MHz; however, these bands may be placed at any frequency within the specified frequency range in 1 MHz steps.

A transistor preamplifier is used to maintain a low receiver noise temperature.

The power amplifiers for the S band transmitter are solid state, providing an output power of 24.5 watts. This is reduced by line losses to 12.5 watts at the antenna yielding the required 47 dBw EIRP. The power

TABLE 3-44. VHF RECEIVER PARAMETERS

Noise figure	3.9 dB
Input band	136 to 138 MHz
Output band	91 to 93 MHz, 96 to 98 MHz
Bandwidth	2 MHz
Input power	2.1 watts
Gain	59 ±6 dB
Weight (two receivers)	3.5 kg

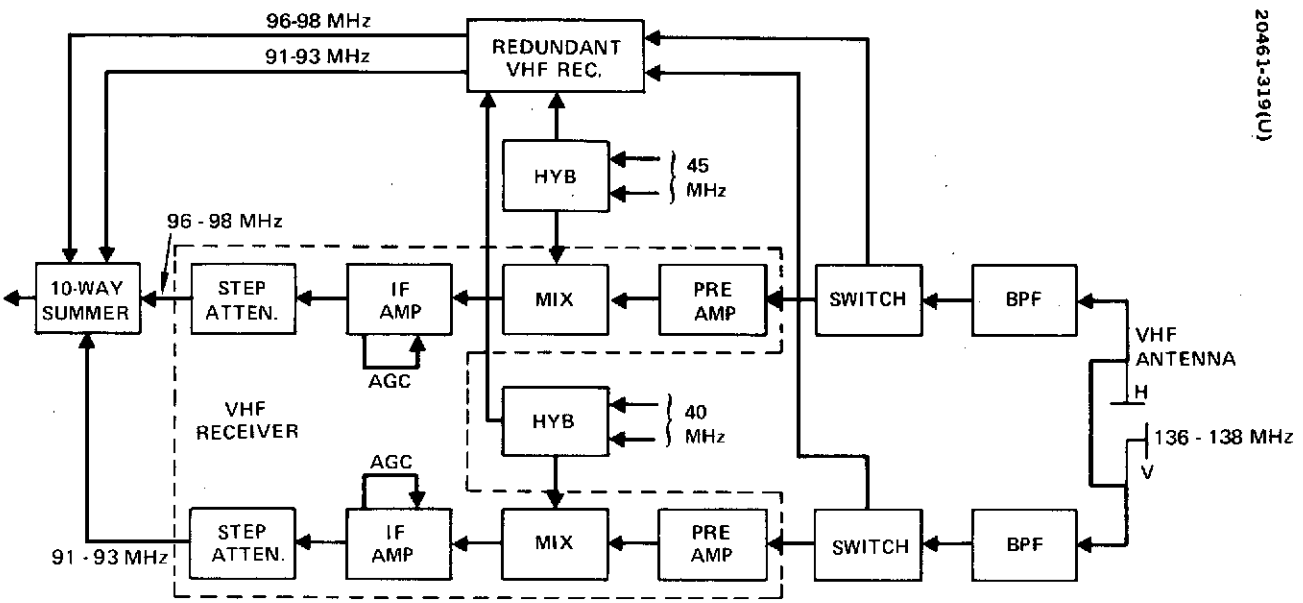

Figure 3-114. VHF Receiver

amplifier can also supply a lower output power of 3.2 watts at the spacecraft antenna. Figure 3-115 illustrates the design.

The S band transmitter input center frequency from the six way power divider is 45 MHz. The output frequency at the antenna input varies between 2035 and 2120 MHz and may be stepped in 1 MHz steps. The instantaneous bandwidth of the S band transmitter is 10 MHz. The dc input power is 20 or 88 watts depending on the power output mode. The overall gain of the transmitter is 50 dB, and the weight for two transmitters is 7.33 kg. These parameters are summarized in Table 3-45.

The S band receiver has a noise figure of 3.9 dB. The input frequency range is 2200 to 2300 MHz. The output frequency of the receiver is 108 MHz. This has an instantaneous bandwidth of 10 MHz. The required receiver input power is 0.9 watts from a 24.5 volt bus and the overall gain is 63±3 dB. The weight for two receivers is 1.4 kg. These parameters are summarized in Table 3-46.

3.4.2.6 Order Wire Receiver

The order wire S band receiver is designed as a reception link, which provides continuous coverage over the entire earth area and offers the opportunity for any user to use the main S band link to signal the earth station through the TDRS he desires. The order wire receiver uses an earth coverage antenna. The input frequency is 2201 MHz. The noise figure and antenna gain of this receiver allow approximately 1 kHz of data to be transmitted by the user to the ground station via the TDRS. Figure 3-116 illustrates the receiver design.

TABLE 3-45. S BAND TRANSMITTER PARAMETERS

Power output (at antenna)	3.2/12.5 watts
Input frequency	45 MHz
Output frequency	2035 to 2120 MHz
Bandwidth	10 MHz
Input power	20/88 watt
Gain	50/56 dB
Weight (two transmitters)	7.3 kg

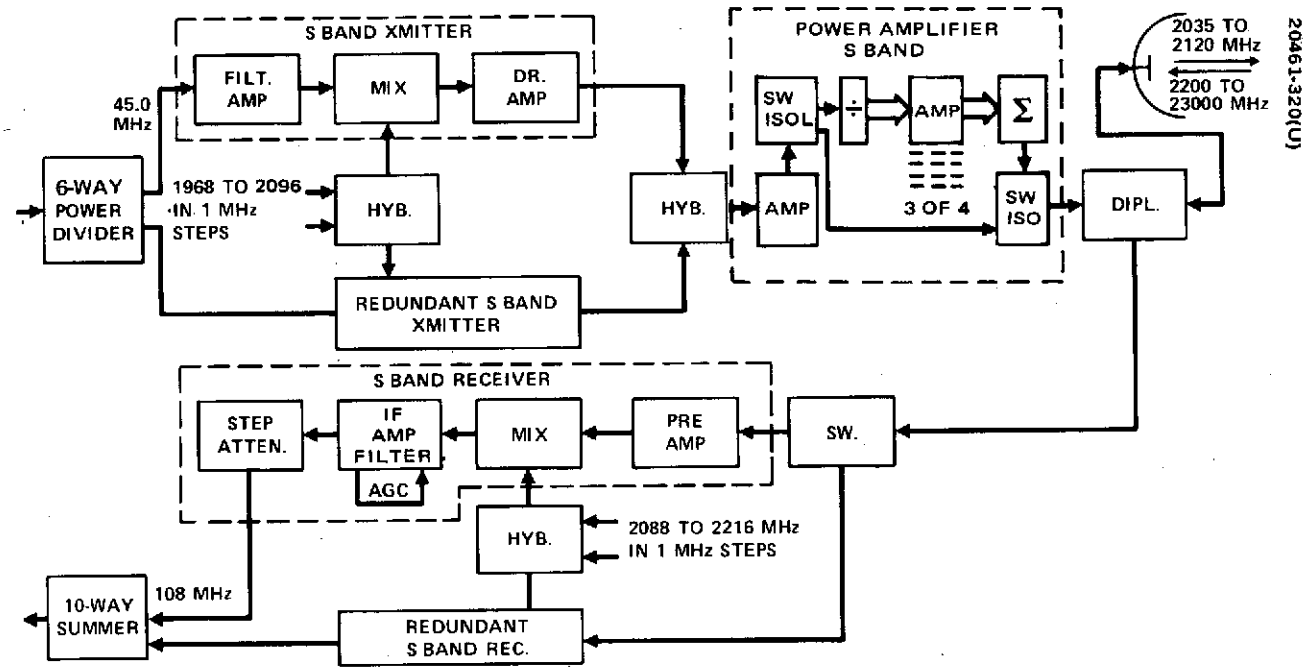

Figure 3-115. S Band Transmitter and Receiver

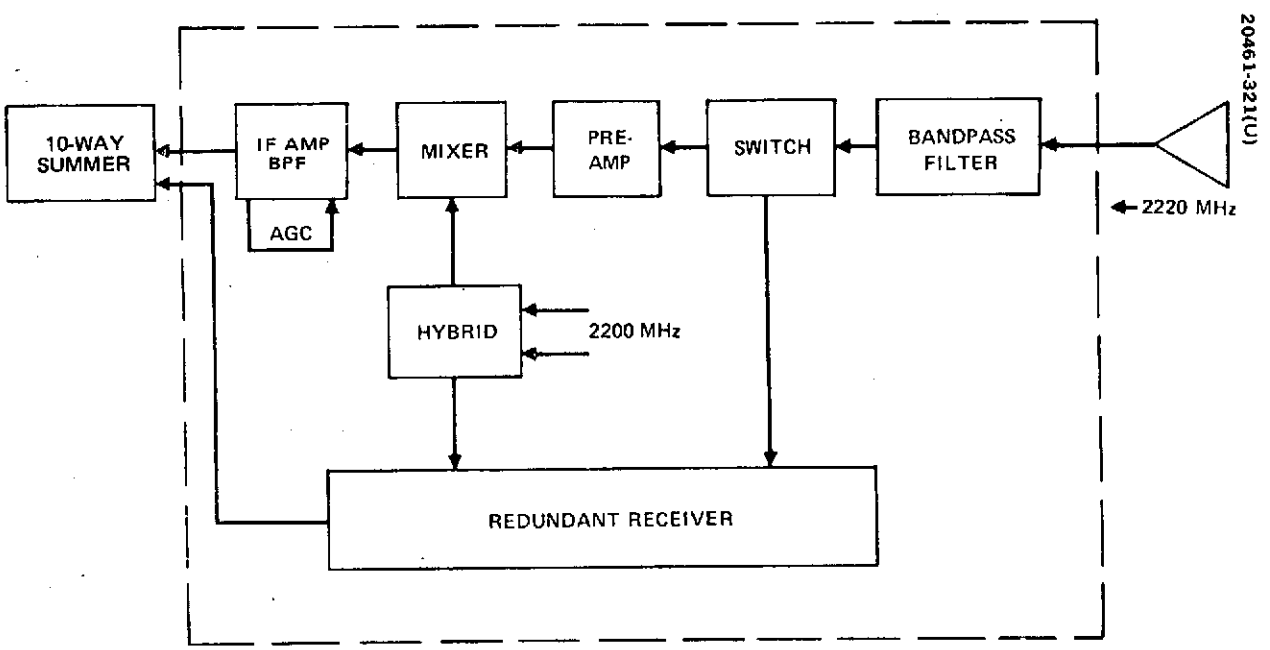

Figure 3-116. Order Wire Receiver

TABLE 3-46. S BAND RECEIVER PARAMETERS

Noise figure	3.9 dB
Input frequency range	2200 to 2300 MHz
Output frequency	108 MHz
Bandwidth	10 MHz
Input power	0.9 watt
Gain	63±3 dB
Weight (two receivers)	1.4 kg

The S band order wire receiver noise figure is 3.9 dB. The input frequency is 2201 MHz with a bandwidth of 1 MHz. The input power is 0.9 watt from 24.5 volt bus, and the overall gain is 67 dB. The weight for two receivers is 1.9 kg. These parameters are summarized in Table 3-47.

3.4.2.7 K Band Transmitter

The K band transmitter consists of two sections: a K band upconverter and a K band power amplifier. The upconverter receives signals from the spacecraft receivers and internal telemetry, amplifies these signals, and shifts them to the K band microwave frequency. The traveling-wave tube (TWT) power amplifier provides additional amplification and has a maximum power output of 8 watts. Five separate channels are processed by the K band transmitter. Each of these signals operates considerably below the maximum power output to maintain the necessary linearity. The total power output will always be 5 dB below the saturation power of the TWT. Figure 3-117 illustrates the design.

TABLE 3-47. S BAND ORDER WIRE RECEIVER PARAMETERS

Noise figure	3.9 dB
Input frequency	2201 MHz
Bandwidth	1 MHz
Input power	0.9 watt
Gain	67 dB
Weight (two receivers)	1.9 kg

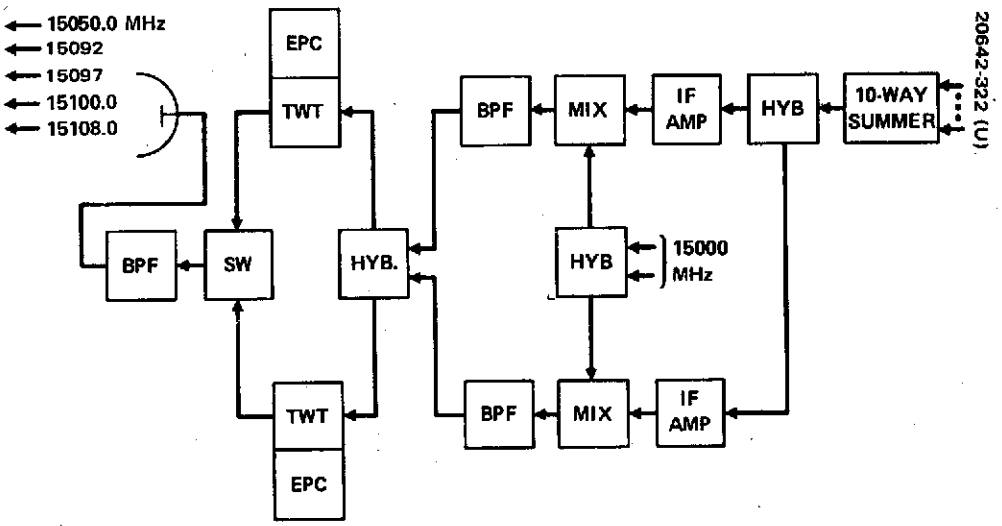

Figure 3-117. K Band Transmitter

The K band transmitter has a maximum power output of 8 watts. The input frequency range is between 50 and 113 MHz to encompass the several individual input spectra. The output frequency varies between 15,050 and 15,113 MHz. This provides a total bandwidth of 63 MHz. The required input power is 26.4 watts from a 24.5 volt bus and the overall maximum gain is 72 dB. The weight for two transmitters is 5.68 kg. These parameters are summarized in Table 3-48.

3.4.3 S Band Transponder

The S band transponder provides for ground link ranging by translating received frequencies in 2286 to 2294 MHz to transmit frequencies in 2041 to 2049 MHz in a single conversion. The input signal contains ranging data within an 8 MHz bandwidth at a received signal level of -120 dBW. A redundant transponder is provided for reliable operation. A block diagram of the S band transponder is shown in Figure 3-118.

The input bandpass filter has a 24 MHz bandwidth and is a four-section coaxial type filter with about 0.5 dB insertion loss. The tunnel diode amplifier after the redundancy switch has 42 dB gain and provides a low (420 K) receiver noise temperature. The amplified signal is wired with 245 MHz from the frequency synthesizer to convert to the 2045 transmit frequency. The transmit frequency is amplified by 43 dB in a solid state multistage amplifier with an AGC circuit to maintain an even drive level to the transmit power amplifier. The final power output is about 6.3 watts. The output filter has a narrow, 8 MHz, bandwidth and requires a large size cylindrical cavity two-section filter design. The S band Transponder parameters are summarized in Table 3-49.

TABLE 3-48. K BAND TRANSMITTER PARAMETERS

Power output (maximum)	8 watts
Input frequency	50 to 113 MHz
Output frequency	15,050 to 15,113 MHz
Bandwidth	63 MHz
Input power	32 watts
Gain	72 dB
Weight (two transmitters)	5.2 kg

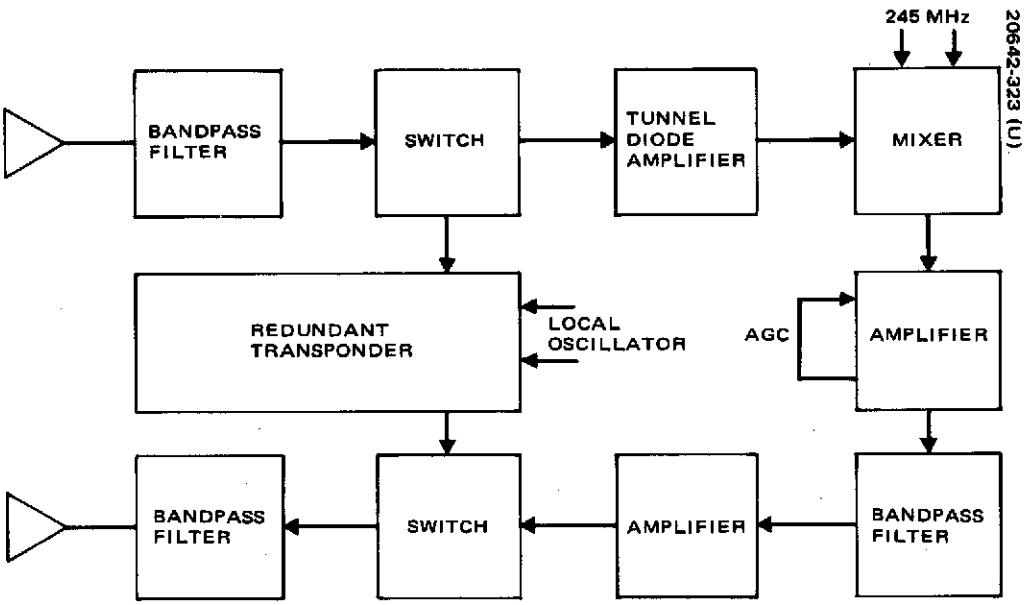

Figure 3-118. S Band Transponder

TABLE 3-49. S BAND TRANSPONDER PARAMETERS

Input frequency	2290 MHz
Output frequency	2045 MHz
Output power	6.3 watts
Bandwidth	8 MHz
Input power (24.5 volt bus)	21 watts
Weight (including redundancy)	7.6 kg

3.4.4 Telemetry and Command

The backup telemetry and command subsystem is a completely independent subsystem operating at VHF. All command decoding and telemetry encoding are accomplished in this unit. It interfaces with the repeater as a digital bit stream. The data bit stream modulates a 100 MHz signal, which is part of the ten-way summer. Similarly, the output of the K band receiver is shifted to a 26.75 MHz signal and amplified and detected to a video bit stream. This is decoded in the command decoders that are part of the telemetry and command subsystem. The output commands from the telemetry and command subsystem go throughout the spacecraft as appropriate. Similarly, all data inputs come into the telemetry and command system for encoding. Figure 3-119 shows the basic elements of this subsystem. More detailed discussion is presented in Volume 5, in subsection 4.2.

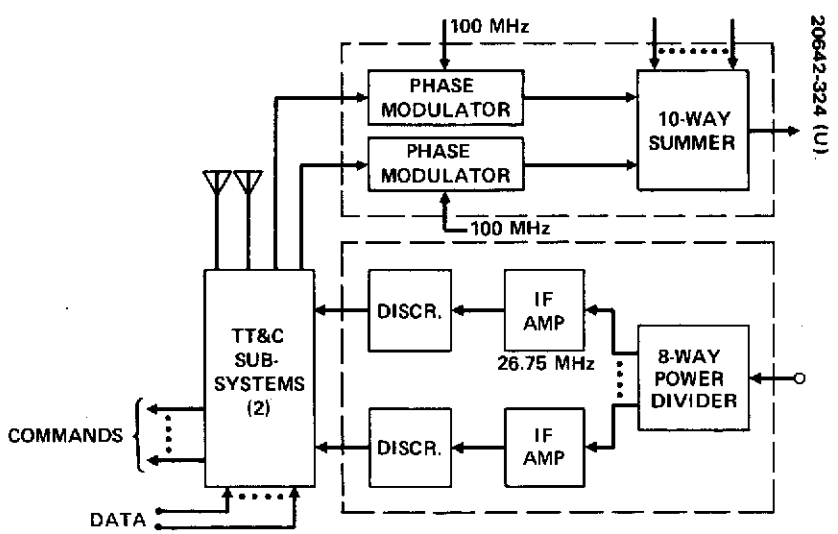

Figure 3-119. Telemetry and Command

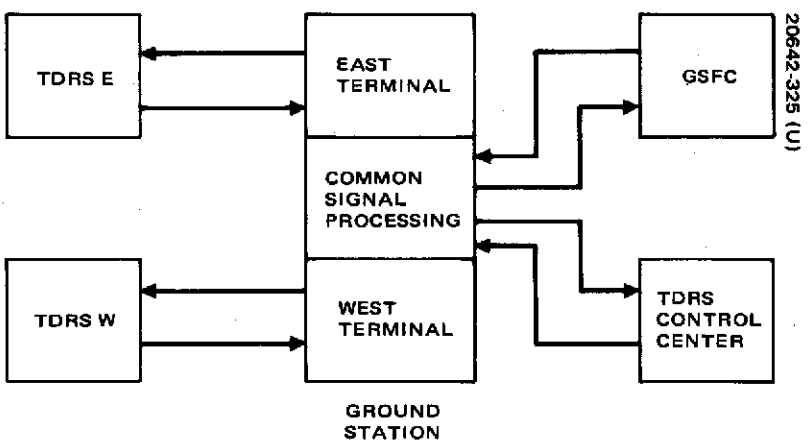

Figure 3-120. Overall Ground Station Concept and External Interfaces

3.5 GROUND STATION DESIGN

The ground station is the interface element between the TDR spacecraft and the two control centers – GSFC and the TDRS control center. The functions of each of these ground elements have been discussed previously in subsection 2.4. The general relationship of the ground station to the other elements is shown in Figure 3-120. Also shown in this figure are three major portions of the basic ground station: 1) a terminal for maintaining RF communication with TDRS E, 2) a terminal for maintaining RF communication with TDRS W, and 3) a common area containing demodulation and processing equipment, which will be applied to signals from both terminals.

The RF terminals are of conventional design as described in the following discussion, but the signal demodulation and processing equipment, although not new in concept, has not been previously applied in the complexity required for simultaneous multiple user communication via the TDRSS.

It should be mentioned that a third terminal may be required for communication with the in-orbit spare TDRS and for redundancy. This will require only a slight increase in the processing equipment and its configuration controls.

The terminals consist of five major portions: 1) the antenna structure, 2) the antenna tracking subsystem, 3) the K band RF/IF subsystem, 4) the VHF backup system, and 5) the TDRS tracking antenna. The signal processing can be functionally separated into six portions:

1) LDR user telemetry demodulation

2) LDR voice demodulation

3) MDR user telemetry demodulation

4) LDR forward link modulation

5) MDR forward link modulation

6) TDRS command, telemetry, and tracking

7) User range and range rate measurements.

These subjects are discussed in the following subsections.

3.5.1 Terminal Design

The major portions and elements of one of the two ground station terminals are illustrated in Figure 3-121.

3.5.1.1 K Band/VHF Antenna

For K band, the antenna consists of a Cassegrain configuration with a 12.8 meter reflector, multimode K band tracking feed, and AZEL mount. Rigidly fixed to the antenna backup structure, behind the reflector, will be the low noise receivers, the monoscan comparator of the tracking system, and the test loop translator; these components interface with the diplexer portion of the feed at its input/output ports. RF power is fed to the diplexer through the elevation and azimuth rotary joints in order to realize gain stability and minimum loss throughout the movements of the reflector.

Projecting from the antenna subreflector and fed through it by its associated duplexer will be the VHF radiators; thus, the 12.8 meter reflector will serve as a near focus fed antenna for the VHF forward and return links.

While the VHF antenna could be implemented independently of the K band unit, its integration with the selected cassegrain antenna is dictated for reasons of economy. Three approaches could be taken to the feed design.

1) Cassegrain feed

2) Focus feed

3) Near focus feed

The third alternative has been selected since it is the simplest and least expensive. A performance penalty of less than 2 dB in VHF gain has been computed with this implementation, but this is within the acceptable bounds of the VHF link. Blockage of the K band subreflector is very small resulting in negligible gain reduction. The effect of VHF feed resonance at K band needs further study, but it appears that the large difference in frequency will minimize this effect. The cassegrain feed approach would require much design work while the focus feed necessitates the use of an expensive transparent subflector.

The major parameters of this antenna are listed in Table 3-50, and Figure 3-122 illustrates its structural configuration.

3.5.1.2 UHF Antenna

The UHF antenna is used for receiving the LDR forward link signal transmitted by the TDRS. This signal, which is modulated by a PN code at the ground station, is used for measuring the range and range rate of the TDRS. The TDRS power is sufficient to allow a low gain antenna to be employed. No specific design has been recommended in this study, but it is expected that an available antenna with 5 dB or more gain would be used. The relatively low gain would allow the antenna to remain fixed, not requiring any motion.

3.5.1.3 Low Noise Receiver

The low noise receiver (LNR) will be an uncooled parametric amplifier with a nominal noise temperature of 400 K. A unit representative of the TDRS LNR terminal requirement is currently available from Comtech Laboratories.

FOLDOUT FRAME

FOLDOUT FRAME 2

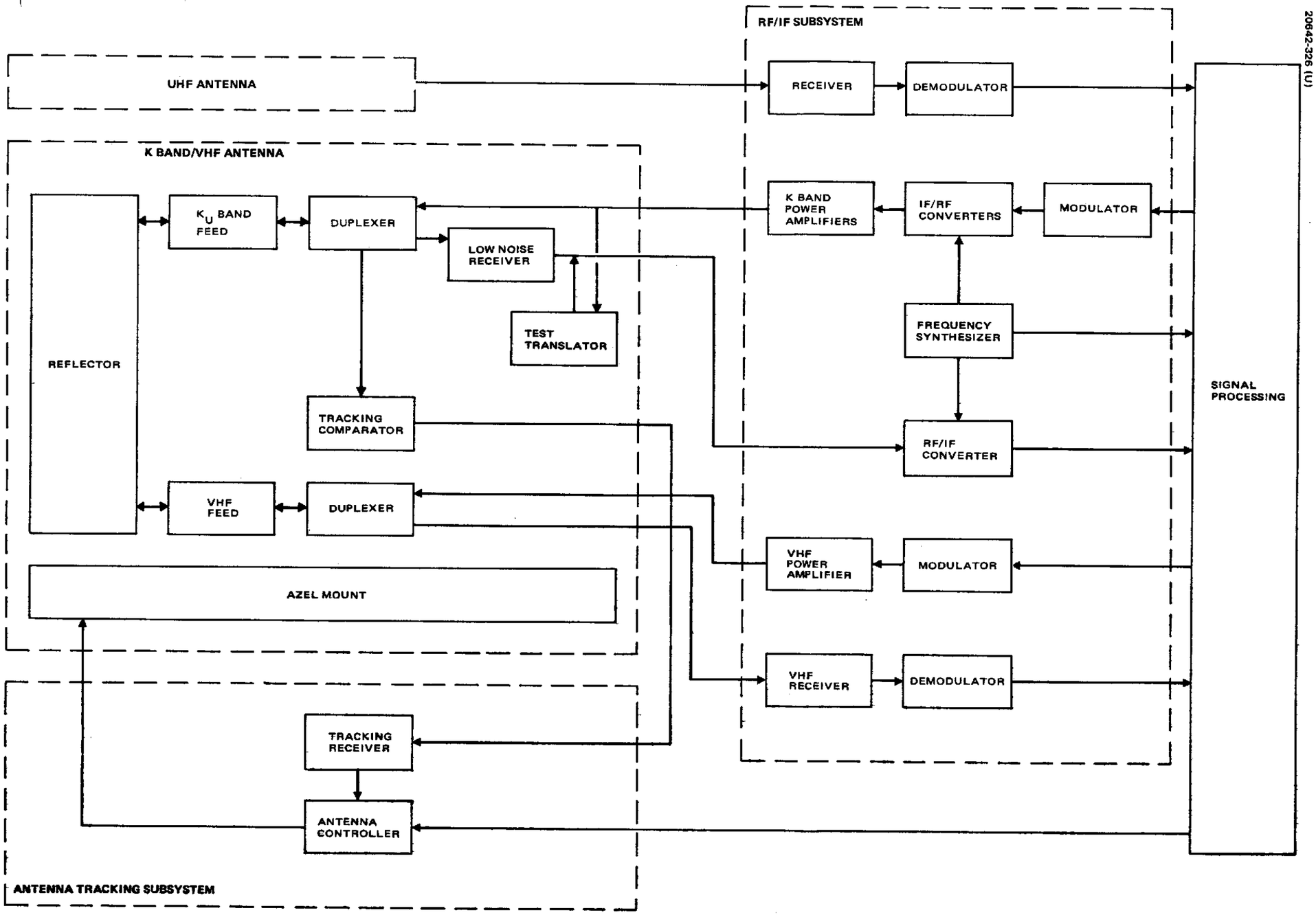

Figure 3-121. Ground Station Terminal Configuration

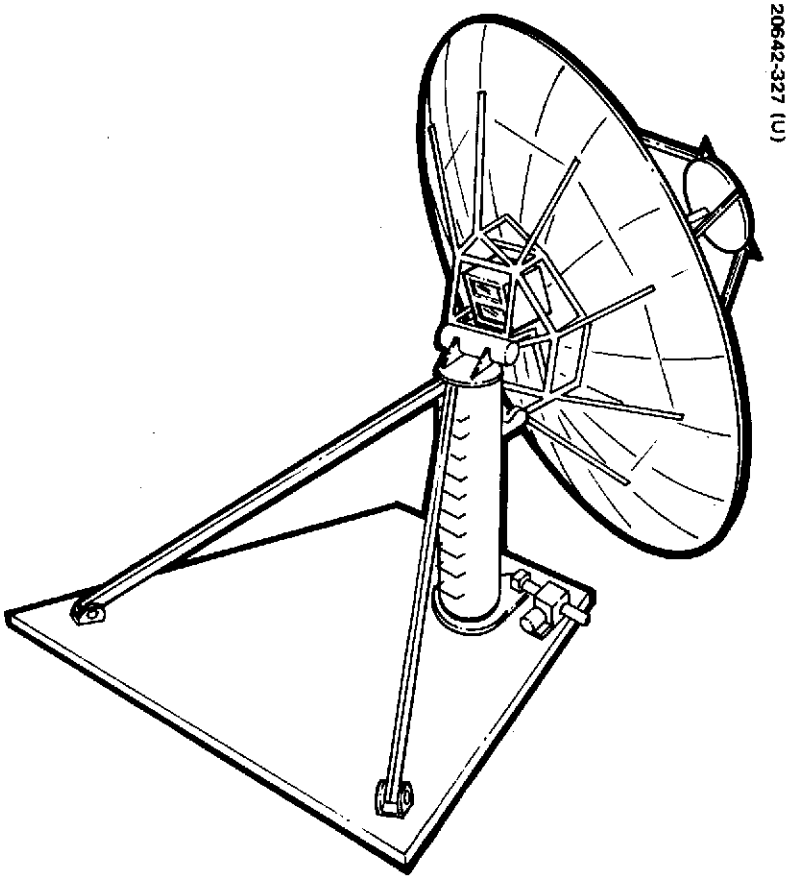

Figure 3-122. Antenna Structure

TABLE 3-50. K BAND/VHF ANTENNA CHARACTERISTICS

Reflector diameter	12.8 meters
Feed type	
K band	Cassegrain transmitter/receiver; tracking type
VHF	Focus fed, transmitter/receiver
Gain at 13.5 GHz 15.0 GHz VHF	62.0 dB 63.0 dB 20.5 dB
Polarization	
K band	Circular, C/CC
VHF	Linear, V/H
Pedestal type	Azimuth/elevation
Coverage	±10 degrees each axis; mount to be resettable to select ±7 degrees coverage over 0 to 90 degrees elevation range and 0 to 160 degrees azimuth range
Axis rates	
Velocity	(0 to 1.75 mr/sec)
Acceleration	(0 to 1.75 mr/sec^2)
Pointing accuracy	0.35 mr
Environmental	
Temperature	219 to 328 K
Humidity	Up to 100 percent
Altitude	Sea level to 3000 km

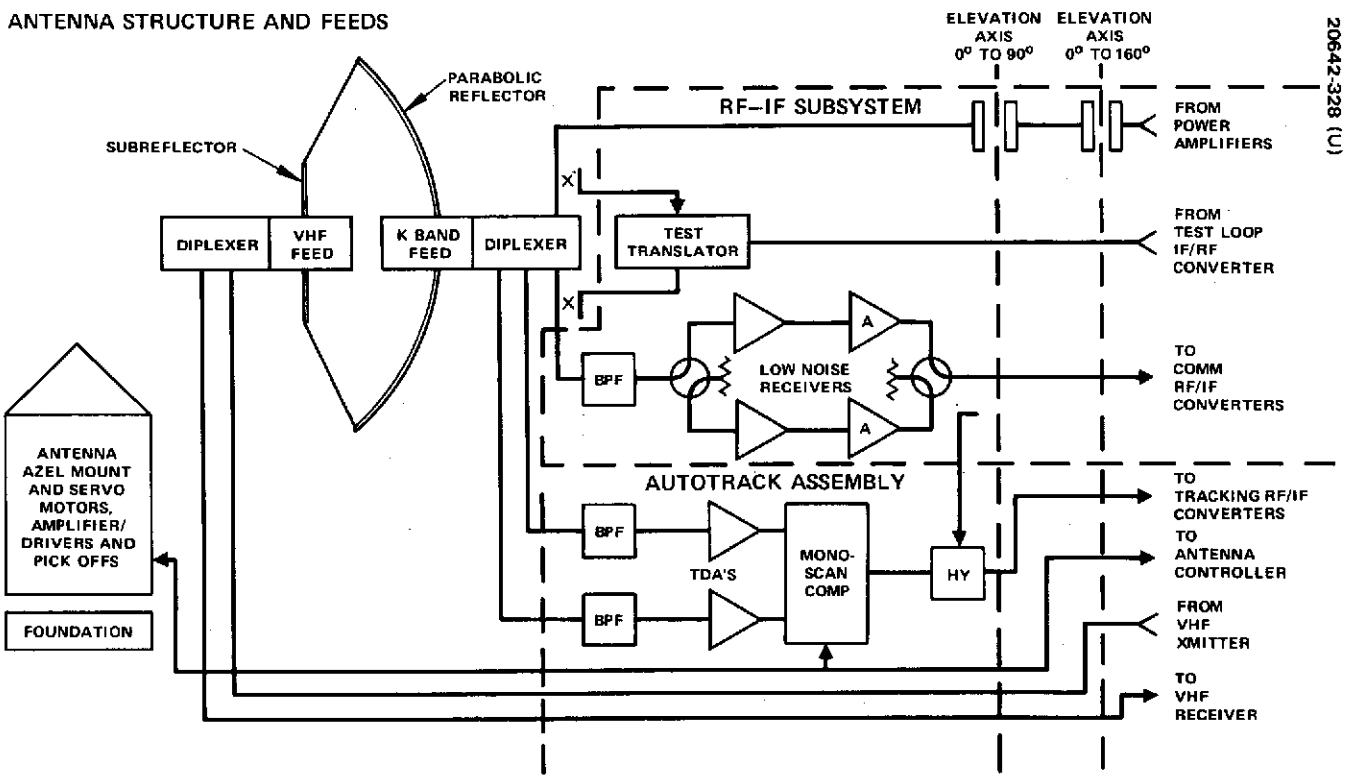

Figure 3-123. The K Band/VHF Antenna/RF-IF Subsystem Interface

3.5.1.4 Reflector Positioning

The tracking system selected for the K band/VHF antenna is a single RF channel, amplitude comparison, monopulse type. The essential advantages of this approach versus the three channel monopulse and conical scan solution are the following:

1) Heavy rotating mechanical parts required for conical scanning are avoided, which results in less critical maintenance.

2) Transmit and receive amplitude modulation inheritent in conical scanning is eliminated.

3) Differential phase shift problems at RF frequencies associated with three channel monopulse tracking are traded off against simpler problems with modulator and demodulator synchronization of low audio frequencies.

4) The use of the single channel type system therefore results in less hardware cost and implementation.

With reference to Table 3-50, the selected antenna mount is resettable over a 0 to 160 degree radian azimuth range. This feature would thus allow redirecting the antenna to the other TDRS satellite if necessary. As presently conceived, this azimuth resetting operation would take approximately 15 minutes to conduct. This repositioning period is considered adequate for the present application; however, the mount slewing mechanism design can be modified at a slight cost increase to shorten the slewing time over a 160 degree arc to a few minutes if deemed necessary.

3.5.1.5 RF/IF Subsystem

The RF/IF subsystem consists of the transmitting and receiving electronics equipment that lies between antenna feeds and the outputs and inputs of the signal processing equipment. The arrangement of the major elements is shown in Figure 3-121. The K band receiver is rightfully a part of this subsystem, but has been discussed above because it is physically attached to the antenna structure. Figure 3-123 provides additional clarification of the interface between the antenna and RF/IF subsystem.

The receivers, frequency synthesizers, converters, and modulators will all be of conventional design. The major topic treated in this study was the power amplifier configuration. Table 3-33 of subsection 3.3.3.2 lists the required ground RF power per channel; they are:

LDR	710 watts
MDR	1500
Beacon	20
TDRS telemetry	20
Total	2550 watts

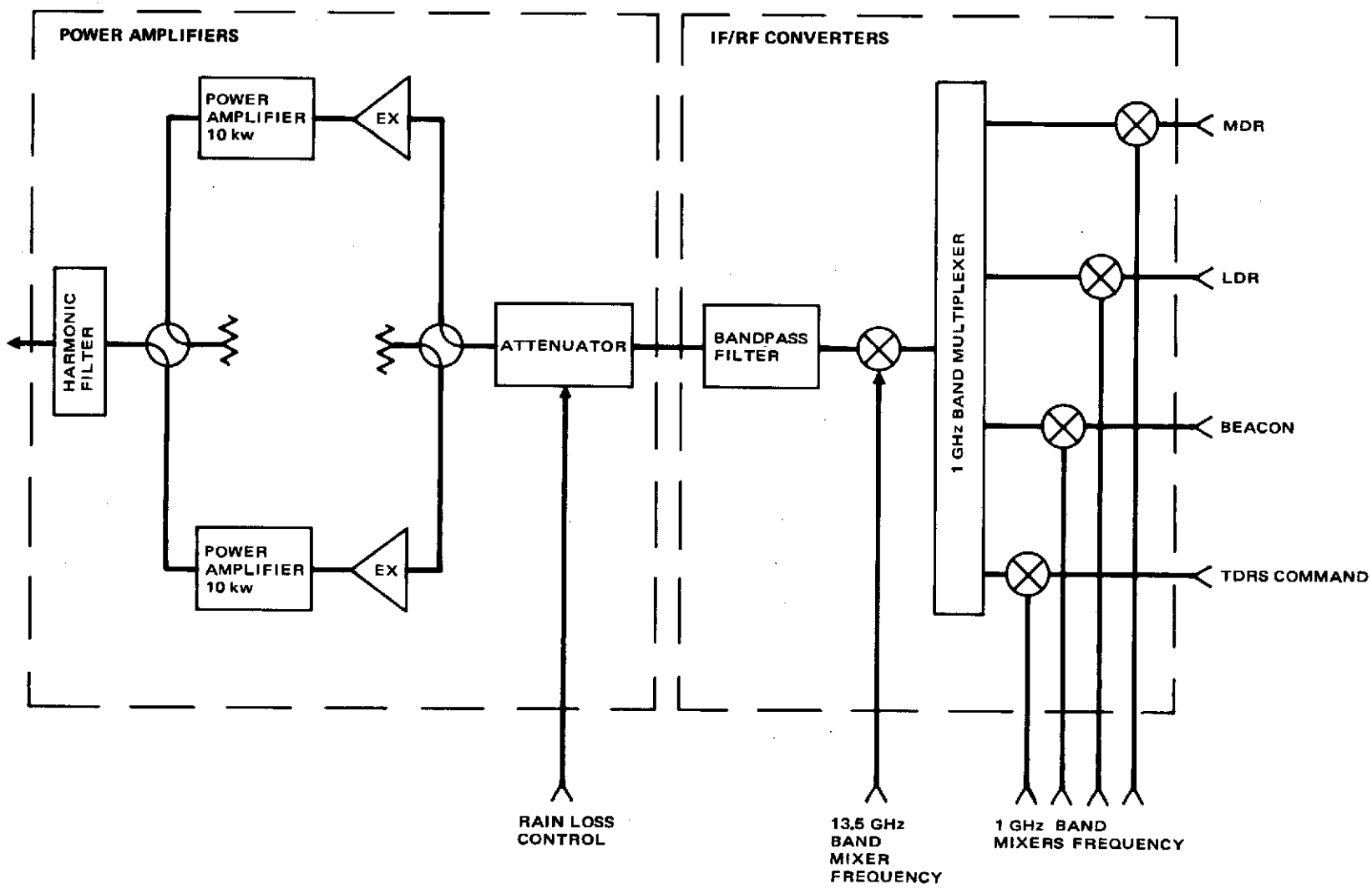

Figure 3-124. Configuration A, Power Amplifier and IF/RF Converters

Three power amplifier configurations were considered and will be briefly discussed.

Configuration A. This approach, which is conceptually the simplest, is shown in Figure 3-124 and utilizes a single 10,000 watt amplifier backed off 6 dB. In spite of its simplicity, some development would be required for the high power amplifier. The backoff is required to keep intermodulation power at acceptably small levels.

Configuration B. To avoid the intermodulation problem while keeping the power output of the individual units to a minimum, Configuration B shown in Figure 3-125 was postulated. The minimum power performance is achieved through use of the 13.5 GHz band multiplexer, which combines with little loss in the beacon and TDRS command signals. To implement this configuration, subject to the requirements and constraints applied earlier, three power amplifier units with outputs of 2 kw, 1 kw, and 100 watts. The problem with this configuration lies in the 13.5 GHz multiplexer, which requires very high Q filters in order to perform its function. The 2 and 1 kw units can be implemented using Varian 882 klystrons, and a TWT can be used for the 100 watt amplifier.

Configuration C. This approach, shown in Figure 3-126, replaces the 13.5 GHz band multiplexer of Configuration B with a 5 dB coupler to eliminate the high Q filter problems. As a result, the 1 kw and 100 watt power amplifier units need replacing with a 2 kw unit. The availability of the Varian 882 klystron for the 2 kw unit was mentioned earlier. Since two of these klystrons, or similar units, will probably be used in Configuration B to simplify procurement, it is logical to use the extra power capability to transmit the three lower power signals with one power amplifier. The only concern is the intermodulation distortion. However, preliminary analysis indicates that the intermodulation power does not lie in the frequency bands of the signal channels. However, with the 2 kw amplifier, 3 dB backoff is provided to reduce intermodulation power.

As a result of the above considerations, Configuration C (Figure 3-126) was chosen as the baseline approach.

3.5.1.6 Cross-Terminal Interference

It is expected that interference produced at either a TDRS or its Ground Station terminal due to transmissions from the other terminal - TDRS pair will be negligible. The two Ground Station antennas will have approximately 160 degrees angular separation between their boresights. The back lobes near this angle can be made more than 50 dB below the boresight peak again. A 17.5 dB margin has been provided in the ground links for attenuation due to rain. Thus, under the most diverse conditions for the two links, the signal to cross-link interference will be greater than 32 dB, and since the links have been designed to provide signal to thermal noise ratios of 20 dB or less, the cross-link interference noise power will be at least 12 dB below thermal noise power under all conditions.

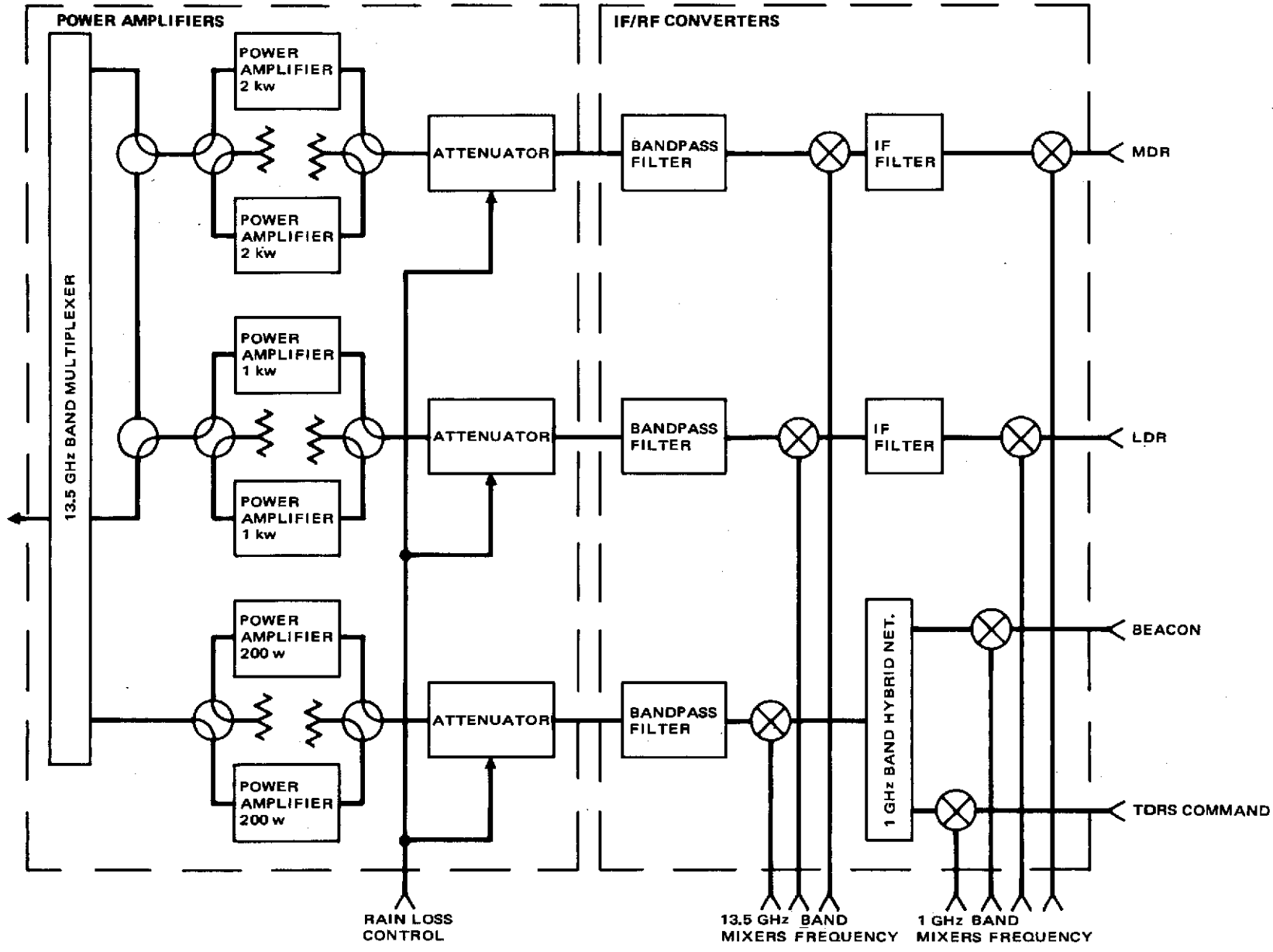

Figure 3-125. Configuration B, Power Amplifier and IF/RF Converters

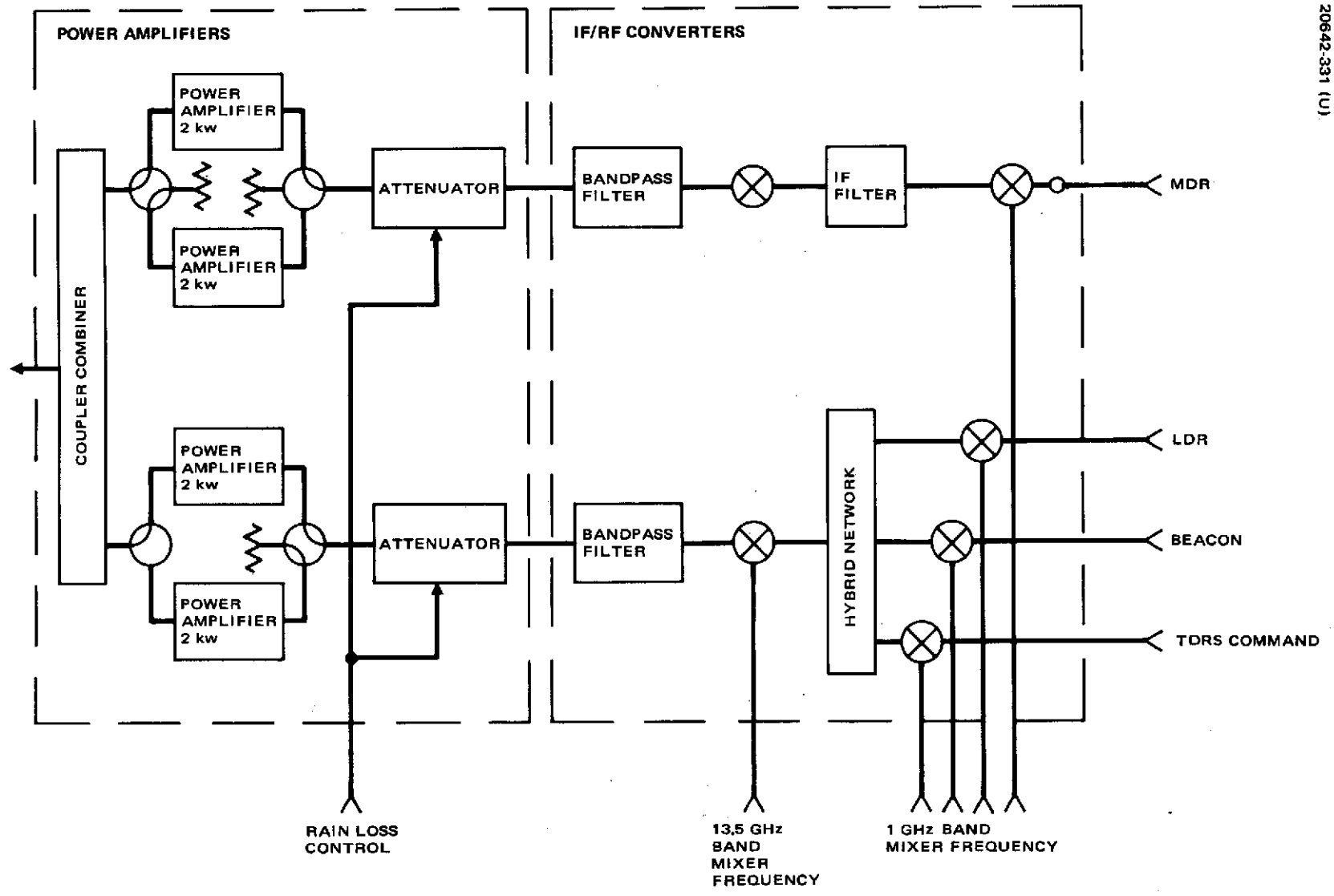

Figure 3-126. Configuration C, Power Amplifier and IF/RF Converters

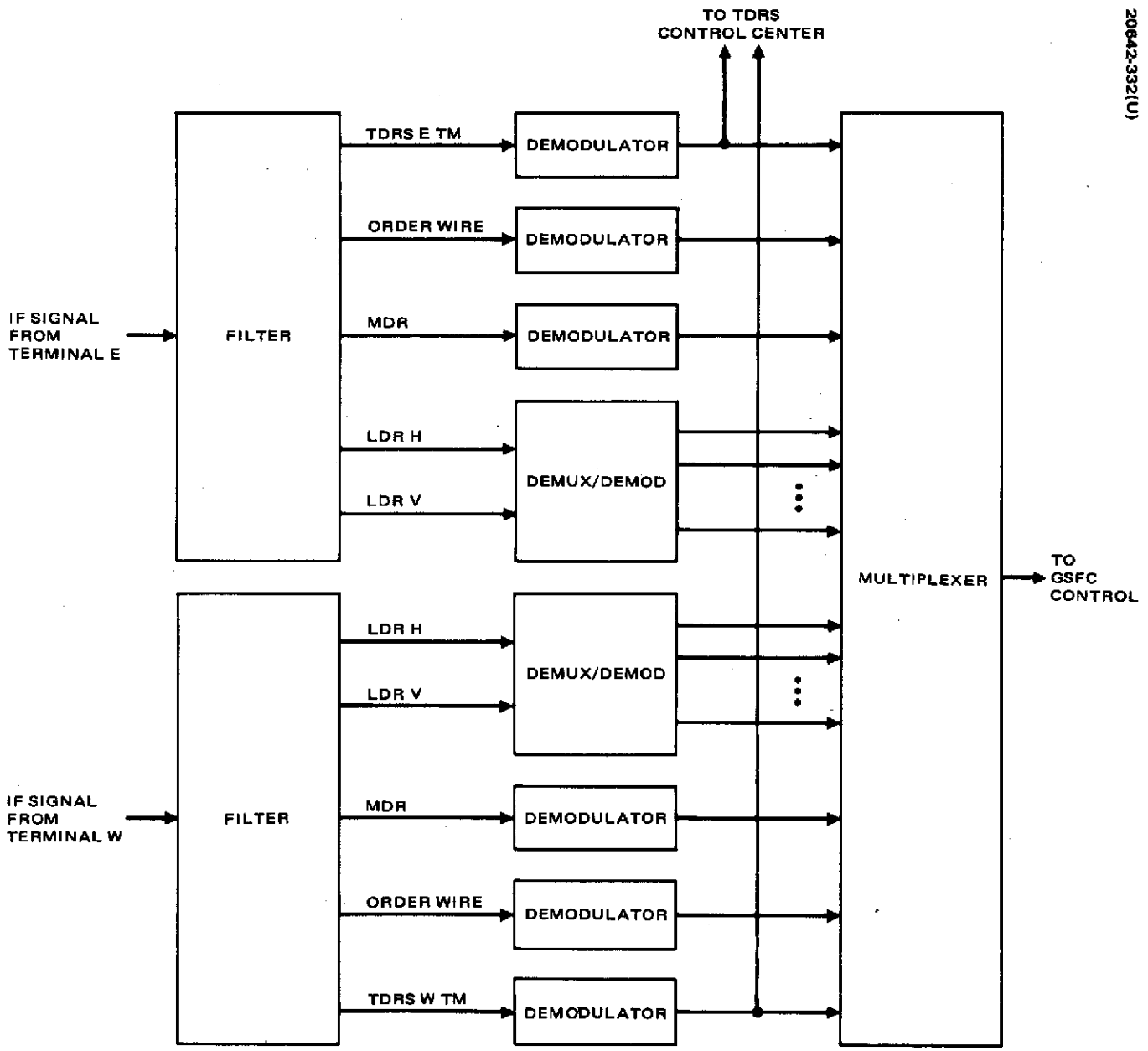

Figure 3-127. Ground Station Return Signal Processing

A worst case condition would require that one ground link experience 17.5 dB attenuation due to rain while the other had no attenuation (clear weather) with both ground antennas in the antenna beams of both TDRSs, i.e., colocated ground antennas. Thus, locating the antennas near each other will not affect link performance, but would provide advantages for installation, maintenance, and operation.

3.5.2 Signal Processing

The ground station return signal processing equipment must separate the individual channels in the two signals from each terminal, demodulate the data signals, and then multiplex all data for transmission to the GSFC telecommunications control center. These functions are illustrated in Figure 3-127 where (for simplicity) range and range rate measurements have been made part of the general demodulation process. The forward signal processing as shown in Figure 3-128 includes demultiplexing the signals from GSFC, modulating the LDR and MDR with PN codes, IF carrier modulation of all signals, and transmission to the two terminals. The voice must be switched to the correct LDR or MDR channel as directed from GSFC

The major task required for the signal processing equipment is one of the integration, control, checkout, maintenance, and replacement provision. All equipment, except the LDR return channel demultiplexing and demodulation equipment, is conceptually conventional. Thus, the remainder of the discussion will treat the LDR equipment.

3.5.2.1 LDR Return Link Processing

The LDR return link processing is the most complex because it requires both code division demultiplexing and demodulation requiring several processes. The basic units required are: 1) acquisition correlator, 2) telemetry correlator, 3) combiner, and 4) decoder.

The overall arrangement of this equipment is important from the standpoint of reliability and cost. Three basic configurations were considered during the study:

1) Dedicating a set of equipment for each user to each of the two terminals.

2) "Pooling" all the equipment and interconnecting a given terminal output to an appropriate set of units as required via a computer controlled switching matrix.

3) "Pooling" strings of electronic units.

The first of the three alternatives is quite costly since many more units would be required. Since at a given time more than half of the user satellites may be visible to one TDRS and not visible to the other, a set of demultiplexer/demodulator equipment for each of the maximum possible number of visible users would be connected to each terminal. Thus, twice this number of demultiplexer/demodulator sets would be required, not including redundancy.

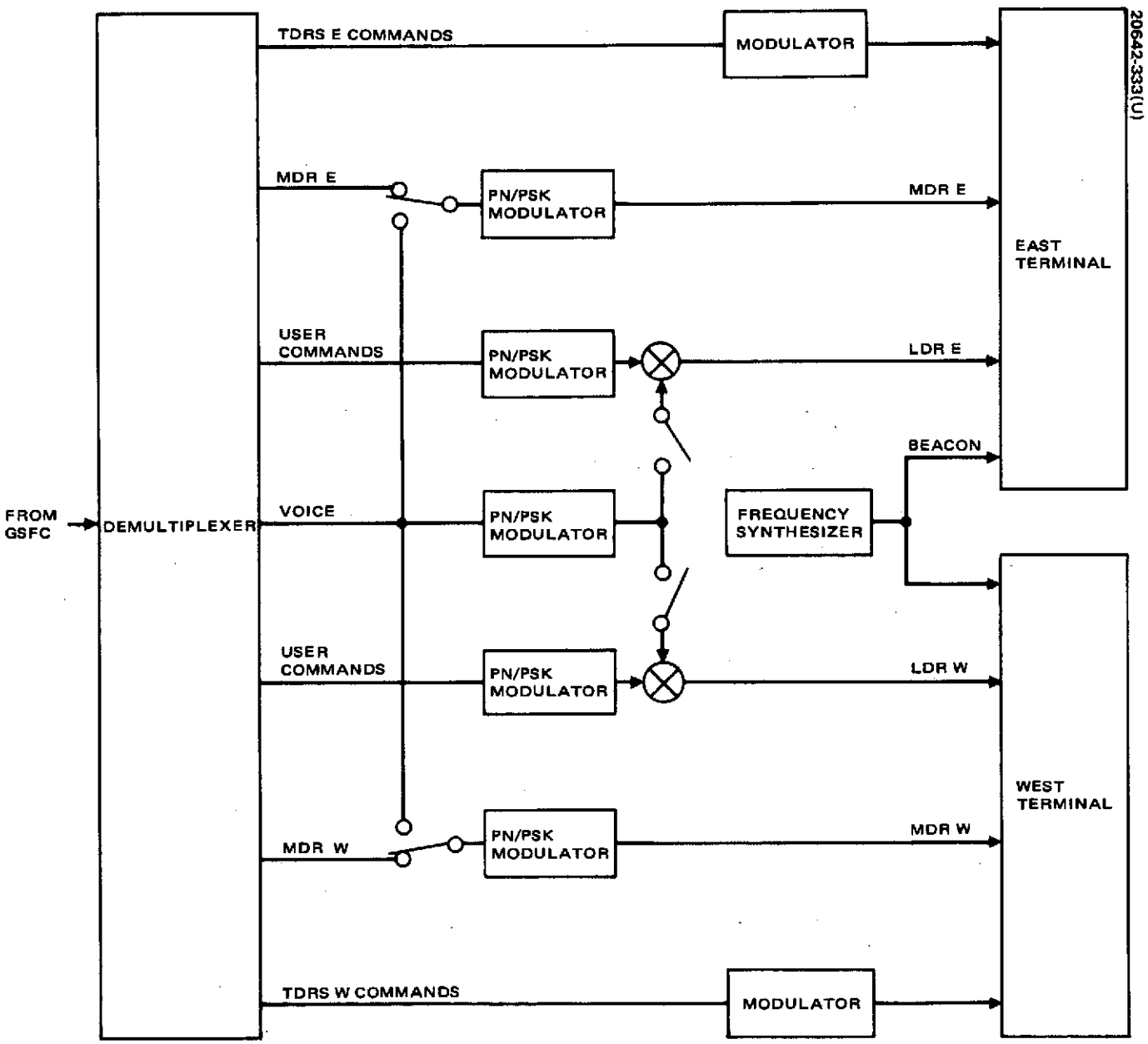

Figure 3-128. Ground Station Forward Signal Processing

The second alternative is attractive because it minimizes the number of individual units, but it requires an extremely complex switching matrix and the additional computational capability to generate the switching control signals. Preliminary estimates of the costs of acquisition and telemetry correlators indicate that a time-sharing of these units is probably not justified considering the system integration and operational difficulties which are inevitable. Thus, a form of the third alternative was selected as the preferred approach.

Figure 3-129 illustrates the general arrangement of the equipment. The demultiplexing/demodulation equipment associated with each user's telemetry is called a data demodulator for convenience. For the full capacity system, 40 data demodulators would be provided each with four inputs corresponding to the two polarization separated channels of the two TDRSs. Each data demodulator is able to provide, without additional equipment, a smooth handover from one set of TDRS signals to another. The following processes are provided by this equipment: 1) signal acquisition, 2) correlation, 3) two-channel combining, 4) convolutional decoding (error correction), and 5) range and range rate measurement. These functions are shown in the baseline arrangement of Figure 3-130.

Adding data demodulators to the set of 40 is an easy means of including redundancy. In the event of a failure, these backup units would be loaded with the code and doppler offset frequency of the failed demodulator.

3.5.2.2 LDR Demodulation Equipment

Notch Filters. Before entering the data demodulators, each composite LDR signal is processed by a bank of notch filters. Hughes Ground Systems Group has built a unit consisting of three banks of automatic tracking notch filters, with six filters in each bank. This electronic unit will normally operate automatically to filter out narrowband RFI sources. Since the frequencies of the sources are fixed with respect to the relay spacecraft, the notch filters need only track out the doppler between the TDRS and ground. The only control required of the unit is to assure that the highest power RFI sources are being tracked.

Telemetry Correlators and Combiners. After filtering, the composite signal from a given TDRS is sent to two telemetry correlators followed by a diversity combiner. These correlators are PN/PSK serial correlators designed to provide maximum coding gain and remain in lock at very low signal-to-noise ratios. They output 5 bit digital words to the combiner along with sync pulses and in-lock/loss-of-lock signals. When both are in-lock, the combiner provides optimum summing of its inputs. If the TDRS noise environment, is such that the noise in the H and V channels is incoherent, the combiner is set to perform maximal-ratio diversity combining. If the noise is better categorized as coherent, it will be set to execute selection combining. This topic was discussed previously under subsection 2.3.3.1. Because of the nature and interaction of the correlators and combiners, they should be procured as a single unit. Both Hughes and the Magnavox Company have built equipment of this type. Figure 3-131 illustrates the major elements of a telemetry correlator.

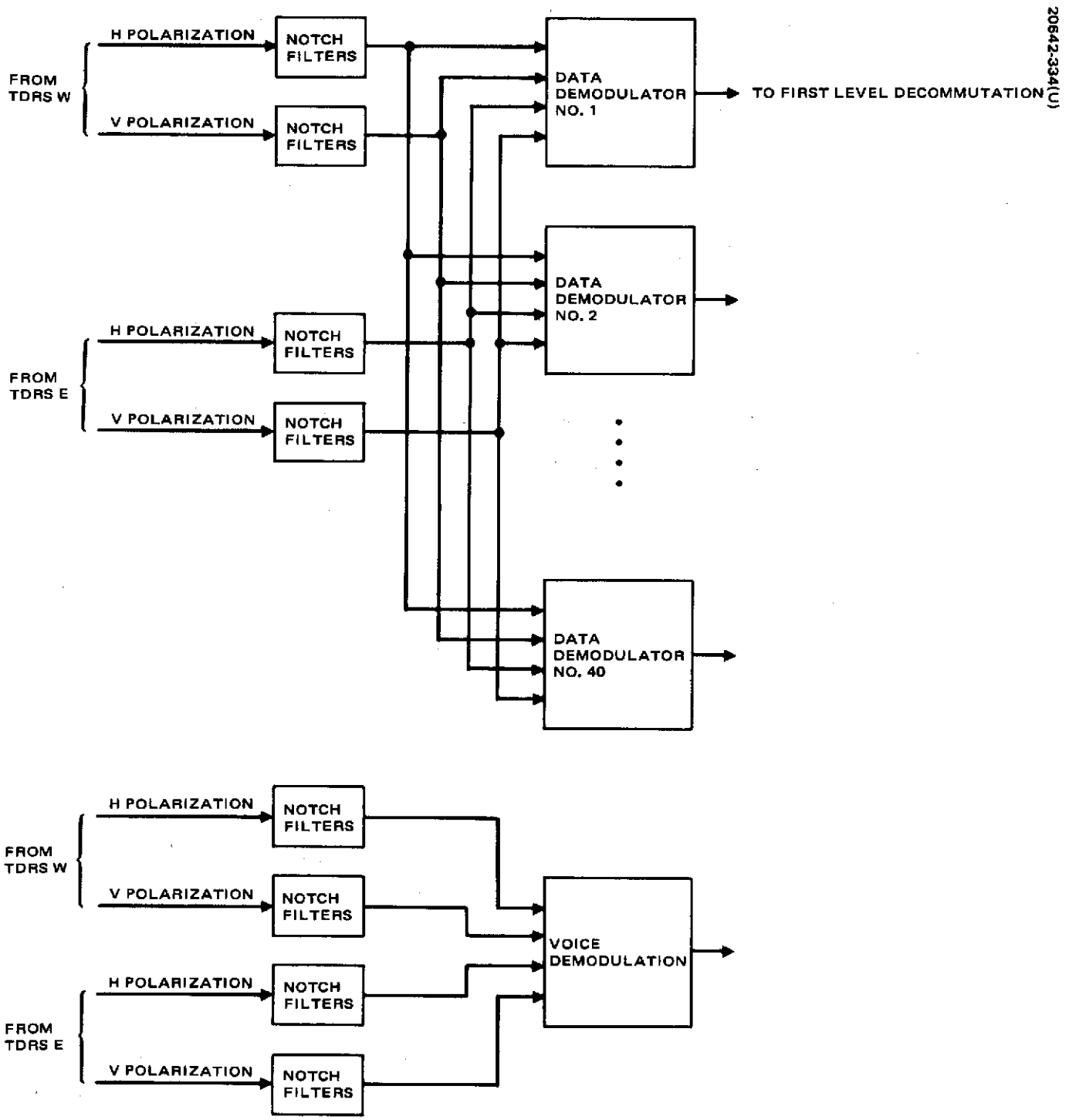

Figure 3-129. Demultiplexing and Demodulation of Return Link Telemetry and Voice

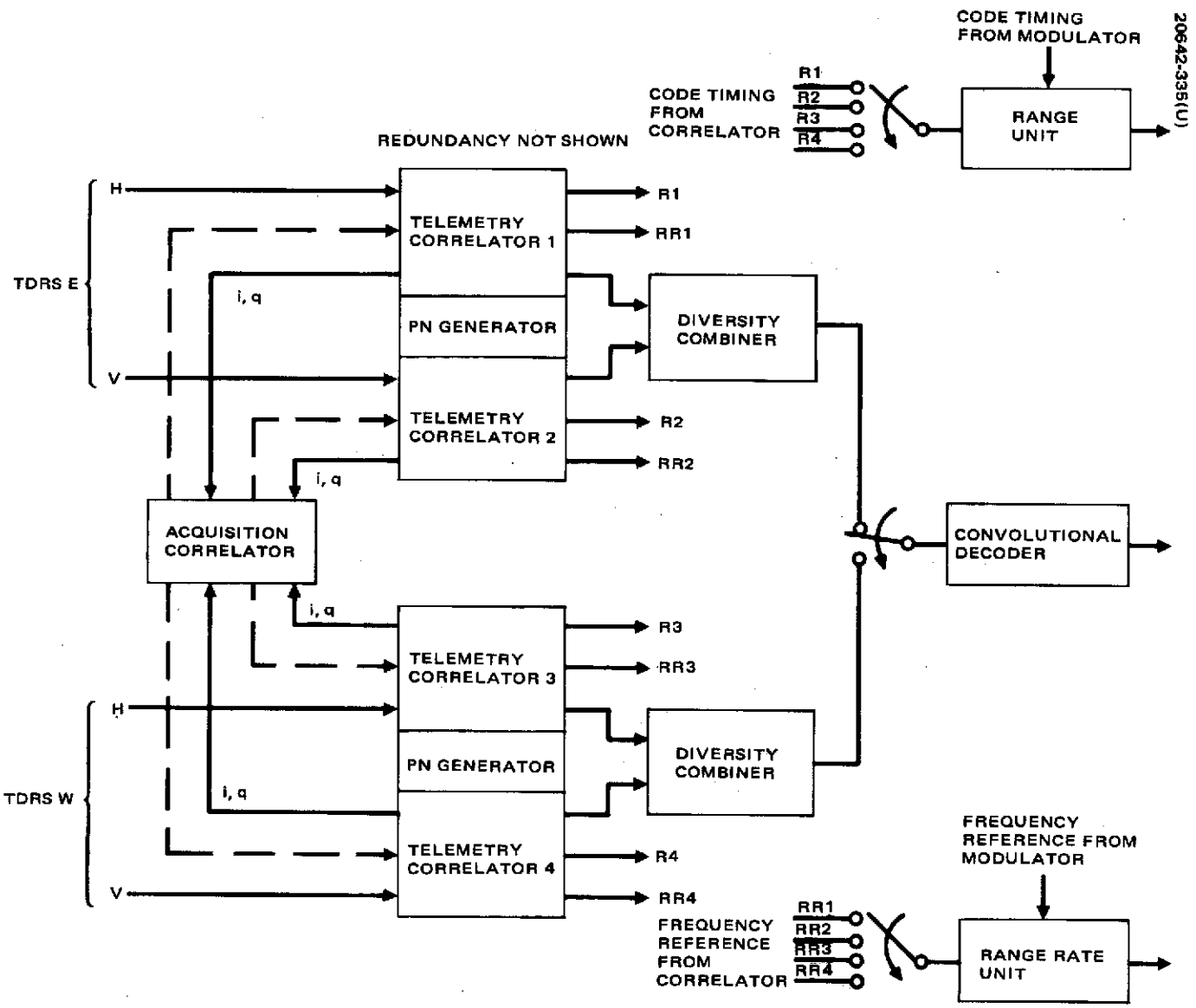

Figure 3-130. Low Data Rate Data Demodulator for Each User

Convolutional Decoder. The convolutional decoder accepts a 3 bit digital word from the active diversity combiner. One such word is accepted every convolutional code symbol time; that is, at twice the output bit rate. Suitable decoding equipment is available from either Linkabit Corp. or Codex. The interfacing circuitry includes deinterleaving logic. It may also prove advantageous to provide two decoders to aid in handover without data loss. However, if the decoder can be made to synchronize within a fraction of a second only one will be required and only a very little data will be lost during handover.

Range and Range Rate Units. Each set of data demodulation equipment also contains range and range-rate extraction units. The complexity of these units is minimal compared to the rest of the assembly and separate boxes are therefore provided for each user. Figure 3-131 shows the interconnection of two telemetry correlators (PN/PSK receivers) and the range and range-rate units. The logic of the active diversity combiner will indicate, which of the four correlator outputs the range and range-rate units should accept. These units are of conventional design.

Acquisition Correlators. When a user spacecraft exists the orbital region excluded from TDRSS coverage, an acquisition sequence will occur, and during user spacecraft transit from the coverage region of one TDRS to that of the other, a handover is required which includes acquisition by the second set of telemetry correlators. Since the dual coverage time is quite large, this handover can be accomplished without data loss. To acquire a given LDR signal two parameters are required: 1) the frequency of the doppler shifted carrier and 2) the start time of the user's Gold code generator. With the communication system in one-way lock, the doppler uncertainty is $\approx$3.6 kHz. At a baseline 1200 bps data rate, the code timing uncertainty is 1/(2 x 1200) second since two code lengths are present per data bit.

Acquisition procedures are generally classed as either serial or parallel. One could search serially first in time and then in frequency or one could, with a sufficient number of correlators, perform parallel correlations with units set to slightly different timing and frequency offsets. The technique selected is called a programmed matched filter correlator. When provided with doppler offset predictions, this parallel correlator can perform extremely fast acquisitions.

The principal design challenge in TDRSS is fast acquisition at a very low signal-to-noise ratio. The E_b/η input to the convolutional decoder can be as low as 4 dB; therefore, E_s/η = 1 dB, where E_s is the energy in a convolutional code symbol or Gold code length. In a given polarization channel only 1/2 this energy may actually be present, therefore the E_s/η drops to -2 dB. At IF, the ratio of Gold code energy-to-noise density is as low as -28 dB in each polarization channel.

The ground terminal acquisition correlator shown in Figure 3-132 has been designed for minimum complexity and maximum speed of operation at minimum input signal-to-noise ratio. The complexity is slightly increased over conventional design by the inclusion of inputs from both the horizontally and vertically polarized antenna channels and by the requirement to acquire while the incoming signal is data modulated.

The approach utilized is to separate the horizontal and vertical channel inputs into two coherent matched filters, each one convolutional code interval (512 PN chips) long, and then to noncoherently combine these into one recirculating register for further signal-to-noise enhancement.

As a worst case, the outputs of the coherent matched filter sections should be no worse than 4 dB rms noise to peak signal. This case corresponds to -28 dB RF signal-to-noise ratio into each of the horizontal and vertical channels and worst timing between the received signal and the receiver sample points. The required 13 dB output signal-to-noise ratio can be obtained by integrating 100 outputs from each channel. Using the approach of Skolnik (Introduction to Radar Systems, Section 2.8) this corresponds to an integration improvement factor of 17 dB.

For the worst case this corresponds to a time constant of less than 0.1 second. At improved signal to noise inputs the time is reduced and the probability of correct first time synchronization is better than 90 percent.

An acquisition involves the following sequence of events:

1) The data correlator's voltage controlled crystal oscillator is set approximately on frequency by command from the computer, or other external input.

2) The received signal samples from two of the telemetry correlators (H and V channels) are routed to the acquisition correlator matched filter.

3) When a potential match between the incoming signal and the stored reference PN pattern is detected, the time of match is transferred to the telemetry correlator. This restarts the telemetry correlator's PN pattern at the predetermined point, which should place it in time synchronization with its incoming signal.

4) The acquisition correlator is then released; the entire sequence to this point should take approximately 0.1 second.

5) The telemetry correlator then tracks and monitors quality on the received signal essentially as with the user spacecraft equipment described in the next subsection.

While the probability of correct timing output from a single trial with the acquisition correlator may be no greater than 0.9 (at minimum signal-to-noise), the probability of acquiring a particular signal should exceed 99.9 percent within 1 second.

Both Hughes and Magnavox have built matched filter acquisition correlators using both digital and acoustic wave techniques. The acoustic wave device built experimentally by Magnavox (see Reference 17) operated satisfactorily, but the design parameters are not those currently needed

Page intentionally left blank

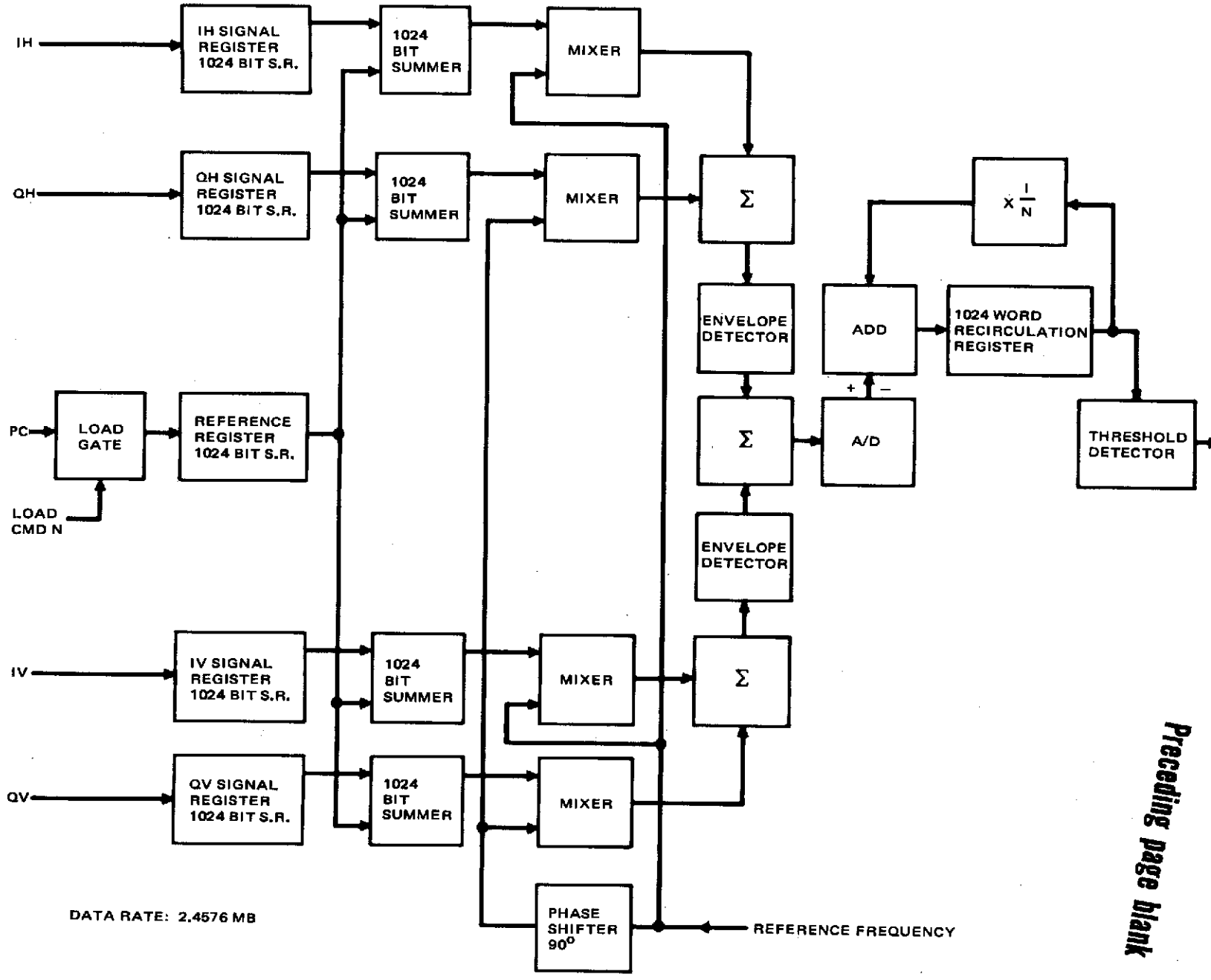

Figure 3-132. Acquisition Correlator

for the TDRSS. Acoustic wave devices are most effective in high data rate systems where the integration time is relatively short compared to those for the LDR data rates.

3.5.2.3 LDR Forward Link Modulation

The use of code division multiplexing (CDM) for voice and user commands in the LDR forward links is novel and provides a great deal of system flexibility as well as reduced TDRS repeater complexity. Figure 3-133 illustrates one possible arrangement of the modulation equipment. Only one command modulator is required per TDRS, since the users are commanded sequentially. And, since all users lock in frequency and time to this signal, the modulator sends transmit references to the range and range-rate units within each data demodulator assembly.

Figure 3-134 shows additional details of a PN/PSK modulator. The command and voice is shown multiplexed in CDM on the same carrier. The two biphase modulators are summed at a low IF frequency directly after modulation. The modulation and summing could also be performed at baseband.

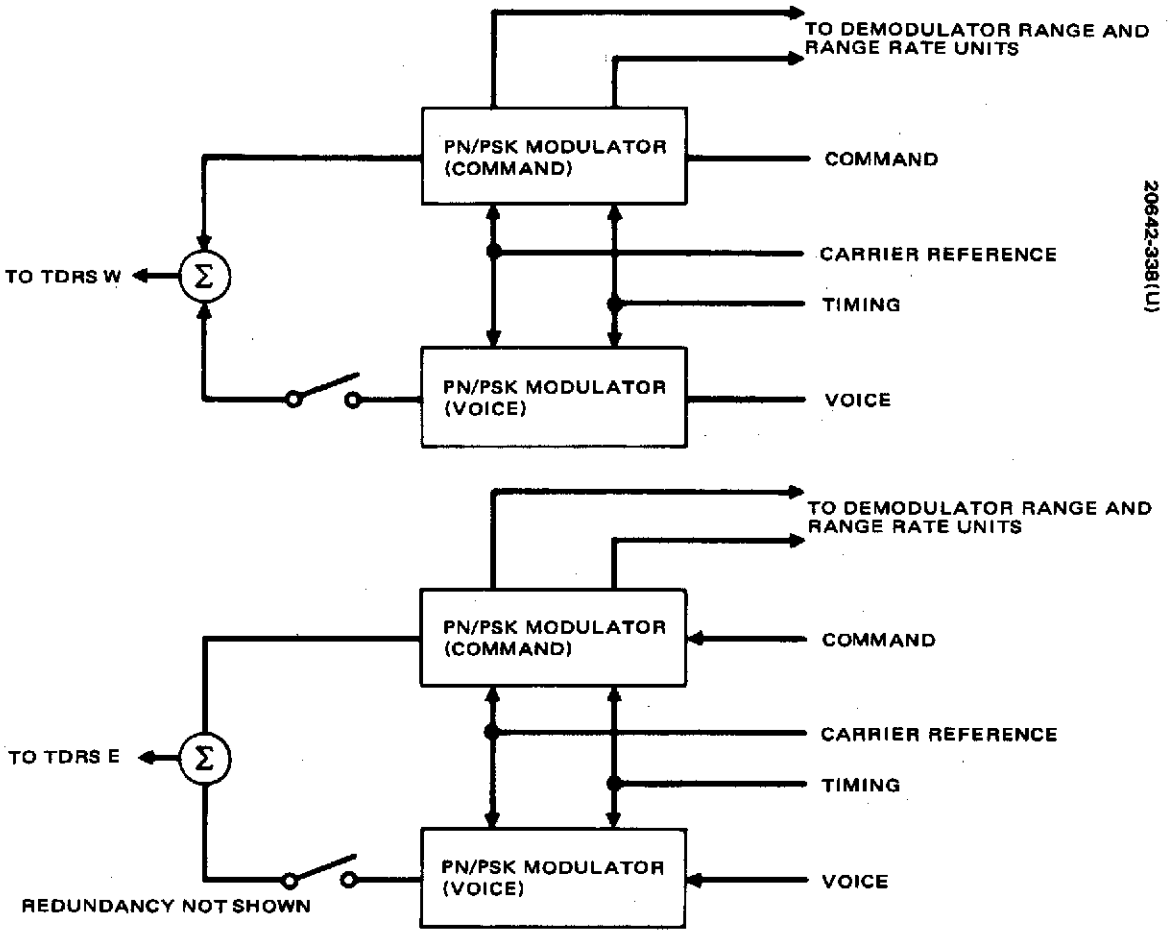

Figure 3-133. Low Data Command and Voice Modulation

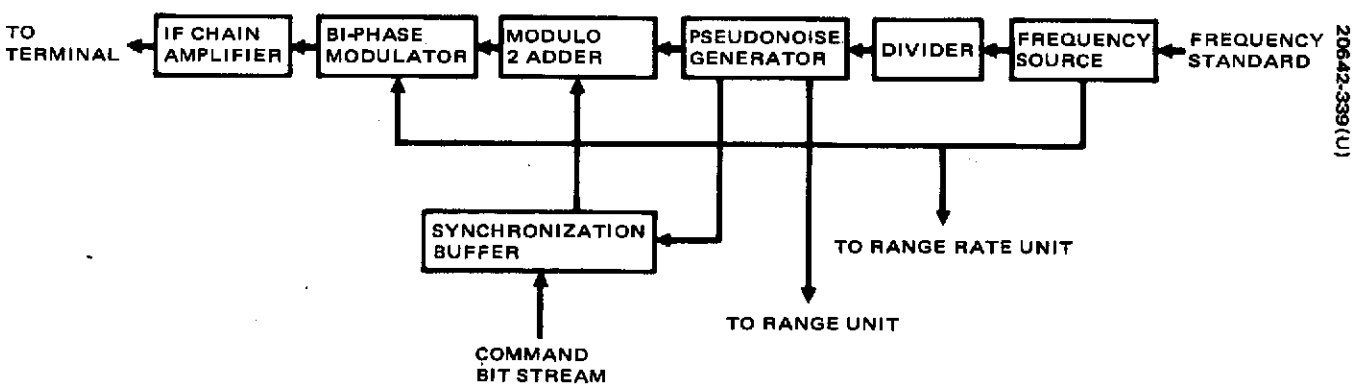

Figure 3-134. Low Data Rate PN/PSK Modulator

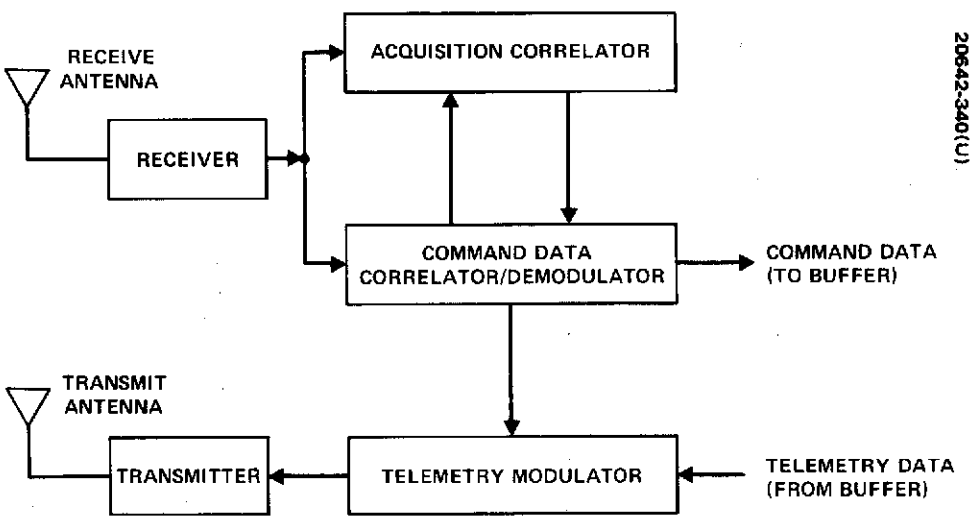

Figure 3-135. User Transceiver

3.6 USER TRANSCEIVER

Both low data rate and medium data rate users will require spread spectrum transceivers. The carrier signals are modulated by binary PN sequences (codes), which in turn have been modulated by data. As was discussed in subsection 3.3.1, the use of PN coding for spectrum spreading accomplishes four objectives: 1) it allows code division multiplexing, 2) it reduces multipath interference, 3) it reduces the earth incident flux density to meet CCIR requirements, and 4) it improves range measurement accuracy. All four of these reasons are important in the LDR system and all but the first are important in the medium data rate system. The low data rate PN symbol (chip) rate is 614 kchip/sec in the allocated 1 MHz (400.5 to 401.5 MHz) band. The bandwidth of the medium data rate service is 10 MHz, and the signal must be spread over most or all of this band to minimize the flux density. Thus, the medium data rate signaling rate may be 10 times greater than that of the low data rate system. However, the transceiver operation will be basically the same for both services. The user transceiver (receiving/transmitting equipment) consists of the following major components, interrelated as shown in Figure 3-135: receiver, command data correlator, telemetry modulator, transmitter, interface buffers, and a signal acquisition, matched filter correlator.

The acquisition correlator permits rapid forward link signal acquisition and provides PN code timing to the command correlator, which maintains pattern and frequency lock after initial acquisition. The telemetry transmitter frequency may be phase locked to the received frequency for ranging but may also be allowed to run free during telemetry data transmission, enabling handover between TDRSs without interrupting data flow.

To operate with the TDRS system, a user spacecraft does not need to replace or modify its NASA ground station-compatible equipment, but must supplement it with the TDRS compatible transceiver and antennas. Two types of standard terminals (transceivers) are envisioned, one for low data rate users and one for medium data rate users. These terminals can be connected with a switch to the regular command decoder and telemetry encoder. The choice between the ground station or TDRSs operation could be made any time during the user's mission by a simple command of the switch setting. If the data and command rates for both modes of operation are different, an interface buffer unit will also be required as part of the transceiver package.

In addition to the standard transceiver, the low data rate users will probably require a UHF antenna. The VHF link to the TDRSs is compatible in frequency with the user to ground station link.

3.6.1 Transceiver Design

This subsection presents a brief discussion of the considerations which led to the baseline transceiver concept. The key functions which must be performed by the user receiver are signal acquisition, signal tracking, and data extraction. In maintaining minimum complexity in a spread spectrum receiver, the approach to signal acquisition must be given prime consideration.

In practice, the signal tracking and data extraction always share much of the same hardware, but the degree to which the signal acquisition hardware must be separate is strongly dependent on specific requirements for signal acquisition time, PN chip rate, doppler frequency, and received signal-to-noise ratio. An increase in any of these factors has the tendency to increase the likelihood of separate signal acquisition hardware and to increase the complexity of that hardware.

One of the first comparisons to be made is between the doppler frequency range and the permissible correlation bandwidth. At the user receiver the maximum doppler range is anticipated to be 24 kHz while the permissible correlation bandwidth is approximately 300 Hz. This frequency uncertainty ratio of 80 (24 kHz/300 Hz) infers a significant frequency search aspect to initial signal acquisition. This uncertainty is too great to consider an unaided phase locked loop, and therefore either a swept frequency or a parallel frequency filter approach will be required. As indicated later a swept frequency search technique has been chosen for the user receiver.

A second significant comparison to be made is between the PN chip duration and the maximum range of timing uncertainty. For signal acquisition purposes at the user receiver, the maximum range of timing uncertainty is equal to the PN pattern duration, and therefore this time uncertainty ratio for the baseline low data rate system is just equal to the PN code length of 2048.

A rough order of magnitude estimate of the median acquisition time for a simple serial search (single correlator sliding in time and frequency) approach is given by

$$T_a \approx U_f \times U_t \times T_i$$

where T_a is the acquisition time, U_f the frequency uncertainty ratio, U_t the time uncertainty ratio, and T_i the time of coherent integration. For the low data rate user receiver the coherent integration time is limited to a maximum of one data interval by the data modulation. For the baseline command bit rate this time is 1/300 second. If the received signal was not data modulated, signal energy to noise considerations would infer an optimum coherent integration time somewhat longer than one data interval. Then the preceding equation, the estimate of median acquisition time, with simple serial search, is approximately 9 minutes. Acquisition with a probability of 99.9 percent would require an order of magnitude more time, and thus the simple serial approach is clearly impractical. In fact, it is about two orders of magnitude too slow.

Since the simple serial search is too slow, three potential approaches of somewhat greater complexity need to be considered as follows: 1) use of multiple sliding correlators, 2) use of a single sliding correlator with multiple frequency filters, and 3) a single matched filter slowly swept in frequency.

In comparing these approaches the relative cost of implementation is a major factor. If only a few (perhaps 10 or less) sliding correlators or frequency filters were required to achieve the desired acquisition time then either of these techniques might be cost effective compared to a single matched filter at a code length of 2048. However, the number of parallel processing channels desired is on the order of 100 and thus the single matched filter is the most cost effective of these three approaches. For a 1 MHz bandwidth and relatively long time duration of 1/3 ms a digital implementation is the most practical.

As a result of the above considerations the primary candidate signal acquisition technique is a single matched filter with a slowly swept mixer frequency input. For a sweep speed that would cover the doppler uncertainty range (±12 kHz) once each second, the probability of acquisition is conservatively estimated at greater than 0.5. This in turn results in achieving 99.9 percent probability of acquisition in about 10 seconds or less.

Figure 3-136 illustrates with additional details the elements and design of the total transceiver with a digital matched filter in the acquisition correlator.

The acquisition correlator consists of two matched filter correlators driven by quadrature signals from the receiver. The signals, sampled at twice the chip rate, are continuously compared to a stored reference PN code pattern. The correlator outputs are squared and summed and the result admitted to a threshold detector. Signals that exceed the threshold are candidate correlation timing pulses which are supplied to the timing and control circuit for verification using the command correlator.

3.6.2 Operation

Upon receipt of a search command (a momentary signal) or upon loss of the receive signal for a period in excess of 1 second, the user transponder receiver will go into a signal acquisition sequence as follows:

1) A 2048 bit PN sequence is loaded into the acquisition correlator. This sequence is derived from the PN code generator and corresponds to the command PN code selected by the "Receive Code A/B" select signal. Also the frequency sweep (search ramp) control is set to its highest value.

2) Upon completion of the loading the receive PN generator is held at a predetermined state and the received signal is sent to the acquisition correlator. Also, the frequency sweep control is activated so as to cause an RF sweep rate of approximately 30 kHz/sec, and the voltage controlled crystal oscillator low pass filter is placed in the wideband mode.

3) When a potential signal match is detected, as indicated by an output from the acquisition correlator, the sweep control is locked in position and the receive PN generator is started. If the potential signal match is correct and not a false alarm, then the receiver PN code timing will match the received signal PN code in the data correlator. Whether or not correct time synchronization has been achieved is determined by the degree of signal integration ($|\int I_c|$).

4) If the signal integration is below a preset quality threshold, a false alarm is assumed and then the receiver returns to the search mode of step (2) with the frequency sweep picked up where it was halted. If no true signal match is obtained when the frequency sweep is completed, then the search process is started over again as in step (1).

5) When the data correlator output is above the preset threshold then a correct signal match, i.e., synchronization is assumed, and the final acquisition phase is started. At this point the voltage controlled crystal oscillator low pass filter is placed in the narrowband mode and the early-late tracking circuits are activated. If the signal match was correct, then these steps will serve to maximize the data output signal-to-noise ratio. As a final check on signal acquisition, the data integrations are continually checked against the preset quality threshold. An up-down counter is used to accumulate the number of times the quality threshold is exceeded minus the number of times it is not reached.

6) When the quality threshold is consistently being exceeded more than half the time the "signal acquired" output signal is turned on. For received signals at usable signal-to-noise ratios the quality monitoring circuits will hold the receiver locked onto the frequency and timing of the received signal.

For the implementation of Figure 3-136 the acquisition correlator gives the following performance when the bit energy-to-noise density, E_b/η at the receiver is 0 dB, which is 10 dB below the link design value:

Mean time to threshold (synchronous signal output)	0.1 second
Probability of correct acquisition	0.99
Probability of a false synchronization output	0.01

3.6.3 Physical Characteristics

Being spaceborne equipment, the weight and power of the user transceiver is of importance. Preliminary estimates of quantities are shown in Table 3-51.

TABLE 3-51. USER TRANSCEIVER EQUIPMENT

Item	Number	Mass, kg	Power, watts
LDR User			
Command receiver	2	2.0	1
Telemetry transmitter	2	4.0	20
Frequency synthesizer	2	2.0	1
Signal processor	2	1.0	3
Antennas	1 Set	2.0	-
Total		11.0	25
MDR User			
Command receiver	2	1.4	1
Telemetry transmitter	2	3.4	20
Frequency synthesizer	2	2.0	1
Signal processor	2	1.0	3
Antenna	1	1.4	-
Gimbal		4.2	-
Gimbal driver	2	1.8	6
Total		15.2	31

3.7 REFERENCES

1. Multipath Study for a Low Altitude Satellite Utilizing a Data Relay Satellite System, Hughes Aircraft Company Report for NASA, Contract No. NAS5-11602, January and August 1969.

2. J. Jenny, D. Gaushell, and P. Shaft, Communication Performance Over the TDRS Multipath/Interference Channel ESL Incorporated, TM239; 19 August 1971.

3. J. Jenny and P. Shaft, The Effects of Multipath and RFI on the TDRSS Command and Telemetry Links — A Final Report, Electromagnetic Systems Laboratories for NASA/GSFC under Contract NAS 5-20228, March 1972.

4. Y. S. Kuo, Test and Evaluation of a Universal Delta Modulator/Demodulator, Lockheed Electronics Company for NASA/GSFC under Contract 9-12200, April 1972.

5. J. N. Birch and N. R. Getzin, Voice Coding and Intelligibility Testing for a Satellite Based Air Traffic Control System, The Magnovox Company for NASA/GSFC under NAS 5-20168, April 1971.

6. S. J. Campanella and J. A. Sciulli, "A Comparison of Voice Communication Techniques for Aeronautical and Marine Applications," COMSAT Technical Review, Vol. 2, No. 1, Spring 1972, pp. 173-704.

7. J. N. Birch, Multipath/Modulation Study for the Tracking and Data Relay Satellite System, Magnavox Company Report for NASA, Contract No. NAS-10744, January 1970.

8. J. W. Hayland, "Information Systems: Performance of Short Constraint Length Convolutional Codes and a Heuristic Code — Construction Algorithm," JPL Space Programs Summary 37-64, Vol. II., pp. 41-44.

9. G. David Forney, Jr., "Coding and its Application in Space Communications," IEEE Spectrum, Vol. 7, No. 6, June 1970.

10. J. A. Jenny and S. J. Weiss, The Effects of Multipath and RFI on the Tracking and Data Relay Satellite System, ESL Incorporated, TM215; 18 March 1971.

11. Final Report for Multipath Modulation Study — Adaptive Techniques, Hekemian Laboratories Report for NASA, GSFC, Contract No. NAS5-10749, March 1970.

12. Parametric Analysis of RF Communications and Tracking Systems for Manned Space Stations, Hughes Aircraft Company under Contract NAS 9-10409 to NASA/MSC, January 1971.

13. E. J. Ferrari, Jr., Selection of Notch Filter Bandwidths for the Cascaded Dynamic Traps, Adcom Memorandum No. G-180-1 to Ralph Taylor of GSFC, 27 April 1971.

14. R. Gold and E. Kopitzke, Study of Correlation Properties of Binary Sequences, AD470697, August 1965.

15. Parametric Analysis of Microwave and Laser Systems for Communication and Tracking, Final Report, Vol. II, Hughes Aircraft Co. under NAS 5-9637 to NASA/GSFC.

16. R. J. Wescott, "Investigation of Multiple f.m./f.d.m. Carriers Through a Satellite TWT Operating Near to Saturation," Proc. IEE (London) 114, 726, June 1967.

17. B. J. Hunsinger, Spread Spectrum Communication Link Using Surface Ware Devices, The Magnavox Co. under NAS5-20198 to NASA/GSFC, November 1971.

APPENDIX A. MULTI-SATELLITE ORBIT DETERMINATION

User Ephemeris Accuracy

The graphs in Figures 1-3 present typical results for the orbit determination accuracy for a user satellite. For simplicity these curves illustrate the orbit uncertainties at their worst values over the user orbit. The user ephemeris accuracy is represented as a 3-dimensional uncertainty in radial, along track, and cross-track directions. Only during the indicated data taking intervals can improvement in the knowledge of the user orbital elements be obtained. Thereafter the ephemeris accuracy degrades due to modeling errors (e.g., earth's gravitational field uncertainties) and uncertainties in the user's orbital elements. This degradation has both periodic and secular variations. Thus, rather than plotting instantaneous fluctuations, Figures 1-3 plot the orbit uncertainties at their worst values over the orbit and connects points with straight lines.

The curves in these figures illustrate how only 10 minutes of data at the same point in each orbit, from a single TDRS, yields good user ephemeris accuracy. These conditions are meant to represent an upper bound on the obtainable accuracy. Nominally the user visibility will allow data to be gathered over much longer intervals, say 40 minutes or more, spaced at various points in the orbit. Furthermore, taking advantage of the geometry improvements afforded by visibility to both TDRS would permit ephemeris determination with greater accuracy than shown in Figures 1-3.

Modeling Error Effects

Modeling errors can also contribute to orbit determination accuracy. However, the usual sources of difficulty do not appear to be significant in this system. The major orbit perturbation is due to solar radiation pressure. Knowing the vehicle orientation, including the direction of the antenna, allows the gross effect of this perturbation to be removed. The fact that each TDRS is located at synchronous altitude also eliminates the need for modeling the sometimes troublesome effect of earth reflected solar radiation pressure. The net result is to eliminate the solar radiation pressure from having any significant effect upon the TDRS ephemeris accuracy between TDRS attitude updates.

A second contributor to degradation in orbit determination accuracy for some systems is the uncertainty introduced by net forces resulting from attitude control torquing required for TDRS antenna slewing. Though this contributor is a definite problem for any 3-axis type system the TDRS gyrostat configuration eliminates it from consideration. The gyrostat slews the antennas by working on the principle of conservation of momentum and not jet firings. Thus, net forces of this type are virtually nonexistent.

Another contributor to orbit determination accuracy is the attitude control of solar torque. The solar torque acts to precess the TDRS attitude in a specific direction away from the nominal value and will be corrected about every two days. By employing a deadband type approach the control torque overcorrects the attitude to one side of the deadband limits. The environmental solar torque then precesses the attitude back through the nominal value until the other limit is reached. Thereupon another correction may take place.

The TDRS orbit would be affected by any net forces resulting from the attitude control torquing, but the uncertainties introduced by these forces would not significantly affect orbit determination accuracy. Accurate estimates of the TDRS orbit can be obtained with 24 hours of tracking data. Since at least two full days will be available between attitude maneuvers any perturbations to the orbit would be determined with extreme accuracy. Of course, if a real time requirement exists, attitude maneuvers may be rescheduled to assure extremely accurate knowledge of the instantaneous TDRS ephemeris. Similar arguments also hold for east-west stationkeeping corrections which will take place at about 100 day intervals.

Special Geometry Factors

The accuracy of orbit determination depends on orbit geometry. The two most significant geometry factors affecting user satellite orbit determination accuracy are absolute inclination of the TDRSS orbits and the relative orientation of the user and TDRSS orbits, the latter being a problem only in the special situation where the user and TDRS orbit planes become coincident.

The first geometry factor occurs because as the TDRSS inclination approaches zero for the synchronous satellite it becomes considerably more difficult to track accurately from the ground. Figure 4 shows the results of a study for low TDRS inclinations as tracked from a single ground station.

At very low inclinations (below 0.1 degrees) tracking from a single ground station would not yield TDRS orbit determination accuracy better than 10 km in the cross track direction even for the smallest ranging errors. The problem arises for 24 hour circular orbits because the perturbations in ground station range data caused by a small change in orbital inclination has the same form as a slight change in eccentricity. Thus, they are indistinguishable and little improvement of the large a priori cross track error is obtained.

It has been observed that the situation could be improved if the TDRS was in a slightly elliptical orbit even though the period was 24 hours. Though small eccentricities are not considered in the TDRS orbital deployment the results are shown in Figure 5 for completeness. As seen in the figure, the coupling of non-zero eccentricity with continuous true anomaly change over the orbit allows the knowledge of orbital inclination to be improved significantly. Alternatively, if two ground stations could be used, the accuracy would be cut to 400 - 1200 meters depending upon the ground station locations[1]. A third ground station would further slice these uncertainties to about 200 meters. The same effect as the addition of a ground station may be obtained by using an inclined, low altitude user. The user would act, geometrically, like a second ground station and soon yield comparable accuracy. These results are shown quite graphically in the greatly improved user accuracies depicted in Figures 1-3. Of course, another solution would be to bias the TDRSS inclination so that the inclination over the mission lifetime would never be below some minimum value.

---

1 - J. L. Cooley, "Error Studies for Ground Tracking of Synchronous Satellites", January, 1972, GSFC report, X551-72-30

The second factor affecting orbit determination accuracy is the degradation of user accuracy as the user - TDRSS orbital planes become coincident. The inability to distinguish out of plane effects degrades the cross track error to unacceptable levels (Figures 6-8). This factor may be eliminated by maintaining an inertial separation between the orbital planes of the TDRS E and TDRS W. Thus the user will never be simultaneously within the same orbital plane of both relay satellites.

As seen in Figure 6, an adequate inertial separation between the orbital planes may be obtained even with both relay satellites at the same inclination provided their inertial nodes differ. The slight humps in the curve at low inclinations are cuased by a small displacement of the maximum user cross track error at the particular ephemeris time of comparison. The curves should be almost symmetric about the 3 degree inclination line though they would improve slightly due to the better TDRSE tracking accuracy at the higher inclination than 3 degrees. Assuming 3 degree inclination as an average value over the mission lifetime, Figure 7 shows that a difference of 10 degrees in TDRS E and TDRS W inertial nodes will ensure user ephemeris tracking accuracies below 0.5 km. Alternatively, Figure 8 shows that a combination of smaller inertial node differences along with inclination differences will yield the same effect.

Figure 1

POLAR USER RADIAL UNCERTAINTY

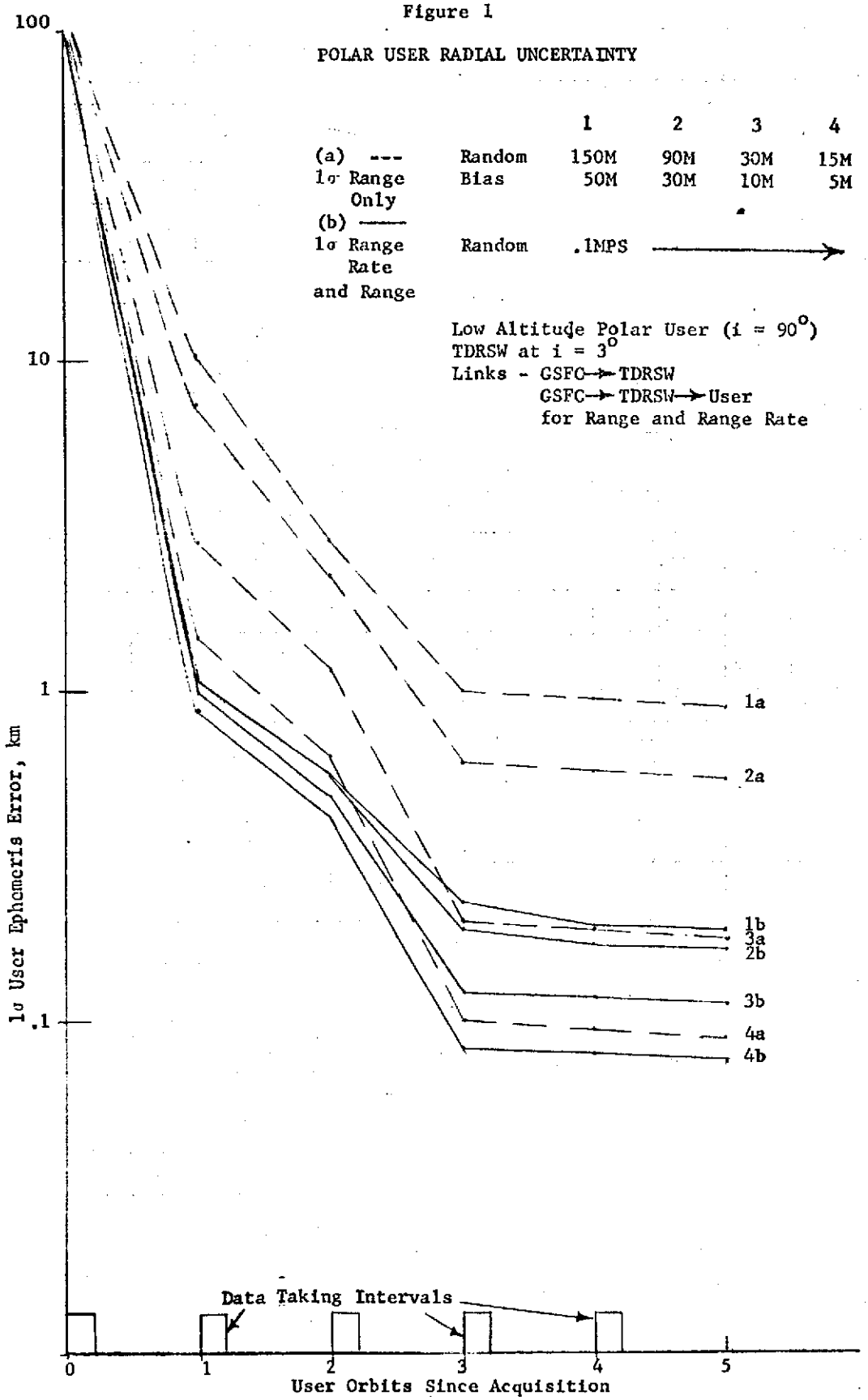

Figure 2

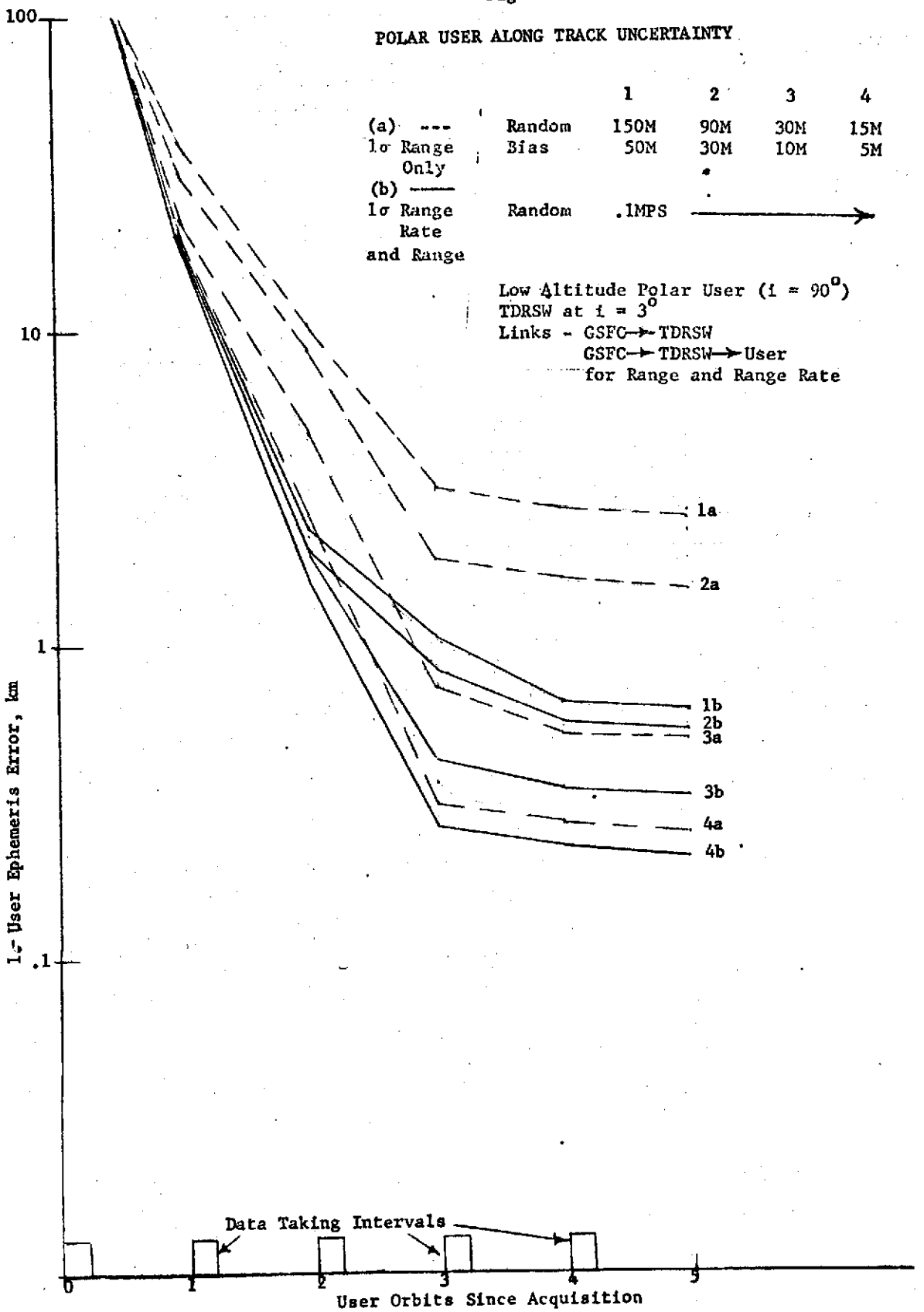
POLAR USER ALONG TRACK UNCERTAINTY
1 2 3 4
(a) --- 1σ Range Only
Random 150M 90M 30M 15M
Bias 50M 30M 10M 5M
(b) —— 1σ Range Rate and Range
Random .1MPS
Low Altitude Polar User (i = 90°)
TDRSW at i = 3°
Links - GSFC→TDRSW
GSFC→TDRSW→User
for Range and Range Rate
1a
2a
1b
2b
3a
3b
4a
4b
100
10
1
.1
1σ User Ephemeris Error, km
Data Taking Intervals
0
1
2
3
4
5
User Orbits Since Acquisition

Figure 3

POLAR USER CROSS TRACK UNCERTAINTY

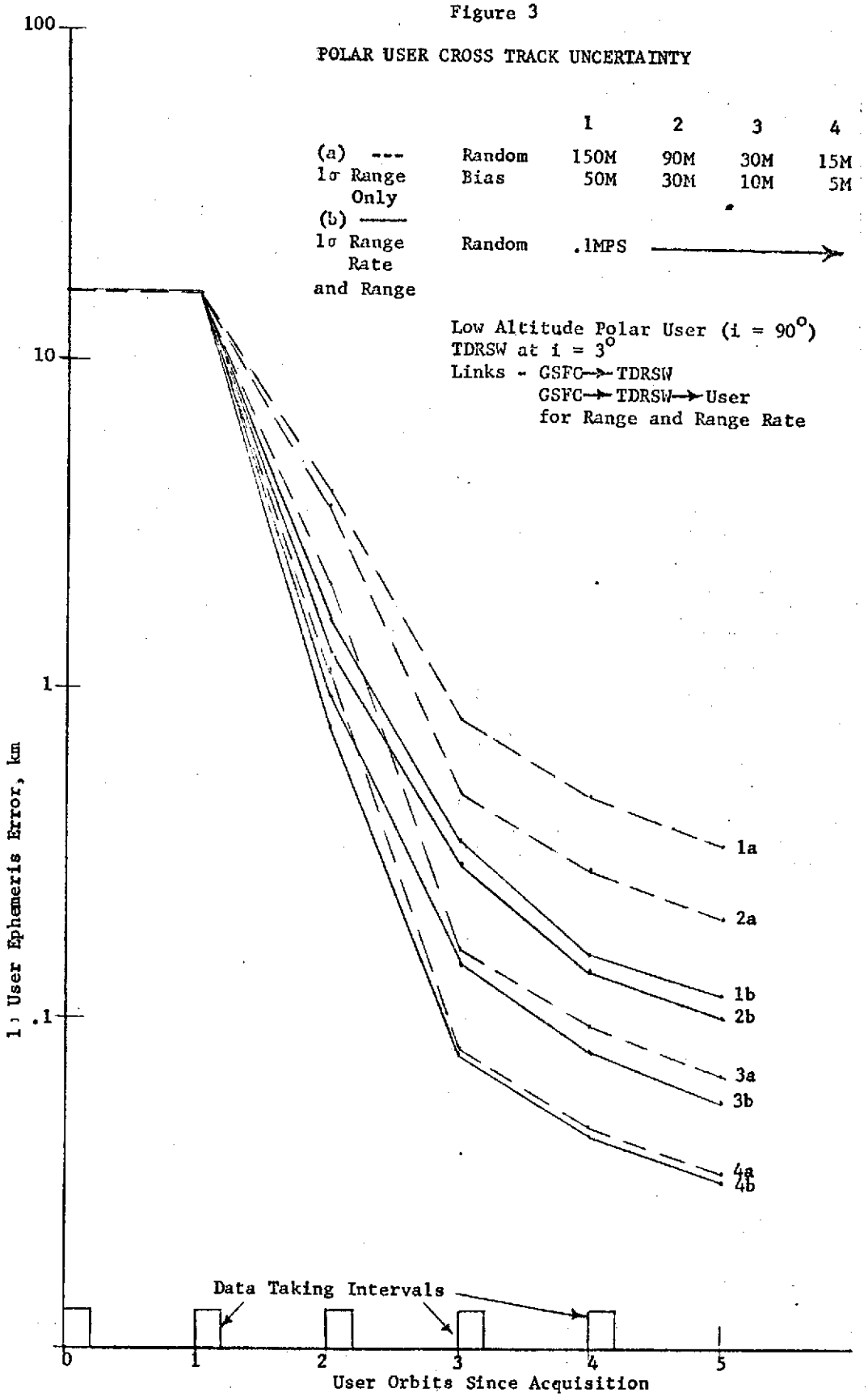

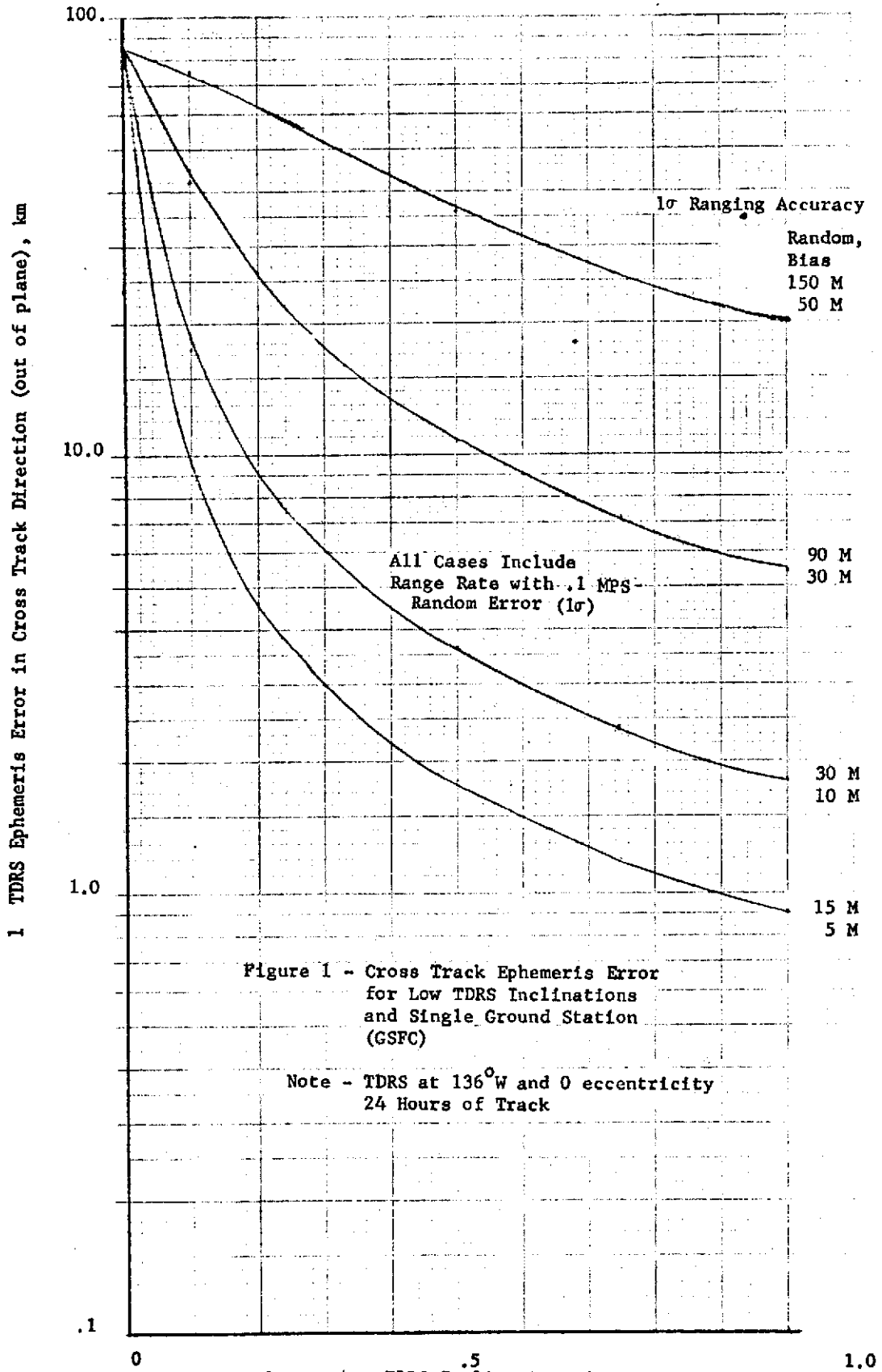

Figure 1 - Cross Track Ephemeris Error for Low TDRS Inclinations and Single Ground Station (GSFC)

Note - TDRS at 136°W and 0 eccentricity
24 Hours of Track

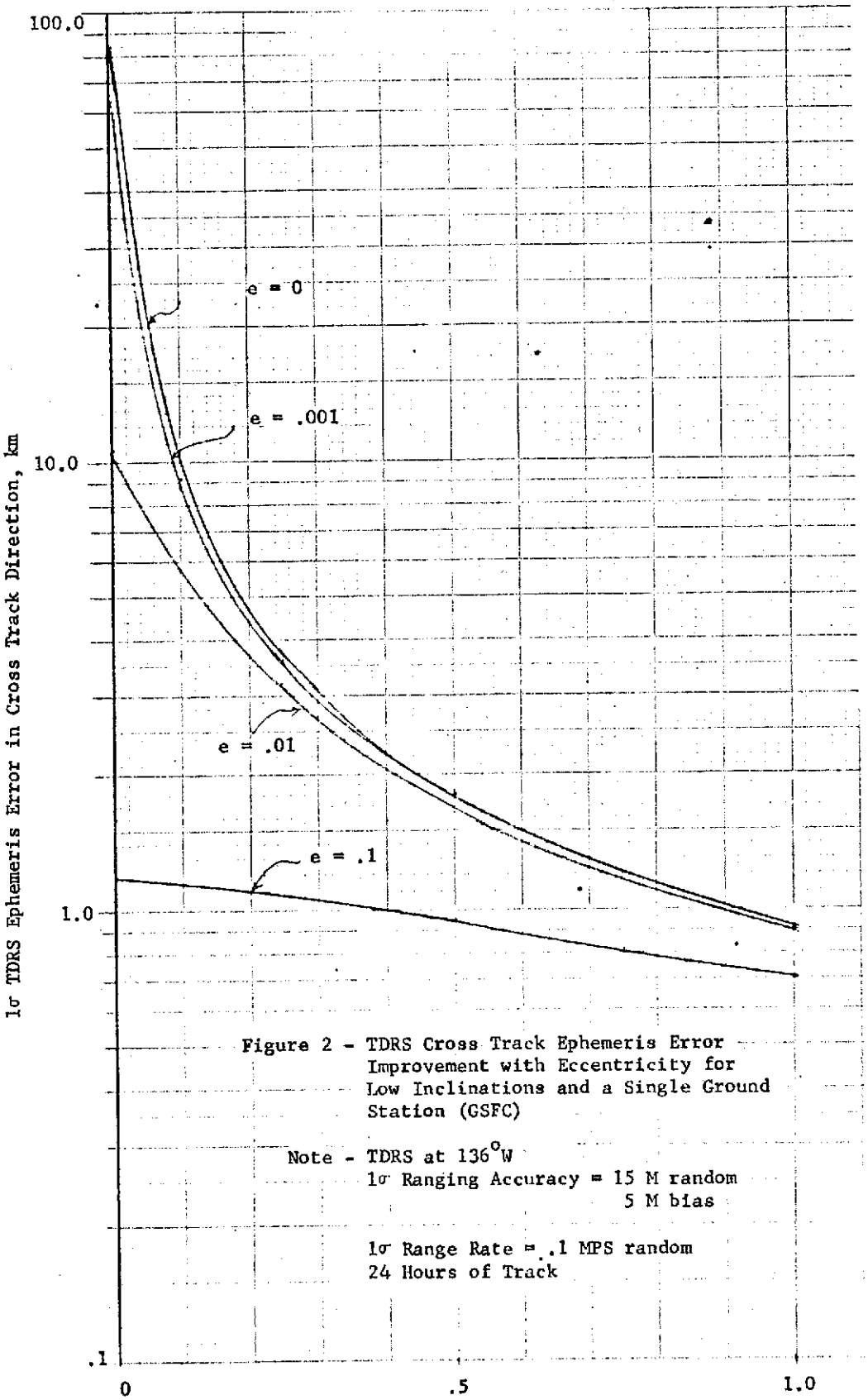

Figure 2 - TDRS Cross Track Ephemeris Error Improvement with Eccentricity for Low Inclinations and a Single Ground Station (GSFC)

Note - TDRS at 136°W
1σ Ranging Accuracy = 15 M random
5 M bias

1σ Range Rate = .1 MPS random
24 Hours of Track

Figure 5 - TDRS Inclination, deg.

Figure 6 - User Ephemeris Accuracy for
Very Nearly Coincident Orbit Planes Geometries

	Inclination	Ascending Mode	Location	Period	Eccentricity
User	3°	270°	90°W	2 hr.	0.
TDRSW	3°	270°	136°W	sync.	0.
TDRSE	Various	Various	18°W	sync.	0.

Note:
- All links include small a priori TDRS errors for normal system operation (<250 M)
- 1σ range = 15 M random, 5 M bias
- 1σ range rate = .1 MPS random
- Tracking for entire user orbit when visibility permits

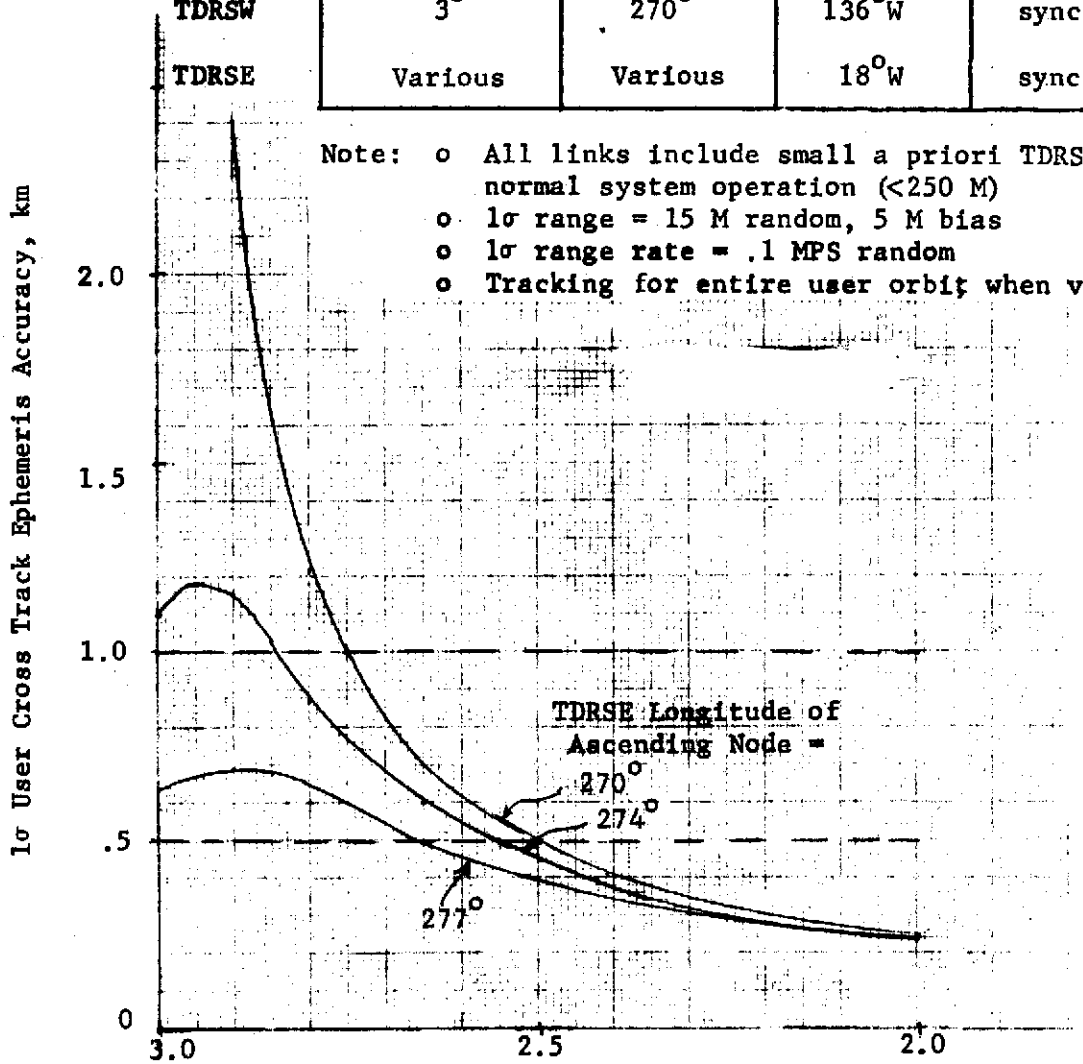

Figure 7 - User Ephemeris Accuracy for
Very Nearly Coincident Orbit Plane Geometries

	Inclination	Ascending Mode	Location	Period	Eccentricity
User	3°	270°	90°W	2 hr.	0.
TDRSW	3°	270°	136°W	sync.	0.
TDRSE	3°	Various	18°W	sync.	0.

Note:
- o All links include small a priori TDRS errors for normal system operation (<250 M)
- o 1σ range = 15 M random, 5 M bias
- o 1σ range rate = .1 MPS random
- o Tracking for entire user orbit when visibility permits

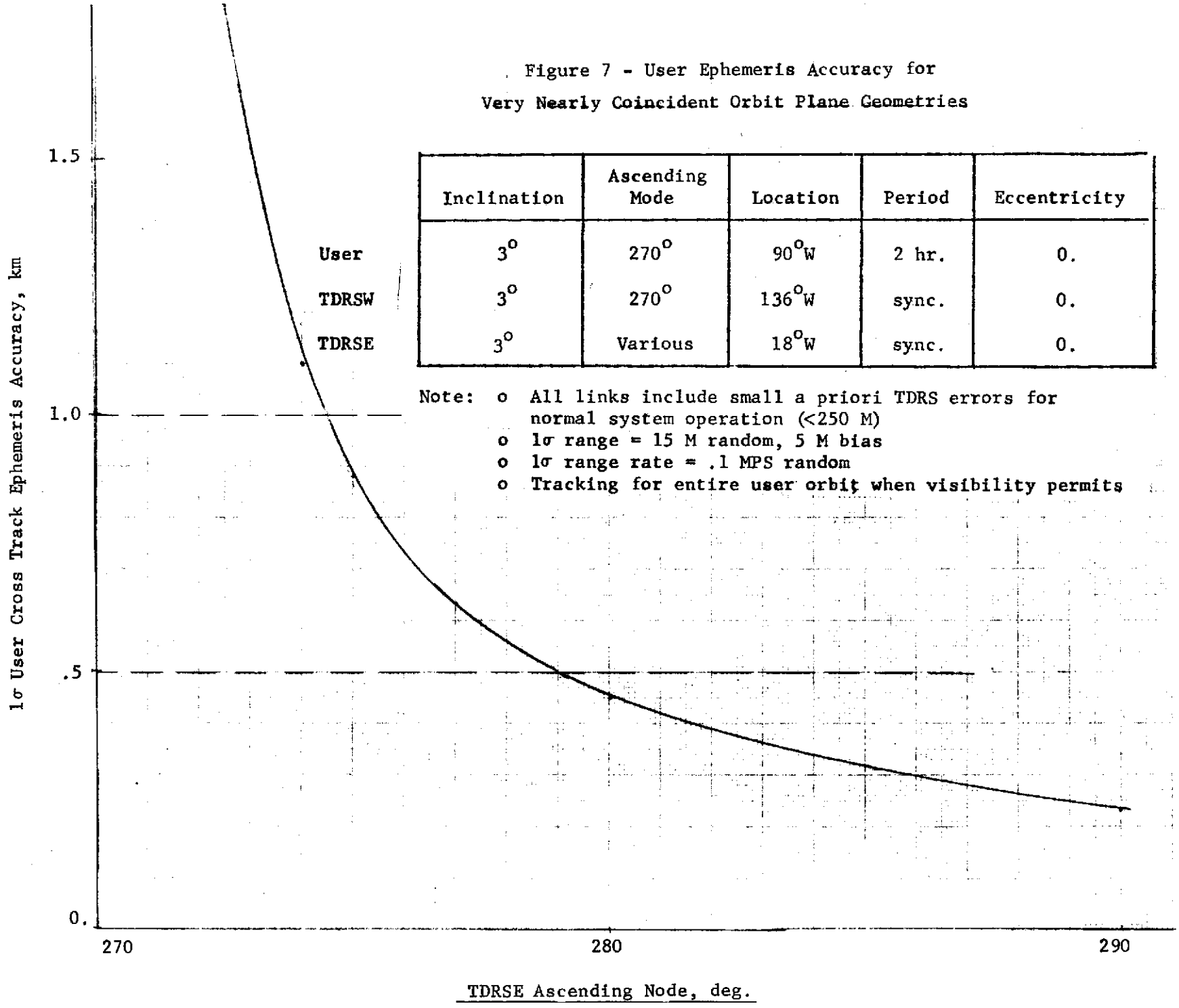

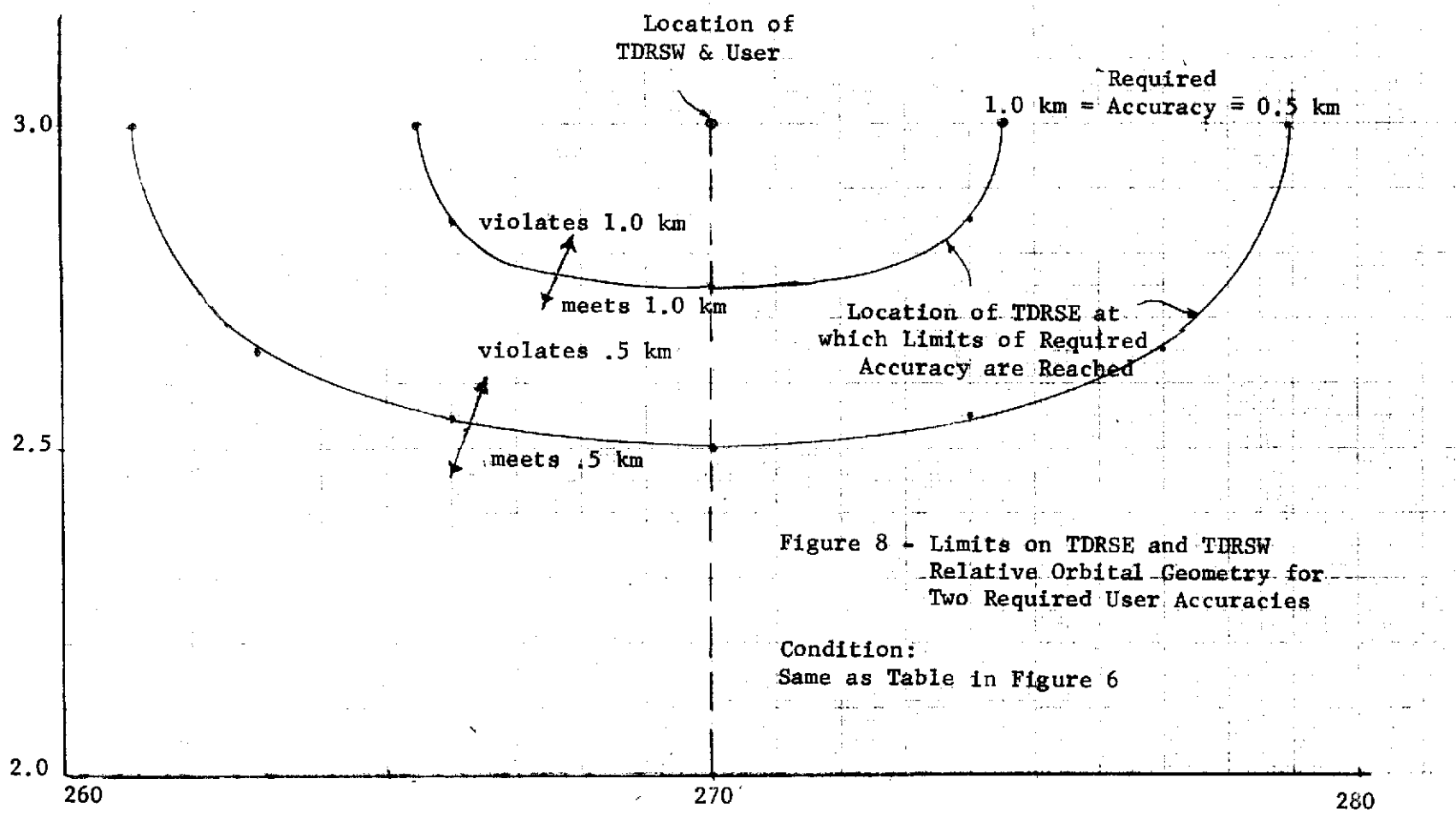

Figure 8 - Limits on TDRSE and TDRSW Relative Orbital Geometry for Two Required User Accuracies

Condition:
Same as Table in Figure 6

Figure 8 - TDRSE Ascending Node, deg

APPENDIX B. SURVEY OF ALGEBRAIC TECHNIQUES FOR SELECTING CODES WITH LOW CROSSCORRELATION

ABSTRACT

This appendix summarizes some of the more useful algebraic properties of linear feedback shift register sequences. The primary objective of the present study is the selection of codes for a code division multiple access system operating in a multipath environment. If the system can take advantage of full correlations (i.e., correlations over integral multiples of the period of the sequences involved), then the problem has essentially been solved (References 7, 8, 9, and 10) and the results are summarized in this appendix. If only partial correlations (correlations over non-integral multiples of the period of the sequences) are possible in the CDMA system, then the problem has not been solved. The only available method of arriving at the solution to the partial correlation problem seems to be through computer evaluation. A computer program to determine partial crosscorrelation has been developed and some limited results have been obtained. The partial correlation problem will be the subject of a future correspondence and will not be discussed in further detail here.

1. INTRODUCTION

One of the central problems in designing a code division multiple access (CDMA) system is the selection of codes with good cross-correlation properties. When the system must also overcome multipath interference then the codes must have good autocorrelation properties. Maximal length linear shift register sequences (often called PN codes) provide very good autocorrelation properties and, by a careful selection process, classes of sequences can be constructed which have good cross-correlation properties as well. The analysis and selection of such sequences is the subject of a study which is now in progress. By considering non-maximal length codes it is possible to find very large families of sequences with good cross-correlation properties if some of the autocorrelation properties are sacrificed. These non-maximal length sequences are derived, however, from maximal length sequences. Thus, the emphasis in the present study is on codes which are maximal length or are derived from maximal length sequences.

The mathematical study of maximal length shift register sequences seems to have started in the mid-1950's. About that time E. N. Gilbert, Neal Zierler, Solomon Golomb, and Lloyd Welch independently derived the theory of linear feedback shift register sequences which is summarized in this paper. However, almost twenty years of study have not answered many important questions concerning the properties of these sequences. Golomb, in his book [1] published in 1967, states that "far stronger regularities" (with respect to cross-correlation between two maximal length sequences) have been observed experimentally than are predicted by theory. Analytical techniques for choosing classes of maximal length sequences with good cross-correlation properties are still not perfected although some results have been obtained in recent years. The main purpose of this correspondence is to present some of these results and discuss methods by which codes may be selected for use in a CDMA system operating in a multipath environment.

2. INTRODUCTION TO THE THEORY OF MAXIMAL LENGTH SHIFT REGISTER SEQUENCES

For purposes of introducing notation and presenting certain results that will be needed in the analysis and construction of efficient codes for code division multiple access (CDMA) over multipath channels some basic properties of maximal length linear sequences (m-sequences) and their generators will be presented. Most of the material included in this section can be found in References [1], [2], and [3].

It is well known that a shift register with feedback can be used to generate certain classes of codes. For the present it will be assumed that the feedback is a linear function of the contents of the shift register memory elements. In particular for the general linear feedback shift register shown in Figure 1, the element $\sum_{i=1}^{n} C_i X_i$ is the next input to the 1st stage of the register where C_i is 0 or 1 depending on whether register i is connected to the adder or not, X_i denotes the present contents of the ith stage, and the indicated

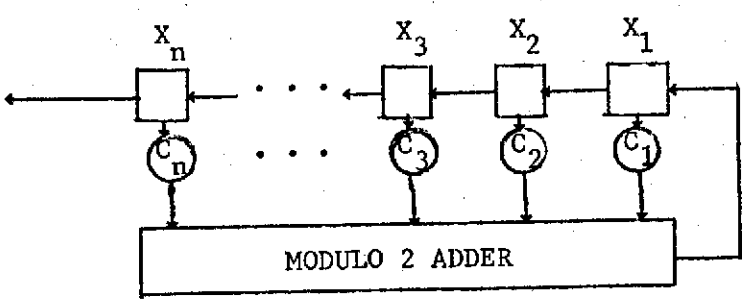

FIGURE 1. General Linear Feedback Shift Register

sums and products are taken modulo 2. Thus, the output sequence is completely determined by the initial conditions of the n registers (i.e., initial values of $X_1, X_2, \ldots, X_n$) and the feedback coefficients $C_1, C_2, \ldots, C_n$. If the initial content of the j^{th} register is denoted by a_{-j} then the sequence denoted (a_j) describing the history of the first stage after the first clock pulse will be $a_0, a_1, a_2, \ldots$ where a_j satisfies the linear recurrence relation

$$a_j = \sum_{i=1}^{n} C_i \, a_{j-i} \qquad \text{for } j=0, 1, 2, \ldots$$

and the sum is again modulo 2.

Regardless of the initial conditions, the sequence (a_j) will be periodic with period $p \leq 2^n-1$. In the special case where $p=2^n-1$ the resulting sequence (a_j) is known as a maximal length linear shift register sequence or simply an m-sequence. This special case is the case of interest for most applications and it is therefore necessary to consider the conditions under which the sequence will be of maximal length. For purposes of the following discussion it is assumed that the initial conditions are given by $a_j=0$ for $j=-1, -2, \ldots, 1-n$ and $a_{-n}=1$ unless otherwise noted. The characteristic polynomial of the sequence (a_j) (and of the shift register that generated it) is given by

$$f(x) = 1 + \sum_{i=1}^{n} C_i \, x^i$$

where all operations are performed modulo 2. This equation specifies completely the properties of the sequence (a_j) for any specified initial conditions.

A polynomial f(x) is said to divide a polynomial g(x), denoted f(x)|g(x), if there exists a polynomial h(x) of degree not less than 1 such that g(x)=f(x)h(A polynomial f(x) of degree n is said to be irreducible if there does not exist a polynomial g(x) of degree not less than 1 and not greater than n such that g(x)|f(x). In order to determine the requirements on maximal length sequence generators several theorems are needed which deal with the characteristic polynomial f(x) for the n-stage linear feedback shift register. Proofs of these theorems are given in [1] or [2].

The first of the theorems gives a necessary (but not sufficient) condition for a shift register sequence to be of maximal length for any set of initial conditions:

THEOREM: If (a_j) is a maximal length linear recurring sequence, its associated characteristic polynomial f(x) is irreducible.

In general, however, f(x) may not be irreducible (i.e., f(x) may factor as a product of irreducible polynomials). The following theorem gives the period of the corresponding sequence:

THEOREM: For the stated initial conditions, the sequence (a_j) from an n-stage linear feedback shift register will have period p if p is the smallest positive integer for which the characteristic polynomial f(x) associated with the sequence divides the polynomial $1-x^p$.

The next theorem gives a sufficient condition for a polynomial f(x) to correspond to a maximal linear shift register sequence.

THEOREM: If f(x) is an irreducible polynomial of degree n then the period p of its associated linear recurring sequence divides 2^n-1. Thus, if 2^n-1 is prime, every irreducible polynmial of degree n corresponds to a maximal length linear recurring sequence.

Note that this does not say that if 2^n-1 is not prime that a given irreducible polynomial does not correspond to a maximal length sequence. The case when 2^n-1 is prime is an important special case, however. If 2^n-1 is prime it is called a Mersenne prime. It will be seen later that m-sequences generated by n-stage linear feedback shift registers where 2^n-1 is a Mersenne prime will have certain desirable cross-correlation properties.

For our purposes, two sequences (a_j) and (b_j) are the same if they are generated by the same characteristic polynomial, since in this case one of the sequences is merely a shift of the other (i.e., for some fixed integer k, $a_j = b_{j+k}$ for j=0, 1, 2, ...). Two sequences which are not generated by the same characteristic polynomial are call distinct in the followimg discussion. Two functions which are important in number theory and combinatorial analysis are the Euler ϕ-function[1] and the Möbius μ-function[4]. The first of these is defined by

$$\phi(n) = \begin{cases} 1 & \text{if } n=1 \\ \prod_{i=1}^{k} p_i^{\alpha_i - 1}(p_i - 1) & \text{if } n>1 \end{cases}$$

where for n>1, n is a unique product of powers of k distinct prime numbers p_i so $n = \prod_{i=1}^{k} p_i^{\alpha_i}$ for some set of $\alpha_i \geq 1$ for i = 1, 2, ..., k. The Möbius function is defined by

$$\mu(n) = \begin{cases} 1 & \text{if } n=1 \\ 0 & \text{if } \prod_{i=1}^{k} \alpha_i > 1 \\ (-1)^k & \text{otherwise} \end{cases}$$

The fact that there are $\phi(n)$ numbers from 1 to n which are relatively prime to n is often used to define the Euler ϕ-function.

The following theorem gives the number of different irreducible polynomials of degree n and the number of polynomials of degree n which correspond to m-sequences of length p in terms of these two functions, where $p=2^n-1$.

THEOREM: The number of irreducible polynomials of degree n is $\psi(n)$ where

$$\psi(n) = \frac{1}{n} \sum_{d/n} 2^d \mu\left(\frac{n}{\alpha}\right)$$

and the number of irreducible polynomials corresponding to maximal length linear shift register sequences is $\lambda(n)$ where

$$\lambda(n) = \frac{1}{n}\,\phi(2^n-1)$$

In the important special case when 2^n-1 is prime

$$\psi(n) = \lambda(n) = \frac{2^n-2}{n}$$

Thus, if 2^n-1 is a Mersenne prime, all irreducible polynomials of degree n correspond to maximal length linear shift register sequences. If 2^n-1 is not prime then some of the irreducible polynomials will not generate maximal length sequences.

As an example, m-sequences of length 127 (which are of interest for further investigations) are generated by 7-stage linear feedback shift registers corresponding to some irreducible polynomial of degree 7. Since $2^7-1=127$ is a Mersenne prime then any irreducible polynomial of degree 7 will correspond to a sequence with period p=127. Since $\psi(7) = \lambda(7) = \frac{2^7-2}{7} = 18$ then there are 18 distinct sequences of period 127. It should be emphasized that for the present application, all sequences with the same characteristic polynomial are identical as was previously discussed.

3. AUTOCORRELATION PROPERTIES OF A MAXIMAL LENGTH SHIFT REGISTER SEQUENCE

The reason that maximal length shift register sequences are useful in communications systems is that they have certain properties often referred to as "randomness properties". Of course, there is nothing at all random about such a sequence since it is completely specified by its characteristic polynomial and initial conditions (i.e., the feedback tap connections and initial register contents). However, some of the characteristics of these sequences make them seem as though they were random in some sense and consequently, maximal length sequences are often called pseudo random (PR) or pseudo noise (PN) sequences.

The so-called randomness properties of a maximal length sequence are essentially that the difference between the number of ones and the number of zeros in any period of the sequence is one, every possible binary word of length n except the all zero word occurs exactly once per code period, and if the sequence is compared with a shift of itself then in any 2^n-1 consecutive positions, the number of positions in which the two have the same element will be one less than the number of positions in which they differ. These properties can be stated more explicitly as follows:

THEOREM: If (a_j) is a maximal length sequence from an n-stage linear feedback shift register then

1. $\sum_{j=k}^{k+2^n-1} a_j = 2^{n-1}-1$ for k=0, 1, 2, ...

2. In any 2^n+n-2 consecutive elements of (a_j) the binary word representing each of the integers 1, 2, 3, ..., 2^n-1 appears exactly once

3. The autocorrelation function $C(\tau) = \frac{1}{2^n-1} \sum_{j=1}^{2^n-1} (-1)^{a_j \oplus a_{j+\tau}}$

satisfies

$$C(\tau) = \begin{cases} 1 & \text{if } \tau=0 \\ -\frac{1}{2^n-1} & \text{if } \tau = 1, 2, 3, \ldots, 2^n-2 \end{cases}$$

The proof of this theorem is given in [1]. The primary reason that these sequences are used in synchronization, ranging, anti-multipath, and many other applications is due to property 3 above.

The autocorrelation function has many equivalent representations including the following two, which appear frequently in the literature:

1. $C(\tau) = \frac{A(a,a^\tau) - D(a,a^\tau)}{A(a,a^\tau) + D(a,a^\tau)}$

   where $A(a,a^\tau)$ is the number of positions in which the codes a and a^τ agree over a period

   $D(a,a^\tau)$ is the number of positions in which the codes a and a^τ disagree over a period

   and $a = (a_j)$, $a^\tau = (a_{j+\tau})$

2. Consider the (isomorphic) mapping $T: \alpha \longmapsto (-1)^\alpha$ which maps the group consisting of $I_2=\{0,1\}$ under addition modulo 2 onto the group consisting of $G=\{+1, -1\}$ such that the group operation is denoted $\cdot$ and obeys the group operation table

$\cdot$	1	-1
1	1	-1
-1	-1	1

Since the mapping preserves operations then in particular if $\alpha, \beta \in I_2$ then $T(\alpha \oplus \beta) = T(\alpha) \cdot T(\beta)$ where $T(\alpha), T(\beta) \in G$. Therefore,

$$C(\tau) = \frac{1}{2^n-1} \sum_{j=1}^{2^n-1} T(a_j \oplus a_{j+\tau}) = \frac{1}{2^n-1} \sum_{j=1}^{2^n-1} T(a_j) \cdot T(a_{j+\tau}$$

Thus, in the sequence (a_j) if 0's are replaced by 1's and 1's are replaced by -1's (in general, a_j is replaced by $\alpha_j = (-1)^{a_j}$) then we get the equivalent expression for the autocorrelation function of a maximal length sequence

$$C(\tau) = \frac{1}{2^n-1} \sum_{j=1}^{2^n-1} \alpha_j \cdot \alpha_{j+\tau} \qquad \tau = 0, 1, \ldots, 2^n-1$$

The reason for introducing this representation is that the actual transmitted waveform is usually a sequence of positive and negative rectangular pulses rather than binary 1's and 0's. Consequently, in communication systems the representation indicated above is often more natural. Since the two are equivalent (in the sense that they are isomorphic) the all of the algebraic structure is preserved in going from one representation to the other. In many applications it is more convenient to use the unnormalized autocorrelation function

$$\theta(\tau) = \sum_{j=1}^{2^n-1} (-1)^{a_j \oplus a_{j+\tau}} = \sum_{j=1}^{2^n-1} \alpha_j \cdot \alpha_{j+\tau}$$

For a maximal length sequence

$$\theta(\tau) = \begin{cases} 2^n-1 & \text{for } \tau=0 \\ -1 & \tau=1,2,\ldots, 2^n-1 \end{cases} .$$

4. MATHEMATICAL STRUCTURE OF MAXIMAL LENGTH SEQUENCES

In order to select codes for code division multiple access (CDMA) systems it is necessary to find classes of codes that in some sense "look different" from each other. In a more precise mathematical sense this amounts to choosing a class of sequences such that any two sequences in the class have a uniformly small cross-correlation function. In particular, sequences which are merely time shifts of each other are not suitable for most CDMA applications. The purpose of this section is to present a method of forming classes of sequences whereby all sequences in a class are identical except for starting point. This method is outlined in the following paragraphs for the case of prime period. Let $p=2^n-1$ be prime. The $\phi(p) = p-1$ integers from 1 to p-1 form a group under multiplication modulo p. The set of integers $C_1=\{2^k | k=0,1,\ldots, n-1\}$ forms a subgroup and cosets can be formed relative to this subgroup. That is, if ℓ is a positive integer not greater than p such that $\ell \notin C_1$ then

$$C_2 = \{\ell \cdot m \bmod p \mid m \in C_1\}$$

is a coset of the subgroup C_1 with coset leader ℓ. The process is continued by choosing an element not in the subgroup nor any of the previous cosets and forming a coset with that element as a coset leader. In general, the process terminates when all of the elements are in the subgroup or in a coset. The number of cosets including C_1 is $\phi(p)/n$. The usefulness of this coset decomposition stems from the following theorem:

THEOREM: Let (a_j) be a maximal length sequence of period $p=2^{n-1}$ where p is prime. Then the sequence (a_{mj}) is the same as the sequence (a_{kj}) except for starting point if m and k are in the same coset.

Assuming p is prime, all of the irreducible polynomials of degree n (where $p=2^{n-1}$) correspond to characteristic polynomials of maximal length sequences of period p. If $p=2^{n-1}$ is prime then there is a one-to-one correspondence between the cosets previously mentioned and the irreducible polynomials of degree n. This correspondence is established by considering polynomials modulo M(x) where M(x) is an irreducible polynomial of degree n. A detailed discussion of the theory of the algebra of polynomials modulo M(x) requires more algebraic background than has been developed here (see [3], [5], or [6]) so only the results will be presented. If α is a primitive element of the Galois field $GF(2^n)$ such that M(x) is the minimal polynomial of α then α^m and α^k are roots of the same characteristic polynomial if m and k are in the same coset. Thus, all of the elements in a coset correspond to roots of the same irreducible polynomial and therefore elements within a coset correspond to shifts of the same maximal length sequence.

For example for n=3, $p=2^n-1=7$ is prime. The set of integers $\{1,2,\ldots,7\}$ is a group under multiplication mod 7 with subgroup $C_1=\{1,2,4\}$ and only one cose $C_2=\{3,6,5\}$. Thus, letting $M(x)=x^3+x+1$ have root α then α^1, α^2, and α^4 are all roots of x^3+x+1 which is irreducible while α^3, α^6, and α^5 are roots of the only other irreducible polynomial of degree 3 which is x^3+x^2+1. Each maximal length sequence of period 7 has one of these two sequences as characteristic polynomial. If (a_j) is a maximal length sequence with period 7 then (a_j), (a_{2j}) and (a_{4j}) are the same sequence except for starting point. Similarly the three sequences (a_{3j}), (a_{6j}) and (a_{5j}) are the same except for starting point. Thus, for period p=7 only two different sequences are available.

In general for p prime, $\frac{p-1}{n}$ different sequences are available and for a proper choice of q any sequence can be generated from a given maximal length

sequences (a_j) by taking every q^{th} symbol and therefore forming (a_{qj}). In the n=3 example, the sequence corresponding to irreducible polynomial x^3+x+1 is ...10011101001110... The same sequence is obtained by taking every second symbol (q=2) which is ...10100111010011 1... By taking every third symbol (q=3), however, the only other maximal sequence of period 7 is obtained which is

...11001011100101...

Note that this latter sequence is just the original sequence "running in reverse". This corresponds to the fact that the multiplicative inverse of 3 mod 7 is 5 which is in the same coset as 1. Thus, $(\alpha^3)^{-1}=\alpha^5$ and the minimal polynomial of α^3 is x^3+x^2+1 while the minimal polynomial of α^5 is the same as the minimal polynomial of α.

If p is not prime, the situation is somewhat different. For example the cosets will not all contain the same number of elements. Furthermore, not all irreducible polynomials will correspond to maximal length sequences. For arbitrary positive integers p, it is the primitive polynomials which are characteristic polynomials of maximal length sequences. A polynomial g(x) of degree n is primitive when g(x) divides x^m-1 for $m=2^n-1$ but g(x) does not divide x^m-1 for any integer m less than 2^n-1. The number of different primitive polynomials of degree n is $\frac{1}{n}\phi(2^n-1)$, hence the number of different maximal length sequences of period $p=2^n-1$ is $\frac{1}{n}\phi(2^n-1)$. When 2^n-1 is prime then a polynomial is primitive if and only if it is irreducible. However, when 2^n-1 is not prime there will be many more irreducible polynomials of degree n than primitive polynomials of degree n. For the case n=13, for example, only 144 of the 335 irreducible polynomials are primitive.

C4

5. CROSS-CORRELATION PROPERTIES OF MAXIMAL LENGTH SHIFT REGISTER SEQUENCES

The coset decomposition procedure presented in the previous section is useful in determining classes of sequences which have good cross-correlation properties. As was previously discussed, each coset corresponds to a characteristic polynomial of a maximal length sequence. In general, the cross-correlation between any two different maximal length sequences can be very large which in a CDMA system can result in a significant decrease in performance and perhaps loss of synchronization. Thus, it is desirable to find families of maximal length sequences having low cross-correlation between any two sequences in the family.

The construction of such families, called maximal connected sets of sequences, has largely been a computational process in the past. Some results have been obtained algebraically, however, such as the following theorem:

> THEOREM (Gold, [7]) Let α be any primitive element of $GF(2^n)$. If f_1 is the minimal polynomial of α and f_t is the minimal polynomial of α^t where $t = 2^{(n+1)/2}+1$ for n odd or $t = 2^{(n+2)/2}+1$ for n even then any sequence generated by f_1 and any sequence generated by f_t will have cross-correlation $\theta(\tau)$ satisfying $|\theta(\tau)| \leq t$ for all shifts τ.

Any two primitive polynomials obtained in this manner are said to form a preferred pair of primitive polynomials. Gold [8,9] has experimentally determined that for all $n \leq 13$ the sequences generated by the polynomials f_1 and f_t have the three-valued cross-correlation function. (The three values are -1, $-2^{(n+1)/2}-1$, and $2^{(n+1)/2}-1$ for n odd and -1, $-2^{(n+2)/2}-1$, and $2^{(n+2)/2}-1$ for n even.) Other cases which lead to the three-valued cross-correlation are summarized by Niho ([10]). It should be emphasized that the term preferred pair is restricted to primitive polynomials. For $n \not\equiv 0 \bmod 4$, the polynomial f_t will be primitive and therefore the theorem will give a pair of maximal length sequences.

Gold and Kopitzke [9] experimentally determined the maximal connected sets for $n \leq 13$. Recall that any two polynomials from the same maximal connected set will have the bounded, three-valued cross-correlation function as was previously discussed. Unfortunately, the number of polynomials in these sets is rather small. For $n \leq 13$ the maximal connected sets have at most six polynomials which occurs for $n = 7$. For $n = 6$ and 9 there are only two polynomials in a maximal connected set and for $n = 8$ and $n = 12$ there are no three-valued cross-correlation functions. (Recall that for $n \equiv 0 \bmod 4$ the theorem does not guarantee the existence of a preferred pair of primitive polynomials.)

The example for $n = 7$ will illustrate the method of finding preferred pairs of primitive polynomials. Let α be a primitive element of $GF(2^7)$. If f_1 is the minimal polynomial of α then by the theorem, for $t = 17$, $\{f_t, f_1\}$ is a preferred pair of primitive polynomials since $7 \not\equiv 0 \bmod 4$. Using the tables of irreducible polynomials published by Peterson and Weldon [3] we can find

the polynomials f_1 and f_t and the corresponding feedback shift register tap connections. The exponent 17 does not appear in this table, but since $17(2^3) = 136 \equiv 9 \pmod{127}$ then 17 is in the same coset as 9. The exponent 9 does appear and has corresponding primitive polynomial $f_9(x) = x^7+x^5+x^4+x^3+x^2+x+1$ and the original polynomial is $f_1(x) = x^7 + x + 1$. The sequences generated by the shift registers with tap connections 1011111 and 1000001 will then be maximal length and have the bounded three-valued cross-correlation function.

6. NON-MAXIMAL LENGTH SEQUENCES WITH GOOD CROSS-CORRELATION

As was discussed in the previous section, there exist classes of codes of length $p = 2^n-1$ having cross-correlation function $\theta(\tau)$ bounded in magnitude by $2^{(n+1)/2}+1$ for n odd and by $2^{(n+2)/2}+1$ for n even as long as $n \not\equiv 0 \bmod 4$ (i.e., all positive n except n=4, 8, 12, 16, ...). For example, there are no such classes of codes of length $p = 2^8-1 = 255$ or $p = 2^{12}-1 = 4095$. As was mentioned, the size of these classes is small for values of n of interest. It is therefore desirable for CDMA applications to consider other classes of codes which have good cross-correlation properties.

Gold [7] discovered large classes of codes having cross-correlation satisfying the same bound as given previously for the maximal connected sets. These codes (called Gold codes) are not maximal length and therefore do not have the two-valued autocorrelation function that maximal length sequences have. The out-of-phase autocorrelation for the Gold codes does, however, satisfy the same bound as the cross-correlation. Gold's result is summarized in the following theorem:

> THEOREM (Gold, [7]): Let f_1 and f_t be a preferred pair of primitive polynomials of degree n (as defined in the previous section). The shift register corresponding to the product polynomial $f_1 f_t$ will generate 2^n+1 different sequences each having period 2^n-1. Any pair of such sequences has cross-correlation function bounded in magnitude by $2^{(n+1)/2}+1$ for n odd and by $2^{(n+2)/2}+1$ for n even ($n \not\equiv 0 \bmod 4$).

The generation of the 2^n+1 different sequences is accomplished by properly selecting 2^n+1 different binary words of length 2n as initial conditions for the shift register. Note that subsets of binary words of length 2n can be formed such that any two words in the same subset when used as initial conditions will

produce the same sequence. There will be 2^n-1 different words in each subset corresponding to the 2^n-1 different words of length 2n in any sequence of period 2^n-1 that is generated by a shift register of length 2n. Two words taken from different subsets will produce two different sequences of period 2^n-1. Since the total number of binary words of length 2n is $2^{2n}-1$ (excluding the all zeros word) then there are a total of $2^{2n}-1$ different initial conditions. Thus, there are a total of $\frac{2^{2n}-1}{2^n-1} = 2^n+1$ different sequences that can be generated by the shift register corresponding to the polynomial $f_1 f_t$.

SUMMARY

Maximal length shift register sequences exist with period $p=2^n-1$ for all positive integers n where n is the number of registers required in the linear feedback shift register which generates the sequence. Those sets of sequences which are merely shifts of each other are not useful in CDMA applications unless extremely precise time synchronization is maintained (which is not usually the case). The number of different maximal length sequences (i.e., not merely time shifts of each other) of period $p = 2^n-1$ is $\frac{1}{n}\phi(2^n-1)$ where ϕ is Euler's ϕ-function defined by the property that $\phi(k)$ is the number of positive integers less than k which are relatively prime to k. Of these $\frac{1}{n}\phi(2^n-1)$ different maximal length sequences, however, only a small subset can be selected which have good cross-correlation. These subsets, when they exist, have the property that any two sequences in the subset have a three-valued cross-correlation function bounded in magnitude by $2^{\frac{n+1}{2}}+1$ for n odd and by $2^{\frac{n+2}{2}}+1$ for n even. A list of the number of maximal length sequences in these subsets (called maximal connected sets) is given in Table 1 for $5 \leq n \leq 13$.

Larger classes of codes exist, called Gold codes, which have good cross-correlation properties but are not maximal length and therefore do not have the good autocorrelation properties possessed by codes in the maximal connected sets. Gold codes exist for all period $p=2^n-1$ having non-empty maximal connected sets. In particular, Gold codes do not exist for $p = 255$ or $p = 4095$ as indicated in Table 2.

TABLE 1. Size of Maximal Connected Sets

n	p	Size of Set (Number of Sequences)	Bound on Unnormalized Cross-Correlation
5	31	3	9
6	63	2	17
7	127	6	17
8	255	0	--
9	511	2	33
10	1023	3	65
11	2047	4	65
12	4095	0	--
13	8191	4	129

TABLE 2. Gold Codes

n	p	Number of Codes	Bound on Unnormalized Cross-Correlation
5	31	33	9
6	63	65	17
7	127	129	17
8	255	0	-
9	511	513	33
10	1023	1025	65
11	2047	2049	65
12	4095	0	-
13	8191	8193	129

REFERENCES

[1] Solomon W. Golomb, Shift Register Sequences, Holden-Day, 1967.

[2] Neal Zierler, "Linear Recurring Sequences," J. Soc. Indust. Appl. Math., Vol. 7, No. 1, March, 1959.

[3] W. Wesley Peterson and E. J. Weldon, Jr., Error Correcting Codes, Second Edition, M.I.T. Press, 1972.

[4] Marshall Hall, Jr., Combinatorial Theory, Blaisdell Publishing Company, 1967.

[5] Elwyn R. Berlekamp, Algebraic Coding Theory, McGraw-Hill, 1968.

[6] Shu Lin, Introduction to Error-Correcting Codes, Prentice-Hall, 1970.

[7] Robert Gold, "Optimal Binary Sequences for Spread Spectrum Multiplexing," IEEE Transactions on Information Theory, Vol. 13, No. 4, October 1967, pp. 619-621.

[8] Robert Gold, "Study of Correlation Properties of Binary Sequences," Technical Report AFAL-TR-66-234, Air Force Avionics Laboratory, August 1966. (AD 488 858)

[9] Robert Gold and Edmund Kopitzke, "Study of Correlation Properties of Binary Sequences," Interim Technical Report, Number 1, Contract No. AF33(615)2595, Air Force Avionics Laboratory, August 1965.

[10] Yoji Niho, "Multi-Valued Cross-Correlation Functions between Two Maximal Linear Recursive Sequences," University of Southern California Report USCEE 409, January 1972.

APPENDIX C. RECEIVER PERFORMANCE ANALYSIS FOR CODE DIVISION MULTIPLE ACCESS SYSTEM

ABSTRACT

This appendix is concerned with the analysis of the performance of correlation receivers for a code division multiple access system. The signal-to-noise ratio at the output of the receiver is determined in terms of the partial crosscorrelation functions for the codes used in the system.

INTRODUCTION

The analytical model for the correlation receiver is shown in Figure 1. In general the received signal consists of K code division multiplexed signals corrupted by additive white Gaussian noise n(t) which has two-sided spectral density $N_o/2$ watts/Hz. That is,

$$r(t) = \sum_{i=1}^{K} \sqrt{2P}\, a_i(t-\tau_i)b_i(t-\tau_i)\cos(\omega_c t+\theta_i)+n(t) \qquad (1)$$

where a_i represents the code waveform for the i^{th} signal, b_i represents the data waveform for the i^{th} signal, the random variables θ_i are independent and uniform on $[0,2\pi]$, and the random variables τ_i are independent and uniform on $[0,T]$ where T is the common data symbol duration for the K signals. We assume that for each i, $|a_i(t)| = |b_i(t)| = 1$ for all t so that the power in each of the K signals is P. For purposes of the present analysis we assume that the receiver is completely synchronized to the first signal and we are interested in the effect of the other K-1 signals on the quality of the first signal. Due to the large number of computations required in the numerical evaluation of the exact solution for the error probability (approximately N^K computations are required where N is the number of code symbols per information symbol) we will compute the signal-to-noise ratio at the output of the receiver. For cases of interest ($K \approx 40$, $N > 1000$) the signal-to-noise ratio is the most useful performance parameter that can be obtained with a reasonable amount of computational effort.

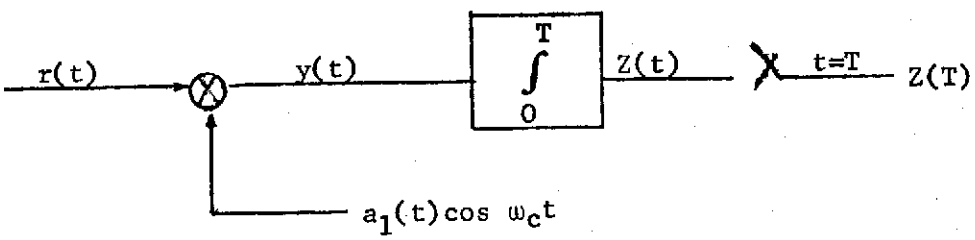

FIGURE 1. Analytical Model

ANALYSIS

Since we assume the receiver is synchronized to the first signal, we can let $\theta_1 = 0$ and $\tau_1 = 0$. The random variables $\theta_2, \theta_3, \ldots, \theta_K, \tau_2, \tau_3, \ldots, \tau_K$ then represent differential phase shifts and time delays with respect to the first signal. The output of the multiplier of Figure 1 is

$$y(t) = \sum_{i=1}^{K} \sqrt{\tfrac{1}{2}P}\, a_i(t-\tau_i)b_i(t-\tau_i)a_1(t)[\cos\theta_i + \cos(2\omega_c t+\theta_i)] + n(t)a_1(t)\cos\omega_c t$$

The frequency response of a realistic hardware implementation for the system of Figure 1 is such that the effect of the double frequency component in y(t) is negligible if $f_c \gg 1/T$. The significant input to the integrator is therefore

$$\hat{y}(t) = \sum_{i=1}^{K} \sqrt{\tfrac{1}{2}P}\, a_i(t-\tau_i)b_i(t-\tau_i)a(t)\cos\theta_i + n(t)a_1(t)\cos\omega_c t \qquad (2)$$

The corresponding output at t=T is

$$Z(T) = \sqrt{\tfrac{1}{2}P} \sum_{i=1}^{K} \int_0^T a_i(t-\tau_i)b_i(t-\tau_i)a_1(t)\cos\theta_i\, dt + \int_0^T a_1(t)n(t)\cos\omega_c t \qquad (3)$$

Writing equation (3) as desired signal plus interference plus noise we have

$$Z(T) = \sqrt{\tfrac{1}{2}P} \int_0^T a_1^2(t)b_1(t)dt + \sqrt{\tfrac{1}{2}P} \sum_{i=2}^{K} \int_0^T a_i(t-\tau_i)b_i(t-\tau_i)a_1(t)dt\cos\theta_i + \int_0^T a_1(t)n(t)\cos\omega_c t\, dt \qquad (4)$$

The information signals b_i are defined by

$$b_i(t) = \sum_{n=-\infty}^{\infty} b_{i,n}\, p_T(t-nT) \qquad (5)$$

$$\mathrm{Var}\{Z(T)\} = \tfrac{1}{4}P \sum_{i=2}^{K} \frac{1}{T} \int_0^T E\left\{\left[b_{i,n} \int_0^{\tau_i} a_i(t-\tau_i)a_1(t)dt + b_{i,o} \int_{\tau_i}^{T} a_i(t-\tau_i)a_1(t)dt \right]^2\right\} d\tau_i$$

$$+ \left(\frac{N_o}{2}\right) \int_0^T a_1^2(t)\cos^2 \omega_c t \, dt \qquad (7)$$

which can expressed in terms of the partial cross-correlation functions R_{i1} and $\hat{R}_{i1}$ defined by

$$R_{i1}(\tau_i) = \int_0^{\tau_i} a_i(t-\tau_i)a_1(t)dt \qquad (8)$$

$$\hat{R}_{i1}(\tau_i) = \int_{\tau_i}^{T} a_i(t-\tau_i)a_1(t)dt \qquad (9)$$

The code waveforms a_i are defined by

$$a_i(t) = \sum_{j=-\infty}^{\infty} a_j^{(i)} \, p_{T_c}(t-jT_c) \qquad (10)$$

where $a^{(i)}$ is the code sequence for the i^{th} signal which satisfies $|a_j^{(i)}|=1$ for each j, and $a_j^{(i)}=a_{j+p}^{(i)}$ for some p and any j (i.e., $a^{(i)}$ is a sequence of +1's and -1's which is periodic with period p). For the present analysis we assume that period p divides $N = T/T_c$ so that there are an integral number N of code periods in the information symbol interval [0,T].

Using (8), (9), and (10) we can write (7) as

$$\mathrm{Var}\{Z(T)\} = \frac{P}{4T} \sum_{i=2}^{K} \int_0^T E\left\{\left[b_{i,-1} \, R_{i1}(\tau_i) + b_{i,o} \hat{R}_{i1}(\tau_i) \right]^2\right\} d\tau_i$$

$$+ \left(\frac{N_o}{2}\right)\left(\frac{T}{2} + \frac{\sin 2\omega_c T}{2\omega_c}\right) \qquad (11)$$

For $\omega_c \gg \frac{1}{T}$ we can neglect the double frequency term in (11) and since $b_{i,-1}$ and $b_{i,o}$ are independent zero mean random variables with $|b_{i,n}|=1$ with probability 1 then

where the $b_{i,n}$ are independent identically distributed random variables taking values +1 and -1 with equal probability and the function p_T is the rectangular pulse function defined by

$$p_T(\lambda) = \begin{cases} 1 & 0 \leq \lambda < T \\ 0 & \text{otherwise} \end{cases}$$

The magnitude of the desired signal component of Z(T) is $\left|E\{Z(T)\,|\,b_{1,0}\}\right| = \sqrt{\tfrac{1}{2}P}\ T$ while the variance of Z(T) for a given $b_{1,0}$ is

$$\text{Var}\,\{Z(T)\} = \tfrac{1}{2}P \sum_{i=2}^{K} E\left\{\left[\int_0^T a_i(t-\tau_i)b_i(t-\tau)a_1(t)dt\right]^2 \cos^2\theta_i\right\}$$

$$+\ E\left\{\left[\int_0^T a_1(t)n(t)\cos\omega_c t\ dt\right]^2\right\}$$

$$= \tfrac{1}{2}P \sum_{i=2}^{K} 1/T\int_0^T E\left\{\left[\int_0^T a_i(t-\tau_i)b_i(t-\tau_i)a_1(t)\ dt\right]^2\right\}d\tau_i$$

$$+\ \int_0^T a_1^2(t)\left(N_o/2\right)\cos^2\omega_c t\ dt \qquad (6)$$

The integral $\int_0^T a_i(t-\tau_i)b_i(t-\tau_i)a_1(t)dt$ represents the cross-correlation of the codes a_i and a_1 if $b_i(t-\tau_i)$ is of the same sign for all $t \in [0,T]$. However, according to (5), $b_i(t-\tau_i)$ will change sign with probability $\frac{1}{2}$ in the internal $[0,T]$ so that in general we do not get full cross-correlations. In fact, by substituting from equation (5) into equation (6) we have for a given $b_{1,0}$

$$\mathrm{Var}\{Z(T)\} = \frac{P}{4T} \sum_{i=1}^{K} \int_{0}^{T} R_{i1}^2(\tau_i)+\hat{R}_{i1}^2(\tau_i)d\tau_i + \frac{N_o T}{4} \tag{12}$$

$$= \frac{P}{4T} \sum_{i=1}^{K} \sum_{\ell=0}^{N-1} \int_{\ell T_c}^{(\ell+1)T_c} R_{i1}^2(\tau_i)+\hat{R}_{i1}^2(\tau_i)d\tau_i + \frac{N_o T}{4} \tag{13}$$

For any nonnegative integer ℓ less than N we note that R_{i1} and $\hat{R}_{i1}$ are linear continuous functions on the interval $[\ell T_c, (\ell+1)T_c]$. Furthermore,

$$R_{i1}(\ell T_c) = \int_{0}^{\ell T_c} a_i(t-\ell T_c)a_1(t)dt = \sum_{j=0}^{\ell-1} \int_{jT_c}^{(j+1)T_c} a_i(t-\ell T_c)a_1(t)dt \tag{14}$$

$$\hat{R}_{i1}(\ell T_c) = \int_{\ell T_c}^{T} a_i(t-\ell T_c)a_1(t)dt = \sum_{j=\ell}^{N-1} \int_{jT_c}^{(j+1)T_c} a_i(t-\ell T_c)a_1(t)dt \tag{15}$$

We define the discrete partial cross-correlation functions ρ_{i1} and $\hat{\rho}_{i1}$ by

$$\rho_{i1}(\ell) = \sum_{j=0}^{\ell-1} a_{j-\ell}^{(i)} a_j^{(1)}$$

$$\hat{\rho}_{i1}(\ell) = \sum_{j=\ell}^{N-1} a_{j-\ell}^{(i)} a_j^{(1)}$$

From (10) we see that $a_i(t)$ is constant on the interval $[jT_c, (\ell+1)T_c]$, so that (14) and (15) become

$$R_{il}(\ell T_c) = \sum_{j=0}^{\ell-1} a_{j-\ell}^{(i)} a_j^{(1)} T_c = \rho_{il}(\ell)\, T_c$$

$$\hat{R}_{il}(\ell T_c) = \sum_{j=\ell}^{N-1} a_{j-\ell}^{(i)} a_j^{(1)} T_c = \hat{\rho}_{il}(\ell)\, T_c$$

Since R_{il} and $\hat{R}_{il}$ are linear on $[\ell T_c, (\ell+1)]$, then for $\tau_i \in [\ell T_c, (\ell+1)T_c]$

$$R_{il}(\tau_i) = \rho_{il}(\ell)T_c + [\rho_{il}(\ell+1)-\rho_{il}(\ell)]\,(\tau_i - \ell T_c) \qquad (16)$$

$$\hat{R}_{il}(\tau_i) = \hat{\rho}_{il}(\ell)T_c + [\rho_{il}(\ell+1)-\rho_{il}(\ell)]\,(\tau_i - \ell T_c) \qquad (17)$$

Therefore

$$\int_{\ell T_c}^{(\ell+1)T_c} R_{il}^2(\tau_i) + \hat{R}_{il}^2(\tau_i)\, d\tau_i = \int_0^{T_c} R_{il}^2(\lambda+\ell T_c) + \hat{R}^2(\lambda+\ell T_c)\, d\lambda$$

$$= \int_0^{T_c} \rho_{il}^2(\ell)T_c^2 + \hat{\rho}_{il}^2(\ell)T_c^2 + 2\tau T_c\{\rho_{il}(\ell)[\rho_{il}(\ell+1)-\rho_{il}(\ell)] + \hat{\rho}_{il}[\hat{\rho}_{il}(\ell+1)-\hat{\rho}_{il}(\ell)]\}$$

$$+ \tau^2\{[\rho_{il}(\ell+1)-\rho_{il}(\ell)]^2 + [\rho_{il}(\ell+1)-\rho_{il}(\ell)]^2\}\, d\tau$$

$$= T_c^3\{\rho_{il}^2(\ell) + \hat{\rho}_{il}^2(\ell) + \rho_{il}(\ell)[\rho_{il}(\ell+1)-\rho_{il}(\ell)] + \hat{\rho}_i(\ell)[\hat{\rho}_{il}(\ell+1)-\hat{\rho}_{il}(\ell)]$$

$$+ \tfrac{1}{3}[\rho_{il}(\ell+1)-\rho_{il}(\ell)]^2 + \tfrac{1}{3}[\hat{\rho}_{il}(\ell+1)-\hat{\rho}_{il}(\ell)]^2\}$$

$$= \frac{T_c^3}{3}\{\rho_{il}^2(\ell) + \rho_{il}(\ell)\rho_{il}(\ell+1) + \rho_{il}^2(\ell+1) + \hat{\rho}_{il}^2(\ell) + \hat{\rho}_{il}(\ell)\hat{\rho}_{il}(\ell+1) + \hat{\rho}_{il}^2(\ell+1)\}$$

(18)

By substituting this into (13) we have

$$\mathrm{Var}\{Z(T)\} = \frac{PT_c^3}{12T} \sum_{i=2}^{K} \sum_{\ell=0}^{N-1} [\rho_{i1}^2(\ell)+\rho_{i1}(\ell)\rho_{i1}(\ell+1)+\rho_{i1}^2(\ell+1)+\hat{\rho}_{i1}^2(\ell)+\hat{\rho}_{i1}(\ell)\hat{\rho}_{i1}(\ell+1)+\hat{\rho}_{i1}^2($$

$$+ \frac{N_o T}{4} \qquad (19)$$

Defining $\nu_{i1} = \sum_{\ell=0}^{N} \rho_{i1}^2(\ell)$, $\hat{\nu}_{i1} = \sum_{\ell=0}^{N} \hat{\rho}_{i1}^2(\ell)$, $\mu_{i1} = \sum_{\ell=0}^{N-1} \rho_{i1}(\ell)\rho_{i1}(\ell+1)$, and $\hat{\mu}_{i1} = \sum_{\ell=0}^{N-1} \hat{\rho}_{i1}(\ell)\hat{\rho}_{i1}(\ell+1)$ then

$$\mathrm{Var}\{Z(T)\} = \frac{PT_c^3}{12T} \sum_{i=2}^{K} [2\nu_{i1}-\rho_{i1}^2(0)-\rho_{i1}^2(N)+2\hat{\nu}_{i1}-\hat{\rho}_{i1}^2(0)-\hat{\rho}_{i1}^2(N)+\mu_{i1}+\hat{\mu}_{i1}] + \frac{N_o T}{4}$$

(20)

Note that $\hat{\rho}_{i1}(0) = \sum_{j=0}^{N-1} a_j^{(i)} a_j^{(1)} = \sum_{j=0}^{N-1} a_{j-N}^{(i)} a_j^{(1)} = \rho_{i1}(N)$ which is the full cross-correlation of code $a^{(i)}$ with code $a^{(1)}$ and that $\rho_{i1}(0) = \hat{\rho}_{i1}(N) = 0$.

Therefore, if we define the signal-to-noise ratio as

$$S/N = |E\{Z(T)\}| \Big/ \sqrt{\mathrm{Var}\{Z(T)\}}$$

where all expectations are conditioned on a given $b_{1,0}$ then

$$S/N = \sqrt{\tfrac{1}{2}P}\, T \left\{ \frac{PT_c^3}{12T} \sum_{i=2}^{K} [2\nu_{i1}+2\hat{\nu}_{i1}+\mu_{i1}+\hat{\mu}_{i1}-2\rho_{i1}^2(N)] + \frac{N_o T}{4} \right\}^{-\frac{1}{2}}$$

$$= \left\{ \frac{T_c^3}{3T^3} \sum_{i=2}^{K} [\nu_{i1}+\hat{\nu}_{i1}+\tfrac{1}{2}(\mu_{i1}+\hat{\mu}_{i1})-\rho_{i1}^2(N)] + \frac{N_o}{2PT} \right\}^{-\frac{1}{2}}$$

(21)

Since the bit energy E is related to the power P by E = PT and since $T=NT_c$ then (21) gives

$$S/N = \left\{ \frac{1}{3N^3} \sum_{i=2}^{K} [\nu_{i1}+\hat{\nu}_{i1}+\tfrac{1}{2}(\mu_{i1}+\hat{\mu}_{i1})-\rho_{i1}^2(N)] + \frac{N_o}{2E} \right\}^{-\frac{1}{2}} \qquad (22)$$

which gives the signal voltage-to-rms noise voltage ratio at the output of the correlator at the sampling instant in terms of the partial cross-correlation functions, the number N of code symbols per data symbol, and the bit energy to noise power density ratio E/N_o.

A computer program has been written to compute the partial cross-correlation functions and the parameters ν_{i1}, $\hat{\nu}_{i1}$, μ_{i1}, and $\hat{\mu}_{i1}$ for arbitrary periodic sequences $a^{(i)}$ and $a^{(1)}$. The results of this computer program will be used in equation (22) to select good codes for the code division multiple access system and to predict system performance. (See Appendix C.)

APPENDIX D. ANALYSIS OF CODE DIVISION MULTIPLE ACCESS SYSTEMS

This appendix is concerned with the generation of codes for a code division multiple access (CDMA) system and the analysis of performance of the system for a specific set of codes. This appendix represents the final phase of the study of the performance of an asynchronous (in time) CDMA system. The study has consisted of an investigation of the properties of codes which are suitable for use in CDMA systems (Appendix A) and the analysis of the system in terms of signal-to-noise ratio at the output of the correlation receiver including the effects of partial cross-correlation (Appendix B). In addition, an analysis of the system leading to expressions for the probability of data symbol detection error (which is a more realistic measure of system performance) is essentially complete, but lack of funding prohibits numerical evaluation of the equations that have been derived.

Generation of Gold Codes

A detailed discussion of the properties and method of generation of classes of codes with small cross-correlation is given in Appendix A. This section briefly summarizes the method of constructing one such class of codes know as Gold codes. The determination of the characteristic polynomial for the class of Gold codes with period 511 will be given as an example of the application of the technique.

The existence of large classes of binary sequences with good cross-correlation properties was shown by Gold (Ref. [3]). These sequences, called Gold codes, exist for any $n \not\equiv 0 \pmod 4$ and have the property that the cross-correlation between any two codes in the same class does not exceed $2^{\left[\frac{n+2}{2}\right]}+1$ where "[ ]" denotes "integer part of". For each $n \not\equiv 0 \pmod 4$, the class of Gold codes of period 2^n-1 consists of 2^n+1 different sequences.

Let α be any primitive element of the Galois field $GF(2^n)$ and and let f_1 be the minimal polynomial of α. If $t = 2^{\left[\frac{n+2}{2}\right]}+1$ and if f_t is the minimal polynomial of α^t then the linear feedback shift register of length 2n with the product polynomial $f_1 f_t$ as characteristic polynomial will generate the class of Gold codes of period 2^n-1. The 2^n+1 different sequences are generated by properly selecting binary words of length 2n as initial conditions for the shift register.

For the case n=9 the class of Gold codes consists of 513 sequences of period 511. The maximum magnitude of the cross-correlation between any two sequences in the class is $2^{\left[\frac{11}{2}\right]}+1 = 33$. Let α be a primitive element of $GF(2^9)$ with minimal polynomial 1021 (in octal). Since $t = 2^{\left[\frac{11}{2}\right]}+1=3$ then we must determine the minimal polynomial of α^{33}. To do this we use the table of irreducible polynomials published by Peterson and Weldon (Ref. [4]). The exponent 33 does not appear in this table but since $33(2^4) = 528 \equiv 17 \pmod{511}$ then the exponent 33 is in the same coset as the exponent 17 which does appear in the table of irreducible polynomials with corresponding minimal polynomial 1333 (in octal). Thus the desired polynomials are:

$$f_1(x) = x^9 + x^4 + 1$$

$$f_{33}(x) = f_{17}(x) = x^9+x^7+x^6+x^4+x^3+x+1$$

The product polynomial is then

$$(f_1 f_{33})(x) = f_1(x)f_{33}(x) = x^{18}+x^{16}+x^{15}+x^{12}+x^{11}+x^8+x^6+x^5+x+1$$

which is 1 3 1 4 5 5 3 in octal. The Gold codes of period 511 are then generated by using this polynomial as the characteristic polynomial for a linear feedback shift register of length 18.

A computer program (Ref. [5]) has been developed to determine the initial conditions that give the Gold codes. A partial listing of the results of this program is given in Table 1. The 40 numbers listed in Table 1 when converted to binary and used as initial conditions for the 18 stage linear feedback shift register with characteristic polynomial $f_1 f_{33}$ will generate 40 different Gold sequences.

TABLE 1. Decimal Representation of Initial Conditions for Generating 40 Gold Sequences of Period 511

1	31	57	89
5	33	61	93
9	35	65	97
11	37	67	101
13	39	71	105
15	41	73	107
17	45	77	111
21	49	83	113
25	51	85	123
27	55	87	125

Performance of Correlation Receivers in a CDMA System Using Gold Codes

An analysis of the performance of correlation receivers for a CDMA system is given in Appendix B where an equation for the signal-to-noise ratio at the output of the receiver is derived in terms of the partial cross-correlation functions for the codes used in the system.

In general the received signal consists of K code division multiplexed signals corrupted by additive white Gaussian noise n(t) which has two-sided spectral density $N_o/2$ watts/Hz. That is, the received signal r(t) is given by

$$r(t) = \sum_{i=1}^{K} \sqrt{2P}\, a_i(t-\tau_i)b_i(t-\tau_i)\cos(\omega_c t+\theta_i)+n(t) \qquad (1)$$

where a_i represents the code waveform for the i^{th} signal, b_i represents the data waveform for the i^{th} signal, the random variables θ_i are independent and uniform on $[0,2\pi]$, and the random variables τ_i are independent and uniform on $[0,T]$ where T is the common data symbol duration for the K signals. We assume that for each i, $|a_i(t)| = |b_i(t)| = 1$ for all t so that the power in each of the K signals is P. We assume that the receiver is completely synchronized to the first signal and we are interested in the effect of the other K-1 signals on the quality of the first signal.

The information signals b_i are defined by

$$b_i(t) = \sum_{j=-\infty}^{\infty} b_{i,n} p_T(t-nT)$$

where the $b_{i,n}$ are independent identically distributed random variables taking values +1 and -1 with equal probability and the function p_T is the rectangular pulse function defined by

$$p_T(\lambda) = \begin{cases} 1 & 0 \le \lambda < T \\ 0 & \text{otherwise} \end{cases}$$

The code waveforms a_i are defined by

$$a_i(t) = \sum_{j=-\infty}^{\infty} a_j^{(i)} p_{T_c}(t-jT_c)$$

where $a^{(i)}$ is the code sequence for the i^{th} signal which satisfies $|a_j^{(i)}|=1$ for each j, and $a_j^{(i)} = a_{j+p}^{(i)}$ for some p and any j (i.e., $a^{(i)}$ is a sequence of +1's and -1's which is periodic with period p). We assume that period p divides $N = T/T_c$ so that there are an integral number N of of code periods in the information symbol interval [0,T].

The peak signal voltage-to-rms noise voltage ratio at the output of the correlation receiver is given by (Ref. [2]).

$$S/N = \left\{ \frac{1}{3N^3} \sum_{i=2}^{K} [\nu_{i1} + \hat{\nu}_{i1} + \tfrac{1}{2}(\mu_{i1} + \hat{\mu}_{i1}) - \rho_{i1}^2(N)] + \frac{N_o}{2E} \right\}^{-\frac{1}{2}} \quad (2)$$

where $\nu_{i1} = \sum_{\ell=0}^{N} \rho_{i1}^2(\ell)$, $\hat{\nu}_{i1} = \sum_{\ell=0}^{N} \hat{\rho}_{i1}^2(\ell)$, $\mu_{i1} = \sum_{\ell=0}^{N-1} \rho_{i1}(\ell)\rho_{i1}(\ell+1)$, and $\hat{\mu}_{i1} = \sum_{\ell=0}^{N-1} \hat{\rho}_{i1}(\ell)\hat{\rho}_{i1}(\ell+1)$ depend on the discrete partial cross-correlation functions ρ_{i1} and $\hat{\rho}_{i1}$ defined by

$$\rho_{i1}(\ell) = \sum_{j=0}^{\ell-1} a_{j-\ell}^{(i)} a_j^{(1)}$$

$$\hat{\rho}_{i1}(\ell) = \sum_{j=\ell}^{N-1} a_{j-\ell}^{(i)} a_j^{(1)}$$

A computer program (Ref. [5]) has been written to compute the partial cross-correlation functions ρ_{i1} and $\hat{\rho}_{i1}$ for any periodic sequences $a^{(1)}$ and $a^{(i)}$ such that the period divides $N = T/T_c$.

The results of this computer program applied to equation (2) for a CDMA system using Gold codes of period 511 with one code period per data symbol are shown in Figure 1 and Figure 2. In Figure 1, the

quantity $20 \log_{10} S/N$ is shown as a function of the data symbol energy to noise power density E/N_o for various values of K. In Figure 2, the degradation $\delta = 20 \log_{10} \{\sqrt{2E/N_o}\ (S/N)^{-1}\}$ is shown as a function of E/N_o for various values of K.

The exact evaluation of Equation (2) for K=40 requires the calculation of 39 partial cross-correlation functions. To reduce computation time, it was decided to compute a few of the partial cross-correlations and select a representative value to be used for all 39 cross-correlations. The results of this calculation are summarized in Equation (1). Code sequence 1, corresponding to code waveform a_1 in Equation (1), is the Gold sequenced generated with polynomial $f_1 f_{33}$ by using initial condition 1 (in decimal). The other six codes listed in Table 2 were picked arbitrarily from Table 1.

The quantity $C_{i1} = \frac{1}{3N^3}\left[\nu_{i1} + \hat{\nu}_{i1} + \frac{1}{2}(\mu_{i1} + \hat{\mu}_{i1}) - \rho_{i1}^2(N)\right]$ is needed to evaluate the signal-to-noise ratio from Equation (2). This was computed for i = 2, 3, 4, 5, 6, and 32 where the index i corresponds to the i^{th} smallest decimal number listed in Table 1. A representative value of C_{i1} of 7.1×10^{-4} was selected in order to serve as a "worst case" correlation value. Thus, the results shown in Figures 1 and 2 may be slightly pessimistic. However, a "worst case" value for C_{i1} seems to be appropriate since only 6 out of a possible 39 correlations were actually computed. In fact, if we consider all possible cross-correlations between the 40 codes listed in Table 2, then we must compute $\binom{40}{2} = 780$ correlations which would require an excessive amount of computer time.

TABLE 2

code Number, i	Initial Condition for Shift Register	C_{il}
2	5	6.39×10^{-4}
3	9	6.89×10^{-4}
4	11	7.04×10^{-4}
5	13	6.37×10^{-4}
6	15	6.41×10^{-4}
32	93	6.12×10^{-4}

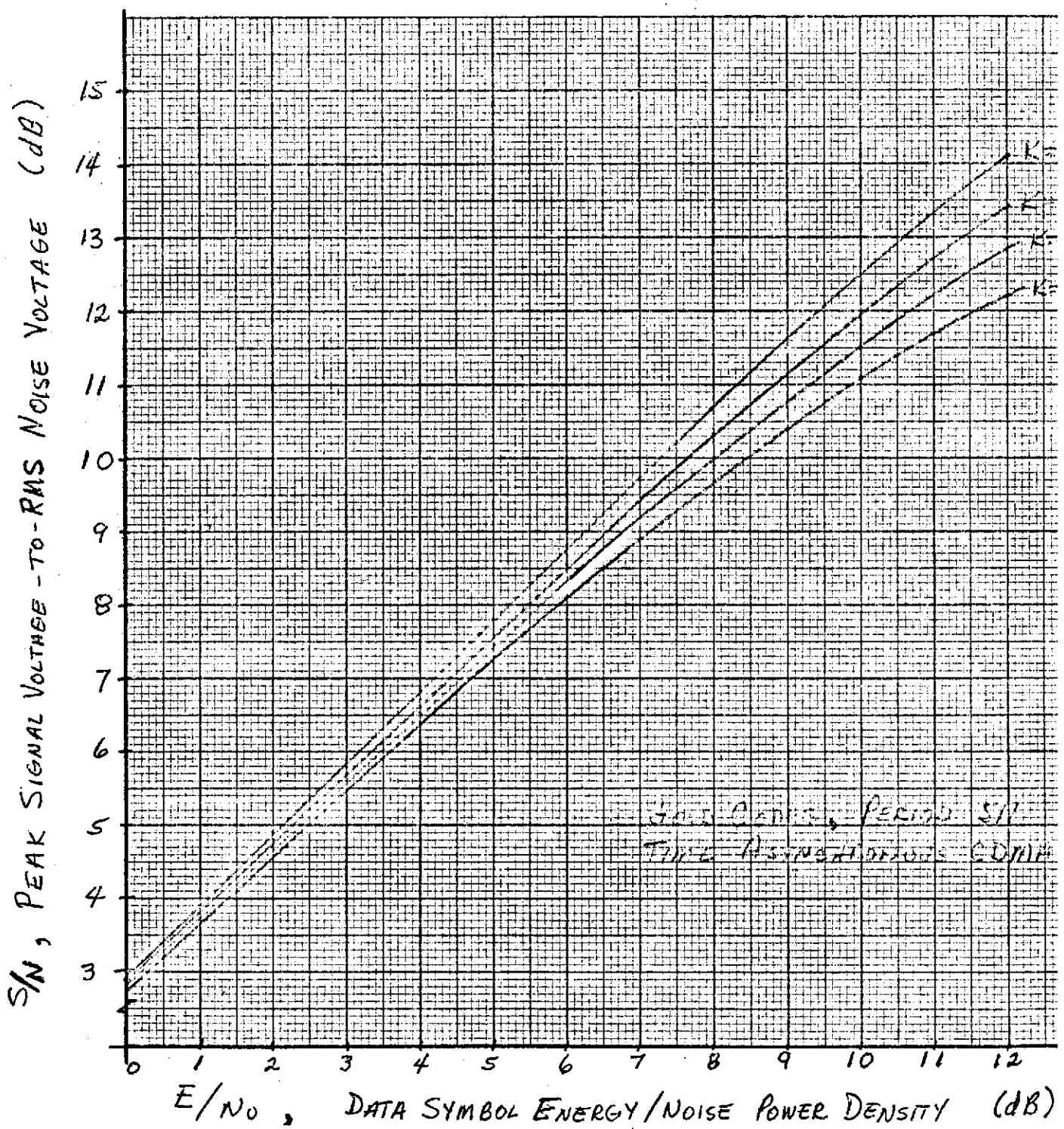
S/N, PEAK SIGNAL VOLTAGE-TO-RMS NOISE VOLTAGE (dB)
15
14
13
12
11
10
9
8
7
6
5
4
3
0
1
2
3
4
5
6
7
8
9
10
11
12
E/N0, DATA SYMBOL ENERGY/NOISE POWER DENSITY (dB)

FIGURE 1

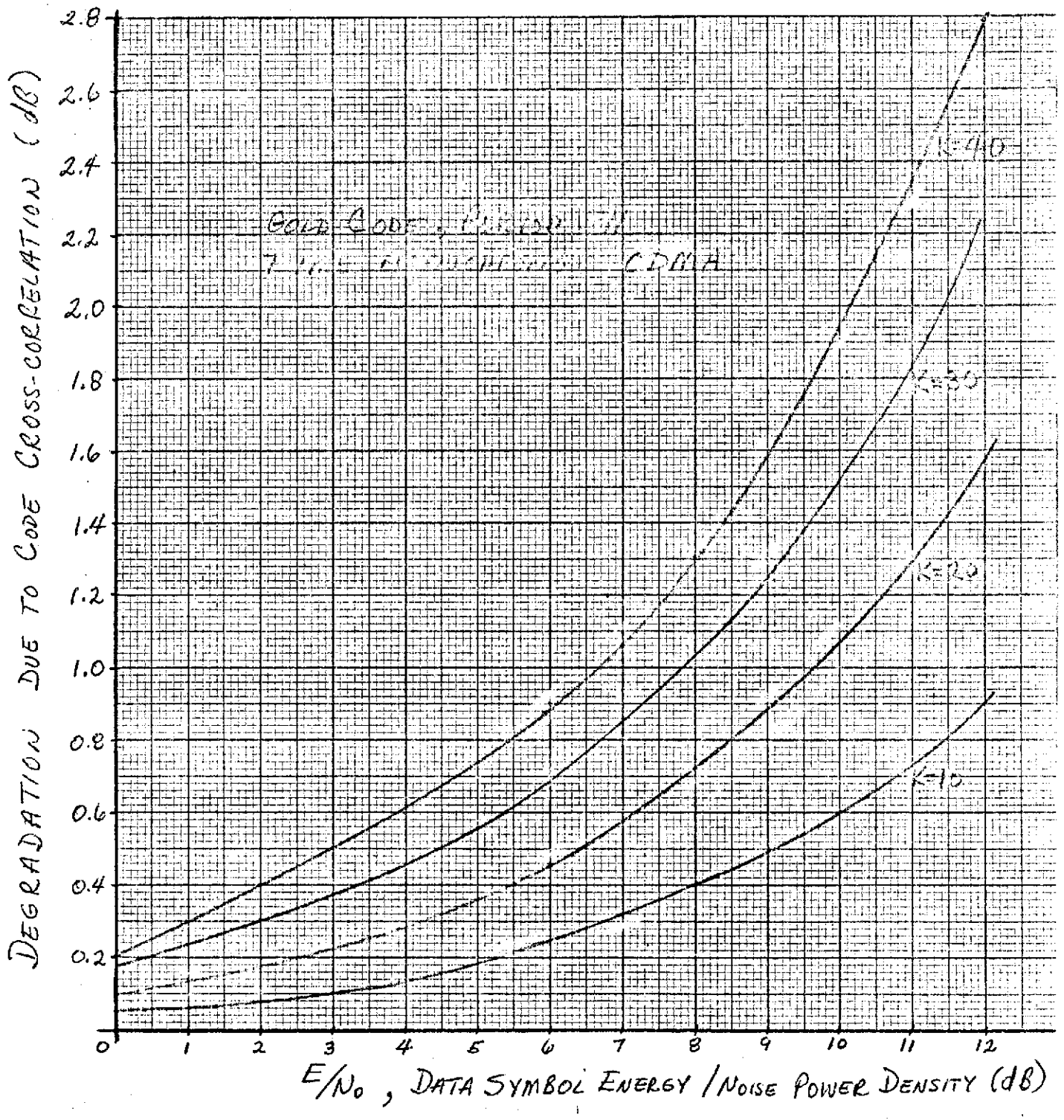
DEGRADATION DUE TO CODE CROSS-CORRELATION (dB)
2.8
2.6
2.4
2.2
2.0
1.8
1.6
1.4
1.2
1.0
0.8
0.6
0.4
0.2
0
1
2
3
4
5
6
7
8
9
10
11
12
E/N0 , DATA SYMBOL ENERGY / NOISE POWER DENSITY (dB)
K=40
K=30
K=20
K=10

FIGURE 2

REFERENCES

[1] M. B. Pursley, "A Survey of Algebraic Techniques for Selecting Codes with Low Cross-Correlation," Hughes IDC 4091.1/162 (HS337/0088), May 1, 1972.

[2] M. B. Pursley, "Receiver Performance Analysis for a Code Division Multiple Access System," Hughes IDC 4091.1/178, June 12, 1972.

[3] Robert Gold, "Optimal Binary Sequences for Spread Spectrum Multiplexing," IEEE Transactions on Information Theory (Correspondence), Vol. IT-13, No. 4, pp. 619-621, October 1967.

[4] W. W. Peterson and E. J. Weldon, Jr., Error Correcting Codes, Second Edition, MIT Press 1972.

[5] Diana Lange, Hughes IDC, to be published.

APPENDIX E. CORRELATION FUNCTIONS OF FILTERED PN SEQUENCES

Correlation functions are given for PN sequences which have been passed through one of the following elementary filters: single-pole, low pass; second-order Butterworth; or ideal rectangular low pass.

INTRODUCTION

The distortion of pseudo-random signals during transmission can potentially reduce their desirable correlation properties. In the TDRSS, PN signals have been proposed which have maximum autocorrelation (for use in combating multipath and in ranging) and minimum cross-correlation (for multiple access). This paper gives preliminary results on the degradation of a signal's autocorrelation when passed through elementary linear filters assuming an ideal autocorrelation at the input.

The earliest available analysis of filtered PN sequences was done by Gilchriest and Springett [1], [2]. However, these results are not directly applicable to TDRSS because a "split phase" signal was used and the PN sequence did not fully modulate the carrier. A recent paper by Koerner [3] describes a detailed filter study performed for JPL's TDRSN study. Again a clock signal was superimposed upon the PN signal. A paper by Gupta and Painter gives a very useful analytical approach, but few examples are provided. [4]

SYSTEM MODEL

Figure 1.A. shows a linear model for the TDRSS VHF user command channel. This model can be further simplified for the purposes of this memo to that shown in Figure 1.B. The input to the user's correlation receiver is assumed to a PN waveform which has been passed through a composite Filter $H_1(W)$. The command data will also be assumed to be all "ones" (no code inversions), but when $T_B \gg T_C$ this restriction is not necessary for the approach used below.

ANALYSIS APPROACH

Figure 2 diagrams the basic analytical approach. The "output" cross-correlation function, $\Phi_{y_1 y_2}(t)$, will be computed from the ideal "input"

autocorrelation $\phi_{xx}(t)$. Since pseudo-random sequences possess periodic autocorrelation functions which are composed of straight line segments only, Gupta and Painter have shown that the analysis of PN sequences in linear systems essentially reduces to finding the Laplace transform of the second derivative of the input autocorrelation. For the PN autocorrelation $\phi_{xx}(t)$,

$$\ddot{\phi}_{xx}^{T_B}(\tau) = \frac{1}{T_c}\delta(\tau) - \frac{2}{T_c}\delta(\tau-T_c) + \frac{1}{T_c}\delta(\tau-2T_c), \quad 0 \leq \tau < T_B ,$$

where the origin has been shifted by $-T_c$ for convenience.

$$\psi_{xx}^{T_B}(s) = \frac{1}{T_c} - \frac{2}{T_c} e^{-T_c s} + \frac{1}{T_c} e^{-2T_c s}$$

and by the periodicity property of Laplace transforms

$$\psi_{xx}(s) = \psi_{xx}^{T_B}(s) \cdot \frac{1}{1-\exp(-sT_B)} .$$

Table 1 summarizes the cases of interest and the quantities which must be computed in each instance.

EXAMPLES

Case I - Single pole low pass filter

$$\phi_{y_1 x}(\tau) = \frac{1}{2\pi j} \int_{\sigma_T - j\infty}^{\sigma_T + j\infty} \frac{1}{s^2} H_1(s)\, \psi_{xx}(s) \exp(s\tau)\, ds$$

$$= \frac{1}{2\pi j} \int_{\sigma_T - j\infty}^{\sigma_T + j\infty} \frac{1}{s^2} \frac{p}{s+p} \sum_{k=0}^{2} \alpha_k \exp(-skT_c) \exp(s\tau)\, ds$$

where $\alpha_1 = \frac{1}{T_c}$, $\alpha_2 = \frac{-2}{T_c}$, $\alpha_3 = \frac{1}{T_c}$

$$= \frac{1}{2\pi j}\sum_{k=0}^{2}\alpha_k \int_{\sigma_T - j\infty}^{\sigma_T + j\infty} \frac{p}{s^2(s+p)} \exp[(\tau - kT_c)s]ds$$

$$\Phi_{y_1x}(\tau) = \sum_{k=0}^{2}\alpha_k \left\{ \frac{-1}{p} + (\tau - kT_c) + \frac{1}{p}\exp[-p(\tau - kT_c)] \right\} h[\tau - kT_c]$$
(single pole)

Case I - Double pole low pass filter

For $H_1(s) = \frac{p_1 p_2}{(s+p_1)(s+p_2)}$,

$$p_1 = a(1+j),\ p_2 = a(1-j)$$

$$\Phi_{y_1x}(\tau) = \sum_{k=0}^{2}\alpha_k \left\{ (\tau - kT_c) - \frac{1}{a} + \frac{1}{a}\cos[(\tau - kT_c)]\exp[-a(\tau - kT_c)] \right\} h[\tau - kT_c]$$
(double pole)

Case I or Case II - Ideal low pass filter

When an ideal sharp cut-off filter is assumed, a more direct approach can be used (Ref. 5, p.93). In this case, we can simply inverse transform the filtered PN spectrum. The power spectrum of a PN waveform is given by

$$|S(\omega)|^2 = T_c \left[\frac{\sin(\frac{\omega T_c}{2})}{\frac{\omega T_c}{2}} \right]^2 .$$

$$\Phi_{y_1x}(\tau) = \frac{1}{2\pi}\int_{-\omega_B}^{+\omega_B} \left| S(\omega) \right|^2 \exp(j\omega\tau)d\omega$$
(ideal)

$$= \frac{2}{\pi} \left\{ \frac{-\sin^2 X \cos \lambda X}{X} + \frac{2+\lambda}{4} \, \mathrm{Si}[(2+\lambda)X] \right.$$

$$\left. + \frac{(2-\lambda)}{4} \, \mathrm{Si}[(2-\lambda)X] - \frac{\lambda}{2} \, \mathrm{Si}[\lambda X] \right\}$$

where $X = \frac{\omega_B T_c}{2}$, $\lambda = \frac{2\tau}{T_c}$

RESULTS

Figures 3, 4, and 5 show the output correlation functions for the three filters discussed above. Note that the curves become greatly distorted for $BW/R_c < .25$. For $BW/R_c > 1.0$ the curve shapes appear to be very close to the optimum. Even for $BW/R_c = .25$ the correlation is 10 dB down at a delay of three chip times. Protection against specular multipath would be 20 dB if the differential delay were greater than $3T_c$.

REFERENCES

[1] C. E. Gilchriest, "Correlation Functions of Filtered PN Sequences," JPL Space Programs Summary 37-16, pp. 81-93.

[2] C. Gilchriest and J. C. Sprigett, "Pseudonoise System Lock-In," JPL Research Summary No. 36-10, pp. 54-63.

[3] M. A. Koerner, "Effect of Premodulation Filtering on the Correlation and Error Signals in a Pseudonoise Receiver," JPL Space Programs Summary 37-64, Vol. III, pp. 51-59.

[4] S. C. Gupta and J. H. Painter, "Correlation Analyses of Linearly Processed Pseudo-Random Sequences," IEEE Trans on Com Tech, Vol. COM-14, Dec. 1966, pp. 796-801.

[5] J. N. Birch, "Multipath/Modulation Study for the TDRS System -- Final Report," The Magnavox Co. for NASA/GSFC under NAS 5-10744, January 1970.

TABLE 1

CASES OF INTEREST

CASE I No Filtering of Reference

$$H_2(\omega) = 1 \text{ For all } \omega$$

Compute $$\Phi_{y_1 x}(s) = \frac{1}{s^2} H_1(s)\, \Psi_{xx}(s)$$

CASE II Reference Filter Identical to Channel Filter

$$H_1(s) = H_2(s) = H(s)$$

Compute $$\Phi_{yy}(s) = \frac{1}{s^2} H(s)\, H(-s)\, \Psi_{xx}(s)$$

CASE III Reference Filter not Identical to Channel Filter

$$H_1(s) = H_2(s)$$

Compute $$\Phi_{y_1 y_2}(s) = \frac{1}{s^2} \left\{ \frac{H_1(s)H_2(-s) + H_2(s)H_1(-s)}{2} \right\} \Psi_{xx}(s)$$

where $$\Psi_{xx}(s) = \text{Transform} \left\{ \ddot{\phi}_{xx}(\tau) \right\}$$

FIGURE 1

A. Linear Model of the VHF User Command Channel

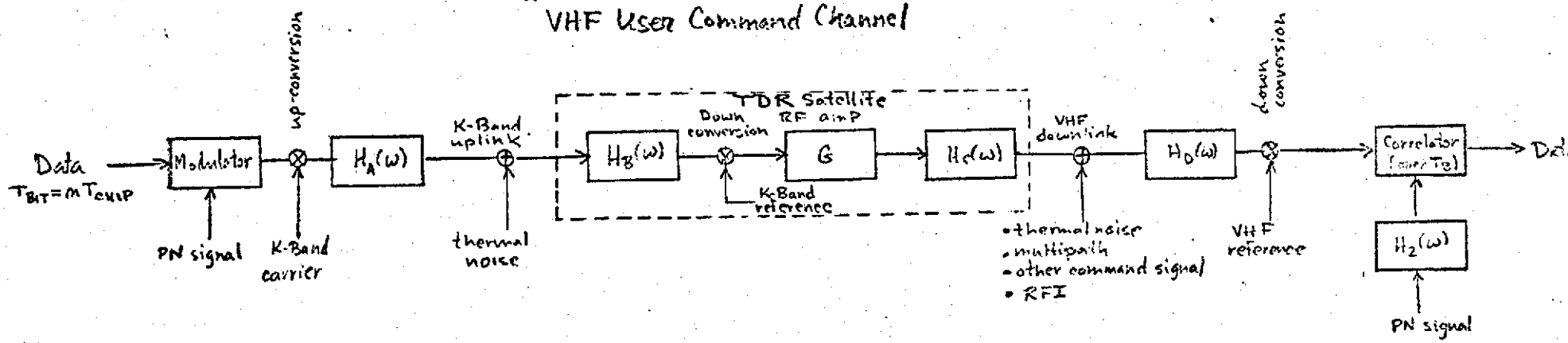

B. Simplified Linear Model

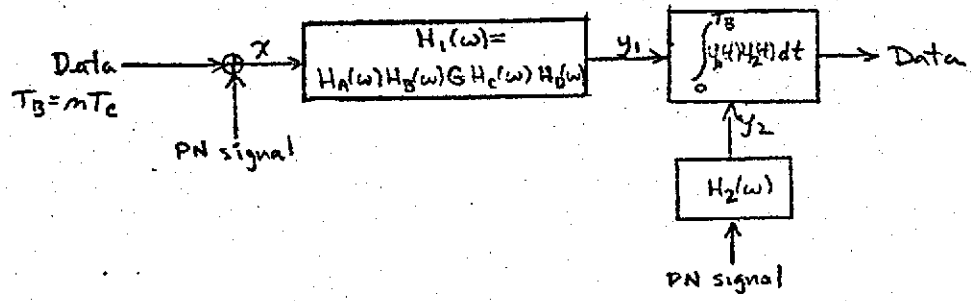

FIGURE 2

ANALYSIS APPROACH

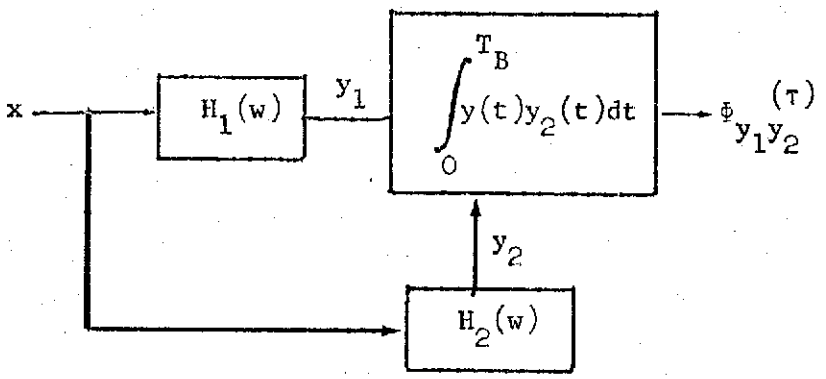

$\Phi_{y_1y_2}(\tau)$ will be computed from the "ideal" autocorrelation where

$\Phi_{xx}(0) = 1$ and $\Phi_{xx}(-T_{c+}) = \frac{1}{T_c}$.

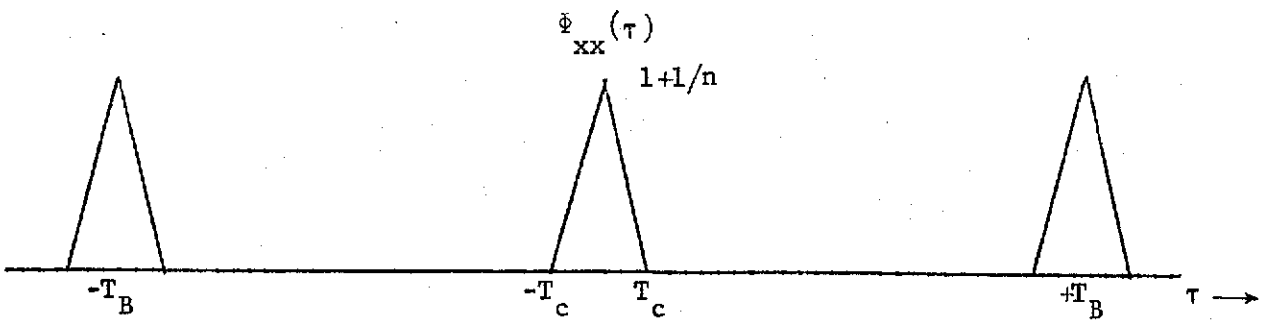

Note: for $n \gtrsim 100$ the peak correlation $\simeq 1$.

FIGURE 3

CROSS CORRELATION FUNCTION — 1 pole channel filter

- single pole low pass filter : $\frac{1}{s+1}$
- ideal reference waveform

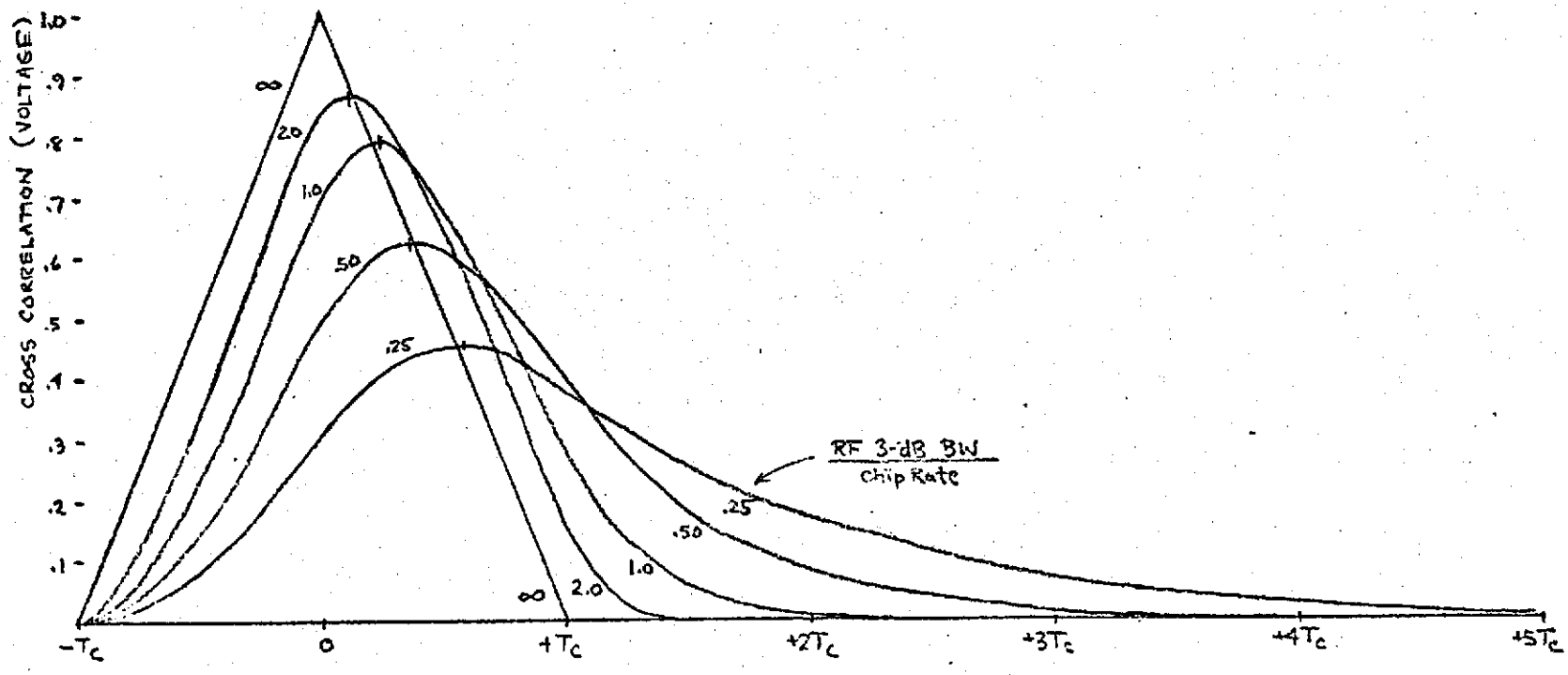

Note: Receiver will track out group delay

FIGURE 4

CROSS CORRELATION FUNCTION — 2 pole channel filter

- 2 pole low pass filter with $\zeta = .707$: $\frac{1}{s^2+\sqrt{2}s+1}$
- ideal reference waveform

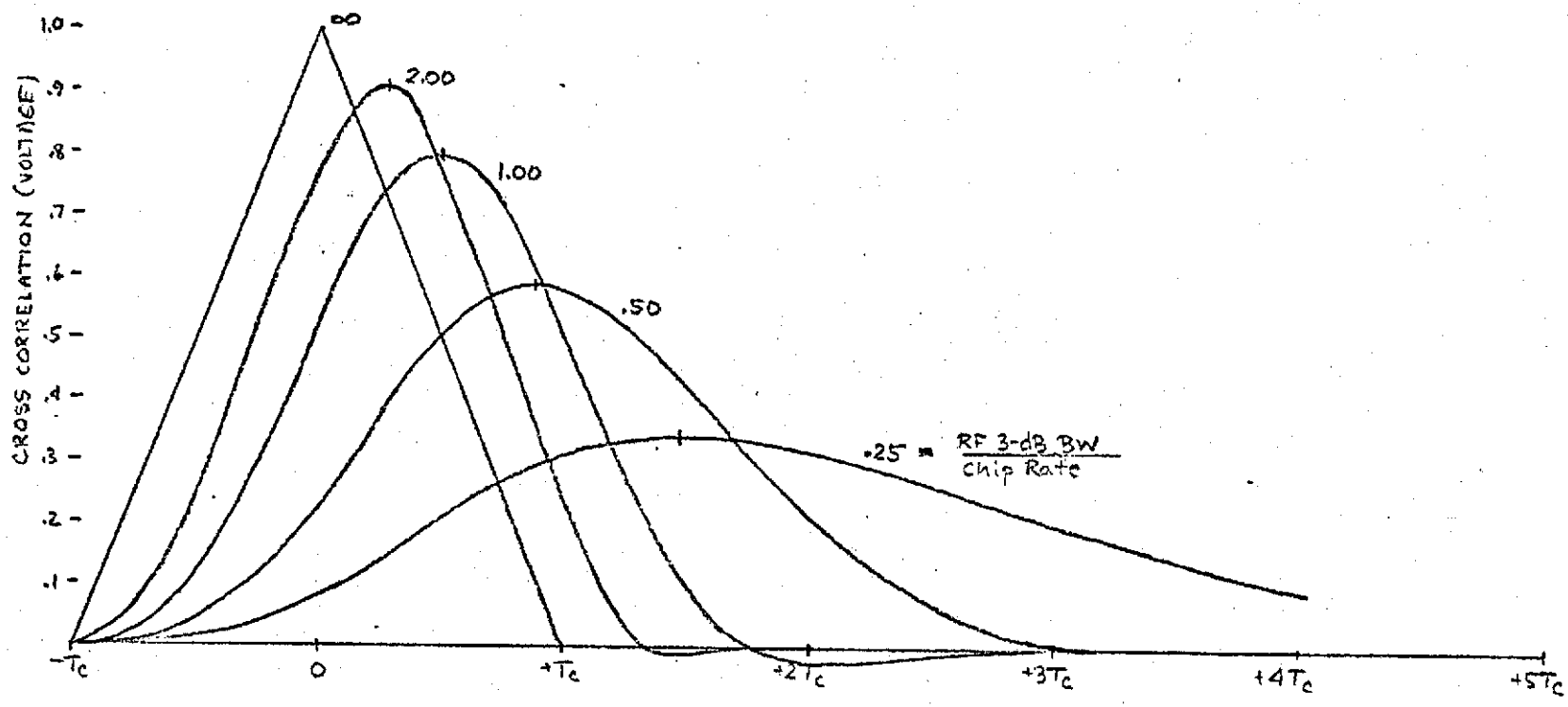

Note: Receiver will track out group delay

FIGURE 5

CROSS CORRELATION FUNCTION - rectangular filter

• ideal reference waveform

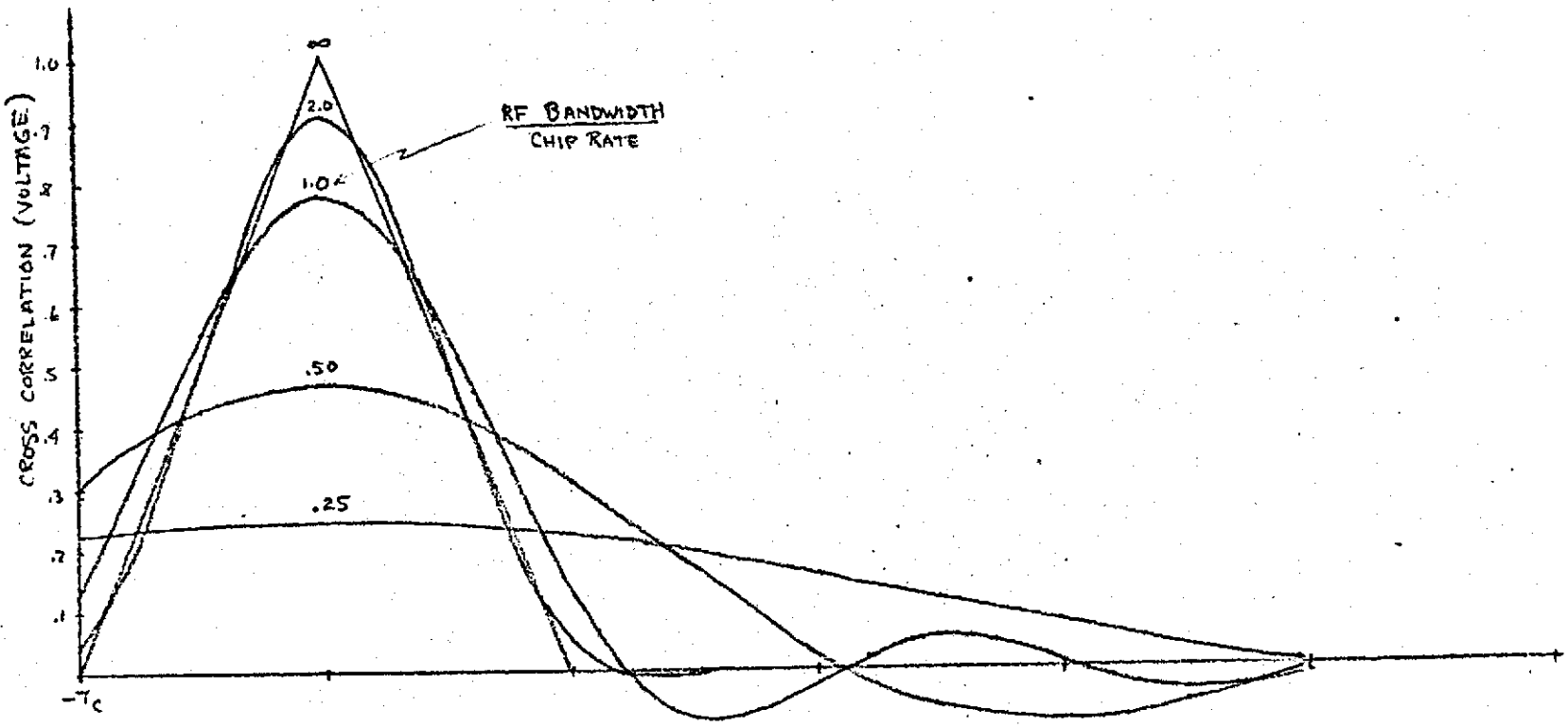

APPENDIX F. CHIP RATE SELECTION IN PN SYSTEMS

ABSTRACT

Bandlimiting in PN systems can degrade both the communications performance and the ranging performance. These degradations are computed for bandlimiting by an ideal rectangular filter. The analysis also permits performance maximization for a given bandwidth by indicating the PN chip rate required. When maximizing the coding gain against diffuse multipath, the chip rate should be less than 1.0 times the available RF bandwidth.

COMMUNICATIONS PERFORMANCE

Consider the performance of a PN system in which a bandlimited waveform, $y_1(t)$, is used to transmit data in the presence of white Gaussian noise. The received unmodulated waveform is given by:

$$r(t) = \sqrt{2P}\, y_1(t) \cos(\omega_c t) + n(t)$$

where we assume that the correlation receiver is in phase-lock and code time-lock.

The output of the demodulator's multiplier is then:

$$z(t) = [r(t)] \times [y_2(t) \cos(\omega_c t)],$$

where $y_2(t)$ is another bandlimited version of the ideal PN waveform. Expanding the above expression,

$$z(t) = \sqrt{2P}\, y_1(t)\, y_2(t) \left[\frac{\cos(2\omega_c t)+1}{2} \right] + n(t)\, y_2(t) \cos(\omega_c t$$

Since the harmonic term will not be passed by the demodulator,

$$z(t) = \sqrt{\tfrac{1}{2}P}\, y_1(t) y_2(t) + n(t)\, y_2(t) \cos(\omega_c t).$$

The integration of z(t) from t=0 to $t=T_{BIT}$ produces the decision variable used by the demodulator

$$z(t) = \sqrt{\tfrac{1}{2}P} \int_0^T y_1(t) y_2(t) dt + \int_0^T n(t) y_2(t) \cos(\omega_c t) dt$$

$$= \sqrt{\tfrac{1}{2}P}\; T\, \Phi_{y_1 y_2}(o) + \int_0^T n(t) y_2(t) \cos(\omega_c t) dt$$

With Gaussian noise the performance of the demoudlator is completely described by the mean and variance of Z(T).

$$E[Z(T)] = \sqrt{\tfrac{1}{2}P}\; T\, \Phi_{y_1 y_2}(o)$$

$$E[Z^2(T)] = E\left\{ \left[\sqrt{\tfrac{1}{2}P}\; T\, \Phi_{y_1 y_2}(o) + \int_0^T n(t) y_2(t) \cos(\omega_c t) dt \right]^2 \right\}$$

$$= E^2[Z(T)] + \frac{N_o}{2} \frac{T}{2} \Phi_{y_2y_2}(o)$$

$$\text{Var}[Z(T)] = \frac{N_o}{2} \frac{T}{2} \Phi_{y_2y_2}(o)$$

Then the probability of error is given by

$$P_E = \text{erfc}\left[\frac{\sqrt{\frac{1}{2}P}\ T\ \Phi_{y_1y_2}(o)}{\sqrt{\frac{N_o}{2}\frac{T}{2}\Phi_{y_2y_2}(o)}}\right]$$

$$= \text{erfc}\sqrt{\frac{2P\ T\ \Phi^2_{y_1y_2}(o)}{N_o\ \Phi_{y_2y_2}(o)}} .$$

Bandlimited autocorrelations effectively reduce the received $\frac{E_{BIT}}{N_o}$ by a factor

$$F = \frac{\Phi^2_{y_1y_2}(o)}{\Phi_{y_2y_2}(o)} .$$

If the reference PN waveform is ideal, $\Phi_{y_2y_2}(o) = 1$ and $F = \Phi^2_{y_1y_2}(o)$. If both the received waveform and the reference waveform are identically filtered, then $F = \Phi_{yy}(o)$.

It was shown in Appendix D that for an ideal rectangular filter

$$\Phi_{yy}(\tau) = \frac{2}{\pi}\left\{\frac{-\sin^2 X\cos\lambda X}{X} + \frac{2+\lambda}{4}\ \text{Si}[(2+\lambda)X]\right.$$

$$\left. + \frac{(2-\lambda)}{4}\ \text{Si}[\lambda X] - \frac{\lambda}{2}\ \text{Si}[\lambda X]\right\}$$

where $X = \frac{\omega\ T_c}{2}$, $\lambda = \frac{2\tau}{T_c}$

Defining $\omega=1$, then since $\omega=2\pi f$ the two sided receiver bandwidth $B_{RF}=2f=\frac{1}{\pi}$. If we define the chip time as $T_c = b\pi$ then the parameter b is the time-bandwidth product $B_{RF}T_c = \frac{1}{\pi}\, b\pi = b$.

The value of the above autocorrelation at $\tau=0$ is

$$\Phi(o) = \frac{2}{\pi}\left\{\frac{-\sin^2 X}{X} + \tfrac{1}{2}\,\mathrm{Si}[2X] - \tfrac{1}{2}\,\mathrm{Si}[2X] + 0\right\} .$$

In terms of b, the time-bandwidth product,

$$\Phi(o) = \frac{2}{\pi}\left\{\frac{\cos(b\pi)-1}{b\pi} + \mathrm{Si}[b\pi]\right\}$$

Plots of this function are shown in Figure 1, with b as the independent variable. As shown above, this function also gives the effective decrease in E_b/N_o for the link. However, the design problem is not concerned with selecting a bandwidth for minimum degradation in $\Phi(o)$, but rather with selecting a chip rate which maximizes the coding gain. Although the coding gain increases linearly with the chip rate for an infinite bandwidth channel, the degradations encountered in a bandlimited channel fix an upper limit on the achievable coding gain. Figure 2 shows that for an ideal rectangular filter that the gain is within 1 dB of theoretical fo$B_{RF}/R_c<1.0$. Note that increasing the chip rate within reasonable limits will neither improve nor degrade the performance.

Ranging Performance

As shown by Fountain[2], the rms tracking error of a delay-lock correlation receiver is given by

$$\epsilon_{rms} = \frac{1}{\sqrt{\frac{S}{N}}} \quad \frac{\sqrt{2\Phi_{y_2y_2}(o) - \Phi_{y_2y_2}(+2d) - \Phi_{y_2y_2}(-2d)}}{\Phi'_{y_1y_2}(-d) - \Phi'_{y_1y_2}(+d)}$$

where d = receiver displacement in chips

$\frac{S}{N}$ = average signal-to-noise power ratio in the tracking loop bandwidth.

Typically, the receiver "displacement" is $T_c/2$; the correlator circuitry then operates at a rate twice the chip rate. With $d = T_c/2$ and assuming a symmetric autocorrelation

$$\epsilon_{rms} = \frac{1}{\sqrt{\frac{S}{N}}} \alpha$$

where $$\alpha = \frac{\sqrt{2\Phi(o) - 2\Phi(T_c)}}{2\Phi'(\frac{T_c}{2})} .$$

In order to evaluate the expression for rms error, we require the autocorrelation value at $\pm T_c$ or $\lambda=2$.

$$\Phi(T_c) = \frac{2}{\pi} \left\{ \frac{-\sin^2 X \cos 2X}{X} + Si[4X] + 0 - Si[2X] \right\}$$

$$= \frac{2}{\pi} \left\{ \frac{\cos^2 b\pi - \cos b\pi}{b\pi} + Si[2b\pi] - Si[b\pi] \right\}$$

And also the value for the derivative of $\Phi(\tau)$, evaluated at $\frac{1}{2}T_c$ or $\lambda=1$.

$$\Phi'(\tau) = \frac{2}{\pi} \left\{ \frac{-\sin^2 X}{X} (-\dot{\lambda} X \sin \lambda X) + \frac{(2+\dot{\lambda})}{4} Si[(2-\lambda)X] \right.$$

$$+ \frac{2+\lambda}{4} \frac{\sin[(2+\lambda)X]}{[(2+\lambda)X]} (\dot{\lambda}X) + \frac{(2-\dot{\lambda})}{4} Si[(2-\lambda)X]$$

$$\left. + \frac{2-\lambda}{4} \frac{\sin[(2-\lambda)X]}{[(2-\lambda)X]} (-\dot{\lambda}X) - \frac{\dot{\lambda}}{2} Si[\lambda X] - \frac{\lambda}{2} \frac{\sin(\lambda X)}{(\lambda X)} (\dot{\lambda}X) \right\}$$

Recalling that $X = T_c/2$ and $\lambda = 2\tau/T_c$ and that $T_c \equiv b\pi$, we have at $\tau = T_c/2$

$$X = \frac{b\pi}{2},\ \lambda = 1,\ \dot{X} = 0,\ \dot{\lambda} = \frac{2}{b\pi},\ \text{and}\ X\dot{\lambda} = 1.$$

$$\Phi'(T_c/2) = \frac{2}{\pi}\left\{\frac{+\sin^3 X}{X} + \frac{2-1/X}{4}\,\mathrm{Si}[3X] + \frac{3}{4}\,\frac{\sin 3X}{3X} + \frac{2-1/X}{4}\,\mathrm{Si}[X] - \tfrac{1}{4}\,\frac{\sin X}{X} - \frac{1}{2X}\,\mathrm{Si}[X] - \tfrac{1}{2}\,\frac{\sin X}{X}\right\}$$

$$= \frac{2}{\pi}\left\{\frac{2+\frac{2}{b\pi}}{4}\,\mathrm{Si}\left[3\,\frac{b\pi}{2}\right] + \frac{2-\frac{6}{b\pi}}{4}\,\mathrm{Si}\left[\frac{b\pi}{2}\right]\right\}$$

Combining all the above expressions

$$\alpha = \frac{\sqrt{\pi\left\{\frac{-(\cos b\pi - 1)^2}{b\pi} + 2\mathrm{Si}[b\pi] - \mathrm{Si}[2b\pi]\right\}}}{(1 + \frac{1}{b\pi})\mathrm{Si}[3\frac{b\pi}{2}] + (1 - \frac{3}{b\pi})\mathrm{Si}[\frac{b\pi}{2}]}$$

The rms tracking error versus the time-bandwidth product is plotted in Figure 3. The curve assumes a signal-to-noise ratio of unity and gives the error as a fraction of the chip time. However, in such a plot, the chip time influences both the dependent and independent variables. The design problem requires selection of the chip time (or chip rate) which minimizes the rms error. This trade is shown in Figure 4 where the performance for $B_{RF}T_c = 4$ has been selected as a reference. Note that the rms error decreases monotonically with T_c for a fixed bandwidth. Caution is required in extrapolating the curve to very low values of $B_{RF}\ T_c$; the analysis assumptions may be inappropriate in this region.

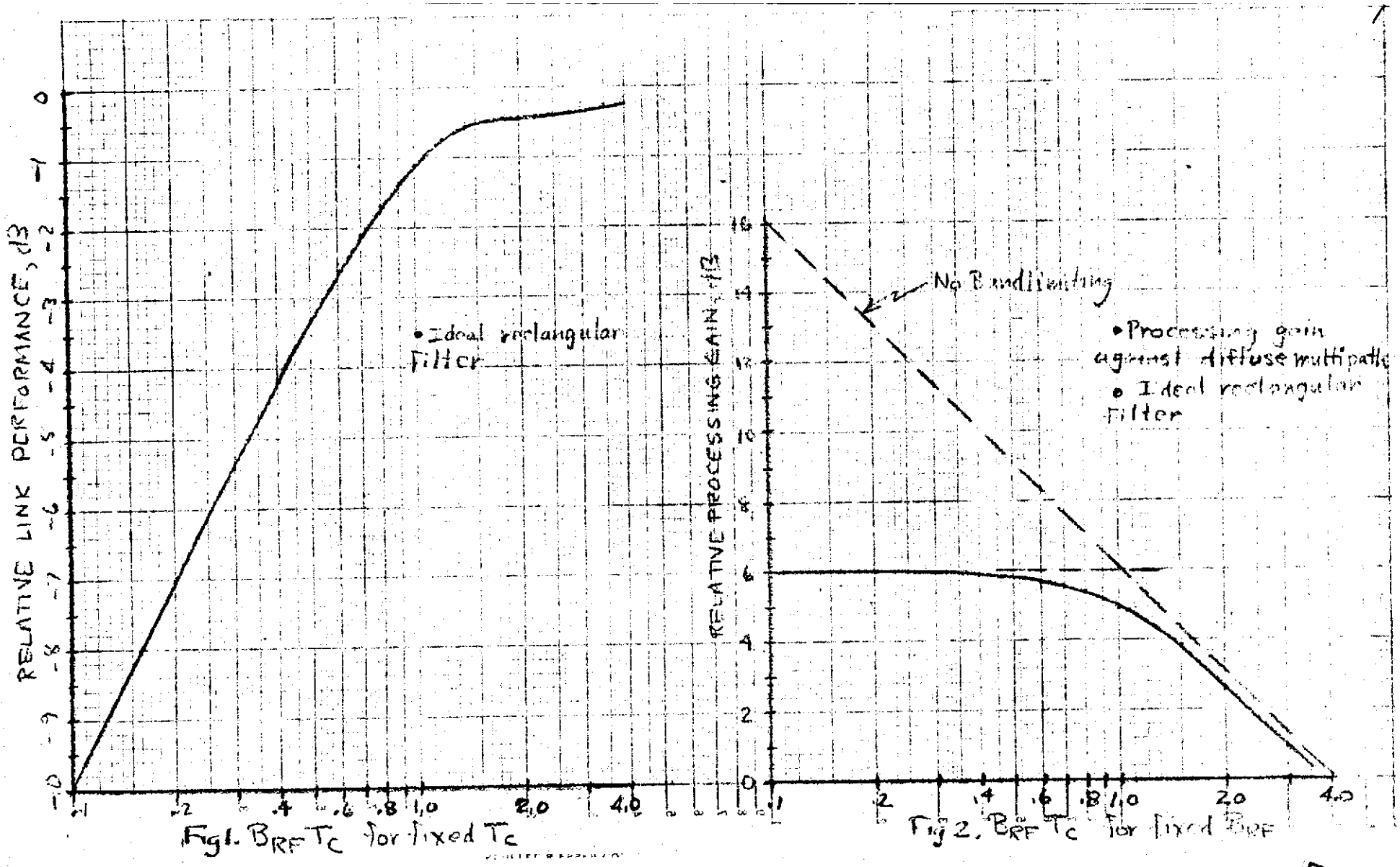

Fig 1. $B_{RF}T_c$ for fixed T_c

Fig 2. $B_{RF}T_c$ for fixed B_{RF}

COMMUNICATION PERFORMANCE OF BANDLIMITED PN SYSTEMS

Fig 3, $B_{RF}T_c$ for fixed T_c

$$\epsilon_{RMS} = \frac{1}{\frac{S}{N}\frac{B_{RF}}{2}} \, d_L$$

• ideal tracking loop filter

Fig 4 $B_{RF}T_c$ for fixed P_{ERR}

TRACKING PERFORMANCE OF
BANDLIMITED DN SYSTEMS